Identifying Genetic Loci for Metabolic Disorders Affecting the Renal Tract

A thesis submitted in fulfilment of the requirements for the degree of Doctor of Philosophy in the University of Glasgow

by

Saurav Ghimire

Institute of Molecular, Cell and Systems Biology

College of Medical, Veterinary and Life Sciences

The University of Glasgow,

Glasgow G12 8QQ

UK

August 2019

The research reported within this thesis is my work except where otherwise stated and has not been submitted for any other degree.

Saurav Ghimire

Abstract

Introduction and Objectives: Nephrolithiasis is one of the most common renal diseases, but with poorly understood pathophysiology. The current understanding of how genetic, environmental, and metabolic factors act singly or in concert to trigger stone formation remains patchy, and the progress of medical therapy has been very modest. Vertebrate models for nephrolithiasis are limited in their ability to rapidly screen multiple and varied interventions that modulate urinary stone formation. Therefore, we hypothesis that the basic research directed at model systems that elucidate the pathophysiology of stone disease is the best hope for advancing the field and leading to the development of new therapeutic approaches that have the potential to reduce the morbidity, mortality, and cost associated with this disease. Further, most studies have confounded that age and temperature share some contribution in precipitation of kidney stones. We also hypothesise that change in temperature (from colder to warmer, low temperature to higher temperature) may have a greater impact on the formation rate of nephrolithiasis.

Methods: A short lifespan, rapid deployment of transgenic lines and conception of rapid stone formation makes *Drosophila melanogaster* an ideal system to screen large numbers of interventions to assess their effect on kidney stone formation. Knockdown of gene candidates for their ability to vary the formation of urinary stones was employed utilising *Drosophila*. Microdissection, imaging and quantification facilitate identification and collection of fly stones within the lumen of the *Drosophila* Malpighian tubules (the functional equivalent of the human renal tubule). Further, *UAS-RNAi* knockdown efficiency was validated by qPCR . The genes which upon knockdown modulated the concentration of accumulated stones were further studied using various genetic, immunostaining and molecular techniques. In addition to that I also identified role of temperature and age in kidney stone formation by rearing flies at 18, 22, 26 and 29 for different time frame (day 7, day 14, day 21 and day 28) and quantifying accumulated stones during that period. The stones obtained were further validated by genetic, temperature switch, colorimetric and biochemical assays.

Results: Calcium oxalate stone formation was associated with the stones accumulated intraluminally in parental lines and gene knockdown or mutant

panel of genes fed with sodium oxalate (0.2% for 2 days). An unbiased knockdown screen of more than 20 RNAi lines was performed utilising the *GAL4*-UAS RNAi system and identified 8 genes that rescued kidney stone accumulation compared to parental lines. Microdissection and microscopy confirmed that five genes decreased stone formation in the fly, including genes *Waterwitch* (*Wtrw*), *Serine Pyruvate Amino Transferase* (*Spat*), *Cinnamon* (Cin), *Na^{+}-dependent inorganic Phosphate Co-transporter* (*NaPi-T*), *Sarcoplasmic Calcium-binding Protein 2* (*Scp2*) and *Secretory Pathway Ca^{2+}/Mn^{2+}-ATPase* (*SPoCK*). From the hits, I showed that mutation of *SRY interacting protein (Sip1)* in *Drosophila* MTs Stellate cells resulted in the accumulation of uric acid stones with a particularly notable interaction with Moesin and NHE2. I also demonstrated a combined impact of age and temperature in stone formation. Critically, I confirmed that they cause an accumulation of stones due to variation in expression of phosphate transporters *NaPi-T* and *Picot*. Our work also provides more precise insight into the impact of age and temperature in stone formation, given that we have shown that stone accumulation increases with age and in flies reared at high temperature compared to flies reared at a lower temperature.

Conclusions: A *Drosophila* urinary stone model was leveraged to perform large scale genetic screens to identify novel genes that modulate calculi formation. Our hits may now be screened as a candidate gene in future cases with a clinical presentation. Our study documents the first case of uric-acid stone formation caused by mutations of a gene using *Drosophila* as a model organism. Confirmation of these mutations as a causative factor and that the stones accumulated were uric acid stones was done by genetic, molecular and physiological experiments.

Keywords: Kidney stones, calcium oxalate monohydrate, stone accumulation, temperature, *Sip1*, *NaPi-T*

Subject Terms: Calcium Oxalate monohydrate, polarised optical microscopy, Immunostaining, crystallisation.

Terms and Terminologies

Kidney stones: Throughout the thesis different terms as nephrolithiasis, urolithiasis, concretions, stones refer to kidney stones.

Sip1: Sip1 in this thesis represents SRY interacting protein.

Table of Contents

Index of Figures

Index of Tables

Acknowledgements

There are a number of people whose contributions made this thesis possible and deserve mention. Special gratitude goes to my supervisors, Professor Julian Dow, Professor Shireen A. Davies and Dr Selim Terhzaz for their support and guidance throughout my thesis. Julian gave me an opportunity of being a graduate student! Being his student inspired me to become not only a better scientist but conduct quality research. Shireen was a great source of knowledge and guidance at various stages along the way. Selim has been continuing to be very supportive not only with my studies but non-academic advices. All these three persons are not only great supervisors, but I also consider them as a valuable person in my life. Thank you!

I am grateful to the Marie-Curie Horizon 2020 Scholarship, for funding this PhD project. I also like to thank all the partner institutes and academicians in this consortium for being with me throughout the PhD.

Many thanks to Pablo Cabrero, who was a great source of knowledge and guidance in performing most of the experiments of my thesis. His support and advice were invaluable. Further, thank you for being along with me throughout the research and also for coffee breaks.

Thanks to Guillermo Martinez Corrales for being a fantastic friend, sharing my highs and lows and supporting me in every way possible. I do not have any words to express my gratitude to you as you have been with me in every step of PhD for the first day until last.

Also, thanks to Dr Anthony Dornan for providing guidance and input at various stages along the way. I could never imagine getting chemicals or any office related work done without your help. Be relaxed now, no more disturbances.

Thanks to the present members of Dow/Davies lab for their help and support during the last three years. I would like to thank Mr Anir Pandit and Dr Lucy Alford for being with me along the way. A special thanks to Sue for her wild type flies and cookies.

I would like to thank Professor Michael Romero, Mayo Clinic, Minnesota USA for his co-operation, support and help during my internship in his lab. Thank you for teaching various skills in *Xenopus* model.

To my wonderful parents (Mr Dipak Ghimire and Ms Gita Sharma) and brother, I will always be grateful for the patience you have shown and never bothered me with any other things during the period. Their love, encouragement and tremendous support have helped me get here and finish my PhD. I dedicate this thesis to them!

Definitions/Abbreviations

Symbols	Abbreviations
˚C	Degree Celsius
µg	Microgram
µl	Microliter
µM	Micromolar
AGT	Amino glyoxylate transferase
AMP	Adenosine monophosphate
ANOVA	Analysis of Variance
bp	Base pair
BSA	Bovine serum albumin
Ca^{2+}	Calcium ions
CAH1	Carbonic anhydrase 1
CaOx	Calcium oxalate
CapaR	Capa receptor
cDNA	Complementary DNA
cAMP	3′,5′-cyclic adenosine monophosphate
cm	Centi-meter
CS	Canton-special
CFP	Green fluorescent protein
Cin	Cinnamon
DhpD	Dihydropterin deaminase
EG	Ethylene Glycol
EMS	Ethyl methanesulphonate
ER	Endoplasmic reticulum
ESRD	Early stage renal disease
g	Centripetal force = to gravitational acceleration
GAG's	Glycosaminoglycans
GDA	Guanine deaminase
GR	Glyoxylate reductase
HA	Hyaluronic acid
HGPRT	Hypoxanthine-guanine phosphoribosyltransferase
HLP	Hydroxyl-L-proline
HPR	Hydroxy-pyruvate reductase
ICC	Immunocytochemistry
IEM	Inborn errors of metabolism
kb	Kilobases
Ksp	Thermodynamic solubility product
M	Molar
mL	Millilitre
mm	Millimetre
mM	Millimolar

min	Minute
M	Molar
MCP-1	Monocyte chemoattractant protein-1
MD	Monogenic disorders
MeS	Metabolic syndrome
Moco	Molybdenum cofactor
Moe	Moesin
MTs	Malpighian tubules
NaCl	Sodium chloride
NaOx	Sodium oxalate
NaPi-T	Sodium Phosphate co-transporter
ng	Nanogram
ng	Nanogram
NHANES	National Health and Nutrition Examination Survey
OPN	Osteopontin
PBS	Phosphate buffered saline
PCR	Polymerase chain reaction
P^H	Primary hyperoxaluria
PRPP	Phosphoribosylpyrophosphate
qRT-PCR	Quantitative reverse transcriptase PCR
RNA	Ribonucleic acid
ROS	Reactive oxygen species
RNAi	RNA interference
ry	Rosy
RT	Room temperature
SA	Sialic acid
Scp2	Sarcoplasmic calcium-binding protein 2
Sec or s	Second
Sip1	SRY interacting protein
Spat	Serine pyruvate aminotransferase
SPCAs	Secretory pathway Ca2+/Mn2+-ATPases
SPoCK	Secretory Pathway Calcium ATPase
THP	Tamm–Horsfall glycoproteins
Tm	Melting temperature
TRP	Transient receptor potential
UAS	Upstream activating sequence
UAT	Urate transporter
V-ATPase	Vacuolar-type H^+ -ATPase
WT	Wild type
Wtrw	Water witch
XDH	Xanthine dehydrogenase

Chapter 1 Introduction

1.1 Summary

Nephrolithiasis is a metabolic and biochemical disorder, with an increasing incidence (in the year 2000, an incidence of 1116 per 100,000 was reported for 18- to 64-year) and prevalence (5-10% globally), which has substantial economic impact associated with its medical costs and morbidity. Despite all these, our fundamental understanding of the pathogenesis, as well as their prevention and cure, remains rudimentary. Hence to overcome the issue, there is an urgent need to develop reliable animal models to study the aetiology of stone formation and to assess novel interventions. Here in this chapter, I describe various kinds of kidney stones, their formation mechanisms, and different organisms used for kidney stone studies for the discovery of novel genes involved in stones formation. Further, I describe the importance of *Drosophila melanogaster*, an emerging model for kidney stone disease research. I also explain the suitability of this model as a high throughput functional drug screening platform for different drugs to treat various human diseases. In summary, this chapter explains the importance of *Drosophila*, *Drosophila genetics* and opens the valid reason for using Drosophila in the identification of the genetic basis of kidney stone disease.

1.2 Human Genetic Diseases

Human genetic diseases are categorised based on the observed inheritance of traits in offspring. Pedigrees charting the inheritance of traits within a family tree help to conceptualise a novel means for the transmission of disease susceptibility via heritable or genetic factors (Acheson et al., 2000). The heritability of a wide range of traits and diseases has been explored through family-based studies that looked at phenotypic heritability between related individuals who consequently were less genetically heterogeneous compared to the general population (Fischer, 2007).

Genetic disorders are traditionally classified into three main groups: a single gene involved disorders (Monogenic), multiple genes involved multifactorial disorders (Polygenic) and chromosomal disorders (Mahdieh and Rabbani, 2013).

1.2.1 Monogenic disorders

Monogenic Disorders (MDs) are the conditions caused due to mutation of a single gene. Several studies have identified approximately 10,000 types of monogenic disorders (Jimenez-Sanchez et al., 2001). Though these diseases are relatively rare, they affect millions of people globally. The symptoms and nature of the disease caused due to these disorders depend on the functions performed by the modified gene. Hence, once the gene gets modified, it causes a disorder which is rare and mostly unpredictable. These conditions are most common in the underdeveloped countries, more specifically in the rural areas where consanguineous marriage is common, e.g. Sickle cell anaemia, Huntington's disease, Fragile X syndrome. Pedigree analyses of large families with many affected members are very useful for determining the inheritance pattern of single-gene diseases. These disorders run in the families and can be dominant or recessive and autosomal or sex-linked (Chial, 2008).

Human has two sets or copies of each gene which is also known as “allele”; one copy on each side of the chromosome pair. Mutation or damage in this allele causes monogenic disorders.

a. **Dominant diseases are monogenic disorders that** involve damage to only one gene copy. As this mutation is carried on an autosome, both males and females are equally affected. Because this inheritance pattern is dominant, the chance of it being passed on during pregnancy is 50% for each pregnancy. If the faulty gene is inherited, it will result in an affected individual. This disease includes severe and most common genetic disorders like Huntington’s disease, polycystic kidney disease.

b. **Recessive or minor unexpressed disorder are monogenic disorders that damage to** both copies or allele. Usually, in these cases, the parents are carriers of the mutated gene. The risk of an affected child being born is 25% for each pregnancy, e.g. Tay Sachs disease.

c. **The X-linked disorder** is monogenic disorders which can be either be dominant or recessive. The mutation in the X-chromosomal gene of the sex chromosomes leads to numerous disorders which are said to be X-Linked Disorders. Usually, the mother carries the affected gene on the X chromosome. Hence females are careers and that usually only males are affected by the disorder e.g. Fragile X syndrome.

1.2.2 Polygenic disorders

Polygenic disorders are caused by the joint contribution of several independently functioning or interacting polymorphic genes, accompanied by non-genetic factors like lifestyle and environmental factors. These disorders are often clustered within the families, but they do not have a clear pattern of inheritance; hence the individual contribution of each gene may be small or even unnoticeable (Lvovs et al., 2012). The carriage of a specific combination of genes determines the occurrence of clinically heterogeneous forms of the disease, thereby simplifying the efficacy of treatment. On a pedigree, polygenic diseases tend to "run in families", but the inheritance does not fit simple patterns with Mendelian diseases. In humans, polygenic disorders are more frequent than monogenic disorders; hence, it has an adverse impact on social and economic aspects. Polygenic disorders cause various diseases like asthma, autoimmune diseases such as multiple sclerosis, cancers, cleft palate, diabetes, heart disease and hypertension (Lvovs et al., 2012, Mitchell, 2012, Curtis et al., 2001).

1.2.3 Chromosomal disorders

Chromosomal disorders result due to change in the number or structure of the chromosomes. The number of chromosome changes when there are either more or fewer copies of chromosomes. The change in the structure of the chromosome happens when the material in an individual chromosome is disrupted or rearranged (Eichenlaub-Ritter, 1996). The major causes of chromosomal disorders are described below.

1.2.3.1 Change in chromosome number

A normal human cell contains 46 chromosomes. Whenever there are fewer or more chromosome numbers in the baby, it causes genetic disorders. For example, Down syndrome is a condition caused because of an extra chromosome with three copies of chromosome 21 instead of two (Mahdieh and Rabbani, 2013).

1.2.3.2 Change in chromosome structure

Changes in the structure of the chromosomes occur when the material in an individual chromosome is broken or rearranged (Salem, 2016). It may involve addition or removal of the chromosomal material.

1.3 Inborn errors of metabolism (IEMs)

Metabolism is defined as the chemical processes that occur within a living organism to maintain life. Complications in metabolism can cause numerous human diseases. While most of them are the consequences of the diet and lifestyle (e.g., diabetes, obesity, atherosclerosis), there is a high proportion due to genetic mutations. Such disorders with a genetic base and which are also an outcome of failure in biochemical pathways are called inborn errors of metabolism (IEMs). IEMs occur if the enzyme(s) is missing or the enzyme function(s) is deficient. However, even if the enzyme/protein is present at an optimum concentration, the transport system might fail, or the regulation of the metabolic pathway may be disrupted, all of which are associated with IEMs (Dent and Philpot, 1954, Martins, 1999).

IEMs were first described by Sir Archibald Garrod, the British physician, in 1908, during the famous Croonian lectures on the inborn errors of metabolism, i.e., alkaptonuria, cystinuria, albinism and pentosuria (Scriver, 2008). Since then, the use of the word IEMs has been ever-expanding, and also named/known as inherited metabolic disorders, hereditary metabolic disorders, or congenital metabolic diseases. For simplicity, IEMs has been used throughout the thesis.

1.3.1 Classification of IEMs

IEMs are also classified based on the metabolic and molecular mechanism of inherited disease. On this basis, they can be mainly classified into two major categories: I and II.

a. Category I

IEMs affecting the functional as well the anatomical system such as endocrine system, immune system or coagulation factors or lipoproteins fall under this category. The indications of the majority of disorders are uniform, and hence, the correct diagnosis is usually easy because the basis of the biochemical defect incorporates the given consequence. For example, the tendency to bleed as a consequence of coagulation defects (Garrod and Harris, 1909).

b. Category II

This category includes the conditions in which the biochemical basis affects one metabolic pathway common to a significant number of cells or organs (e.g., problems in storage diseases due to lysosomal disorders), or is restricted to one organ with humoral and systemic consequences, such as hyperammonaemia in defects of the urea cycle or hypoglycaemia in hepatic glycogenesis (Martins, 1999).

1.3.2 Nephrolithiasis related to inborn metabolic diseases

Nephrolithiasis associated with inborn metabolic diseases is a rare condition which may occur with many kinds, but with common characteristics: early onset of symptoms, family history, associated tubular impairment, bilateral, multiple and recurrent stones, and association with nephrocalcinosis. The initial symptoms could be primary hyperoxaluria, cystinuria and the late symptom could be the occurrence of glycogen storage disorders. Such diseases may lead to life-threatening conditions, not only because of persistent kidney damage but also because of the progressive extra-renal factors involvement (Torres et al., 2007).

Furthermore, patients with other inborn metabolic diseases present only with recurrent stone formation, such as cystinuria, adenine phosphoribosyl-transferase deficiency, xanthine deficiency (Weinstein et al., 2001). Furthermore, nephrolithiasis may be the consequence of other metabolic diseases, such as glycogen storage disease type 1 or inborn errors of metabolism leading to Fanconi syndrome (nephropathic cystinosis, tyrosinemia type 1 (Cochat et al., 2010), fructose intolerance, Wilson's disease, respiratory chain disorders) as shown in **Table 1.1**. Furthermore, urine supersaturation may be related to the biochemical defect itself (oxalate, cysteine) or a secondary disorder (urate, citrate).

Nephrolithiasis due to the metabolic defect itself	Nephrolithiasis due to the secondary metabolic effect
1. Nephrolithiasis is usually an initial/early symptom 2. Primary hyperoxaluria types 1 and 2 3. Cystinuria 4. Disorders of purine and pyrimidine metabolism, e.g. Xanthinuria	1. Nephrolithiasis occurs during the evolution 2. Glycogen storage disease type 1 3. Treatment of secondary Fanconi syndrome

Table 1.1. Nephrolithiasis associated with inborn metabolic diseases due to presentation and pathophysiology. Adapted from (Cochat et al., 2010).

1.4 Kidney stones

1.4.1 Overview

Kidney stones, also known as renal calculi (singular calculus) or nephrolithiasis, is the most common kidney disease and known risk factor of chronic kidney diseases (Moe, 2006). These unwanted mineral aggregations can result in extreme pain, morbidity, and is often related to other chronic diseases such as high blood pressure, coronary artery disease and diabetes mellitus. This

condition has afflicted humans for centuries, affecting populations of every region, race, culture, gender and age (López and Hoppe, 2010). So far, precise mechanisms behind the stone formation and pathophysiology behind it have been largely unknown. Nephrolithiasis is often misunderstood as Urolithiasis. However, they have some difference; urolithiasis refers to stones originating anywhere in the urinary system, including the kidneys and bladder. However, nephrolithiasis refers to the presence of such stones in the kidneys.

Kidney stones are one of the most painful medical conditions to afflict human beings, with an approximate incidence of 1116 per 100,000 per 16-64-year-old persons in the USA in 2000 (Romero et al., 2010). It is a common problem worldwide with a marked increase in prevalence (12% of the world population) and recurrence rate (Alelign and Petros, 2018). After an initial stone, there is a 50% chance of forming a second stone within seven years (Sutherland et al., 1985). Numerous epidemiologic studies suggest that the prevalence of stone disease over the last 35 years has increased dramatically (3.8% in the late 1970s to 8.8% in the late 2000s) (Curhan, 2007). Importantly, it affects mainly productive young individuals, with a peak incidence in the third and fourth decades of life. Interestingly, the gender distribution among these patients, which initially was reported to have a ratio of three to one male to female predominance, has now been reported to be moving closer to parity (Romero et al., 2010).

A kidney stone begins as a little precipitate to form a nidus which subsequently grows to a stone. They are a crystal aggregation formed in the kidney (renal pelvis) from dietary minerals in the urine. The physical process of stone formation is a complex cascade of events. It begins with urine that becomes supersaturated with stone-forming salts (e.g., calcium, oxalate, uric acid, magnesium, phosphate) resulting in their precipitation out of solution to form crystals (Shafiee Jr, 2012). The aetiology of the first precipitation is heterogeneous (Ratkalkar and Kleinman, 2011). A detachment of the stone from the tissue will cause it to travel through the urinary tract, thereby showing initial symptoms of kidney stones or injury.

The pathogenesis of kidney stone is complex and diverse and include an understanding of how genetic and non-genetic risk factors act singly or in

concert to trigger stone formation. Recent studies have reported a significant percentage of adult kidney stone patients identified due to the monogenic causes (cystinuria being the most prevalent i.e. about 1% of all stones and up to 7% of stones in children (Goldfarb, 2014). Perhaps this might be one of the primary reasons why research efforts to elucidate the pathophysiology of kidney stone formation has been severely hampered. It causes uncertainty in the identification of the genes involved in the formation of stones.

Therefore, this thesis explores the issues by performing basic research directed at model systems (*Drosophila*) that elucidate the pathophysiology of stone disease in combination with clinical research in order to advance the field and, ultimately, leading to the development of new therapeutic approaches that have the potential to reduce the morbidity, mortality, and cost associated with the disease. Furthermore, the thesis also encompasses investigation about the different genetic disorders that cause kidney stones and focuses on the importance of understanding the role of genes on kidney stones development.

1.4.2 Causes of Kidney Stones

Kidney stone disease is widespread, with a lifetime incidence estimated at 1% to 15% (Campbell et al., 2007, Halbritter et al., 2015). Stones are formed due to the various etiological factors which result in various dysfunction or damage to the function of the kidney. The probability of developing kidney stones varies with numerous factors including age, gender, race, geographic location and body mass index (Stamatelou et al., 2003). Several studies support an increased incidence of the stone disease to be influenced by dietary habits and lifestyle, predominantly decrease in consumption of green vegetables and an increase in the consumption of animal proteins (Turney et al., 2012). The significant risk factors can be divided into two major categories: urinary risk factors and pre-urinary risk factors.

1.4.2.1 Urinary risk factors

Some urinary factors have been suggested as the major risk factors for renal stones formation. Disease conditions such as hypercalciuria, hyperoxaluria, hyperuricosuria and hypocitraturia, have been associated with urinary risk

factors. Change in the urine due to the below-mentioned factors is believed to influence stone formation.

a. Urinary salt concentration

Urinary salt concentration plays a critical process in kidney stones formation (detail in section 1.4.4). In normal conditions, various forms of urinary salts such as calcium oxalate, uric acid stones, cystine or xanthine dissolve in urine and are excreted. With an increase in the number of crystals, the excretion of the urine decreases significantly, thereby reaching the supersaturation point favouring the precipitating and formation of the crystals.

In vitro studies have shown that oxalate, either in crystalline or insoluble form is responsible for the formation of the crystals. Activation of the cytosolic phospholipase A2 plays a vital role in oxalate actions, thereby triggering the signalling cascade and mediating the crystal attachment (Yoo et al., 2001). Similarly, increased production of the reactive oxygen species (ROS) also triggers the formation of crystals. ROS causes an increment in cell death and induction of genes involved in cell survival, some of which may also promote proliferation for the replacement of damaged cells or may promote the secretion of urinary macromolecules that serve to modulate crystals formation (Nita and Grzybowski, 2016). Additionally, it was also found that calcium oxalate monohydrate gets precipitated at membrane lipid rafts (Backov et al., 2000).

b. Urinary volume

Urinary volume is one of the most critical factors for crystallisation. When the urine volume increases, it dilutes the crystallisation phenomena, thereby decreasing the oxalate load to calcium and phosphate, which finally reduces the number of accumulated crystals (Borghi et al., 1999).

c. Urinary pH

Urinary pH plays an essential role in uric acid stone formation. Uric acid is frequent in patients with urine pH below 5.5. It is very insoluble in urine at pH 5 but becomes significantly more soluble in urine at pH 7. Any combination of low

urinary pH concentrated urine and increased uric acid excretion make one at risk for the uric acid stone disease. In some patients, this very low urine pH is caused by a defect in renal ammonia secretion that results in less buffering of secreted hydrogen ion and low urine pH (Alelign and Petros, 2018).

d. Enzymes in urine

The initial step in the pathogenesis of kidney stones formation is the precipitation of an organic matrix of mucoprotein (detail 1.4.4). An essential factor in this process may be the activity and/or concentration of the urinary enzyme urokinase, which would affect the level of urinary mucoprotein. A decrease has been observed in urinary urokinase concentration of renal stones patients, which again underlines the possible involvement of urokinase in renal stone formation (Du Toit et al., 1997).

1.4.2.2 Pre-urinary factors

These factors could be both intrinsic and extrinsic in nature. Intrinsic factors include hereditary, age and sex. While, extrinsic factors include geographical location, climatic factors, dietary factors and total water intake.

a. Age

Idiopathic kidney stones are relatively uncommon before the age of 20, but the rate increases rapidly (10.6% of men and 18.4% of women) until the age of 40-60 years and then declines after the age of 65 and beyond (Romero et al., 2010, Marshall et al., 1975, Lieske et al., 2014). Further details are in **Chapter 4**.

b. Gender

Typically, men are more susceptible to kidney stone formation as compared to females. The inhibition of calcium oxalate crystal growth is influenced by a combination of both gender and sex. With age vigorous ability to inhibit crystallisation is reduced (Krambeck et al., 2013, Lieske et al., 2014, Soucie et al., 1994). Urinary citrate and magnesium excretion are lower, and glycosaminoglycan and zinc excretion are higher in men as compared to women. Furthermore, the citrate creatinine excretion ratio is significantly higher in

women, which may explain the lower incidence of calcium stones in women compared to men. Details about the influence of age and gender in kidney stone formation are in **Chapter 4.**

c. Race

Interestingly, Caucasian people are more susceptible to kidney stones occurrence as compared to the African descents and mixed-race people together. (Denstedt and Fuller, 2012). According to Reyes et al., there is a racial difference in electrolyte excretion related to lithogenesis such as sodium and magnesium (Akoudad et al., 2010, Reyes et al., 2002). Idiopathic kidney stones are more common in Caucasians as compared to African Americans regardless of the geographical location of residence, e.g. 5.9% vs 1.7% in the US. The difference is not maintained when dietary habits and environmental factors are the same. There was a significant increase in the prevalence of urolithiasis in African Americans once they had adopted Caucasian dietary habits (López and Hoppe, 2010).

d. Geographical location

Kidney stone disease is highly prevalent in hot, arid, or dry climates such as in mountains, deserts, or tropical areas, as geographic variability tends to reflect environmental factors. Previously, it has been reported that warmer areas had higher stone prevalence in the US, British Isles, Scandinavian and Mediterranean countries, northern India and Pakistan, northern Australia, Central Europe, portions of the Malay peninsula, and China (Mente et al., 2007). Further details are in **Chapter 4**.

e. Genetics

25% of new patients with kidney stones have a family history (1st-degree relatives). However, there is a less known fact whether the risk of disease is due to the genetics alone or combination of genetics with other factors including environmental or socio-economic combinations. A positive family history of urolithiasis has been reported in 16-37% of patients who have formed kidney

stones, compared with 4-22% of healthy people with no history (Park et al., 2010).

Similarly, a study by Curhan et al. showed that family history and the risk of urolithiasis in a cohort of 37,999 male participants, with a follow-up of 8 years; 4873 (12.8%) had a family history of kidney stones, 2957 of which (7.8%) reported a personal history of kidney stones. Finally, the study confirmed that men who had urolithiasis are approximately three times more likely to report a family history of kidney stones (Curhan et al., 1997, Türk et al., 2010). Also, there are also intrinsic epidemiological factors, such as autosomal recessive syndromes, with increased susceptibility to stone formation (Martínez et al., 2007).

1.4.2.3 Primary hyperoxaluria

Primary hyperoxaluria (PH) instigates a broad spectrum of diseases, ranging from occasional stone passage to systemic oxalosis in infants. Two distinct inherited enzyme defects have been related to primary hyperoxaluria. On this basis, they are divided into two major categories: PH1, a condition which is a defect in enzyme alanine: glyoxylate aminotransferase (AGT) and PH2 which is a defect in enzyme glyoxylate reductase/hydroxy-pyruvate reductase (GR/HPR).

PH1 is an autosomal recessive disorder (~1:120,000 live births per year in Europe), caused by the functional defect of the hepatic, peroxisomal, pyridoxal phosphate-dependent enzyme AGT. This condition leads to oxalate overproduction; the disease occurs because AGT activity is either absent or mistargeted to the mitochondria (Cochat et al., 1995). Similarly, PH2 has been documented in fewer cases; and in this condition, glyoxylate and hydroxypyruvate are metabolised by lactate dehydrogenase to oxalate and l-glycerate, respectively (Rumsby et al., 2001). Further details are in **chapter 3.**

1.4.2.4 Inborn errors of amino acid metabolism

Inborn errors of metabolism which can be detected by the accumulation of specific amino acids as metabolites in body fluids like serum and urine are inborn errors of amino acid metabolism. Amino acid metabolism uses active trans-tubular transport, which is usually associated with active sodium transport;

such tubular transport may be specific to either one single amino acid (e.g. glycine, histidine) or a group of amino acids (e.g. cysteine, lysine, ornithine and arginine) (Schmidt-Nielsen and Sands, 2001).

a. Fanconi syndrome

Hyperaminoaciduria (mainly histidine, glycine, serine, alanine and glutamine) is a marker of proximal tubular dysfunction together with variable increased urinary excretion of glucose, phosphate, bicarbonate, potassium, calcium, uric acid, carnitine, etc. Such Fanconi syndrome may either be primary (idiopathic primary Fanconi syndrome), or it may occur secondarily to various inherited metabolic disorders, i.e. cystinosis (cystinosin), tyrosinemia type 1 (fumarylacetoacetate hydrolase), fructose intolerance (fructose 1,6-bisphosphate aldolase), Wilson's disease (copper-transporting P-type ATPase, *ATP7B* gene), glycogen storage disease type 1 (glucose-6-phosphatase), respiratory chain disorders, Fanconi–Bickel syndrome (GLUT-2), lysinuric protein intolerance (y+LAT1 protein encoded by *SLC7A7* gene), etc (Wilson et al., 1983).

b. Cystinuria

Cystinuria is an autosomal recessive inherited aminoaciduria that leads to recurrent nephrolithiasis with a prevalence between 1 in 2,500 and 1 in 100,000. Cystine represents 4–8 % of all renal stones in children in France (Daudon and Jungers, 2004). The solubility of these stones is pH-dependent, with a modest increase if pH rises to 7·5, and a steeper increase with a pH above 7·5. However, the solubility of these stones also depends on the urinary pH, owing to the solubilising action of electrolytes and macromolecules. With a urine pH<7, cystine solubility is generally exceeded when the urinary cystine concentration is higher than 250 mg/L. In Type I cystinuria, mutations in the gene for the dibasic amino acid transporter (*SLC3A1*) have been uncovered. The molecular defects in Type II and III cystinuria have not yet been determined (Daudon et al., 2003).

1.4.2.5 Inborn errors of purine and pyrimidine metabolism

Inborn errors of purine and pyrimidine metabolism are often associated with nephrolithiasis of various composition and pathophysiology. They represent 1–3%

of renal stones in children in France (Daudon and Jungers, 2004). All these calculi are primarily radiolucent, but they can be identified by ultrasound, which usually does not show any nephrocalcinosis. Some of the common disorders under this group are:

a. Phosphoribosylpyrophosphate synthetase superactivity

Phosphoribosylpyrophosphate (PRPP) synthetase superactivity is an inborn error linked to X-linked inheritance. The disease usually shows in young male patients with gouty arthritis and uric acid nephrolithiasis, sometimes leading to early-stage renal disease (ESRD). Under abnormal conditions plasma uric acid may reach maximum up to 600–900 μmol/l (average adult values 170–320 μmol/l), and urine uric acid concentration might increase so that the urinary uric acid to creatinine ratio approaches 2.5 mmol/mmol (average adult values 0.2–0.3 mmol/mmol). The condition mentioned above may appear during infancy, together with neurological abnormalities, i.e. sensorineural deafness, hypotonia, motor delay, ataxia and autistic features (Becker et al., 1988).

b. Hypoxanthine-guanine phosphoribosyltransferase deficiency: Lesch–Nyhan syndrome

Deficiency of hypoxanthine-guanine phosphoribosyltransferase (HGPRT) activity is an inborn error of purine metabolism associated with uric acid overproduction and various degrees of neurological disorders, depending on the amount of enzyme deficiency. The prevalence is estimated at 1 in 380,000 live births in Canada and 1 in 235,000 in Spain (Torres et al., 2007).

c. Adenine phosphoribosyltransferase deficiency

The deficiency may lead to clinical manifestations in early childhood, but it can also remain silent for decades. Symptoms include the passage of crystals, gravel, and stones. Such nephrolithiasis is responsible for abdominal colic, dysuria, haematuria, urinary tract infection, and, sometimes, acute anuric renal failure (Di Pietro et al., 2007).

d. Xanthine-Oxidase deficiency

Two deficiencies of xanthine oxidase (or dehydrogenase) are known: isolated hereditary xanthinuria (type 1, with nephrolithiasis) and combined xanthine oxidase and sulphite oxidase deficiency (type 2, with prominent neurological involvement). Isolated xanthine oxidase deficiency can be asymptomatic, but one-third of affected patients suffer from kidney stones. Xanthine stones are not visible on X-ray and may appear at any age. Studies have shown that some patients with myopathy are also associated with crystalline xanthine deposits (Ichida et al., 1997).

e. Hereditary renal hypouricemia

Familial renal hypouricemia is a sporadic disease caused by mutations in the *SLC22A12* gene. The disease condition is caused by a defect in the tubular reabsorption of urate.

1.4.3 Epidemiology of Kidney stones

Globally, the prevalence and recurrence rate of kidney stone disease is increasing (3.25% in the 1980s and 5.64% in the 1990s), with limited options for effective drugs (Campbell et al., 2007). It affects about 12% of the world population at some stage in their lifetime (Chauhan et al., 2009). The prevalence of kidney stones varies with age, sex, and race but occurs more frequently in men than in women within the age of 20–60 years, exceeding 12% in men and 6% in women (Moe, 2006, Romero et al., 2010, Edvardsson et al., 2013). Recent studies have reported that the prevalence of kidney stones has been increasing in the past decades in both developed and developing countries (**Figure 1.1)**. This growing trend is believed to be associated with a change in lifestyles such as lack of physical activity, exercise, dietary habits and global warming (Moe, 2006, Alelign and Petros, 2018).

In England, in between 2009-2010, there were over 83,000 recorded hospital episodes due to kidney stones (Turney et al., 2012). The data represents a 63% increase over the previous 10 years and an 11% calculated lifetime risk of forming a stone. In the US, kidney stone affects 1 in 11 people (Scales Jr et al.,

2012), and it is estimated that 600,000 Americans suffer from urinary stones every year (Kovshilovskaya et al., 2012). Furthermore, the US nationwide occurrence and prevalence of kidney stone were investigated in two major studies. The first study, which was carried for two periods in between 1976 to 1980 and second from 1988 to 1994, revealed that the prevalence of kidney stones increased from 3.8 % ± 0.21% in the first period to 5.2 % ± 0.34% in the second (Romero et al., 2010). Apart from six states, there was an average of 41% increase in urinary stone rates. Also, assuming 50 years of exposure, 12% of the total US population will experience kidney stones at some point in their lifetime **Figure 1.1.**

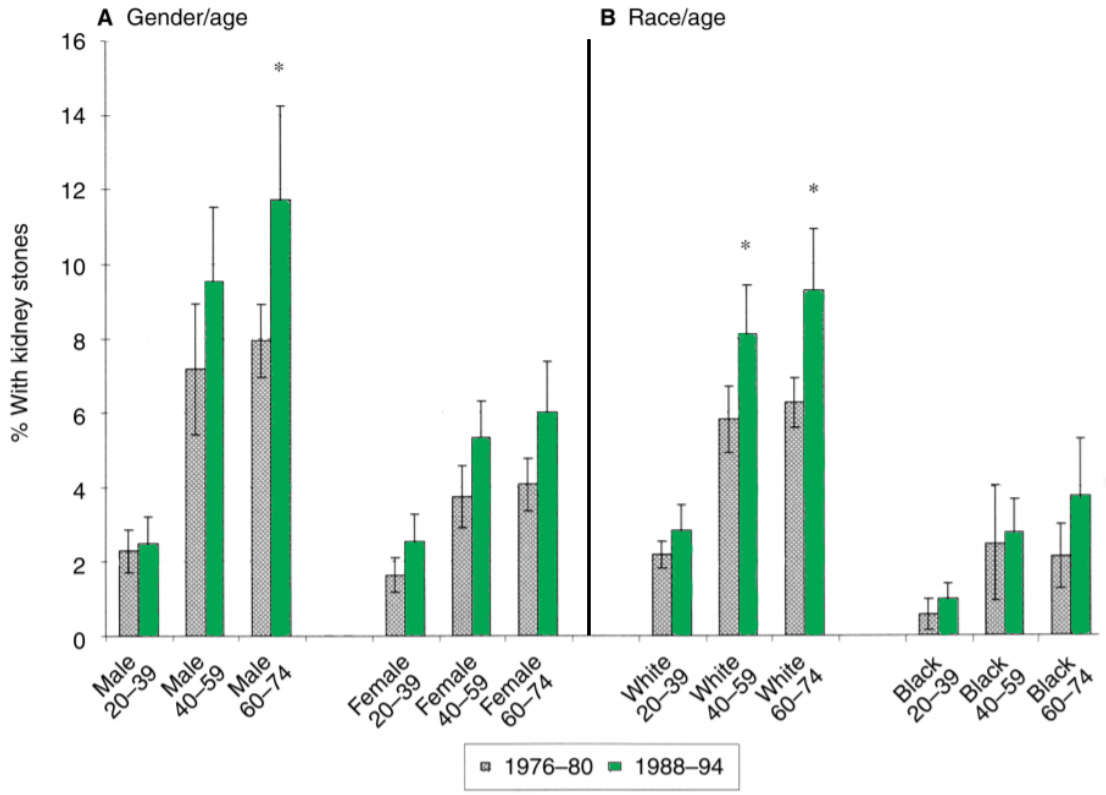

Figure 1.1. Percentage prevalence of a history of kidney stones in the US for two different time frames; 1976 to 1980 and 1988 to 1994 in each age group for (A) Gender and (B) race group. Reproduced with permission from (Stamatelou et al., 2003).

Furthermore, the study showed that the prevalence was gender and age-dependent. Men were more prone to the disease compared to females. Similarly, regular kidney stone occurrence was observed with increasing age, up to the age of 70 for men and 60 years of age for women (Stamatelou et al., 2003). For both genders, age groups between 20 and 39 years were the least affected. A similar

trend was also observed in other countries in the world, such as Argentina, Brazil, Canada, Germany, United Kingdom, Italy, Sweden, Turkey, Japan, and South Africa. The detail is described in **section 1.4.2**.

In the US and during the period between 1988 and 1994, non-Hispanic Caucasians (5.9 %± 0.43%) were more affected by kidney stones compared to Mexican Americans (2.6 %± 0.19%) or non-Hispanic African Americans (1.7 %± 0.16%) (Stamatelou et al., 2003). Asian Americans also had lower kidney stone incidence than White Americans. The variation in kidney stone prevalence among the different races was attributed to lifestyle factors such as dietary habits and socioeconomic differences of the study subjects. The lower occurrence of kidney stones in the African American community in the US or other countries such as South Africa is due to (1) lower serum and urinary calcium levels because of lower intake and absorption of calcium (Sorensen, 2014), (2) higher carbohydrate intake resulting in higher urine volume (Reddy et al., 2002), and (3) higher liver damage in this group which fails to metabolise circulating oestrogens resulting in increased urinary citrate excretion (Kovacs, 2000).

Early reports suggest that if kidney stones are left untreated, the likelihood of forming another stone after the initial episode averages 30 to 40% at 5 years (Johnson et al., 1979), for all stone types. These figures from observational studies are similar to the recurrence rates in the control samples of published randomised trials (Ettinger et al., 1986, Resnick et al., 1968). Encouragingly, the treatment arms of many of the randomised trials have shown dramatic reductions in recurrence rates by 50% or more. These reductions by medication or dietary interventions emphasise that recurrent stone disease may be preventable. In this regard, recurrence rates of 50% after 10 years and 75% after 20 years has been reported.

1.4.4 Mechanism of stone formation

The mechanism of kidney stone formation is a complex process which remains incompletely understood. It is a biochemical sequence that is the consequence of an increase in urinary supersaturation due to excess of crystalline particles and low urinary volume. Supersaturation leads to the formation of the crystals

which further form a concretion beyond which there is no further dissolution. When the concentration of two ions exceeds their saturation point in the solution crystallisation occurs. Although all types of stones share a similar mechanism of formation, the sequence of events leading to their formation differs depending on the type of stones, urinary pH and urine chemistry. For instance, crystallisation of calcium-based stones (calcium oxalate or calcium phosphate) occurs in supersaturated urine with low concentrations of inhibitors (Ratkalkar and Kleinman, 2011).

The transformation of a liquid to a solid phase is influenced by pH and solubility of the substances. If more salt is added, it crystallises in solution, provided the temperature and pH remains unchanged (Ratkalkar and Kleinman, 2011). The concentration at which saturation is attained and crystallisation begins are called the thermodynamic solubility product (Ksp). Thus, the crystallisation process depends on Ksp and kinetics of a supersaturated solution. Hence, prevention of supersaturation can decrease the formation of the stones (Alelign and Petros, 2018). Additionally, stone formation depends on the imbalance between urinary stone promoters and inhibitors (Evan et al., 2015). If the concentration of inhibitors of crystallisation, becomes low, then it results in nephrolithiasis.

The schematic diagram for Kidney stone formation is represented in **Figure 1.2**. The detailed process is explained below:

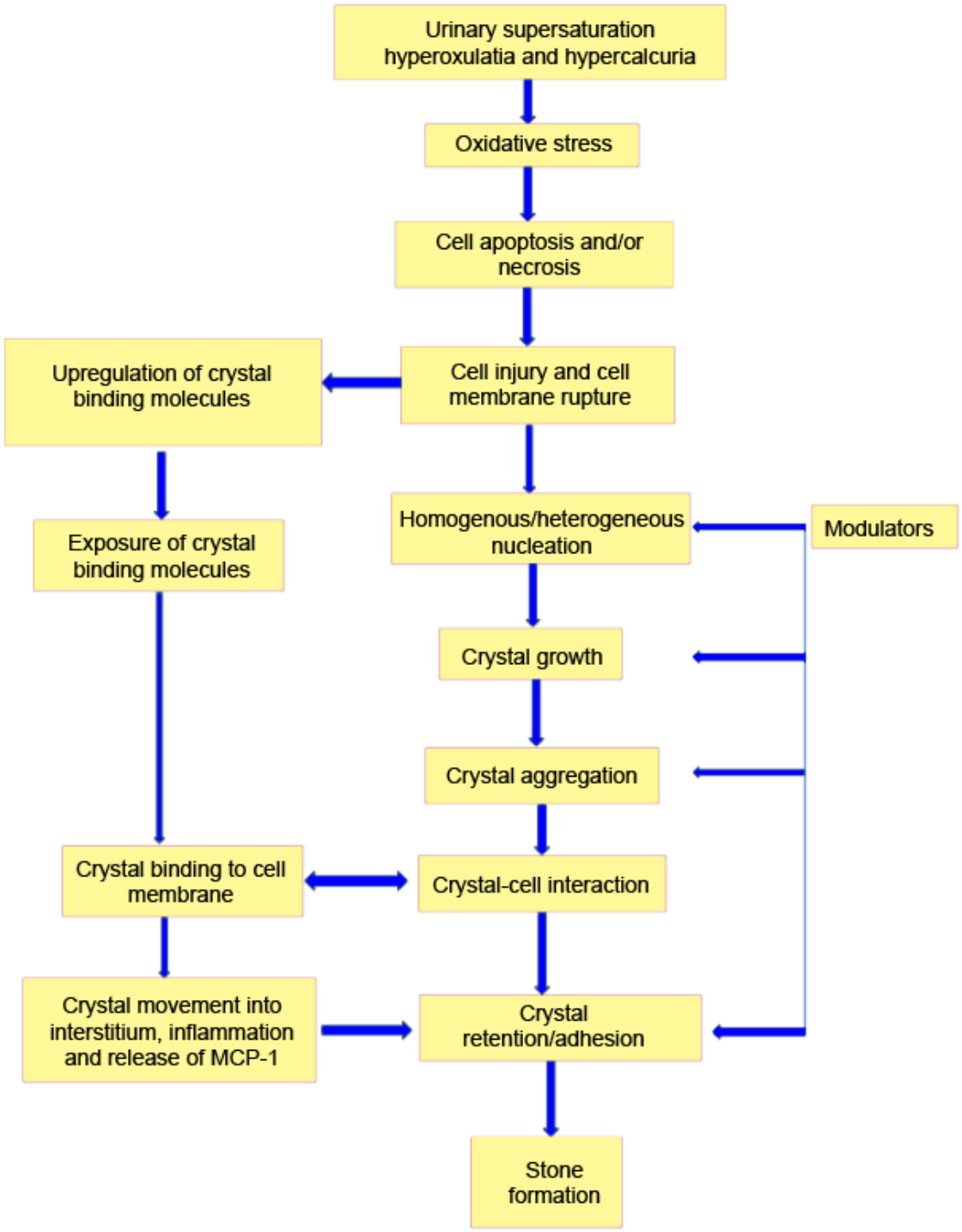

Figure 1.2. Schematic representation of various cellular and extracellular events during stone formation. *(OPN: osteopontin, HA: hyaluronic acid, SA: sialic acid, MCP-1: monocyte chemoattractant protein-1). Adapted from (Aggarwal et al., 2013).

1.4.4.1 Nucleation:

It is an early step for the formation of the solid crystals from liquid forms. It begins with the combination of stones and salts into clusters forming a nucleus (termed as nidus) which gradually increases in size, thereby forming new

components or clusters. Nuclei form the first crystals in the characteristic lattice pattern by heterogeneous nucleation (Alelign and Petros, 2018). Once the nucleus is created, crystallisation can occur at lower chemical pressure for the formation of the initial nucleus.

Epithelial cells, urinary casts, RBCs, and other crystals can act as binding agents by increasing heterogeneous nucleation and crystal aggregation (Alelign and Petros, 2018). On the other hand, nanobacteria form apatite structures serving as a crystallisation centre for stone formation. Furthermore, renal tubular cell injury also promotes crystallisation of CaOx crystals, thereby providing substances for their heterogeneous nucleation. *In vitro* cell degradation following renal tubular cell, injury produces numerous membrane vesicles, which are good nucleators of calcium crystals. *In vivo* crystals observed in the renal tubules of hyperoxaluric rats are always associated with cellular degradation products (Tsujihata, 2008).

1.4.4.2 Growth

Once a crystal nucleus has achieved a critical size, and relative supersaturation remains above one, the overall free energy is decreased by adding new crystal components to the nucleus. This process is called crystal growth. The process of stone growth is a slow and long-lasting process. It was reported that the crystal surface binding substance, which is found in CaOx crystals generated from whole human urine, is a potent inhibitor of CaOx crystal growth and contains proteins mainly the Tamm–Horsfall glycoprotein, also known as uromodulin, and osteopontin also known as bone sialoprotein I (Aggarwal et al., 2013). Under *in vitro* study, crystals induced in human urine demonstrated an intimate association between calcium-containing crystals and organic matrix (lipids and proteins) (Basavaraj et al., 2007).

1.4.4.3 Aggregation

This is the most crucial step in stone formation in which all the crystals within the solution stick together to form a more massive particle. This process is slow because the crystals are small, and it takes a long time to obstruct the renal

tubules and show its impact; hence, this process is thought to be the most critical step.

1.4.4.4 Crystal-cell interaction

This is the complex and unexplored step of stone formation. In this step, there is an attachment of the grown crystals with the renal tubule lining of epithelial cells due to crystal retention or crystal-cell interaction. These structural and functional studies of crystal-cell interactions indicate that calcium oxalate monohydrate (COM) crystals rapidly adhere to microvilli on the cell surface and are subsequently internalised. Khan et al. concluded that crystal-cell interaction is an essential element in the development of urinary stone disease (Khan et al., 1999).

In hyperoxaluric patients, renal tubular epithelial cells are injured due to exposure to high oxalate concentrations or sharp COM crystals. Crystal-cell interaction results in the movement of crystals from the basolateral side of cells to the basement membrane. Further, crystals could be taken into cells and anchored to the basement membrane of the kidneys. The interaction of COM crystals with the surface of renal epithelial cells could be a critical initiating event in nephrolithiasis. An increased retention force between the crystal and injured renal tubule epithelial cells promotes CaOx crystallisation. Most of the crystals attached to epithelial cells are thought to be digested by macrophages and/or lysosomes inside cells and then discharged with the urine. A role for crystal uptake in renal stone disease is disputed because intracellular crystals seldom are observed in the kidney and in cell culture, crystals are taken up by proximal tubular cells where crystals are expected to be formed (*e.g.*, the distal tubule, collecting ducts). Studies by Kok and Khan observed crystal attachment to the brush border of proximal tubules in rats (Khan et al., 1999). Experimental induction of CaOx urolithiasis starts with hyperoxaluria followed by crystalluria and deposition in the kidney.

1.4.4.5 Infection stones

During the infection of the urinary tract with urea-splitting organisms (*Proteus sp., Haemophilus sp., Ureaplasma urealyticum, Klebsiella sp.*), the hydrolysis of

urea yields ammonium and hydroxyl ions (Sakhaee et al., 2012), which further results in infection stones formation. The consequent alkaline pH of the urine increases the dissociation of phosphate to form trivalent phosphate, and there is supersaturation of struvite (magnesium ammonium phosphate) and carbonate apatite.

1.4.4.6 Endocytosis of CaOx Crystals

Endocytosis or engulfment of crystals by renal tubular cells is the initial process in the formation of kidney stones. Studies by Lieske noted that engulfment of crystals into tubular epithelial cells and cell proliferation in a transplanted kidney in a patient with PH1 indicated that COM crystals rapidly adhere to microvilli on the cell surface and subsequently internalised (Lieske et al., 1992). Further, they also confirmed this phenomenon experimentally using calcium-containing crystals and tubular cells in culture. Various substances inhibit the effect on CaOx endocytosis in tubular fluid/urine such as glycosaminoglycans, glycoproteins, and citrate may coat crystals and inhibit the binding of COM crystals to the cell membrane. Tamm–Horsfall glycoproteins (THP) leads to a decrease in COM endocytosis by 34%, suggesting that it promotes renal stone formation by interaction with COM crystals with distal tubular cells. Further, the inhibitory effect of fibronectin (FN) on CaOx crystal endocytosis was only 18.4% at the physiological concentration of excreted FN (0.5 mg/mL), though morphological examination revealed that FN inhibited the endocytosis of crystals by renal tubular cells (Tsujihata, 2008).

1.4.4.7 Randall's Plaques

Randall's plaques appear to be the precursor to the origin of renal stone. However, the pathogenesis of Randall's plaque itself is not precisely known (Ettinger et al., 1986). The majority of CaOx stones are found to be attached with renal papillae at the sites of Randall's plaque (Lieske et al., 2014). It is located at the interstitial basolateral membrane in the loop of Henle (Evan et al., 2003, Evan et al., 2006). Calcium phosphate (apatite), and purine crystal compositions were identified in plaques, whereas the quantity of apatite is dominant (Daudon et al., 2015). Initially, calcium phosphate crystals and organic matrix are deposited along the basement membranes of the thin loops of Henle

and extend further into the interstitial space to the urothelium, constituting the so-called Randall's plaques. Evidence suggests that a primary interstitial apatite crystal also leads to CaOx stone formation (Knoll, 2010). In supersaturated urine, crystals adhere to the urothelium, which may enhance subsequent stone growth (Dawson and Tomson, 2012).

Due to renal cell injury, the plaque is exposed to supersaturated urine. Renal epithelial cell degradation product promotes heterogeneous nucleation and crystal adherence in renal cells. Randall's plaque calcification is triggered by oxidative stress. Cells may express molecules at distal and collecting tubules which act as crystal binding sites such as phosphatidylserine, CD44, osteopontin, and hyaluronan (Joseph et al., 2005, Yuen et al., 2010). Renal epithelial cells of the loop of Henle or collecting ducts produce membrane vesicles at the basal side, which leads to plaque formation (Khan, 2014). Thus, apatite crystal deposits have been proposed to act as a nidus for CaOx stone formation by attachment on further matrix molecules (Khan, 2014, Hayes, 2015). However, the driving forces in plaque formation and the involved matrix molecules remain elusive.

Kidney stones are either attached to the renal papillae or found freely (Kok and Khan, 1994). According to the fixed particle pathway, the beginning of CaP deposition in the interstitium establishes a nucleus for CaOx formation. CaP formed in the basement membrane of the loops of Henle, the inner medullary collecting ducts, and ducts of Bellini serves as an attachment site for stone development. Idiopathic stone formers develop CaOx attached to fixed sites of interstitial plaque. Stones of the distal tubular acidosis attach to plugs protruding from dilated ducts of Bellini, whereas cystinuria stones do not attach to the renal plagues (found freely)(Evan, 2010). CaP, uric acid, or cystine crystals formed in the renal tubules plug at the terminal collecting ducts. When mineralisation reaches the renal papillary surface, plaques rupture exposing CaP crystals to the pelvic urine. Then, urinary macromolecules deposit over the exposed CaP crystals and promote CaOx deposition on CaP.

1.4.5 Types of stones

There are different types of stones categorised based on their nature (physical and chemical) and percentage of occurrence **Figure 1.3**.

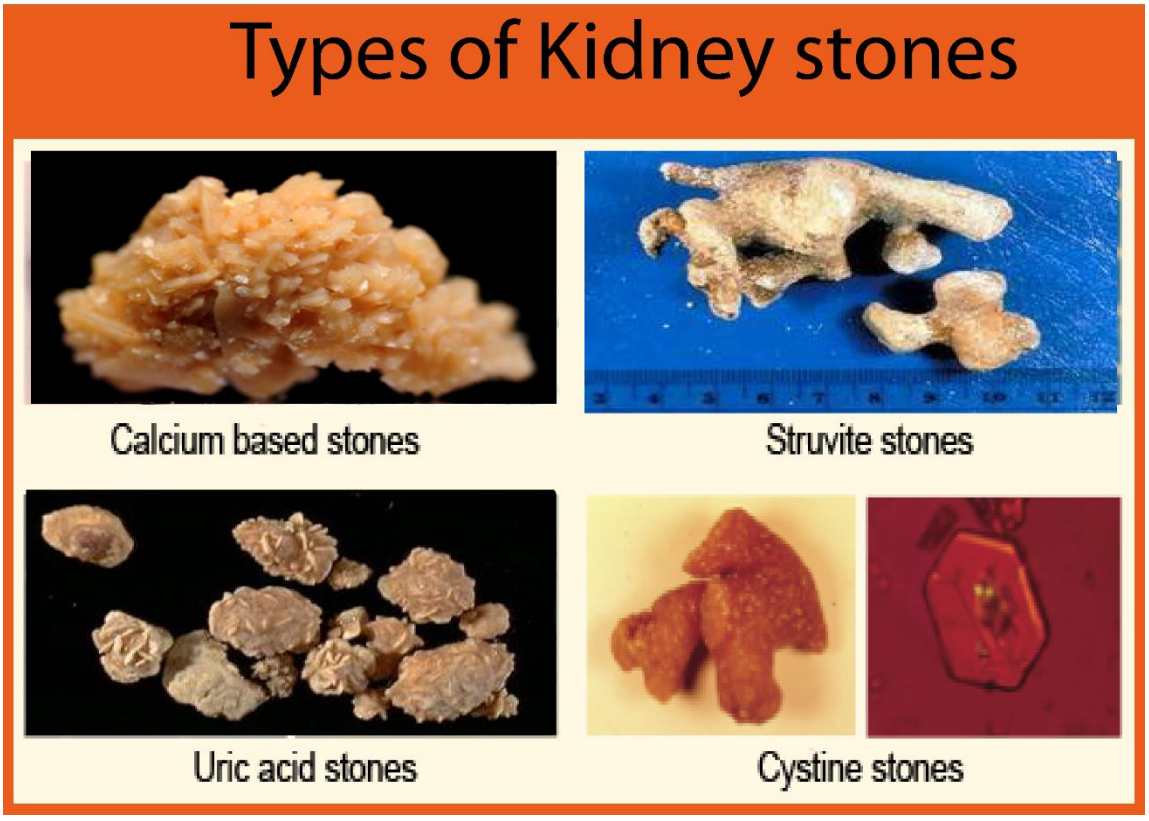

Figure 1.3. Some of the different types of kidney stones.

1.4.5.1 Calcium stones

Calcium stones in the form of oxalate or phosphate are the predominant form of renal stones comprising about 80% of the total urinary calculi (Coe et al., 2005), i.e. Calcium Oxalate (CaOx; 50%), calcium phosphate(CaP; 5%) and a mixture of both around 45% (Chaudhary et al., 2010). The primary constituent of the calcium stones is brushite (calcium hydrogen phosphate or hydroxyapatite). Calcium oxalate also exists in the different form of CaOx monohydrate (COM, termed as weddellite; $CaC_2O_4.H_2O$) and CaOx dihydrate (COD, weddellite, $CaC_2O_4{\cdot}2H_2O$), or as a combination of both, with the monohydrates accounting for more than 60% of total stones (Alelign and Petros, 2018). COM is the most

thermodynamically stable form of stone and is, therefore, more frequently observed than COD.

In the human body, many factors are responsible for calcium oxalate stone formation such as hypercalciuria, hyperuricosuria, hyperoxaluria, hypocitraturia, hypomagnesuria and hyper cystinuria (Dal Moro et al., 2005) (detailed in section 1.4.2.5). These stones are mostly dependent on urinary pH, i.e. urinary pH of 5.0 to 6.5 promotes CaOx stones, whereas CaP stones occur in pH greater than 7.5 (Dal Moro et al., 2005, Coe and Coe, 1983). The recurrence of calcium stones is higher than other types of stones.

1.4.5.2 Struvite or Magnesium Ammonium Phosphate Stones

Struvite stones often referred to as infection stones or triple phosphate stones; are the second most abundant (10-15%) stone types. These stones are most frequent among patients with a history of chronic urinary tract infections that produces an enzyme called urease. Urease is most commonly produced by *Proteus mirabilis*, and less common pathogens, including *Klebsiella pneumonia*, *Pseudomonas aeruginosa*, and *Enterobacter* (Barbas et al., 2002, Coe et al., 2005). However, *Escherichia coli* is bacteria not capable of splitting urea and is therefore not associated with the formation of struvite stones (Griffith, 1978, Dursun et al., 2015).

1.4.5.3 Uric acid stones of Urate

Uric acid stones are the third most common stones accounting 3-10% of total stones (Giannossi and Summa, 2012, Coe et al., 2005). These stones are frequent among patients eating high purine diets, especially those containing high protein diets such as meat and fish, which results in hyperuricosuria, low urine volume, and low urinary pH (pH<5.5) (Barbas et al., 2002, Coe et al., 1992). The most prevalent cause of uric acid stones is idiopathic, and these stones are more common in men compared to women. The detail in **Chapter 5**.

1.4.5.4 Cystine stones

These stones account for around 2% of the total kidney stones population and are triggered by a mutation in the transport of amino acid and cystine. These

stones cause cystinuria, an autosomal recessive disorder instigated due to a defective *SLC3A1* (*rBAT*) gene on chromosome 2, resulting in impaired renal tubular absorption of cystine or leaking cystine into the urine. These stones are not soluble in urine; hence patients with cystinuria excrete more than 100 millimoles insoluble cystine per day (Parmar, 2004, Scales Jr et al., 2012, Wells et al., 2012). The development of urinary cystine is the only diagnosis of the disease.

1.4.5.5 Drug-induced stones

These stones are the least common stones accounting for around 1% of the total occurrence rate. They are formed from the aggregation of lithogenic agents due to the side effects of drugs such as guaifenesin, triamterene, atazanavir, and sulfa-containing drugs. For instance, people who take the protease inhibitor indinavir sulphate, a drug used to treat HIV infection, are at risk of developing kidney stones. Such lithogenic drugs or/and its metabolites may deposit to form a nidus or on renal calculi already present. On the other hand, these drugs may induce the formation of calculi through its metabolic action by interfering with calcium oxalate or purine metabolisms (Daudon et al., 2018).

1.4.6 Kidney stone diagnosis and treatment

Significant advances were seen over the past three decades in the diagnosis and treatment of kidney stones. Helical computed tomography (CT) imaging and ultrasound coupled with X-ray, provide a powerful diagnostic tool. Relatively non-invasive techniques, such as shock wave lithotripsy (SWL), percutaneous nephrolithotomy (PNL), and ureteroscopy (URS) have eased the treatment of this disease. However, it remains challenging to visualise remaining kidney stone fragments after SWL, and hence, these remaining fragments can act as nidi, or sources of origins, for another episode of stone disease. Besides the aforementioned method, stone can be treated without operating it, called medical expulsive therapy (MET). MET is the use of pharmacologic agents to promote ureteral stone passage by relaxing ureteral smooth muscle. Both α-adrenergic blockers and calcium-channel blockers have been shown to increase the likelihood of spontaneous stone passage. However, a recent meta-analysis found that α-adrenergic blockers were superior to the calcium-channel blocker

nifedipine and as such may be the preferred agent for MET. MET is commonly utilised now in patients who undergo conservative/expectant management for ureteric stones.

1.5 Animal models for Kidney stones

Nephrolithiasis may also be associated with nephrocalcinosis, *i.e.*, crystal depositions in the tubular lumen, an entity which suggests specific pathological processes. Stones are common in obese and diabetic individuals.

Several animal models, including rodents' have been studied to understand the pathophysiology of intrarenal crystal formation (Tzou et al., 2016). Here in this part of the thesis, the benefits and limitations of different model organisms have been reviewed in preference to their uses in kidney stone studies.

1.5.1 Rat

Rat represents a well-established model for mimicking the urinary stones diseases. These models replicate two primary conditions (hypercalciuria and hyperoxaluria), like humans and play a vital role in the observation of the pathophysiological changes associated with these conditions.

1.5.1.1 Anatomic and physiological comparison of a rat with humans

The kidneys of rats are uni-papillary, but the kidneys of human are multi-papillary. Similarly, an average human has around 170 g of the kidney with around one million nephrons, but an average mouse has 0.75-1.3 g kidney with around 30,000 nephrons. Despite these gross differences, the cortex-medulla ratio (2:1) of the rat is similar to humans (Khan, 2013). Therefore, the mouse can be a good model for the following type of stone studies:

a. Hypercalciuria

Hypercalciuria is one of the most common risk factors for the development of urinary stone diseases (Coe et al., 1992, Bushinsky et al., 1995). Researchers have established a strain of multigeneration inbred Sprague-Dawley rats to produce hypercalciuric progeny (Bushinsky and Favus, 1988). Different studies

have shown that an increased number of vitamin D receptors in the GI tract, kidneys and bone leads to increased calcium absorption in rats (Li et al., 1993, Yao et al., 1998, Krieger et al., 1996).

b. Hyperoxaluria

This is a disease condition in which patients excrete an excessive amount of oxalate in urine. Individuals with hyperoxaluria often have calcium oxalate kidney stones. For the induction of kidney stones, different lithogenic agents causing oxalate stones need to be supplemented externally, for example, feeding rats with sodium oxalate, ethylene glycol (EG), glycolic acid and hydroxy L-Proline. The summary is inlisted in (**Table 1.2**). Administration of such agents causes physiological changes in rats and induces stones.

Type of approach	Lithogenic agent, reference	Diet/administration	Effects
Crossbreeding	Inbreeding hypercalciuric progeny (Bushinsky et al., 2000, Bushinsky et al., 2002)	• Multiple generation inbred • Multiple diets/agents applied	• Hypercalciuria • Hyperoxaluria • CaOx crystals • CaP crystals
Exogenous induction	Sodium oxalate (Khan et al., 1979, Khan et al., 1992, Khan and Hackett, 1993)	• Intraperitoneal injection of 10 mg/kg sodium oxalate	• Prompt CaOx crystal deposits • Crystal aggregation in the ducts of Bellini
	Glycolic acid (Ogawa et al., 1990)	• Free drinking of water with powdered 3% glycolic acid	• Hyperoxaluria • Hypocitraturia • CaOx crystal deposits
	Ethylene Glycol (EG) (Khan et al., 1992, Boeve et al., 1996, Thamilselvan et al., 1997)	• 0.75% EG in water with/without ammonium chloride, vitamin D, calcium chloride	• Hyperoxaluria • CaOx crystalluria • CaOx crystal deposits • Renal toxicity
	Hydroxy-L-proline (HLP) (Tawashi et al., 1980, Khan et al., 2006, Bushinsky et al., 2002)	• 0.75% EG in water with/without ammonium chloride, vitamin D, calcium chloride	• Hyperoxaluria • CaOx crystal deposits • Less toxic compared to other agents
Dietary manipulation	Potassium oxalate supplement (Wiessner et al., 2011)	• 5% level of potassium oxalate	• CaOx crystal deposits
	Magnesium (Mg) deficiency (Rushton and Spector, 1982)	• Dietary Mg deprivation	• Increase of CaP crystal deposits
	Vitamin B6 (pyridoxine) deficiency (Andrus et al., 1960, Gershoff and Andrus, 1961)	• Dietary intentional deficiency of pyridoxine	• Hyperoxaluria • Hypocitraturia • CaOx crystal deposits

Table 1.2. Rat models related to hypercalciuria and hyperoxaluria. Adapted from (Tzou et al., 2016).

c. Dietary Manipulation

An alternative method of induction of stone formation is an alteration of the diet by adding external components. Dahl salt-sensitive and Brown Norway male rats were fed with 5% of potassium oxalate in order to develop calcium oxalate stones (Wiessner et al., 2011). Meanwhile, hyperoxaluric rats deprived of dietary Mg demonstrated increased production of calcium phosphate (apatite) stones (Rushton and Spector, 1982). These methods of induction of kidney stones in rat help us to understand the underlying biological progress as well to access the pathophysiological changes in the body.

1.5.1.2 Limitations of a Rat model

As a vertebrate the rat requires ethical approval for performing experiments and the cost of rearing is also. (DiMasi et al., 2003). Rats are coprophagic (eat their own stool), and therefore consume unnecessary elements hence might not be relevant to compare with a human. Additionally, very few humans suffer from primary hyperoxaluria, which makes the study limited to few numbers practically.

1.5.2 Mouse

Beside rat models, the mouse is also a useful model organism for the prevention and treatment of kidney stones. Furthermore, the genetic and physiological complexities of the mouse are similar to human and can be used to observe the variation on the primary process underlying stones formation.

1.5.2.1 Genomic/anatomic/physiologic comparison between mice and humans

The respective genomes of mice and humans are similar as both genomes contain approximately 3.1 billion base pairs and are ~85%identical on average, with some greater than 95% identical. Mice generally weigh between 25 and 35 g, approximately 1/2500 the size of humans(Liebelt, 1998). However, the mean weight of mouse kidney comprises 0.8% of the total mouse weight whereas in human, it comprises 0.2% of body weight (Meneton et al., 2000, Sands and Layton, 2009). Meanwhile, maximal urine concentration of mice is around 3.3

times higher as compared to a human. Under microscopic examination, mouse kidneys have a distinct; cortex, medullary components, glomerular, tubular structure and vascular framework (Liebelt, 1998).

a. Hyperoxaluria

Hyperoxaluria is the most common risk factor for the development of urinary stone diseases. In mouse, hyperoxaluria is induced by feeding with lithogenic agents like EG, HLP and sodium oxalate to develop oxalate stones. Chemical food treatment of mouse develops not only hyperoxaluria but also form sodium oxalate crystals in the kidney (Khan and Glenton, 2010, Okada et al., 2007). This helps investigators to establish the role of a gene in stones formation. Summary of the use of a mouse model for different stones formation is in (**Table 1.3**). For example, researchers found that the selective knockout of osteopontin (OPN) and Tamm-Horsfall protein (THP) established the critical role of macromolecules in stones formation (Okada et al., 2007).

Mouse; References	Exogenous method	Urinary features	Nephrocalcinosis
Slc7a9 KO (Feliubadaló et al., 2003)	Normal diet	Cystinuria, cystine crystalluria	Cystine stone in pelvis and bladder
OPN KO (Wesson et al., 2003)	4 weeks administration of 1% EG in drinking water	hyperoxaluria, COD/COM crystalluria	intratubular COM crystals
THP KO (Mo et al., 2004, Mo et al., 2007)	normal diet or 4 weeks administration of 1% EG and 4 IU/ml VitD3 in drinking water	not described	intratubular and interstitial CaOx crystals
NHERF-1 KO (Weinman et al., 2006)	normal diet	hypercalciuria, hyperphosphaturia, hyperuricosuria	interstitial CaOx crystals
Slc26a6 (Jiang et al., 2006)	normal diet	hyperoxaluria, CaOx crystalluria	intratubular COD/COM crystals
C57BL/6 (Okada et al., 2007)	daily 80 mg/kg GOX intraperitoneal injection	hyperoxaluria, high CaOx index	intratubular COM crystals
Npt2a KO (Khan and Glenton, 2010)	4 weeks administration of 1.5% GOX or 5% HLP in chow	COD/COM crystalluria	intratubular/interstitial CaOx crystals and interstitial CaP crystals
Sat1 (Slc26a1) KO (Dawson et al., 2010)	normal diet	hyperoxaluria	intratubular CaOx crystals and bladder stone
MetS model (Taguchi et al., 2015)	2 weeks administration of 1% EG in drinking water and high-fat diet	hyperoxaluria, hypercalciuria	intratubular CaOx crystals

Table 1.3. Summary of mice models of nephrocalcinosis. CaP=calcium phosphate, COD=calcium oxalate dihydrate, COM=calcium oxalate monohydrate, EG=ethylene glycol, GOX=glyoxalate, HLP=hydroxy-L-proline, KO=knockout, MetS=metabolic syndrome, THP=Tamm Horsfall protein Adapted from (Tzou et al., 2016).

b. Transport knockout model

Several studies have been conducted by knocking out different transporters in the mouse model to induce hyperoxaluria, hypercalciuria, hyperuricosuria and cystinuria.

1.5.2.2 Limitations of Mouse model

Despite the advantage of having its genome sequenced, its overall accuracy and consistency in relation to human kidney stone disease have always been controversial among researchers. So, is mouse an ideal model for the study of kidney stones? Although this model imitates similar pathophysiological changes experienced in human models suffering kidney stones, it can be only useful for the study of hyperoxaluria. Also, the prevalence of cystinuria is rare (less than 1% of urolithiasis patients). Therefore these mice models are not representative of most humans who suffer from the urinary stone disease.

1.5.3 *Drosophila*

Studies performed by the laboratory of Julian Dow (Hirata et al., 2012) and Marshall Stoller (Chi et al., 2015) now present *Drosophila melanogaster* as a model for kidney stones research. They have shown that *Drosophila* has numerous advantages over vertebrates for the study of kidney stones.

1.5.3.1 Anatomic/Physiologic comparison between fly and humans

Drosophila is often overlooked as an ideal model organism for kidney stone studies. The previous study by Hirata and colleagues have presented and validated CaOx nephrolithiasis in the fruit fly. The fly Malpighian tubules (MTs) are considered the fly kidney and represent the excretory and osmoregulatory system similar to that of a human. Some of the significant differences between them are:

1) *Drosophila* is invertebrate.

2) *Drosophila* has an open circulatory system with a fluid-filled hemocoel cavity that uses haemolymph to circulate ions and regulation of water and nutrient excretion (Miller et al., 2013).

3) *Drosophila* has two pairs of MTs which have similar functions to human kidney (Dow and Romero, 2010). Homologous to human renal tubules, the Malpighian tubule functions to filter the fly haemolymph similar to how human tubules filter blood. The detail in **section 1.6.**

4) Unlike the vertebrate kidney, the *Drosophila* kidney does not have a glomerular-like structure, so the luminal fluid is not generated by a filtration process (Dow and Romero, 2010, Knauf and Preisig, 2011).

Despite all these differences, the conservation of genetic composition and transport protein structure as well as the similarities of the physiological function of the MTs (Reiter et al., 2001) have facilitated the development of several *Drosophila* stone models, including those of genetically linked and environmentally induced nephrolithiasis (Chung et al., 2016).

a. Diet-induced stones

Similar to other vertebrate models, hyperoxaluria can be induced in *Drosophila* by feeding with lithogenic agents such EG, HLP and sodium oxalate (Chen et al., 2011). The incidence of crystal formation with different lithogenic agents is discussed in **Table 1.4**.

	Crystal formation (%)		
	Male	Female	Total
Control	6.6±3.6	46.8±3.4	24.3±3.0
EG			
0.10%	54.8±9.4*	67.0±4.9*	61.3±2.8*
0.50%	94.2±1.5*	98.4±0.1*	97.7±1.4*
0.75%	100.0±0.0*	100.0±0.0*	100.0±0.0*
1%	100.0±0.0*	100.0±0.0*	100.0±0.0*
HLP			
0.01%	4.6±7.5	90.3±8.3*	38.5±3.1*
0.10%	9.0±5.7	91.2±8.2*	42.4±9.9*
1%	15.3±2.8*	91.6±11.7*	48.7±7.5*
NaOx			
0.01%	49.6±3.5*	98.0±3.4*	73.8±4.3*
0.05%	91.0±5.3*	96.0±3.5*	93.7±4.5*

Table 1.4. The incidence of crystal formation for different lithogenic agents in *Drosophila*. Adapted from (Chen et al., 2011). Abbreviations: EG, ethylene glycol; HLP, hydroxyl-L-proline; NaOx, sodium oxalate. *A probability, P-value of 0.05, was considered significant compared with control. Values were expressed as means±SEM. Statistical evaluation was performed using one-way analysis of variance (ANOVA) followed by Bonferroni test.

Adult *Drosophila* supplemented with EG produced CaOx concretions in as little as 6 h (Chung et al., 2016). Feeding *Drosophila* larvae with sodium oxalate dissolved in standard growth media resulted in CaOx microliths within 2 days (Hirata et al., 2012). However, adult flies fed with sodium oxalate develop crystals within an hour. Polarised light applied to dissected MTs permits the visualisation and quantification of the stones (Bagga et al., 2013, Miller et al., 2013).

b. Genetic models of stone diseases

The previously established GAL4-UAS (details in **section 1.6.2.1**) transgenic expression system allows researchers to perform targeted gene knockdown in *Drosophila* in relation to stone formation in a particular cell type or tissue of interest (Brand and Perrimon, 1993). With the immense resources available for *Drosophila*, investigators can directly order their desired transgenics to express or silence specific gene end products. Besides that, cost and time efficiency also make this model an ideal as compared to available model organisms (Dow and Davies, 2001, Dow and Romero, 2010).

Numerous inborn metabolic diseases such as hyperoxaluria, cystinuria, and hyperaminoaciduria (Fanconi syndrome) manifest with the urinary stone disease in humans. Although these disorders are rare, exploring the genetic basis of these diseases in *Drosophila* may reveal mechanisms underlying stone formation and its regulation that are common to other stone types.

1) Hyperoxaluria: As in the mice model, m*SLC26A6* is an essential oxalate transporter in flies. Hirata and colleagues have shown that *Drosophila* Prestin (dPrestin) is the homologue of m*SLC26A6* (Hirata et al., 2012, Monico et al., 2008). *Drosophila* Prestin has been shown to act as a chloride/oxalate exchanger, analogous to the role of the apical *SLC26A6* Cl^-/Ox^{2-} exchanger in the human kidney (Brand and Perrimon, 1993). Knockdown of dPrestin, mainly in the principal cells of the initial and main segments of the anterior MTs resulted in the reduction of calcium oxalate stones (Hirata et al., 2012).

2) Xanthinuria: Xanthinuria types I and II are a rare autosomal recessive defect in purine metabolism, i.e. deficiency of xanthine oxidase which results in the accumulation of xanthine and hypoxanthine stones (Levartovsky et al., 2000, Ichida et al., 2001). In xanthinuria type I, there is a deficiency of xanthine dehydrogenase, causing hyperxanthinemia with low or absent uric acid and xanthinuria, leading to urolithiasis (Aggarwal et al., 2017, Chi et al., 2015). The gene responsible for type I xanthinuria has been localised to chromosome 2p22-23 (Ichida et al., 1997). Utilising the fly *GAL4*/UAS system, Thomas et al. have silenced xanthine dehydrogenase enzyme in flies, which resulted in the formation of xanthine stones. They performed a series of experiments showing/demonstrating that flies can be an essential model for the study of xanthine stones.

Stone composition

1) Calcium oxalate and hydroxyapatite: As described in the rodent feeding flies with a stone causing lithogenic agents as described in **Error! R eference source not found.** results in the formation of calcium oxalate crystals in the MTs (Chen et al., 2011). Studies using X-Ray diffraction,

scanning electron microscopy (SEM) and energy-dispersive X-ray spectroscopy (EDS) can also be used to identify crystal deposition and composition in flies (Chi et al., 2015, Wessing et al., 1992). Hence in flies, calcium-based stones, as well as non-calcium based human stones, may be generated from a hydroxyapatite nidus (Evan, 2010). This finding highlights potential similarities between *Drosophila* fly stone and human stones (Tzou et al., 2016a).

2) Zinc stones: The majority of human stones are composed of oxalate or uric acid stones. However, other minerals have essential roles in stones formation (Chi et al., 2015). Analysing the mineral components of fly concretions, human Randall's plaques, and human xanthine stones demonstrated that calcium (Ca), magnesium (Mg) and zinc (Zn) were the major metal components within each specimen (Wang et al., 2009). Inductively coupled plasma optical emission spectroscopy (ICP-OES) showed that the relative amount of each of these metals was consistent across the stone source. Additionally, it has been shown that there are traces of zinc in the food which is responsible for stones formation (Yin et al., 2017). Additionally, three *Drosophila* ZnT transporters (CG3994, CG11163, and CG17723) have been reported to be highly expressed in the MTs. Their function is to regulate Zn movement across the cell membrane (Wang et al., 2009, Yepiskoposyan et al., 2006).

1.5.3.2 Limitations of the *Drosophila* model

Despite having many benefits in terms of reliability, duration and cost-effectiveness, there are some limitations to its use and applicability. As an invertebrate, *Drosophila* does not have bones, and hence, they lack a calcium reservoir, so it becomes hard to compare the calcium metabolism as well as transport across the tubules. Next, the fly is not an ambulatory model and relies on a different feeding cycle compared to humans. Additionally, it can be challenging to measure how much food and medication that *Drosophila* ingest. Another limitation is that since the fly's MTs drain into the hindgut, there is a combination of waste products in a single-elimination chamber and the GI tract can contribute to the elimination of electrolyte and water waste.

1.6 Drosophila melanogaster

1.6.1 History of *Drosophila melanogaster*

Drosophila melanogaster (fruit fly or vinegar fly) has been extensively used for scientific research since 1910 when Thomas Morgan described *Drosophila*'s first mutant, *white* (Morgan and Bridges, 1916). In 1933 he was awarded the Nobel Prize for his work in sex-linked gene transmission in *Drosophila*. In 1927, Muller studied the hereditary characteristics of fruit flies and demonstrated that mutations and hereditary changes could be caused by X-ray. in 1946, Muller was awarded the Nobel Prize in physiology or medicine for the same. Again in In 1995, the Nobel Prize in Medicine was awarded to Dr Edward Lewis, Christiane Nuesslein-Volhard, and Eric Wieschaus, for discovering the genes playing a vital role in embryonic development (Lewis, 1978, Nüsslein-Volhard and Wieschaus, 1980). Importantly, these genes have human homologues and also have an essential function in development. Again in 2011, Jules Hoffmann was awarded Noble prize for his contribution in immunology in understanding how human and other organisms protect themselves from the attack of bacteria and other organisms. Recently in 2017, The Nobel Prize in Physiology or Medicine was awarded jointly to Jeffrey C. Hall, Michael Rosbash and Michael W. Young for their discoveries of the molecular mechanism controlling *Drosophila* circadian rhythm. Hence it is apparent that *Drosophila* is one of the most intensely studied organisms in biology and has provided essential general insights into developmental and cellular processes including neuroscience (Crocker and Sehgal, 2008), immunity (Davies and Dow, 2009), sex determination and development (Telonis-Scott et al., 2009), circadian cycle (Sofola et al., 2008), insecticide resistance (Yang et al., 2007),renal function (Terhzaz et al., 2012, Dow et al., 1994) and neurodegenerative researches (Brumby and Richardson, 2005, Reiter et al., 2001).

1.6.2 *Drosophila* as a genetic model

The availability of a complete genome sequence published in 2000, as well as a number of stock centres that can provide strains that carry a mutation in the given gene, makes this model an ideal organism for genetic research. Furthermore, the friendly nature of *Drosophila* researchers worldwide having a

common philosophy of making their resources available to other research groups by sharing it makes this community close and intact.

Therefore, *Drosophila* is considered as an ideal model for studying human disease genes, applying the genetic approach. In addition to the advantages mentioned in **section 1.5.3**, some of the critical reasons behind using *Drosophila* as a model organism are:

a. The life cycle of *Drosophila* is short (around 2 weeks at 22 °C). Hence, it permits investigation for several generations in a relatively short period. Additionally, they are small (2-3 mm long); hence, a considerable number of flies can be kept in small vials.

b. Cost - maintenance of fly lines is inexpensive ($20 per year per fly line) and relatively easy as compared to other model organisms. For example, it costs >$10K/year to keep a single strain of transgenic mouse.

c. In terms of genetics, *Drosophila* is well defined, with the complete sequence of the genome published in 2000 (Adams et al., 2000). This makes *Drosophila* a more comprehensive model with the well-annotated genome, easily manipulated transgenes and an excellent pedigree of physiology. Additionally, about 70% of Drosophila genes (around 13,500) have human homologues (Chien et al., 2002).

d. *Drosophila* is genetically very pliable; gene manipulation has been accessible with the use of transposable elements (e.g., P-elements) (Rubin and Spradling, 1982, Spradling and Rubin, 1982). Systemic mutagenesis has been directed to the production of RNAi lines for nearly all *Drosophila* genes (Dietzl et al., 2007). These lines are available from *Drosophila* stock centres such as the Vienna *Drosophila* RNAi Centre (VDRC) and the Bloomington *Drosophila* Stock Centre (BDSC) for a minimal cost (Dow and Romero, 2010).

e. Presence of specific online resources including Flybase (http://flybase.org/) (Drysdale et al., 2005), FlyAtlas 1(http://flyatlas.org/atlas.cgi) (Chintapalli et al., 2007) and FlyAtlas 2

(http://flyatlas.gla.ac.uk/FlyAtlas2/index.html) (Leader et al., 2017) providing information on gene sequences, transcriptomic data and expression of genes in different tissues. Additionally, FlyBase also provides information about RNAi (RNA interference) knockdown lines, mutant alleles, human disease homologues, etc.

1.6.2.1 The *UAS/GAL4* system

GAL4 is a yeast transcriptional factor, which activates transcription downstream of the yeast promoter Upstream Activating Sequence (*UAS*) in *Drosophila*. *GAL4* does not normally activate *Drosophila* promoter sequences but is capable of driving transgene expression under the control of a *UAS* promoter. P-elements are frequently used in conjunction with the *UAS*/*GAL4* binary system (Brand and Perrimon, 1993). By cloning a transgene into a P-element construct downstream of a *UAS* promoter, it is possible to control transgene expression using a *GAL4* driver to knockdown or overexpress any gene of interest with cell and tissue specificity, **Figure 1.4**.

The first *GAL4* 'driver' line was developed by Brand and Perrimon as an enhancer trap *GAL4* construct (the original P-element plasmid; pGAWB) (Brand and Perrimon, 1993). In the last 25 years, an impressive array of *GAL4*-driver lines has been constructed by modifying pGAWB. It is now possible to drive transgene expression from a subset of neural cells to a whole organ, depending on your tissue of interest. There are many advantages to maintaining *GAL4* lines with specific temporal and spatial expression patterns. Driver lines can be maintained as stable stocks and used to drive expression in any fly line containing a transgene with a UAS promoter, reducing the complexity of cloning when making a new fly line. Many UAS transgenes are lethal or debilitating when expressed in *Drosophila* and would be difficult or impossible to maintain if both the *GAL4*-driver and UAS-transgene elements were inserted in the same line. Maintaining them in separate parental fly-lines means they are much more likely to be viable. It also allows the experimenter to change the UAS-transgene expression pattern by crossing to different *GAL4* parental lines, which is much easier than making and microinjecting a new construct with a different driver.

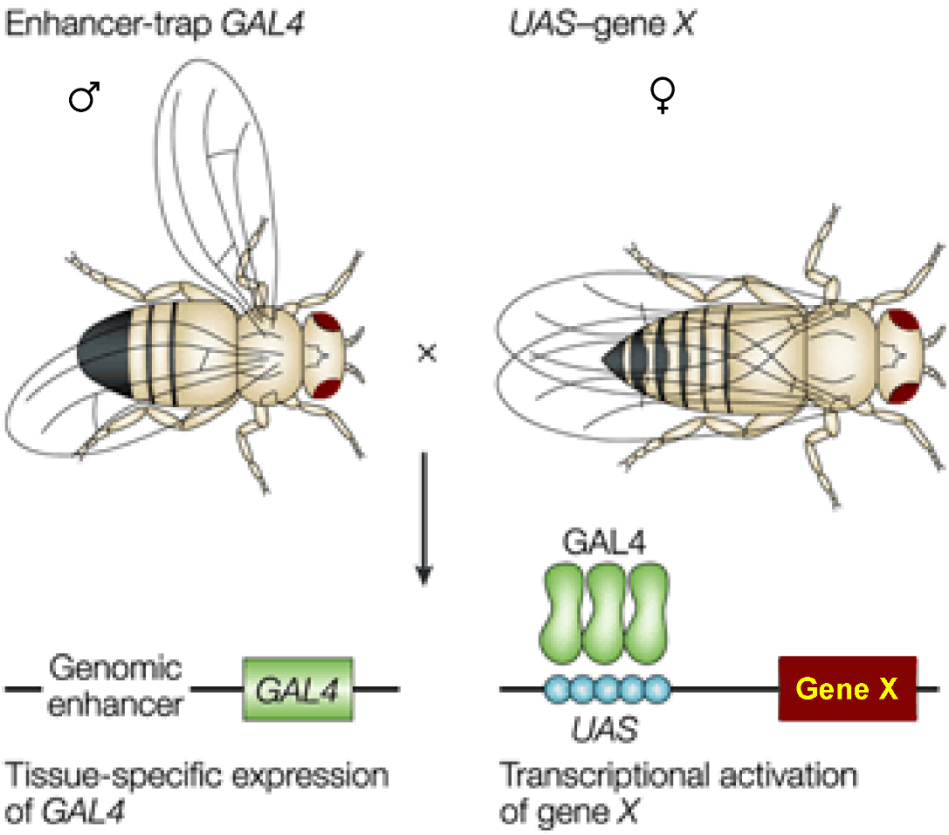

Figure 1.4. The *GAL4*/UAS system used for targeted gene expression. To obtain flies expressing a gene of interest ("Gene X") in a tissue-specific pattern, flies must both contain a transgene expressing the *GAL4* transcriptional activator protein under the control of a tissue-specific enhancer, and a transgene containing the *GAL4* DNA binding sequence adjacent to the reporter gene. The target gene is silent in the absence of *GAL4*. To activate the target gene in a cell- or tissue-specific pattern flies carrying the target (UAS-Gene X) are crossed to flies expressing *GAL4* (Enhancer Trap *GAL4*). In the progeny of this cross, it is possible to activate UAS-Gene X in cells where *GAL4* is expressed and to observe the effect of this directed misexpression on development. Reproduced with permission from (Brand and Perrimon, 1993).

The UAS/*GAL4* system can be used to express full gene sequences for protein over-expression, with or without additional tags. It can also be used for gene knockdown through the action of a specific double-stranded RNA (dsRNA). RNAi lines can be made by inserting a double-stranded hairpin loop sequence into a P-element so that it expresses a dsRNA when driven (Kennerdell and Carthew, 2000). Dicer recognises the dsRNA and breaks it down, along with any other RNA which contains the same sequence as the dsRNA. This decreases the amount of that particular transcript, effectively suppressing the expression of that gene.

In summary, when these two systems (UAS and *GAL4*) or in another word two flies containing different components are crossed together, they will give rise to progeny that have both components. This, in turn, activates the transgene under the control of UAS in a *GAL4*-specific expression manner. As the *GAL4* expression depends on the upstream elements, it was inserted or fused with; this system is useful in elucidating tissue- and cell-specific functions. For example, *ClCa-GAL4* can be placed under the control of the *Sip1* gene promoter as this gene is expressed exclusively in the MTs; the *ClCa-GAL4* line drives transgene expression with exquisite precision in stellate cells (Dow and Davies, 2003).

1.6.2.2 Balancer Chromosomes

One of the advantages of *Drosophila* genetics is the presence of balancer chromosomes. They prevent recombination and enable the maintenance of deleterious mutations in stable fly populations. This is due to the presence of chromosomal inversions in the balancers, which prevent the formation of crossovers. As a result, there is no recombination between homologues chromosomes, and the mutation is maintained. Since most recessive mutations have no phenotype, balancers allow the geneticists to indirectly follow the recessive mutation (by scoring dominant markers on the balancer) without losing the mutation (due to inhibited recombination). Balancers are also used to maintain chromosomal deficiencies that would otherwise be lethal due to the deficiency. Moreover, they carry visible dominant marker genes (such as curly wings or stubbly bristles), which enable selection of progeny, which inherited the balancer. Balancer chromosomes also carry at least one recessive lethal locus in order to maintain mutations in the stocks (Dow and Davies, 2003).

1.6.3 Malpighian tubules

Similar to many other insects, the central excretory tissue in *Drosophila* is the Malpighian tubules (MTs), which performs a renal role analogous to the vertebrate kidney (**Figure 1.5**). The tubules transport excess fluid and solutes from the haemolymph and secrete the primary urine into the hindgut for excretion. They are an excellent model not only for morphogenesis of epithelia

in general but also for transport mechanisms and maintenance of homeostasis, especially in *D. melanogaster* (Dow and Davies, 2003, Dow et al., 1994), which have helped elucidate biological functions at both tissue and single-cell level.

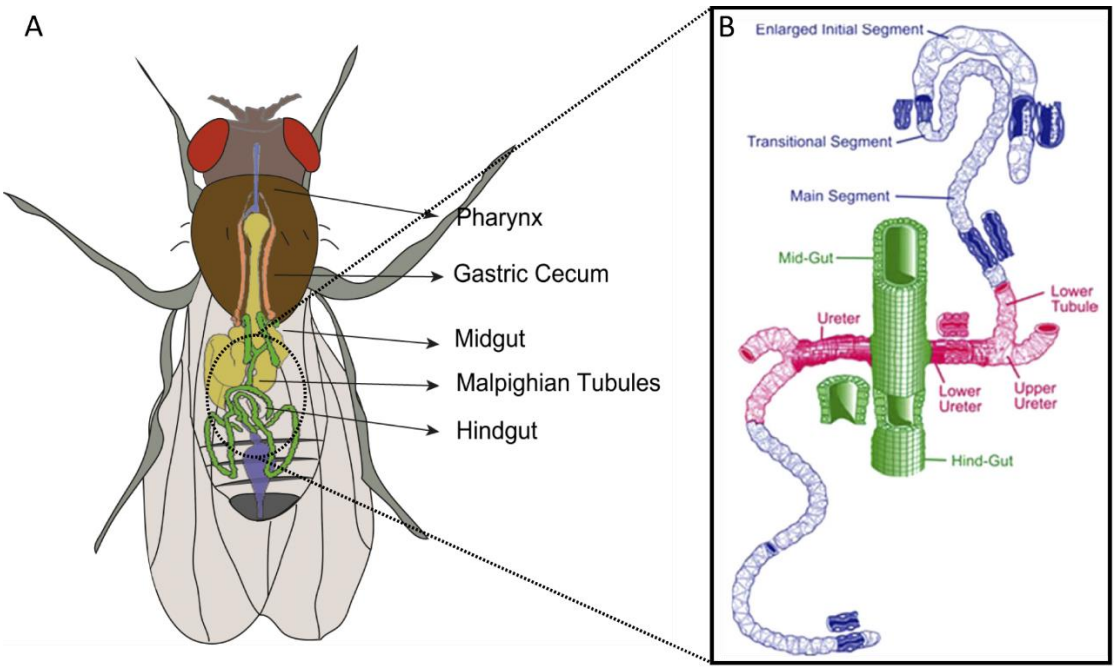

Figure 1.5. Schematic diagram of D. *melanogaster* excretory tract. Two pairs of Malpighian tubules, one anterior and one posterior, are each connected to the gut by a common ureter. All the segments are clearly labelled in the image. Adapted from (Sözen et al., 1997).

1.6.3.1 History

The Malpighian tubules are named after Marcelo Malpighi (1628-1694), who was a physician of the Pope, 500 years ago. Besides his work as a comparative anatomist, he was a pioneer in the use of microscopy, contemporaneously with Hooke, and followed the discoveries of William Harvey on the nature of circulation. This interest allowed him to apply his skills in microscopy to investigate insect anatomy, which further resulted in the discovery of the Malpighian tubules. However, it was not demonstrated until the 20th century, that they could produce urine. Since then, tubules have been extensively studied for their excretory and osmoregulatory functions. Furthermore, various research has been conducted using insect tubules as an epithelial system and a

targeted organ for insecticide development (Dow and Romero, 2010, Miller et al., 2013).

1.6.3.2 Morphology

Drosophila has two pairs of MTs, which are tubular and blind-ended epithelia joined in pairs by a short common ureter to the alimentary canal, which floats freely in the haemocoel (Wessing and Eichelberg, 1979). Each fly possesses a pair of anterior and posterior tubules, which contribute equally to tubule function (O'Donnell and Maddrell, 1995). A single Malpighian tubule is approximately 2 mm in length, with an inner luminal diameter of 17 µm (**Figure 1.6**).

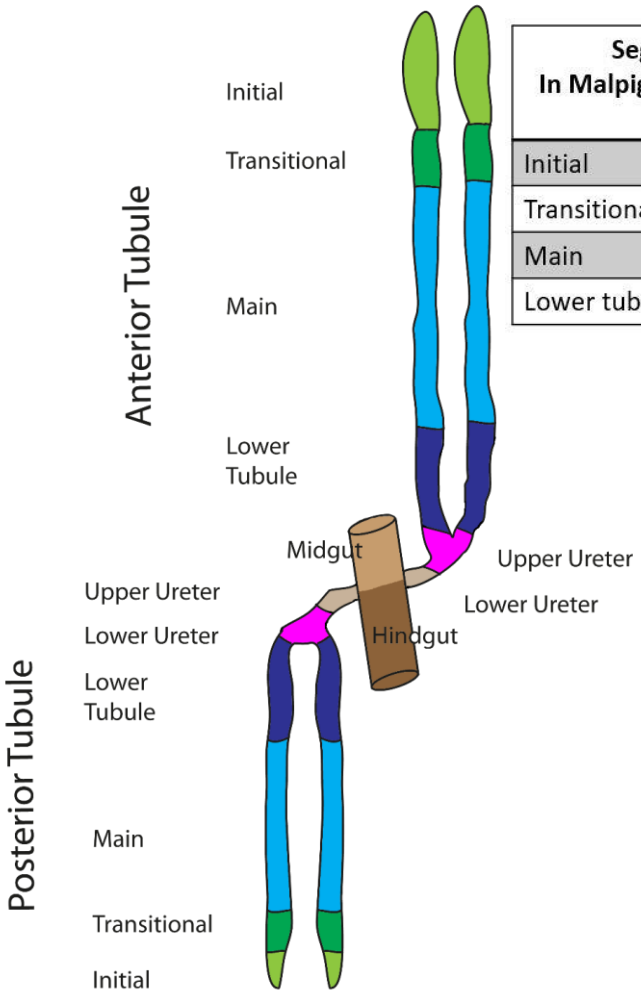

Segments In Malpighian Tubules	No. of cells			
	SCs		PCs	
	Ant	Post	Ant	Post
Initial	7	1	22	4
Transitional	6	1	22	3
Main	20	20	77	75
Lower tubule	0	0	25	23

Figure 1.6. Overview of the *Drosophila* Malpighian tubules showing the six domains of the tubule and the numbers of principal and stellate cells in each. Adapted from (Sözen et al., 1997).

The anterior and posterior tubules can be divided morphologically into three segments; the initial segment, the transitional segment and the main segment, which joins to the common ureter to the alimentary canal (Miller et al., 2013). In contrast to anterior tubules, the posterior pairs have a short initial segment (Weiss et al., 1988, Wessing and Eichelberg, 1979). Furthermore, there is no apparent morphological difference between male and female tubules, although females have bigger size tubules. The main segment of the tubules is composed of two cell types; the large principal cells and the star-shaped stellate cells. The principal cells have deep basal infoldings and long apical microvilli and are more abundant than the stellate cells (Cabrero et al., 2014). The stellate cells are comparatively small and thin, with shallow basal infoldings and short apical microvilli (Wessing and Eichelberg, 1979). Enhancer trapping has been used to investigate the morphology of the tubule and cell-types in great detail, including the bar-shaped cells and tiny cells in the tubule (Singh et al., 2007, Sözen et al., 1997).

1.6.3.3 Physiology

The Malpighian tubules perform a multitude of physiological roles in *Drosophila*, from the normal renal and hepatic roles (detoxification) to a surprising role in immune response (McGettigan et al., 2005). Osmoregulation and ion homeostasis are arguably the defining functions of the tubules, as they are performed continually throughout the lifecycle of the fly. Active cation transport by the tubules is described by the Wieczorek model (Wieczorek et al., 1999, Wieczorek et al., 2009). The model suggests that the principal cells use the apical proton-pumping activity of the Vacuolar ATPase (V-ATPase) to build a favourable transport gradient (Wieczorek et al., 1991, Wieczorek et al., 1999). Apical alkali metal-proton exchangers are then able to drive potassium into the tubule lumen, with water following the potassium due to the osmotic gradient. The Wieczorek model seems to fit the experimental tubule data in *Drosophila*, as V-ATPase inhibitors abolish fluid secretion (Dow et al., 1994), and the V-ATPase subunits are highly enriched and expressed in the principal cells (Wang et al., 2004).

The principal cells are also involved in the active transport of cations (O'Donnell and Maddrell, 1995, Evans et al., 2005). These cells are

concentrated in the main segment of the tubule and contain basolateral ion cotransporters for Na^+, K^+ and Cl^- as well as a Na^+ dependent solute transporter and a Na^+ dependent $Cl^-/HCO3^-$ exchanger (Sözen et al., 1997). Ion transport at the apical cell membrane of the principal cell is accomplished via vacuolar-type H^+-ATPase (Dow et al., 1997), which pumps protons from the cell into the lumen, providing the gradient necessary for the secondary movement of Na^+ and K^+ into the lumen by the Na^+/H^+ and K^+/H^+ exchangers (Romero et al., 2000) **Figure 1.7**.

The stellate cells appear to be the site of transcellular chloride shunt and therefore, water movement (Dow et al., 1997). The stellate cells, which are more evenly distributed throughout the initial, transitional and main segments of the posterior Malpighian tubules, provide mainly chloride transport and water conductance (Dow and Romero, 2010). Chloride shunt is controlled by the hormone Drosokinin and the second messenger intracellular Ca^{2+}, which increase transcellular conductance through chloride channels (Terhzaz et al., 1999, Cabrero et al., 2014).

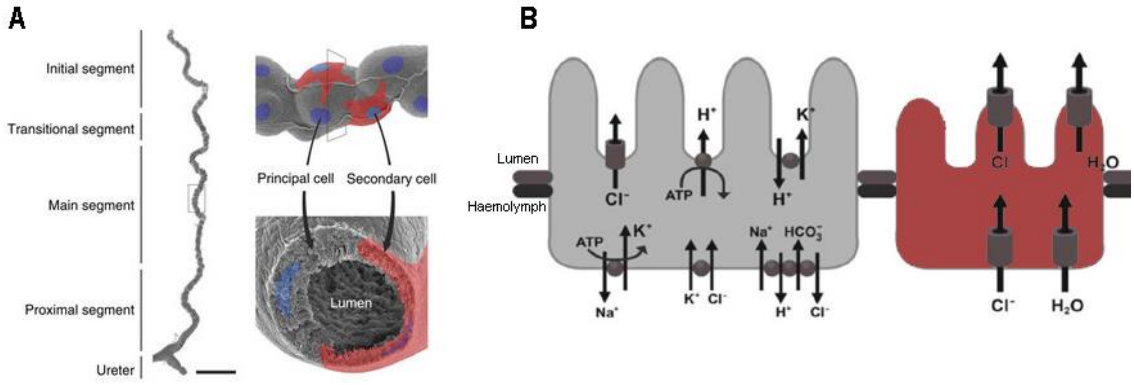

Figure 1.7. *Drosophila* Malpighian tubule morphology. A. Spatial organisation of the *Drosophila* tubule as evidenced by scanning electron microscopy, with superimposed illustrations of principal and secondary cells. B. Classic two-cell-type model: fluid transport is energised by a vacuolar H^+-ATPase (V-ATPase) located in the apical membrane of PCs (grey), which through a K^+/H^+ exchanger, drives net secretion of K^+ into the lumen. Reproduced with permission from (Halberg et al., 2015).

1.7 The aim of the study

1.7.1 General Study Objective

The prevalence of nephrolithiasis is increasing yearly; however, our understanding of the pathophysiology has not kept pace, and new therapeutic approaches have not emerged. Hence, the overall objective of this dissertation is to study the genetic and environmental cause of kidney stone formation using Drosophila as a model organism. Here, we establish a *Drosophila melanogaster* model for stones formation by using genetic, molecular, pharmacological and biochemical studies to open a novel perspective on the aetiology of urinary stones and related diseases, which may lead to the identification of new preventive and therapeutic approaches.

1.7.2 Specific study Objectives

There are four specific study objectives:

1. Identification of the genes involved in nephrolithiasis.

   The 'sensitised background' in which stones form spontaneously at a low dose, will be used to screen RNAi and/or mutant panels for genes that increase or decrease the rate of oxalate stone formation, identify the genes responsible and seek homologous human candidate gene loci. This thesis will provide in detail description and validate the use of *D. melanogaster* as the model system for a screen of different genes in stones formation.

2. In-depth study of selected genes involved in the renal stone accumulation

   By choosing candidate genes (objective 1), genetic and physiological experiments will be performed to determine their role in different types of stones accumulation. It is hypothesised that knockdown or overexpression of a gene will increase or decrease stone quantity. Further, it can be believed that under this objective, the results will

represent two distinct phenomena, a. Determination of the pathophysiological role of the gene in stone formation b. Mechanism of stone formation and accumulation.

3. Identification of the role of temperature and age in the stone development

   To assess whether the risk of calcium phosphate deposition alters with environmental factors flies were reared at different temperature for a different time and the stone formation was quantified. It is hypothesised that the rate of the stone formation deviates with age and temperature of residence. This allows elucidating the complex interplay between proteins, minerals, genes and environmental exposures which are known to influence kidney stone formation.

4. Identification of the role of *Sip1* in kidney stones formation

   In humans, Sodium hydrogen Exchanger Regulatory Factor 1 (*NHERF1*), a homologue of *Drosophila Sip1,* is linked to nephrolithiasis. However, the function of *Sip1* in *Drosophila* has not been previously investigated. Here, we have identified the role of *Sip1* in uric acid stone formation and established a mechanism behind it.

   These research studies should improve our understanding of the genetic, physicochemical and physiological factors that may lead to the formation of a stone.

1.8 Study Hypothesis

1. Given the similarities in tubular structure, function and physiology; conservation of genes in the excretory system, and characteristics of stone formation between D. melanogaster and humans, and the availability of powerful genetic tools in the fly, we hypothesize that D. melanogaster can be utilized as a meaningful model to improve understanding of kidney stone disease and to identify novel therapeutics.

2. It is hypothesized that mutation of the gene causes formation or precipitation of kidney stones; while it is not revealed whether its monogenic or polygenic. This study will determine how mutation of gene causes calcium oxalate, uric acid and phosphate stones and how long the does it take to form the stones. If stone formation occurs due to mutation of the gene, it would be beneficial to determine the role of a gene in calcium oxalate or phosphate or uric acid precipitation.

3. Heat and temperature are one of the risk factors for kidney stone formation. We hypothesise that change in temperature (from colder to warmer, low temperature to higher temperature) may have a more significant impact on the formation rate of nephrolithiasis.

Chapter 2 Materials and Methods

2.1 Summary

This chapter describes the protocols used during the experiments mentioned in this thesis. Further, it summarises the rearing conditions of *Drosophila melanogaster* and describes novel methods which play an essential role to validate *Drosophila* as a model for kidney stone formation studies. Relevant references were used for methods where applicable.

2.2 Drosophila melanogaster

2.2.1 *Drosophila* stocks

The detailed description of all the *Drosophila* stocks used in this work can be found in Error! Reference source not found., including their fly ID, genotype, d escription and the source of origin along with references. A full description of all mutations and balancer chromosomes used can be found in FlyBase (http://www.flybase.co.uk).

Strain	Genotype	Description	Origin
Canton S	*w;+/+;+/+*	Wildtype	DD
Actin-*GAL4*	*w;actin-GAL4/CyO; +/+*	Ubiquitous *GAL4* driver	BDSC
CapaR-*GAL4*	*w⁻; +/+; CapaR-GAL4/ CapaR-GAL4*	Expression of *GAL4* to the tubule principal cells	DD
ClCa-Gal4	*w⁻; +/+; CapaR-GAL4/ C;Ca-GAL4*	Expression of *GAL4* to the tubule Stellate cells	DD
Rosy	*ry* ^{506}		DD
UAS-CG10939 RNAi		Knocks down *CG10939* expression by RNAi	BDSC, VDRC
Sip1 mutant	*Sip1*^{5a} */ CyO*		

NHE2 RNAi		Knocks down *NHE2* expression by RNAi	BDSC
UAS-Moe RNAi		Knocks down *Moesin* expression by RNAi	BDRC
Dihydropterin deaminase (*DhpD*); (*CG18143*)	*y⁻w⁻ ;P{KK108461}VIE-260B; +/+*	Knocks down *DhpD* expression by RNAi	VDRC
	w; CG18143/CyO;+/+		BDSC
Water witch (*Wtrw*); (*CG31284*)	*y⁻w⁻ ;P{attP,y⁺,w³⁺}VIE-260B; +/+*	Knocks down *Wtrw* expression by RNAi	VDRC
	W⁻; +/+; CG31284/CG31284		BDSC
CG11374	*y⁻w⁻ ; P{GD5055}v15561; +/+*	Knocks down *CG11374* expression by RNAi	VDRC
	w⁻ ;CG11374/CyO;+/+		BDSC
Serine pyruvate aminotransferase (*Spat*);(*CG3926*)	*y⁻w⁻ ;P{KK107941}VIE-260B; +/+*	Knocks down *CG3926* expression by RNAi	VDRC
	y¹ v¹; CG3926/CG3926; +/+		BDSC
Cinnamon (*Cin*); (*CG2945*)	*y⁻w⁻ ;P{KK102795}VIE-260B;+/+*	Knocks down *cin* expression by RNAi	VDRC
	y¹ v¹; +/+; CG2945/TM3		BDSC
Molybdenum cofactor synthesis 1 (*Mocs1*); (*CG33048*)	*w; CG33048/CyO; +/+*	Knocks down *Mocs1* expression by RNAi	BDSC
Carbonic anhydrase 1 (*CAH1*); (*CG7820*)	*W;P{KK108727}VIE-260B;+/+*	Knocks down *CAH1* expression by RNAi	VDRC
Sarcoplasmic calcium-binding protein 2 (*Scp2*); (*CG14904*)	*w¹¹¹⁸; P{GD7705}v31916;+ /+*	Knocks down *Scp2* expression by RNAi	VDRC
Na⁺-dependent inorganic	*w;P{KK106711}VIE-260B;+/+*	Knocks down *NaPi-T* expression by RNAi	VDRC

phosphate cotransporter (*NaPi-T*); (*CG10207*)	*W;+/+; CG10207/TM3, Sb1*		BDSC
Secretory Pathway Calcium ATpase (*SPoCk*); (*CG32451*)	$y^{-}w^{-}$ *;P{KK101068}VIE-260B; +/+*	Knocks down *SPoCk* expression by RNAi	VDRC
	y^{1} v^{1}*; +/+; CG32451/TM3*		BDSC

Table 2.1. *Drosophila melanogaster* stocks used for the experiments in this thesis. VDRC: Vienna *Drosophila* Research Center, BDSC: Bloomington *Drosophila* Stock Center, DD: Dow/Davies lab (In house).

2.2.2 *Drosophila* husbandry

All the stocks of *D. melanogaster* (**section 2.2.1**) were maintained in standard conditions unless otherwise specified. An ideal fly husbandry room was tightly regulated with 22°C, 55% atmospheric humidity and a 12:12 h light: dark cycle. Flies were fed with the standard *Drosophila* diet (composition listed in **Table 2.2**).

Initially, 5-7 days old flies were transferred to vials containing freshly prepared food. The flies were transferred to another vial every two weeks to maintain the stock unless flies of specific age where required. For the collection of newly emerged flies, a laying population of around 15 females and 10 males were kept in a vial for 5 days and then transferred to next vial. When the new flies emerged from larvae and pupae stage after 10 days, the 1-day old progeny was collected in vials. This allowed us to determine the age of the flies and perform age-related experiments. All the flies referred to as adult flies throughout the thesis are 5-7 days old flies reared in the standard *Drosophila* diet unless otherwise mentioned.

2.2.2.1 Rearing for age and temperature vs Kidney stones formation experiment

1-day old flies (newly emerged) were subjected to 18°C, 22°C, 26°C and 28°C and they were maintained at that same temperature for 21 days unless mentioned. Furthermore, for the temperature switch experiment, flies were

transferred to another temperature every week, to observe an alteration in stones accumulation. Detailed rearing conditions are described in **Chapter 4.**

2.2.3 *Drosophila* diet

Flies were reared on standard *Drosophila* diet composed of yeast cornmeal, sucrose and agar medium. The recipe of standard diet is enlisted in **Table 2.2**. While preparing the food, all the recipes were mixed and boiled in 1 litre of water, and the mixture was let to simmer for 10 mins. Then the food was left to cool down at 70°C for about 20 minutes, before adding Nipagin and propionic acid. Finally, the food was kept in 50 ml vials and stored at 4°C.

Per 1 litre of food recipe

1. 10 g agar
2. 15 g sucrose
3. 30 g glucose
4. 35 g dried yeast
5. 15 g maize meal
6. 10 g wheat germ
7. 30 g treacle
8. 10 g soy flour
9. 10 ml Nipagin (25 g Nipagin M (Tegosept M, p-hydroxybenzoic acid methyl ester) in 250 ml Ethanol]
10. 5 ml Propionic acid

Table 2.2. The composition of fly food. Adapted from (Cabrero et al., 2014).

2.2.3.1 Preparation of the diet containing Sodium oxalate

For the induction of calcium oxalate stones within the MTs, we introduced Sodium Oxalate in the regular *Drosophila* diet. Different concentration of Na-oxalate (0.1% low; 1% high) were dissolved in 100 ml of standard *Drosophila* diet. The food was kept at 100°C with continuous stirring for 20 minutes in order to mix thoroughly. Then the food was kept in the glass tubes, and the diet was left to set. Diet was freshly prepared to avoid any changes in the concentration of salts due to evaporation/precipitation.

2.2.3.2 Preparation of the diet containing Allopurinol

Allopurinol, containing food used was also freshly prepared before each experiment. Allopurinol [4-hydroxypyrazolo (3,4-d) pyrimidine; Sigma] was

dissolved in standard *Drosophila* diet to make final concentration 250 ng/ml (Zhou and Riddiford, 2008). At this concentration our flies can phenocopy *rosy* mutant flies. To prevent the irregular distribution of the drug and make the solution homogenous, drug was kept in the bottle with constant stirring for about 20 minutes. Then, 5 ml of the mixed solution was added to the vial and was kept at room temperature for 1 day in order to allow allopurinol to be completely absorbed. Flies were fed with allopurinol for 48 hours to observe the therapeutic effect.

2.2.4 *Drosophila* crossing

For the expression of the gene of interest in a particular tissue in *Drosophila*, the UAS-*GAL4* binary system (**section 1.6.2.1**) was employed (Brand and Perrimon, 1993) Virgin female flies of UAS-RNAi lines were crossed to *GAL4* males. Flies were kept at 26°C for 4 days, and the parental lines were transferred to next vials to prevent mixing with the progeny. F1 progeny from the cross was used for experiments as a knockdown fly while UAS-RNAi/+ and UAS-Gal4/+ were regarded as parental controls . The presence of transgene or knockdown was evaluated by visual markers and validated by qPCR (quantitative PCR), respectively.

In order to collect adult virgin female flies, an egg-laying population of around 10 male and 20 females were transferred to the new vials every 3 days. The progeny which emerges from the vials were collected every hour, and virgin female flies were selected. The reciprocal crosses were also made, to test for sex-specificity of gene expression, though this was not observed in this project.

Typical examples of *GAL4*-UAS crosses and selection of appropriate progeny as described below. After mating, flies laid sufficient eggs and adults were transferred into new vials leaving the first vial with larvae. The newly transferred flies were left for several days until sufficient eggs were laid. This process took approximately five to ten days.

Example of a cross:

ClC-a Gal4 is Drosophila Malpighian tubule SC specific Gal4 driver.

1. **UAS and *GAL4* driver lines on different chromosomes**

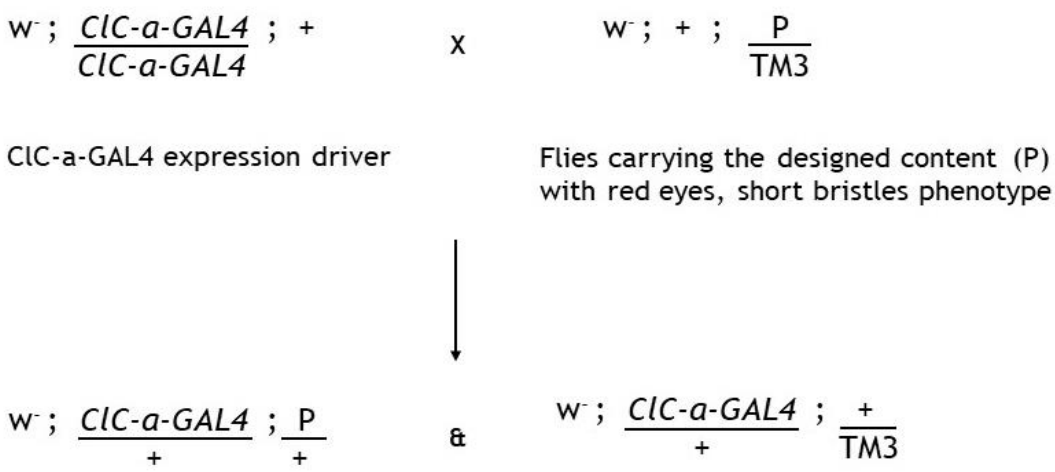

Flies with long bristles were selected from this cross and used for experimentation.

2. **UAS and *GAL4* driver on the same chromosome**

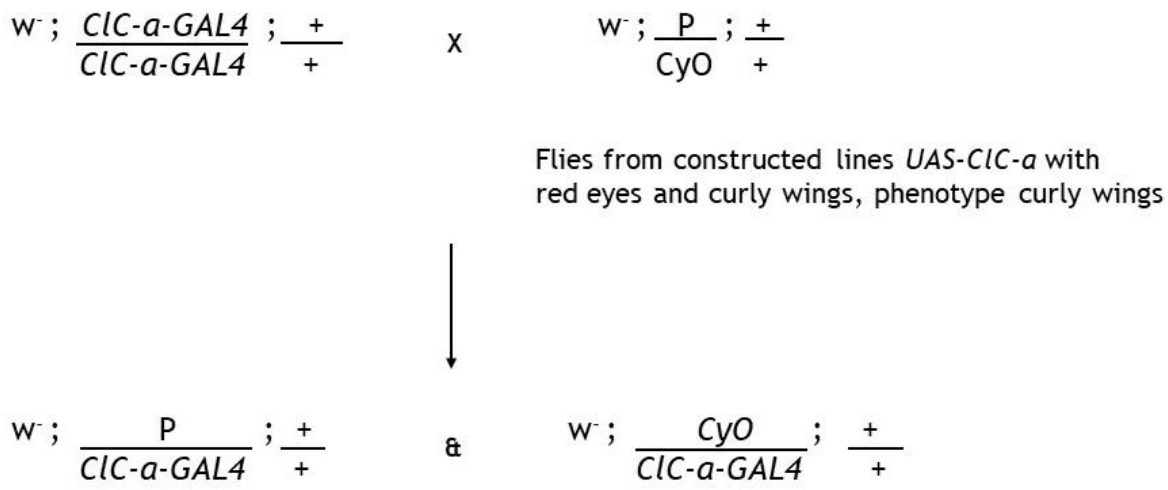

Flies with straight wings were selected from this cross and used for experimentation.

2.2.5 *Drosophila* tissue dissection

Adult flies were anaesthetised on ice and transferred to a Petri dish containing *Drosophila* Schneider's medium (artificial hemolymph). Malpighian tubules were easily dissected by holding a fly firmly by forceps from the thorax region and with the other hand, pulling the very end part gently and slowly. At this point, the Malpighian tubules start to appear, attached in between midgut and

hindgut. The tubules were then pulled out, and the joint between tubules and gut was cut with great care, gently hold the tubules from the ureter (**Figure 2.1**). Importantly, the MTs should be intact for stone imaging experiments. The number of flies dissected for MT collection varied with each experiment. This method was adopted as per previous research articles (Dow et al., 1994, Sullivan and Sullivan, 1975).

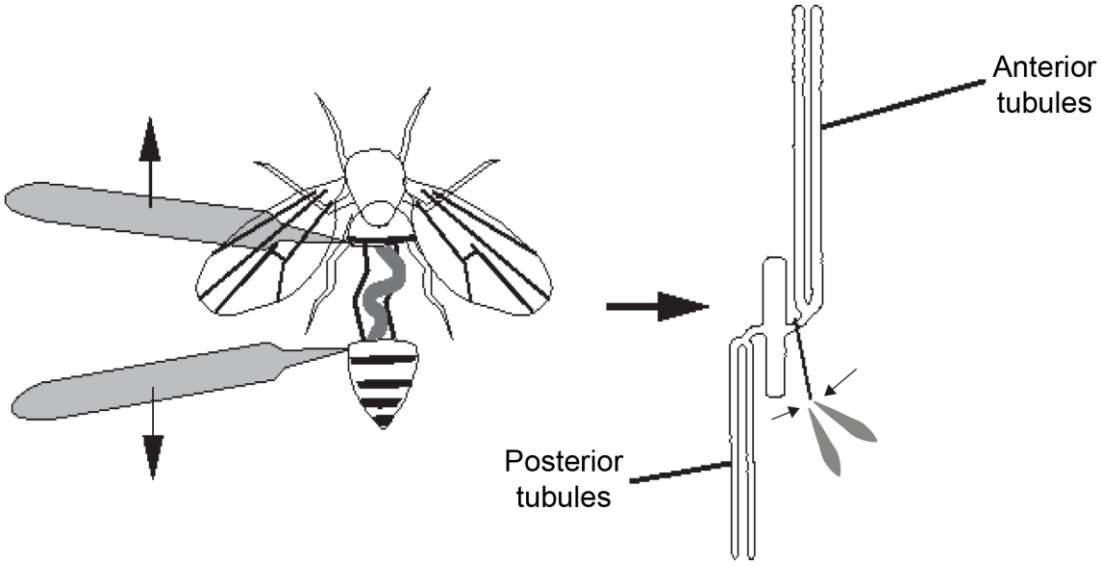

Figure 2.1. MTs dissection method.

2.2.6 Slide preparation

Following the dissection, tubules were mounted on glass slides and immediately transferred to Poly-L-lysine coated slides containing a drop of PBS (pH 7.4). The process of preparation of the slide is shown in **Figure 2.2**. Once the slide samples were prepared, they were imaged and analysed.

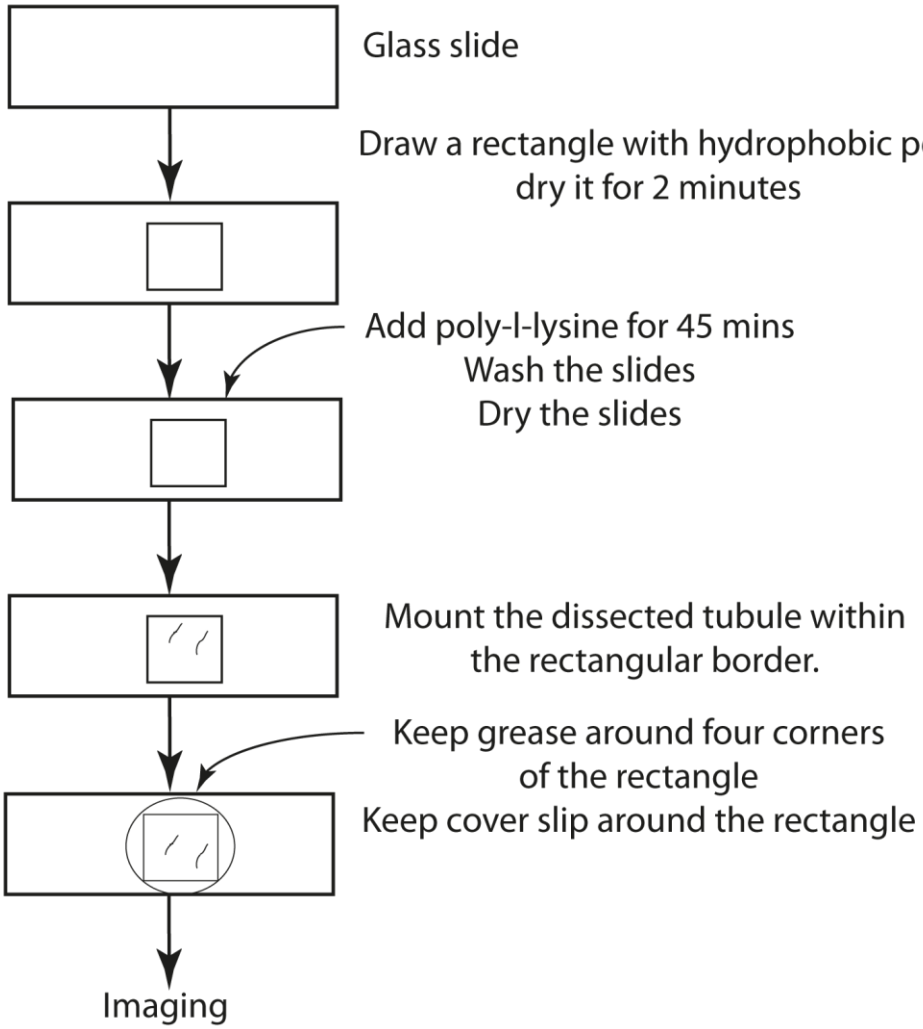

Figure 2.2. The process of preparation of glass slides and tubule samples.

2.2.7 RNA interference kidney stone screen a candidate gene *in vivo* RNAi screen

Candidate genes were screened for impact on oxalate stone deposition by using 20 different RNAi lines (**Error! Reference source not found.**) driven by a t ubule principal cell-specific *GAL4* line (CapaR-*GAL4*). Each transgenic fly strain containing inducible UAS-hairpin RNA elements on their chromosomes towards a single coding protein sequence was obtained from the Bloomington or Vienna *Drosophila* RNAi Center. Knockdown flies were transferred to a fresh Sodium Oxalate containing diet and the tubules assessed for concretion formation.

2.3 RNA extraction

Messenger RNAs (mRNAs) were extracted using the Qiagen RNeasy Mini extraction kit following the manufacturer's instructions. RNA was extracted from Malpighian tubules as well as from whole flies, depending on experimental requirements and detailed below.

2.3.1.1 RNA extraction from whole flies

Adult flies were collected and then homogenised using a micropestle in an eppendorf containing 1 ml of Trizol (Life Technologies, UK). The homogenate was kept at the room temperature (RT) for 5 minutes, and 200 µl of Chloroform was added to the solution. The mixed solution was centrifuged at 12000 *g* at 4°C for 15 min. The aqueous upper layer was transferred to a new 1.5ml eppendorf without touching the interface. Isopropyl alcohol (one half) was then added, followed by precipitation at RT for 10 min. The samples were then centrifuged at 12000 g and 4°C for 10 min. After removing the supernatant, the pellet was washed with 70% ice-cold ethanol and vortexed. Following centrifugation at 8000 g and 4°C for 5 min, the supernatant containing ethanol was discarded without disturbing the pellet. In order to remove any residual ethanol, the pellet was air-dried at RT for ~5 min and then resuspended in 30 µl of RNase-free water and gently mixed. Extracted RNA was immediately used for cDNA synthesis. Remaining RNA was stored at -80°C.

2.3.1.2 RNA extraction using Malpighian Tubules

Messenger RNA (mRNA) was extracted from 50-60 pairs of Malpighian tubules using the Qiagen RNA extraction kit according to the manufacturer's instructions (Qiagen, UK). All the experiments were conducted in a nuclease-free environment.

After obtaining RNA, the total mRNA concentration and purity was analysed using Nanodrop TM 1000. The concentration was measured on the assumption that an OD of 1 at 260 nm corresponds to 50 µg/ml for DNA and 40 µg/ml for RNA. The same elution solution (used in the samples) was used as a control; hence, the value was balanced to zero. The purity was checked by the ratio of

A260/280. Values of 1.8 and above for DNA and 2.0 and above for RNA were considered as of acceptable purity.

2.4 cDNA isolation

First strand cDNA (complementary DNA) was synthesised from messenger RNA using the reverse transcription reaction protocol as described by manufacturers (Qiagen, UK). The reverse transcription reaction contained: 500 ng of total RNA, 0.2 mM of each dNTP (Promega), 40 U RNase OUT (Invitrogen), 10 mM dithiothreitol (DTT), 1X first strand buffer (Invitrogen), 1X oligo-dT (IDT, U.K.), final volume made up with nuclease-free water to 19 µl. The mixture was mixed by pipetting and incubated at 42˚C for 10 min, cooled on ice for 5 min and 1 µl of Superscript II RNase H- Reverse Transcriptase (Invitrogen) was added to each reaction tube. The reaction was incubated at 42˚C for 50 min and then incubated at 70˚C for 15 min to stop the reaction. The cDNA was subsequently quantified and stored at -20˚C.

2.5 PCR

Polymerase Chain Reaction (PCR) is used to amplify specific regions from a DNA template. The area of amplification was designated using specific DNA primers 17 – 22 nucleotides in length. The DNA template was derived from gDNA, mRNA or plasmid DNA. The purpose of amplification was to assess the presence of a specific region in the template or to amplify a specific region of the template for future applications.

2.5.1 Standard PCR

This protocol was used to optimise the annealing temperature of primers used for quantitative real-time PCR. In brief, each 25 µl reaction contained 1 µl of cDNA mixed with left and right primers at a final concentration of 0.5 µM and pre-aliquoted ready-to-use DreamTaq Green PCR Master Mix (Thermo Scientific) that contained 2X DreamTaq Green buffer, dNTPs (0.4 mM each), and 4 mM $MgCl_2$ and enhanced DNA polymerase. The cycling was carried out in 0.2 ml PCR tubes using the PCR Express-Gradient thermocycler for running a gradient of

annealing temperatures across the block at the same time. A typical cycling procedure is described in **Table 2.3**.

Step	Temperature, ˚C	Time	Number of cycles
Initial Denaturation	94˚C	2-5 min	1
Denaturation	94˚C	30 s	35 -40 cycles
Annealing	55-65˚C	30 s	
Extension	72˚C	30 s	
Final Extension	72˚C	5 min	1

Table 2.3. Taq DNA polymerase PCR cycling parameters.

2.5.2 SYBR Green-based qRT-PCR

For this method, gene-specific primers were designed according to the method described in section 2.5.5, that yielded a PCR product of 150-500 bp and wherever possible spanned intron/exon boundaries of each gene of interest in order to control for possible genomic contamination. Each reaction setup contained: 10 µl of 2X SYBR Green real-time PCR master mix (Agilent Technologies), 1 µl of each primer (0.3 µM final concentration) and 2 µl cDNA, made up to a final volume of 20 µl with sterile dH_2O. The SYBR Green real-time PCR master mix which contains the mutant Taq DNA polymerase, dNTPs, Mg^{2+}, a buffer specially formulated for fast cycling, and the double-stranded DNA-binding dye SYBR Green I to detect PCR product as it accumulates during PCR. The cycling was performed used an Opticon 3 thermal cycler according to the protocol described in below **Table 2.4**.

30-40 X	Denaturation	95 ºC	10 min
	Denaturation	95 ºC	10s
	Annealing	50-60 ºC	30s
	Extension	72 ºC	30s
	Absorption reading	76 ºC	10s
	Incubation	72 ºC	5 min
	Melting curve	63 - 90 ºC	Read every 0.2 ºC

Table 2.4. SYBR Green-based qRT-PCR cycling parameters.

qRT-PCR reactions were set up in triplicates with primers of the gene of interest. A standard gene (house-keeping gene), *Rpl32* that encodes for a ribosomal protein was used to quantify the relative amount of each target gene.

Following amplification, each qRT-PCR reaction from a specific sample cDNA was analysed for its Ct (threshold cycle) value particular to the target gene and *Rpl32* gene. Relative quantification for target gene in each sample cDNA was determined by normalising target gene Ct value to its *Rpl32* Ct value. By calculating the ratio of the two compared samples' Ct values and using the $2^{-\Delta\Delta Ct}$ (Schmittgen and Livak, 2008) method, the relative fold change data of target gene between two samples were obtained . It is assumed that during this comparative analysis, the PCR efficiency of the amplicon of interest was steady over all the cycles.

The results were plotted as mean ± SEM using Graph Pad Prism 6.0 software. One-way ANOVA was used to determine the statistical significance of data where multiple samples were used, and a Student's *t*-test was carried out for paired samples of two. qRT-PCR used throughout the thesis had 3 biological replicates, and the results were consistent in all the studies.

2.5.3 Agarose gel electrophoresis

Agarose gel electrophoresis was used to determine the quality and specificity of PCR products or DNA by running it on 1% TBE agarose gels made in 0.5 % TBE, containing 0.1 µg/ml EtBr using 0.5% TBE as the electrophoresis buffer. Before loading, 6x loading dye was added to samples. The size of the samples was compared with the 1 kb DNA ladder (Invitrogen). Typically, electrophoresis was carried out at 100 V, and the DNA was visualised using a high-performance ultraviolet transilluminator (UVP, UK).

2.5.4 PCR/ Gel purification

A DNA fragment of the desired size was excised using a scalpel blade under UV illumination on the transilluminator and transferred to an Eppendorf tube,

weighed, then processed according to the Qiagen Gel Extraction Kit manufacturer's instructions.

2.5.5 Primer sequences design

Oligonucleotide primers were either designed using web source Primer3, NCBI; FlyPrimerBank, DRSC and/or using software MacVector 11.1.1 (MacVector, Inc. UK). The design of the primer pair wherever possible was either (1) extending across an intron, or (2) Some of the primers in the pair were designed across two exon boundaries.

The lyophilised primers (Integrated DNA Technologies; IDT) were resuspended in nuclease-free water as a working concentration of 6.6μM prepared from the stock dilution of 100 μM. Primers were stored at -20 ˚C until further use. The table below (**Table 2.5**) shows the list of the oligonucleotide sequences (forward and reverse primers) used in this study.

Primer	Forward	Reverse
Sip1	GCTGTTCGCTTTCGTTTCGTTTAG	TGTCCTGGTTTCACCTTCTCCG
Moe	AACGCCAAGGATGAGGAGAC	ACGCTTTGTGTTGCCCTTAC
Rpl32	TGACCATCCGCCCAGCATAC	ATCTCGCCGCAGTAAACGC
Wtrw	CTCGCAGGACCCCGTGAAC	CGGATCTTGCCCCACTTGAT
Cin	CAATACGCTTTGCTGCTGGC	TCGGCACCAACAATGCTCTG
Spat	ATGCGCAAGTACAGCGTTGA	GATCCGTCTTGATCCCCAGC
SCP2	CCGATTTCCGCAAAAAGAAGC	TCCATCATCAGGTCGTAGGTCTCC
SPoCK	TTTTCATTGAGGAACAGACGGG	CACCAGAGCAGAACCAAGAAGC
Picot	TCAACCACTTGGACCTCACACC	TGACGCACGACTACGGCTAATAC
NHE2	CACAATGTCCTGGCTGACCTTTC	CTCCACCACCGAGAGATAAAACC

Table 2.5. List of Primers used for qPCR.

2.6 Microscopy

2.6.1 Polarised light microscopy

Polarising microscopy was used to visualise stones (oxalate, phosphate, xanthine and uric acid). Among all the different stones present in the tubule, oxalate and uric acid stones are bright and white under crossed polarising filters due to their birefringent property. Meanwhile, phosphate and xanthine stones are dull and not birefringent. In order to visualise birefringent specimens, the polarised microscope is equipped with two polarisers: one between the light source and the specimen (light path), and the other one (analyser) in the optical pathway between the objective and the observation tubes. The polariser can be rotated through 360 degrees, which enables regulation of the intensity of the polarisation light **Figure 2.3**. When minimum brightness was achieved, samples were visualised for birefringent stones and vice-versa for non- birefringent stones. All the samples were imaged as per the steps mentioned below:

1. All the images were taken in the same microscope.

2. The internal and external light intensity was made constant throughout the imaging.

3. All the microscopic conditions were kept constant like the same objective magnification, exposure, gain, saturation, gamma, iris, transmitted light etc.

4. The same volume of *Drosophila* medium was used for mounting the slides so that the focus of the microscope remains constant.

All the tubules were accurately dissected in one set and images were taken approximately within a minute (since the amount of concretion might be dissolved if kept in the solution for a long time). Using this technique, Malpighian tubules were assessed for the presence or absence of stones. Tubules were dissected, and slides were prepared as described in **section 2.2.5** and quantified, as discussed in **section 2.7**.

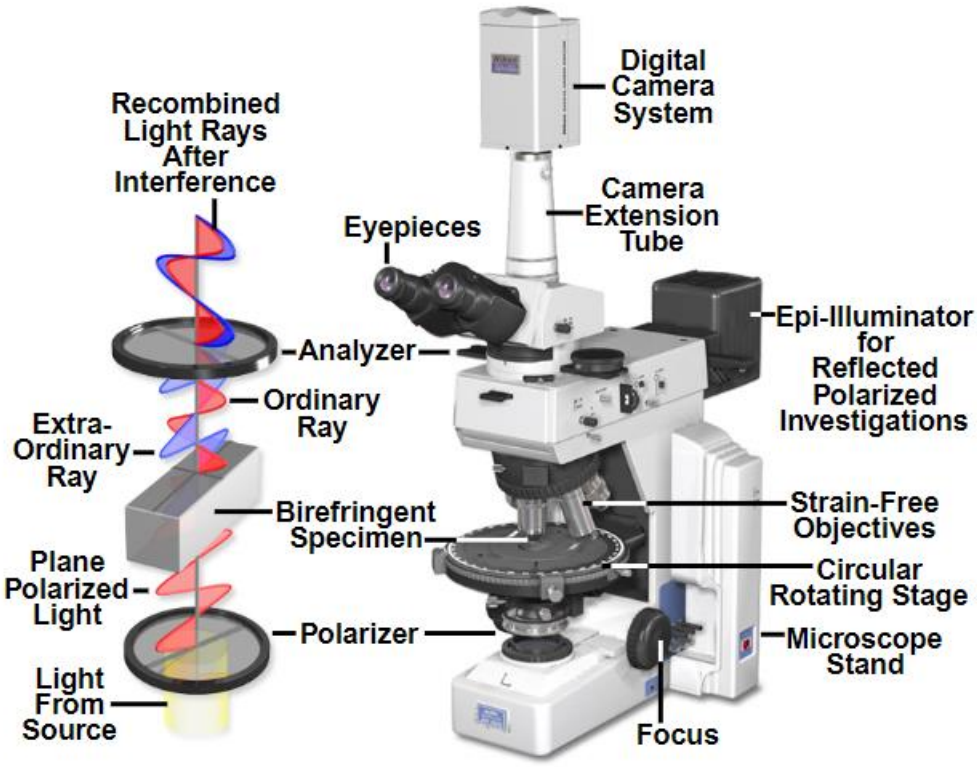

Figure 2.3. Polarized Light Microscope Configuration.

2.6.2 Confocal microscopy

Fluorescent imaging of the MTs was carried out using the LSM 800 confocal microscope system (Zeiss Technologies UK) as described previously (Cabrero et al., 2014). HeNe1 543nm laser and a 561-625 nm bandpass filter were used for imaging the Alexafluor 568. An Argon 488 nm laser and a 505-530 nm bandpass filter were used for imaging the staining. The DAPI was excited using the standard UV source (mercury lamp) and the image captured using the confocal photomultipliers. Either 40x (oil immersion) or 63x objectives was used. All the images were processed with Zen software and Adobe Photoshop/Illustrator CS 5.1.

2.7 Photoshop

Prior to the kidney stones quantification, images taken from the microscope were combined using Photoshop. Once the images were combined, the brightness and contrast of all-electron micrographs of an image was noted, and the same setting was used for all the pictures to make a consistent background

for the analysis. The images were adjusted using Photoshop CS3 version software.

2.8 Quantification of the stones

The samples prepared were viewed and imaged as per the protocol mentioned in **section 2.6.1**. The level of concretion accumulation was quantified using the public domain ImageJ software (http://rsb.info.nih.gov/ij). The process of quantification of the stones is described in detail below:

2.8.1 Quantification of the stones using image J

1. Open image using image J software

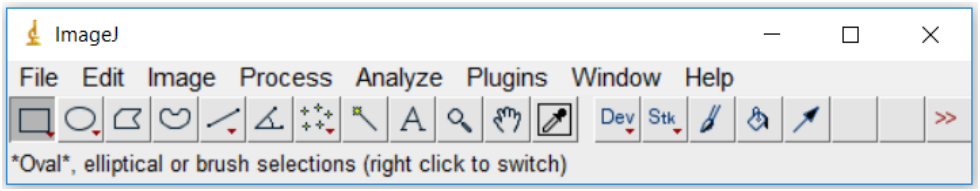

2. Change image format by choosing Edit->Type->32 bit

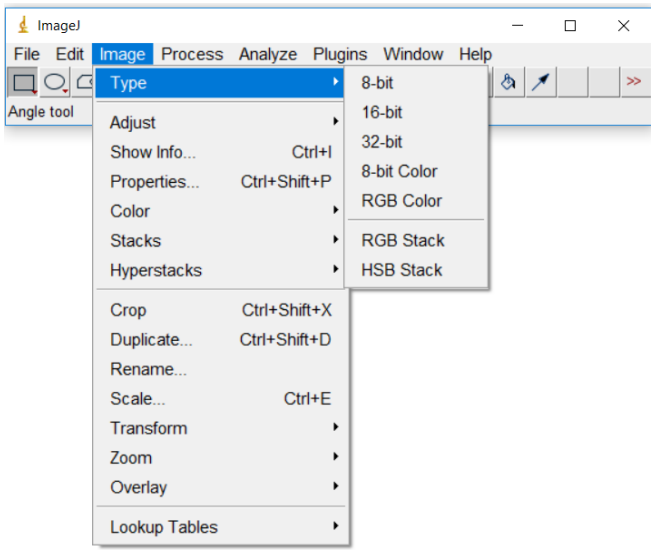

3. Make invert image by choosing Edit->Invert

4. Using “Freehand selections” icons on the toolbar, outline the tubule

5. Go to Analyze->Histogram

6. Make sure “use min/max” is marked. You do not have to change other parameters

7. Click OK

8. Write down Min and Max values (for example min:81, max:220)

9. Close the window

10. Go the Analyze->Histogram again

11. Deselect “use min/max” box

12. Enter min and max values obtained in (8) (for example min:81, max:220)

13. Use the max-min value for Bins (for example 220-81=139)

14. click OK

15. Distribution with Bin width=1 achieved

16. Write down “Count”, which means total tubule area, Mean=average intensity, Std Dev= standard deviation. However, the background intensity needs to be subtracted to get a real mean value. The background is the intensity obtained from an area without tubule on the image.

17. Click “Copy”

18. Open the excel file then “Past”, which will go past all the data on the excel file. The left column is intensity; the right column is the number of pixels corresponding to that intensity, which means an area.

19. After subtracting background, the threshold intensity needs to be determined. We assume that if the intensity is above the threshold, it is concretion. The threshold is determined using a tubule obtained from a

wildtype fly tubule (CS) fed on a normal diet. We decided the threshold value to be “mean+3 x SD”.

20. Sum the pixel number above the threshold

21. Now the total area (From (16)) and the area above the threshold (=concretion) (From (20)) was obtained.

22. Now the tubule area filled with concretion is calculated (%).

Note: This technique was used for birefringent stones. However, in the case of non-birefringent stones, the images are not inverted (step 3); instead, follow all the same process except this step. All the images were taken in the white background instead of dark.

2.8.2 Quantification of the stones using Fiji

1. Open FIJI and Open the .CZI File for the tubule to be analysed (the computer will ask if you would like to Run FIJI; click Run).

2. Go to Image → Type → 8-Bit (this will allow the image to be edited).

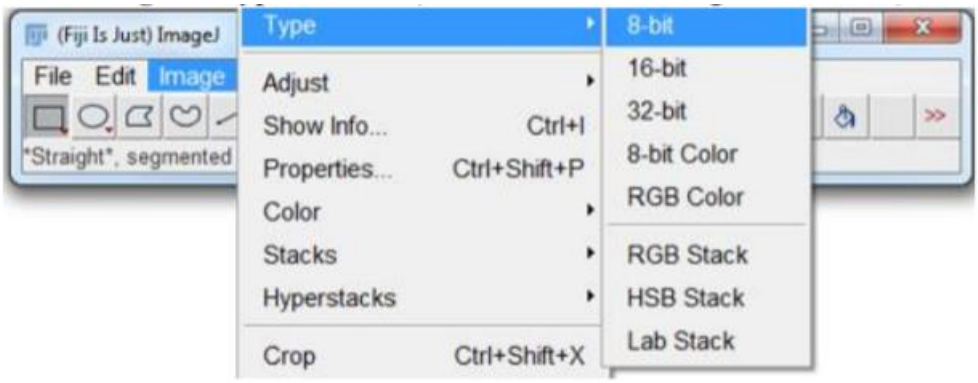

3. Use the straight-line tool to measure the first 600 µm of the tubule.

4. Mark off the regions that are not to be included in the crystal analysis using the Freehand selections tool and Ctrl + F to paint the selected area(s) black.

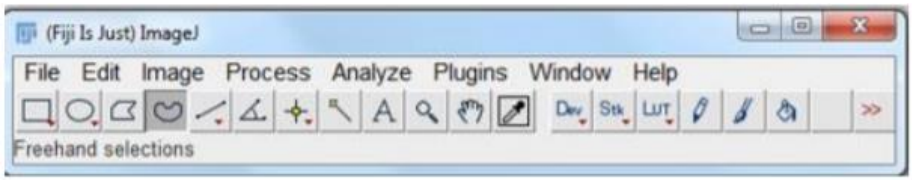

5. Go to Image → Adjust → Brightness/Contrast (or use Ctrl + Shift + C) and move the Minimum slider (the top slider) until most if not all of the tubule tissue disappears leaving only the birefringent crystals. If any of the tubule tissue is still visible select it with the Freehand selections tool and use Ctrl + F to paint the selected area black.

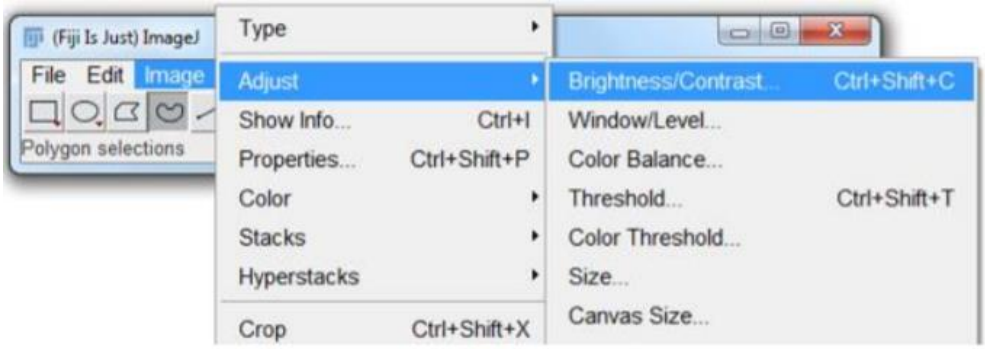

6. Go to Image → Adjust → Threshold (or use Ctrl + Shift + T) and click Apply. If needed how many shades of white/grey are recognised as crystals can be adjusted using the top slider (this step is used to make the image binary so that there is only white and black).

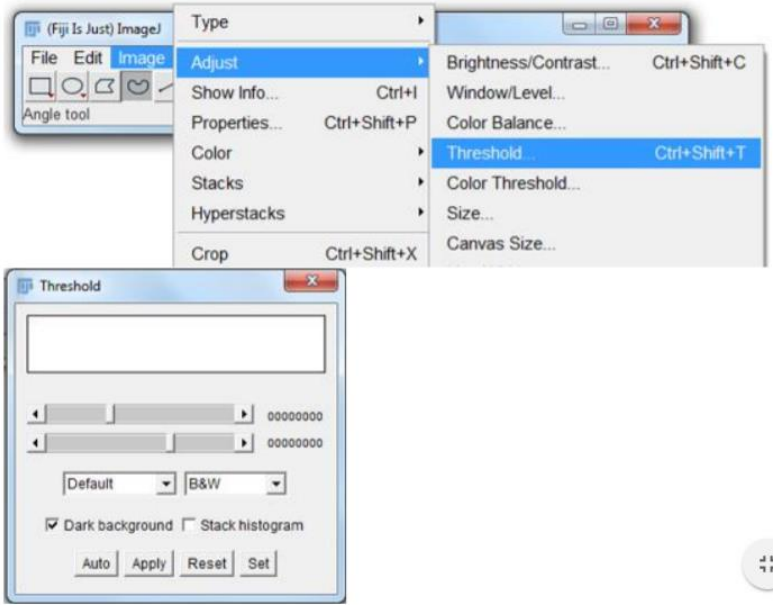

7. Go to Analyse → Analyse Particles.

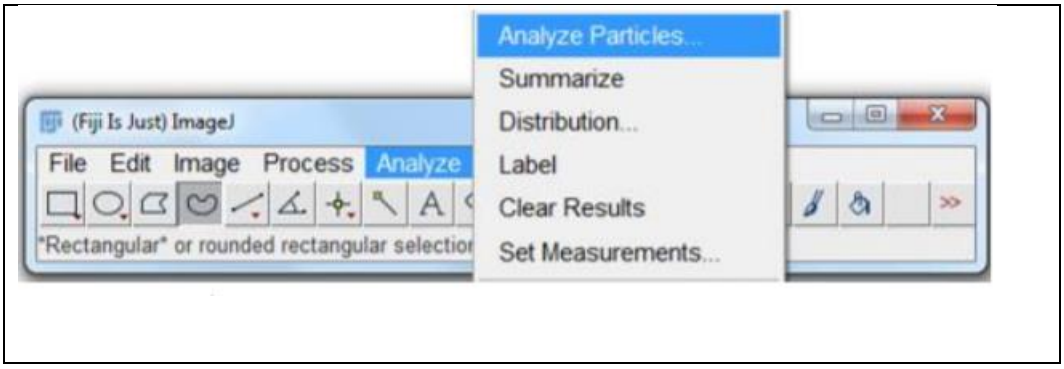

8. Set the top blank to 2 µm (this is the minimum size partcle that will be analysed). Set the Show dropdown to Overlay Masks (this will mark the crystals/particles counted with a teal mask overlay). Check Display Results, Clear Results, Summarize and Include Holes checkboxes. Click OK.

9. Check the teal overlays to make sure only the desired crystals were indeed analysed. Save both the Summary and the Results for further analysis.

2.9 Biochemical assays

2.9.1.1 Determination of concentration of uric acid

The MTs concentration of uric acid was quantified using the Quantichrome Colorimetric Uric acid kit (DIUA-250, BioAssay Systems) according to the manufacturer's instruction. Six adult MTs per sample were homogenised in 12 µl of Tween-20 (Sigma-Aldrich), and 200 µl of working reagent was added to 5 µl of each tubule sample in 96 well plates (3 replicates for each sample). Samples were incubated for 30 minutes at room temperature and the optical density measured at 590nm using a Mithras LB940 automated 96-well plate reader (Berthold Technologies). Data were analysed using the MikroWin software.

Detailed method:

1. 5 flies were homogenised in 100 µl tween (or 6 tubules were suspended in 12 µl if measuring tubules)

2. 10 volumes of reagent A and 1 Volume of reagent B and 1 Volume of reagent C was mixed as per the protocol (all the reagents are provided in the kit).

3. All the standards were set up in the following concentration: (10-5-2.5-1.25-.625 mg/dL).

4. 5 µl of standards and samples were added to clear bottomed 96 well plates. (sample no. can be increased depending on the no. of replicates required).

5. 200 µl of working reagent was added to the mixture, and the mix was tapped.

6. The mixture was incubated for 30 minutes at RT and absorbance measured at 590 nm.

CALCULATION:

The uric acid concentration of the sample is calculated as

$$= \frac{OD_{SAMPLE} - OD_{BLANK}}{OD_{STANDARD} - OD_{BLANK}} \quad X\ 10\ (mg/dL)$$

OD_{BLANK}, $OD_{STANDARD}$ and OD_{SAMPLE} are OD590 nm values of Blank, Standard and Sample, respectively. It is not necessary to prepare a calibration curve, because the concentration of the provided standard lies within the linear range.

Normal serum uric acid values: 1.0 to 7.0 mg/dL.

Conversions: 1 mg/dL uric acid equals 59.5 µM, 0.001% or 10 ppm.

2.9.1.2 Determination of concentration of phosphate

The MTs concentration of phosphate was quantified using the Quantichrome Colorimetric phosphate kit (DIPI-500, BioAssay Systems) according to the manufacturer's instructions. Thirty adult fly MTs per sample were homogenised in 50 µl of nitric acid (Sigma-Aldrich), and 100 µl of working reagent was added to 50 µl of each tubule sample in 96 well plates (3 replicates for each sample). Samples were incubated for 30 minutes at room temperature and the optical density measured at 620 nm using a Mithras LB940 automated 96-well plate reader (Berthold Technologies). Data were analysed using the MikroWin software.

Detailed method:

1. 60 MTs were homogenised in 50 µl 30% HNO_3. A range of HNO_3 concentrations was tried, and this was found to be the optimal concentration.

2. Transfer 50 µL distilled water ("Blank"), Standard and samples in to duplicate wells of a clear bottom 96-well plate. All the standards were set up in the following concentration: (0.28, 0.14, 0.07, 0.035, 0.0175 mg/dl).

3. 100 µl of working reagent was added in the mixture, and the mix was tapped.

4. The mixture was incubated for 30 minutes at RT and measure absorbance at 620nm.

CALCULATION:

The phosphate concentration of sample is calculated as

$$= \frac{OD_{SAMPLE} - OD_{BLANK}}{OD_{STANDARD} - OD_{BLANK}} \quad X\ 0.28\ (mg/dL)$$

OD_{BLANK}, $OD_{STANDARD}$ and OD_{SAMPLE} are OD_{620nm} values of Blank, Standard and Sample, respectively.

Conversions: 1 mg/dL Pi equals 105.3 µM, 0.001% or 10 ppm.

2.10 Statistics

Unpaired two-tailed Student's *t*-test and ANOVA with Dunnett's post hoc test were used for the statistical comparison between two independent groups and more than two independent groups, respectively. For the statistics assays, Prism 6 (Graphpad, CA, USA) was used for data analysis and statistical significance was tested.

2.11 Solubility assay

Adult flies were dissected in Phosphate Buffered Saline (PBS, pH 5), and intact MTs were mounted on glass-slide in PBS adjusted to pH 5 to 10, and immediately imaged using a microscope (Axioskop 2, Zeiss) under polarised light. Images were taken every minute for 30 min and were quantified once the time frame was completed. Imaging conditions were maintained as described previously in **section 2.6.1**. Total stones present within the tubule at 0 min were considered 100% and the stones accumulated after 1, 10, 20 and 30 min were quantified with respect to the initial quantity.

2.12 Immunocytochemistry

Immunocytochemistry (ICC) staining was performed to determine the cell-type localisation of the expressed protein within the *Drosophila* MTs. All the experimental protocol was followed as previously described in (MacPherson et al., 2001). Malpighian tubules were dissected in Schneider's medium and transferred to a 1.5 ml Eppendorf containing 100 µl of PBS. This was aspirated with care taken not to disturb the tubules. 200 µl of fixation solution (4% (w/v) paraformaldehyde in PBS) was then added for 30 min. The fixation solution was removed, and the tubules were washed three times in PBS every 30 min. The tubules were then permeabilized for 30 min with PBS, 0.5% Triton (v/v), 0.15M NaH_2PO_4, 0.1% Sodium Azide (PBTA) (w/v), changing every 10 min. The tubules

were then incubated in PBS, 0.3% (v/v) Triton X-100, 0.5% (w/v) NGS (PAT) for 3 h at RT. Incubation with the primary antibody was carried out overnight at 4˚C. Tubules were then washed 4 x in PAT for 2 h and then blocked with PAT for 3 h. Incubation with secondary antibody was performed in PAT overnight. The tubules were washed three times with PBTA for 30 min each wash. Tubule cell nuclei were stained with DAPI(500 ng/ml in PBS) for 2 min and washed three times with PBTA for 30 min each wash. Finally, the tubules were then washed 2 x 10 min in PBS, mounted in Vectashield (Vector labs, U.K.), and sealed with glycerol/gelatin (Sigma). The samples were viewed using confocal microscopy (**details in section 2.6**).

2.13 Antibody purification

2.13.1 Isolation of IgG fraction from immune serum

The antibody was purified as detailed in (Day et al., 2008). A HiTrap Protein A HP" column (Amersham) was flushed with 5 ml 0.1 M glycine pH 2.5, passed through at ~2ml/min, then equilibrated with 30 ml of PBS. 5 ml of immune serum was filtered through a 0.45 μM filter and then syringed through the column to bind. The column was washed with 30 ml of PBS, and the IgG fraction was eluted with 17 ml of 0.1 M glycine, pH 3.0. The first 2 ml were discarded, and the subsequent 15 ml flow-through was collected in a 50 ml Falcon tube containing 1.5 ml 1 M Tris-HCl pH 8.0. The column was then washed with 5 ml 0.1 M glycine pH 2.5, and stored, sealed, containing ethanol, at 4˚C. The absorbance at 280nm was read to confirm IgG elution, and the IgG eluate was dialysed overnight against a large volume of PBS in a Slide-A-Lyzer dialysis cassette (Pierce).

2.13.2 Preparation of affinity columns

The bottom cap was fitted to a 10 ml polypropylene column (Pierce) and the column filled with deionised water. A frit was pushed to the bottom of the column using the plunger from a disposable syringe. The water was drained by removing the end cap, and 5 ml of Sulfolink slurry (Pierce) was added. When the slurry had sedimented, the slurry buffer was removed down to the surface of the gel and 2 x 25 ml of 50 mM Tris-HCl, 5 mM Na-EDTA pH 8.5 was run

through the column, with the end cap replaced when the buffer reached the slurry. 1 mg of the antibody-specific peptide was dissolved in 4 ml of 50 mM Tris- HCl, 5 mM Na-EDTA, and added to the column. The top cap was added, and the column subjected to the rotation for 15 min at 4˚C. The column was left upright for 45 min, following which the column was drained. 15 ml of 50 mM cysteine in 50 mM Tris-HCl, 5 mM Na-EDTA was added to the column and rotated for 15 min at 4˚C. The column was set upright and allowed to settle for 45 min. The top cap was removed, and the top frit fitted just above the level of the gel. The end cap was removed, and the column drained. 60 ml of 1 M NaCl was then run through the column, followed by 50 ml of PBS and then 40 ml of 0.05 % (w/v) sodium azide in PBS keeping the level above the gel. The end caps were fitted and the column stored at 4˚C until use.

2.13.3 Affinity purification of antibodies

The affinity column was brought to room temperature, and the sodium azide in PBS was drained. The column was equilibrated by passing through 30 ml of PBS, and the IgG fraction was passed through in 5 ml batches. Next followed a wash with 30 ml of PBS and finally, the antibody was eluted with 0.1 M glycine, pH 3.0. A volume of 12 x 1 ml fractions were collected into 12 x 1.5 ml Eppendorfs containing 100 µl Tris-HCl pH 8.0. To determine the yield the absorbance at 280 nm of each fraction was measured and fractions with readings greater than 0.05 were pooled and dialysed overnight against PBS with 0.01 % (w/v) sodium azide. The absorbance at 280 nm was again taken in order to ascertain the final yield using the equation:

Antibody concentration (mg/ml) = OD 280 x 1.35 mg/ml

Aliquots of the antibodies were made and frozen at -20 ºC until use.

2.14 Antibodies used in the study

Tubules were incubated with markers such as 4’,6-diamidino-2-phenylindole (DAPI; Sigma-Aldrich, 1 µg/ml) and Rhodamine-Alexa-633-coupled phalloidin (Thermo Fisher Scientific, 1:100). The primary and secondary antibodies used are listed below. (**Table 2.6**).

Antibody and Source	Concentration and Use
Anti-NHE2 (long isoform), rabbit	1:300 (ICC)
Anti-NHE2 (short isoform), rabbit	1:300 (ICC)
Goat-Anti-Rabbit-Alexa Fluor 488 (Thermo Fisher Scientific)	1:1000 (ICC)
Goat-Anti-Rabbit-Alexa Fluor 546 (Thermo Fisher Scientific)	1:1000 (ICC)
Anti-Rabbit- Alexa Fluor 633 (Sigma)	1:600 (ICC)
Anti-Sip1, Rabbit	1:200 (ICC)
Anti-phosphorylated-Moesin, Rabbit	1:200 (ICC)
Anti-Rabbit-HRP (Amersham)	1:2000 (Immunoblotting)
Anti-Tubulin (Sigma)	1:2000 (Immunoblotting)

Table 2.6. List of antibodies used in the experiment.

2.15 Western blotting

2.15.1 Preparation of sample

2.15.1.1 Preparation of S2 cell lysates

For S2 cell transfections, each transfection was viewed under 20x magnification to assess cell membrane integrity at every stage (as a measure of survival) and resuspended using a transfer pipette. Each transfection was split into two 1.5 ml eppendorfs and spun down for 4 min at 2000 rpm in a Thermo Heraeus centrifuge. The supernatant was removed, and the cell pellets were frozen in a -80°C freezer. When needed, the pellets were resuspended in IGEPAL buffer (150 mM NaCl, 50 mM Tris, 1% IGEPAL) containing protease inhibitor cocktail (Sigma-Aldrich, UK). The lysate was then sonicated on ice. An equal volume of Laemmli 2x buffer (4% SDS, 5% β-Mercaptoethanol, 20% glycerol, 0.004% bromophenol blue, 0.125 M Tris-HCl) was then added, and the samples boiled in a boiling water bath for 3 min.

2.15.1.2 Preparation of sample from MTs

Tissue sample (300 tubules) was transferred into 100 µl of Tris-Lysis buffer (2% (w/v) SDS, 70 mM Tris, pH 6.8) containing 1 µl of protease inhibitor cocktail (Sigma-Aldrich, UK), in a 1.5 ml Eppendorf tube. Next, the sample was homogenised using a hand-held pestle followed by 3 x 1-sec homogenisations with a Microson Ultrasonic Cell Disrupter. The sample was then centrifuged at 14000 g for 10 min to remove debris and the supernatant transferred to a new tube. Samples were stored at -80ºC until the Bradford assay and Western blot were performed.

2.15.2 Bradford assay

The Bradford assay was performed on a 96 well plate. Standards from 0-5 µg (typically 0 µg, 0.5 µg, 1 µg, 1.5 µg, 2 µg, 3 µg, 4 µg, 5 µg) were generated in triplicate using Bovine Serum Albumin (BSA), Fraction V (Roche) in a volume of 50 µl distilled H_20. For each protein sample, 1 µl of the sample was added to 49 µl H_20 in triplicate. To each well, 200 µl of a well mixed 1 in 5 dilutions of Bio-rad protein assay dye reaction concentrate (Biorad) in H_20 was added. Absorbance at 590 nm was read using a plate reader; Quanta smart software was used to generate a standard curve, and from this ascertain the concentration of each protein sample.

2.15.3 Sodium Dodecyl Sulfate Polyacrylamide Gel Electrophoresis

10 or 15 well-resolving gels between 6-20% were prepared according to the size of the protein of interest, as according to (Joseph and David, 2001). Electrophoresis was performed in a Biorad Miniprotean 3 Cell electrophoresis system. Samples were run at 50 V until the dye front had settled at the bottom of the stacking gel, and then at 130 V for 1 hour. Prestained Benchmark Ladder (Invitrogen) was used to determine the exact size of proteins.

2.15.4 Coomassie staining of PAGE gels

PAGE gels were fixed by brief treatment with 40% distilled H_20, 10% acetic acid, 50% methanol on a horizontal shaker. The gel was then added to the same

mix but with the addition of 0.25% by weight Coomassie Brilliant Blue R-250 and incubated for 4 hours to overnight. The gel was then washed in 67.5% distilled H_2O, 7.5% acetic acid, 25% methanol on a horizontal shaker, the solution changed until the excess dye was removed, and the protein bands were clear.

2.15.5 Transfer

Hybond P was incubated in methanol for 5 min and then rinsed in distilled H_20. Western blotting was carried out according to Novex Xcell II Blot Module (Invitrogen) instructions. The transfer was carried out at 60 V for 1 hour, with ice packs to prevent overheating.

2.15.6 Ponceau S Staining

To visualise protein on the membrane, the membrane was rinsed in methanol, then washed in PBST. The membrane was then incubated for 5 min in PBST (PBS with Tween 20)-10% (v/v) Ponceau with rocking, scanned, rinsed in methanol to remove the stain, and then washed in PBST.

2.15.7 Development

The membrane was briefly rinsed with PBS with 0.1 % (v/v) Tween 20 (PBST), and blocking was performed with PBST containing 5% Marvel Milk (w/v), for three hours at RT, or overnight at 4°C. The membrane was then rinsed in PBST. Incubation with a primary antibody was performed in a block with a suitable amount of primary antibody for 1 hour.

The membrane was then extensively washed for an hour with frequent changes of PBST. The membrane was then incubated with an HRP-conjugated secondary antibody in the block for 1 hour. The membrane was then extensively washed for an hour with frequent changes of PBST. All steps were performed on a flatbed shaker.

2.15.8 Signal detection

Chemiluminescence detection was performed using the ECL Western Blotting analysis system (Amersham Pharmacia) following the manufacturer's instructions. Equal volumes of reagent 1 and reagent 2 were mixed and added to a sheet of Saran wrap. The filter was added protein side down and incubated for 1 min. The membrane was then wrapped in Saran Wrap, added to a cassette, and exposed to ECL film (Amersham Pharmacia), before development in an X-OMAT film processor.

2.16 Co-Immunoprecipitation

For Co-IP experiments, 200 tubule tissues were dissected as described in **section 2.2.5**. The Dynabeads™ Co-Immunoprecipitation Kit (Invitrogen, UK) was used to carry out IPs. All the experiment was conducted according to the manufacturer's protocol. In brief, following immobilisation of a particular antibody, the coupled beads were used, and the buffers supplied in the kit for co-immunoprecipitation (co-IP) of proteins, intact protein complexes, or intact protein-nucleic acid complexes and to elute those complexes from the beads. In addition to Dynabeads®, all the buffers were supplied in the kit which was required for efficient antibody coupling, gentle washing, and elution of the co-isolated protein complexes. Once eluted, the protein was loaded onto a standard SDS-PAGE gel and ran as described in **section 2.15**. The samples were developed using the western blot technique.

2.17 Recipes of solutions used in the experiment

2.17.1.1 *Drosophila* Schneider's medium

Commercially available *Drosophila* Schneider's medium (Invitrogen, UK), which resemble the composition of the fly hemolymph, was used throughout the experiment to dissect the flies unless otherwise mentioned. The composition of the Schneider medium is:

Amino Acids (mM)	**Inorganic Salts (mM)**
• Beta-alanine: 5.6 • L-arginine: 2.3 • L-asparagine 0.3 • L-aspartic acid: 4.0 • L-cysteine: 0.5 • L-glutamic acid: 5.4 • L-glutamine: 12.3 • Glutathione: 0.1 • Glycine: 3.3 • L-histidine: 2.6 • L-isoleucine: 1.5 • L-leucine: 1.1 • L-lysine: 11.3 • L-methionine: 5.4 • L-phenylalanine: 1.5 • L-proline: 14.8 • L-serine: 2.5 • L-threonine: 3.5 • L-tryptophan: 1.0 • L-valine: 2.6	• Calcium Chloride ($CaCl_2$-$2H_2O$): 4.1 • Magnesium Sulfate ($MgSO_4$-$7H_2O$):37 • Potassium Chloride (KCl):21.5 • Potassium Phosphate monobasic (KH_2PO_4):5.0 • Sodium Bicarbonate ($NaHCO_3$) • Sodium Chloride (NaCl):35.9 • Sodium Phosphate monobasic (NaH_2PO_4-$2H_2O$):2.8
	Other Components (mM) • Alpha-Ketoglutaric acid: 1.8 • D-Glucose (Dextrose): 11.1 • Fumaric acid: 0.9 • Malic acid: 0.7 • Succinic acid: 0.8 • Trehalose: 5.3 • Yeastolate: 2g • FCS 18%

2.17.1.2 Buffers

Phosphate Buffer Saline

The PBS solution was prepared by mixing the recipes enlisted below. All the chemicals were mixed, and the final volume of 1 L of pH 7.4 was prepared.

- 137 mM NaCl
- 2.7 mM KCl
- 10 mM Na_2PO_4
- 2 mM KH_2PO_4 (pH 7.4)

Lysis RIPA Buffer (in H_2O)

100 mM Tris-Cl (pH 7.4), 300 mM NaCl
- 10% Triton®X100
- 10% Na deoxycholate
- 200mM Phenylmethanesulfonyl fluoride (in isopropranol)

- 10% SDS
- Pierce® protease and phosphatase inhibitor (Thermo)
- 0.01M EDTA (pH 7.4)

Transfer Buffer (in 1 litre of H_2O)

- 20 % (v/v) Methanol
- 14.4 g Glycine
- 3 g Tris Base

Tris/Borate/EDTA Buffer

- 90 mM Tris
- 90 mM boric acid (pH 8.3)
- 2 mM EDTA

Chapter 3 Screening and identification of genes involved in kidney stone formation

3.1 Summary

This chapter describes identification and selection of genes which might be involved in kidney stone accumulation. Kidney stone disorder encompasses a wide range of clinical phenotypes and is genetically heterogeneous. It arises from mutations of the genes which might be effective targets for understanding the mechanisms involved in kidney stone formation. The introduction to this chapter describes the list of genes which are involved in different physiological functions and specifically for the transport of ions. Calcium, phosphate and urate co-transporters are conspicuous candidates among the hits. However, until now, there has been no study regarding a systematic screening of these genes for their involvement in oxalate stone formation. The results presented in this chapter confirms the list of hits and opens an idea to develop a molecular strategy to understand the role of those genes in mineralisation. Crucially, the role of the genes in calcium oxalate stone formation was demonstrated by feeding control and knocked down flies with different dose of sodium oxalate. The particular genes were knocked down using the *UAS/GAL4* system, and RNAi knocked down efficacy was confirmed by qPCR. Taken together, genetic interventions to inhibit the function of the genes and observe their decisive role in calcium oxalate stone formation confirm a critical role of the gene in driving the process of heterogeneous nucleation that eventually leads to stone formation. Our findings open a novel perspective on the aetiology of urinary stones and related diseases, which may lead to the identification of new preventive and therapeutic approaches.

3.2 Introduction

Calcium oxalate (CaOx) is the predominant type of kidney stone, occurring in the majority of the kidney stone population. Interestingly, the formation of calcium oxalate crystals is not limited to individuals who end up developing kidney stones, but several studies have confirmed the existence of calcium

oxalate crystals also in the urine of non-stone formers. Currently, the general consensus is that calcium oxalate crystals in urine appear through a heterogeneous, not homogeneous, nucleation, where the numerous components found in various concentrations in the kidney make heterogeneous nucleation more likely. The identity of materials acting as nidi for kidney stone growth remains unclear. Hence, researchers are searching for a model which can mimic the actual pathogenesis of the human stone disease and allow genetic manipulations with the convenient observation of results as well as being cost-effective and easy to breed (Kovshilovskaya et al., 2012, Miller et al., 2013, Tzou et al., 2016a).

Previous studies have shown that, among different model organisms, oxalate metabolism of human is almost identical to rats (Khan, 1997, Liebow et al., 2017). Kidney stones in humans and hyperoxaluric rats are located on renal papillary surfaces and consist of an organic matrix and crystals of calcium oxalate and/or calcium phosphate (Finlayson, 1978, Robertson and Peacock, 1980). The disease is experimentally induced in rats, either by the administration of excess oxalate or exposure to the toxin ethylene glycol (EG), hydroxyl-L-proline (HLP), sodium oxalate (NaOx), or various nutritional manipulations (Khan, 1991, Khan and Hackett, 1987). A rat model of calcium oxalate nephrolithiasis can be used to investigate the mechanisms involved in human kidney stone formation.

Medical treatment prevention strategies for calcium oxalate nephrolithiasis, in the last two decades, has remained stagnant based on an understanding of the underlying aetiology of the disease (Ali et al., 2018). Current studies show that various drugs like potassium citrate and thiazide diuretics are active agents in the prevention of calcium oxalate stone formation in hypocitraturia and hypercalciuria states (Qaseem et al., 2014, Reilly et al., 2010). However, the progress of the development of new drugs has been limited due to a lack of suitable pre-clinical models that reliably recapitulate the pathophysiology of this disorder. Recent work performed by Hirata and colleagues has shown that *Drosophila* fed with ‘moderate to strong’ (0.1% -1%) doses of sodium oxalate generate CaOx crystals in Malpighian tubules (Hirata et al., 2012, Tsai et al.,

2008). Other studies have also shown that flies can be fed with ethylene glycol (EG) or hydroxyl-L-proline (HLP) to induce oxalate stones (Chen et al., 2011).

3.2.1 Genes involved in stone formation

Certain genes could be predicted to be involved in stone formation. Several genes have been implicated in stone formation (Miller et al., 2013) for e.g., oxalate co-transporters (*SLC26A6*) (Hirata et al., 2012), xanthine dehydrogenase (*xdh*) (Chi et al., 2015, Wang et al., 2009), calcium transporters and zinc transporters (Chintapalli et al., 2012a). In order to assess the involvement of different genes in calcium oxalate stone formation, we screened different genes, via reverse genetic studies in an organotypic context, by visualising and quantifying calcium oxalate stone burden in the *Drosophila* model of calcium oxalate nephrolithiasis. This led to the identification of genes with a possible role in stone formation, allowing us to perform further *in vivo*, physiological and genetic assays. While the fly model may not fully recapitulate mammalian calculi formation processes, we successfully identified genes that, when knocked down, were highly effective in halting calculus formation. This approach indicates that other novel genes can be identified in a similar manner due to the primarily acellular development of kidney stones.

In this study, it was initially planned to screen RNAi and/or mutant panels for genes that increase or decrease the rate of oxalate stones formation and to seek homologues human candidate gene loci. Genes were specifically searched based on three criteria:

a. Genes that had not been previously studied in the context of stone formation, but which had predicted functions in kidney stone formation.

b. *Drosophila* genes with human homologues that had been identified and their function characterised in mineralisation.

c. Genes with enriched expression in Malpighian tubules (MTs).

d. *Drosophila* RNAi, mutant stocks and resources that were already available.

The *Drosophila* homologues were investigated to determine the extent of gene characterisation, and any resources which could be utilised in this study. Based on previous gene characterisation and the availability of *Drosophila* resources, twenty different *Drosophila* RNAi lines corresponding to eleven homologues gene-pairs were selected, and the list of genes is summarised in **Table 3.1**.

S. N.	Genes	Tubule enrichment		Functions
	Name	Larvae	Adult	
1	*Carbonic anhydrase (CAH1); CG7820*	1082.7	978.6	zinc ion binding; carbonate dehydratase activity.
2	*Calcium Binding Protein (Scp2); CG14904*	3962.8	3687.3	GTPase activity Calcium ion binding
3	*Sodium Phosphate symport (NaPiT); CG10207*	1490.9	2613.8	Phosphate transporter
4	*Calcium Pump (SPoCK); CG32451*	28	33	Mg and Ca transporting ATPase activity
5	*Trp-like calcium channel (water witch); CG31284*	261.6	715.1	Cation channel activity Calcium channel activity
6	*UAT; urate transporter CG11374*	8.9	7.5	Galactoside binding, Urate transmembrane transporter activity
7	*Spat; CG3926*	2567.9	1682.1	serine-pyruvate transaminase activity; alanine-glyoxylate transaminase activity
8	*Cinnamon MOCS3; CG2945*	NA	NA	Molybdenum Cofactor synthesis
9	*Dihydropterin deaminase; CG18143*	88.3	193.2	Guanine deaminase activity, Zinc ion binding
10	*MOCS1; CG33048*	25	88	Molybdenum Cofactor synthesis
11	*Sry interacting protein (Sip1); CG10939*	171	369	scaffold and cytoskeletal linker proteins

Table 3.1. List of genes selected for the initial screening. The expression level of the genes in MT was obtained from FlyAtlas (Chintapalli et al., 2007, Leader et al., 2017).

These candidates are described more fully in the following paragraphs.

3.2.1.1 Carbonic anhydrase (CAH1); CG7820

The *carbonic anhydrase* (or *carbonate dehydratases*) are a group of enzymes that catalyses the interconversion between carbon dioxide and water and the dissociated ions of carbonic acid (i.e. bicarbonate and hydrogen ions) (Supuran et al., 2003). Carbonic acid dissociates spontaneously to release protons, which are essential for creating the acidic environment required for the dissolution of bone minerals in the resorption lacunae (Sly et al., 1983). There are 14 known human *carbonic anhydrase isoenzymes* (CAs), and they differ in tissue distribution, subcellular localisation, kinetics and sensitivity to various carbonic anhydrase inhibitors (Shah et al., 2004). Carbonic anhydrase is an essential enzyme for brain, kidney and bone physiology.

Carbonic anhydrase II (CA II) is one of the most widespread of the *CA* isozymes and one with the highest catalytic activity. It is a cytoplasmic isozyme expressed in a variety of cell types in different tissues. The physiological functions of *CA II* include pH regulation, CO_2 and HCO_3^- transport, and production of aqueous humor, cerebrospinal fluid, gastric acidity and pancreatic secretions (Pushkin et al., 2004). The only known inherited deficiency of a carbonic anhydrase of clinical significance is the *CA* II deficiency syndrome, which is inherited as an autosomal recessive trait. It also assists in metabolic pathways such as gluconeogenesis, lipogenesis, ureagenesis and bone resorption and calcification (Mboge et al., 2018). The clinical manifestations include osteopetrosis, renal tubular acidosis, and cerebral calcification. Additional clinical features of the disease include developmental delay, short stature, a history of multiple skeletal fractures by adolescence, and cognitive defects varying from mild learning disabilities to severe mental retardation (Alhuzaim et al., 2015).

Further patients with *CA* deficiency are found to have mixed-type renal tubular acidosis with other features of carbonic anhydrase deficiency. Hence, we knocked down *CG7820* in PCs of *Drosophila* MTs to observe its impact on stone accumulation.

3.2.1.2 SCPs (CG14904)

Sarcoplasmic calcium-binding proteins (SCPs) are proteins that participate in calcium cell signalling pathways and play essential roles in many cellular processes (Hermann and Cox, 1995). SCPs have specific domains that bind to calcium and are known to be heterogeneous. Since Ca^{2+} is an important secondary messenger, it can act as an activator or inhibitor in gene transcription (Ikura et al., 2002). SCPs are found exclusively in invertebrates and have been identified in crustaceans, insects, annelids, molluscs, cephalochordates and other groups (Hermann and Cox, 1995).

SCPs have been selected evolutionarily with a range of affinities, kinetics and capacities to intervene in cell-specific Ca^{2+} signals (Fernández-Boo et al., 2016). A transient rise of the intracellular Ca^{2+} concentration is achieved by the entrance of Ca^{2+} ions either through the plasma membrane from the external compartment via voltage, ligand or stretch-activated ion channels or by being released from various internal stores (endoplasmic/sarcoplasmic reticulum, mitochondria, etc.) (Gees et al., 2010). The rise and fall of the cellular Ca^{2+} concentration or in localised areas within the cytoplasm play a key role in the activation of membrane conductance, secretion, contraction, regulation of enzymes.

Renal calcium-binding proteins have been identified in several biological systems. Previous studies have reported excess excretion of calcium-binding proteins in the kidney leads to the accumulation of the stone formers (Ratkalkar and Kleinman, 2011, Alelign and Petros, 2018). Calcium-binding proteins, as well as molecules like sialic acid, carboxy glutamic acid and phosphatidic acid, allow high local concentrations of calcium inside the cell in hyperoxaluric conditions (Aggarwal et al., 2013). Using calcium oxalate, the existence of CaOx binding protein has been demonstrated in several rat tissues (Selvam and Kalaiselvi, 2003), and the kidney showed the maximum binding activity among the various tissues studied. Renal medulla exhibited higher CaOx binding activity than papilla or cortex. All the above-mentioned calcium oxalate binding proteins are located in different membranes of renal cells which may serve the function of carrier proteins for the transport system.

Purified mitochondrial oxalate binding proteins derived from rat and human kidney showed a promoter effect on CaOx crystallisation (Selvam and Devaraj, 1997). Among them, rat protein showed higher promoter activity, and CaOx binding protein antibody inhibited both oxalate binding activity and crystal growth *in vitro*, suggesting that the oxalate binding site plays a vital role in crystal growth. Hence, we knocked down *CG14904* in *Drosophila* MTs to observe its impact on stone accumulation.

3.2.1.3 NaPi-T (CG10207)

Human has three types of membrane-bound phosphate transporters: type I: *SLC17A1-9, type II: NPT2a*, *NPT2b*, and *NPT2c*, and type III: *Pit1* and *Pit2; which* are thought to be exclusively transporting phosphate across the membrane (Levi and Bruesegem, 2008). In humans (Blaine et al., 2015, Virkki et al., 2007) and rat studies (Villa-Bellosta et al., 2009), it has been shown that the sodium phosphate cotransporters are positioned in the apical membrane of renal proximal tubule cells, to move phosphate from lumen to the cell interior (Curthoys and Moe, 2014b). In *Drosophila* MTs, *NaPi-T* is known as a major player to be involved in elevating intraluminal phosphate concentration that contributes to the kidney disease (Villa-Bellosta et al., 2009, Chintapalli et al., 2012). However, a detailed study has not been conducted. Hence, to better understand the role of NaPi-T in kidney stone formation, I selectively knocked down NaPi-T in Drosophila MTs to observe its impact in stone formation. The detailed characterisation of NaPi-T, for its involvement in kidney stone formation, is explained in **Chapter 4** and **Chapter 6**.

3.2.1.4 SPOCK (CG32451)

Secretory pathway Ca^{2+}/Mn^{2+}-ATPases (SPCAs) represent a new group of ion-motive ATPases consisting of single subunit integral membrane enzymes specifically mediating the ATP-powered uphill transport of either Ca^{2+} or Mn^{2+} from the cytosol into the Golgi lumen. The lumens of the Golgi apparatus (GA), store a high amount of free Ca^{2+}, in the order of 1.0 mM and 0.3–0.4 mM, respectively, compared with those in the external fluids. The $[Ca^{2+}]$ in all these compartments is finely regulated, and the correct Ca^{2+} homeostasis is essential for the majority of intracellular pathways, including the protein trafficking and

secretion (Micaroni, 2010). The mammalian Ca^{2+}-transporting ATPases are encoded by *ATP2C1-2* genes, sarco(endo)plasmic reticulum Ca^{2+}-ATPases (SERCAs; encoded by *ATP2A1–3* genes) and plasma membrane Ca^{2+}-ATPases (PMCAs; encoded by *ATP2B1–4* genes). The biochemical, cell biological, and physiological functions of SERCA and plasma membrane Ca^{2+}-ATPases have been intensively studied (Okunade et al., 2007). Only limited information is available for the SPCAs, which are firmly related to *PMR1*, a P-type Ca^{2+}-ATPase in yeast that is expressed in Golgi membranes and transports both Ca^{2+} and Mn^{2+} (Shull et al., 2011, Okunade et al., 2007).

The focus here is on the SPCA family of Golgi Ca^{2+} pumps, with particular emphasis on disease phenotypes resulting from null mutations in the *ATP2C1* (*SPCA1*) gene in mice and humans and their similarities to disease phenotypes resulting from null mutations in the *ATP2A2* gene (Shull et al., 2011), which encodes *SERCA2*, the major endoplasmic reticulum (ER) Ca^{2+} pump (Liao and Zhang, 2008). *Drosophila* homologue of *SPCA* genes is *SPoCK*, the gene encoding a secretory pathway Ca^{2+}/Mn^{2+}-ATPase that has been mainly characterised in our lab (Southall et al., 2006). However, its role in kidney stone formation is not known. Hence in this chapter, we focus on the impact of *SPoCK* in calcium oxalate stone formation.

3.2.1.5 Waterwitch (Wtrw; CG31284)

Renal and intestinal transcellular calcium absorption plays a crucial role in calcium homeostasis (Blaine et al., 2015). The rate-limiting step in transcellular calcium transport across the apical membrane of the epithelial cell is tightly controlled by 2 members of the transient receptor potential (TRP) superfamily, *TRPV5* and *TRPV6* (Bonvini et al., 2016), which controls renal epithelial, and the small intestine calcium transport respectively, **Figure 3.1** (Sakhaee, 2009).

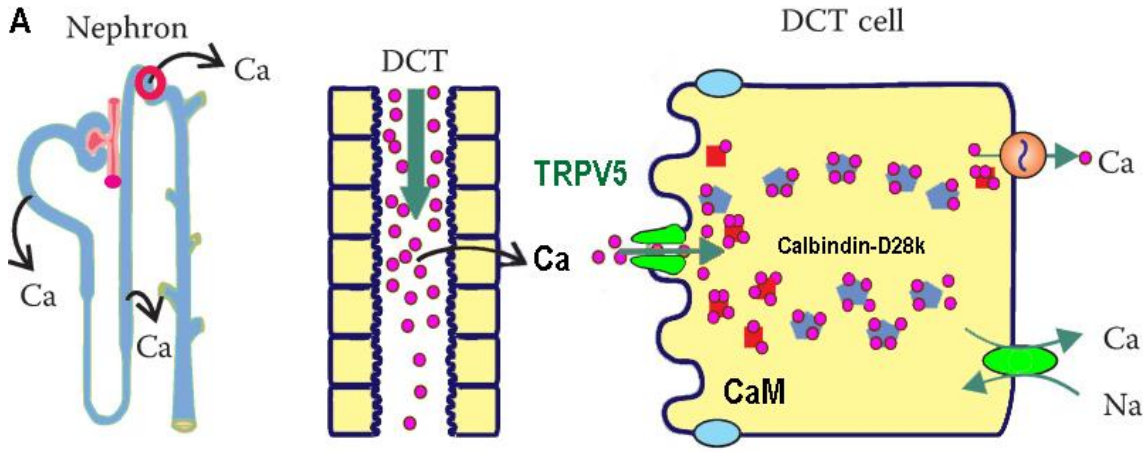

Figure 3.1. TRPV5 function and regulation in active renal Ca^{2+} reabsorption. Adapted from (Peng et al., 2018).

TRPV5 is the main channel responsible for apical Ca^{2+} entry. It is expressed in the distal convoluted tubule and connecting tubule that acts as cellular sensors and regulates a variety of cell functions (Loffing et al., 2001, Suzuki et al., 2008). *TRPV5* channels mediate calcium reabsorption in the kidneys, and their expression is regulated by parathyroid hormone, *1,25 di-hydroxyvitamin D3*, *estrogen* and dietary calcium (Hoenderop et al., 2003). Interestingly, *TRPV5* $^{-/-}$ mice have impaired Ca^{2+} reabsorption and high plasma *1,25 di-hydroxyvitamin D3* with compensatory hyperabsorption of dietary calcium and severe calcium wasting (Renkema et al., 2005). Additionally, a reduced trabecular and cortical bone thickness indicated disturbed bone morphology. Hence, it is interesting to investigate associations of the gene *TRPV5* in kidney stone formation. In our study, we knocked down *Wtrw*, *Drosophila* homologue of human *TRPV5* and observed its impact in oxalate MTs stone accumulation.

3.2.1.6 CG11374

Galectins are an ancient, ubiquitous family of lectins characterised by an evolutionally conserved, approximately 130-amino acid-long carbohydrate recognition domain that binds *ß*-galactosides. *Galectins* include 15 members, among which *Galectin-1* is the family prototype, containing one carbohydrate recognition domain and forming homodimers. *Galectin-1* binds to the *TRPV5 N-glycan* (Nie et al., 2016).

Among all the members of *Galectins*, *Galectin-9* (*UAT; urate transporter*) has also been proposed to be involved in renal urate transport (Lipkowitz et al., 2002). *UAT* was identified by screening a rat kidney cDNA library with a polyclonal antibody to pig liver uricase, and its function was examined using a reconstitution assay (Knorr et al., 1994). *UAT* is expressed ubiquitously and localises to the apical side of the proximal tubule in the kidney. It consists of 322 amino acid residues and contains 4 transmembrane-spanning domains, with a predicted urate binding site on the intracellular loop between transmembrane domains 2 and 3 (Lipkowitz et al., 2002, Hediger et al., 2005). Consequently, *UAT* is supposed to be a multimeric protein related to various functions which are still required to be discovered. Hence, further studies are needed to determine the precise role of *UAT/galectin 9* in urate metabolism. In this study, we knocked down *UAT* in *Drosophila* MTs to observe its impact in oxalate stone formation.

3.2.1.7 Alanine: Glyoxylate Aminotransferase (AGT) – homologue of *Drosophila spat*

Primary Hyperoxaluria Type 1 (PH1) is a severe autosomal recessive kidney stone disease (~1:120,000 live births per year in Europe), caused by loss or dysfunction of the enzyme alanine: glyoxylate aminotransferase (AGT; the AGXT gene product) and characterised by oxalate overproduction and elevated excretion (Adam et al.). AGT is a hepatic peroxisomal enzyme involved in glyoxylate metabolism that detoxifies glyoxylate in the peroxisomes of cells by converting it to glycine. If not degraded, excess glyoxylate results in a build-up of oxalate in all tissues, which is also deposited in the kidneys in the form of calcium oxalate, resulting in nephrocalcinosis, urolithiasis, and renal failure (Danpure, 2005). Since calcium oxalate is poorly soluble in urine, patients with PH1 usually present with symptoms related to the urinary tract. The risk of stone formation is increased when urine oxalate exceeds 0.4 mmol/l, especially if urine calcium concentration is elevated (i.e. more than 4 mmol/l), leading to the formation of monohydrated calcium oxalate (whewellite) crystals (Cochat et al., 1995).

Current knowledge on the role of *AGXT* for PH1 is not fully understood. Enzymes that can significantly degrade oxalate have not been discovered. Over

75 different missense mutations in *AGT* have been found associated with PH1. While some of the mutations are affecting enzyme activity, stability, and/or localisation, approximately half of these mutations are completely uncharacterized (Lage et al., 2014). The *Drosophila* homologue of AGXT is *spat (CG3926)* which functions in catalysing the conversion of glyoxylate to glycine using L-alanine as the amino donor. Hence, we sought to systematically knocked down *spat* in *Drosophila* MTs to observe its effect in the accumulation of oxalate stones.

3.2.1.8 Molybdenum cofactors MOCS

Molybdenum cofactor deficiency (MoCD) is a rare autosomal recessive inborn error of metabolism of sulfur-containing amino acid with an overlapping clinical phenotype and severe neurodegeneration in new-borns. All molybdenum-containing enzymes are other than the bacterial nitrogenase share an identical molybdenum cofactor (MoCo), which is synthesised via a conserved pathway in all organisms and therefore also is called “universal molybdenum cofactor”.

In humans, four different molybdenum enzymes are expressed, known as *sulfite oxidase (SO)*, *xanthine oxidoreductase (XOR)*, *aldehyde oxidase (AO)* and the mitochondrial amidoxime-reducing component, in the form of two isoforms (*mARC1* and *mARC2*) (Reiss and Hahnewald, 2011). Mutations in the genes encoding the biosynthetic MoCo pathway enzymes abrogate the activities of all molybdoenzymes and result in the “combined” form of MoCo deficiency, which is clinically very similar to isolated sulfite oxidase deficiency, caused by mutations in the gene for the corresponding apoenzyme (Reiss and Hahnewald, 2011). Both deficiencies are inherited as an autosomal recessive disease and result in progressive neurological damage and early childhood death in most cases. The majority of mutations leading to *MoCo* deficiency have been identified in the genes *MOCS1* (type A deficiency), *MOCS2* (type B deficiency), with one reported in *GPHN (Reiss, 2000)*. This is summarised in (**Figure 3.2** and **Figure 3.3**).

a. MOCS1

The *MOCS1* gene was the first gene identified in human in this conserved pathway (**Figure 3.2**), leading from GTP to active MoCo (Reiss et al., 1998). Approximately two-thirds of all MoCo-deficient patients are homozygous or compound heterozygous for mutations in the *MOCS1* gene. Mutation in *MOCS1* causes synthesis of all the four MoCo-dependent enzymes; *aldehyde oxidase, mARC, xanthine oxidoreductase,* and *sulfite oxidase*. Classical xanthinuria type I is the result of an isolated xanthine oxidoreductase deficiency, while traditional xanthinuria type II is caused by a defect in the molybdenum cofactor sulfuration by HMCS before incorporation into xanthine oxidoreductase and aldehyde oxidase (Ichida et al., 2006). In the asymptomatic patient, xanthine stones have prominent effects due to elevated levels of xanthine, although they are not life-threatening. Isolated sulphite oxidase deficiency is also an autosomal-recessive genetic disease even rarer than the “combined” MoCo deficiency (Ichida et al., 2001). Furthermore, Isolated sulfite oxidase deficiency and the combined deficiency of all MoCo-dependent enzymes due to MoCo deficiency are clinically indistinguishable and can be differentiated only by biochemical parameters like high xanthine and lowered uric acid as a result of the simultaneous loss of xanthine oxidoreductase deficiency in the combined form.

Similarly, *CG33048* is the *Drosophila* homologue of human *MOCS1*. We knocked down *CG33048* in MTs to observe its impact in oxalate stone formation.

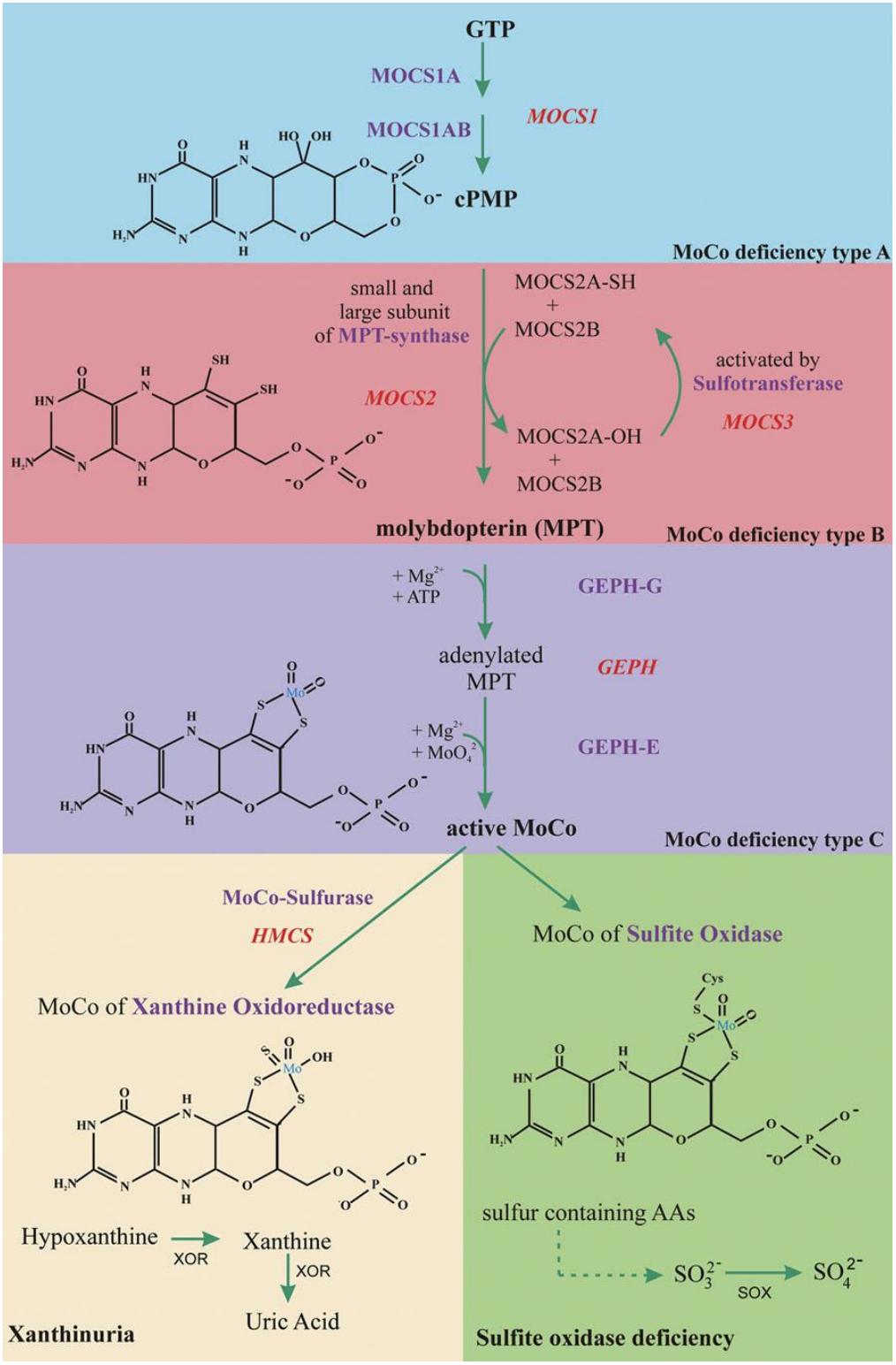

Figure 3.2. Biosynthesis of MoCo via an ancient pathway common to all free-living species and types of diseases as a consequence of mutations in the different genes. Reproduced with permission from (Reiss and Hahnewald, 2011).

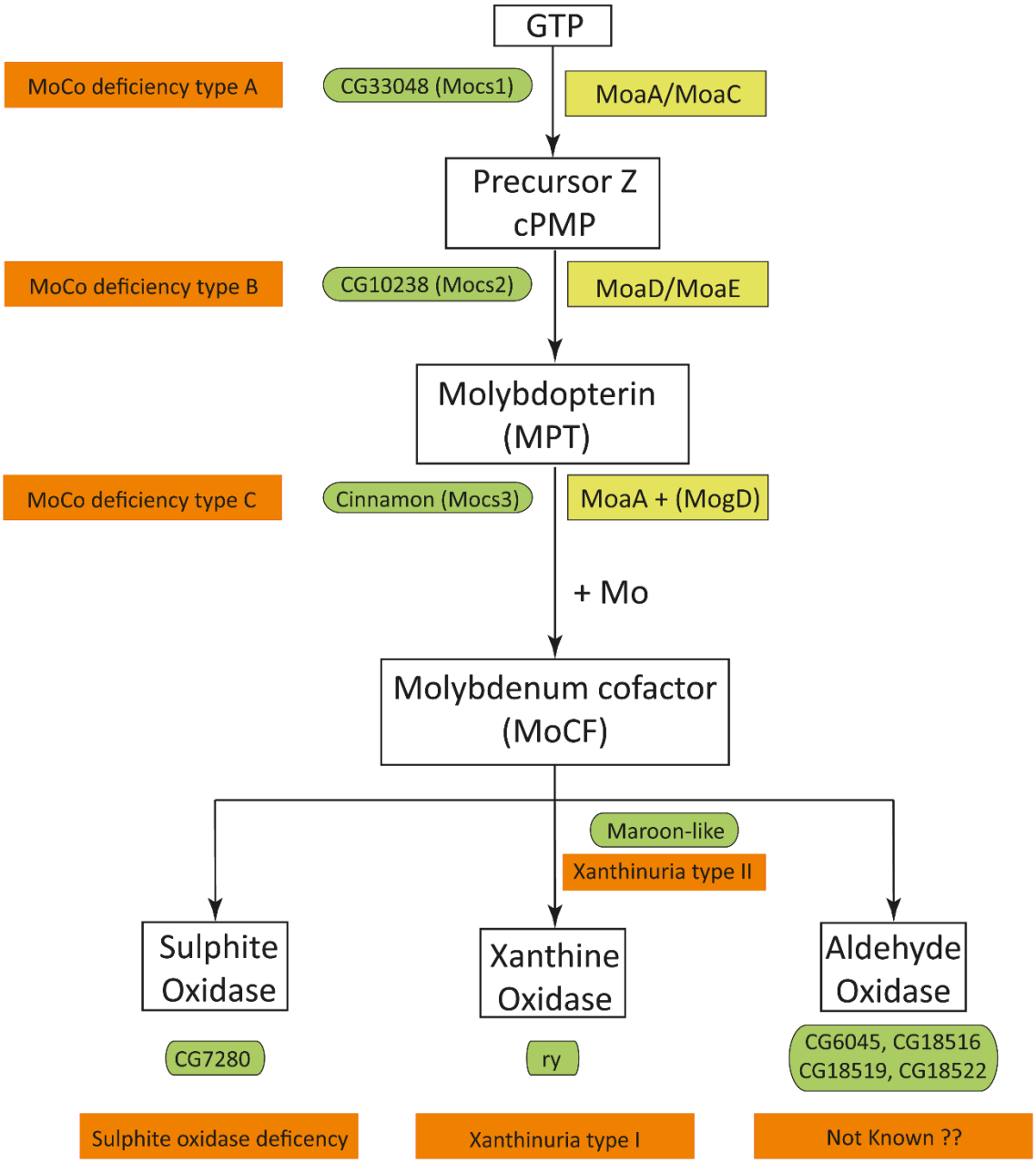

Figure 3.3. MoCo containing enzymes in *Drosophila*. GTP; Guanosine triphosphate, MPT; molybdopterin, MoCo; molybdenum cofactor, SO; sulphite oxidase, XDH; xanthine dehydrogenase, AO; aldehyde oxidase, *cin*; *cinnamon*, *ry*; *rosy*, *mal*; *maroon-like*. Adapted from (Hobani, 2012).

b. MOCS3

MOCS3 is one of the essential genes which encodes a protein believed to catalyse both the adenyl transfer and subsequent thiocarboxylation at the C-terminus of the small subunit of molybdopterin synthase (Matthies et al., 2004), thus providing the sulfur to be incorporated into cPMP. This gene is

located on chromosome 20 and contains no introns. A pseudogene (*MOCS3P1*) is located on chromosome 14 (Reiss and Hahnewald, 2011). Mutations in the genes encoding the biosynthetic MoCo pathway enzymes abrogate the activities of all molybdoenzymes and result in the "combined" form of MoCo deficiency, which is clinically very similar to isolated sulfite oxidase deficiency, caused by mutations in the gene for the corresponding apoenzyme (Reiss and Hahnewald, 2011). Hence, in this study, we knocked down *Cinnamon*, *Drosophila* homologue of human *MOCS3* in *Drosophila* MTs and observed its impact in oxalate stone formation **Figure 3.3**.

3.2.1.9 Guanine Deaminase - homologue of *Drosophila dihydropterin deaminase (CG18143)*

Guanine deaminase (GDA) is a metalloenzyme that catalyses the first step in purine catabolism by converting guanine to xanthine by hydrolytic deamination. *GDA* also regulates the total cellular purine-derived nucleotide pool by converting adenylic derivatives to guanine (**Figure 3.4**) (Saint-Marc and Daignan-Fornier, 2004, Nygaard et al., 2000). Since *GDA* activity is involved in guanine metabolism, this enzyme is essential for the regulation of intracellular levels of guanylic derivatives (Akum et al., 2004). Furthermore, in higher eukaryotes, *GDA* (also known as *cypin*) plays an essential role in the development of neuronal morphology where the dendrite growth/ branch formation by *GDA* is dependent on the breakdown of guanine as substrate (Chen et al., 2005, Chen and Firestein, 2007).

Recent studies have shown that abnormally high levels of *GDA* activity occur in serum from patients suffering from liver diseases as compared to levels in healthy adults. A strong correlation is observed between high *GDA* activity and patients with chronic hepatitis, biliary obstruction, and liver cirrhosis (Kuzmits et al., 1980, Shiota et al., 1989). Although *GDA* serves as an attractive drug target for the prospective treatment of purine metabolism deficiency, liver diseases, and cognitive disorders; novel ligands, which may act as clinically significant inhibitors and/or activators of the enzyme, have not been intensely investigated.

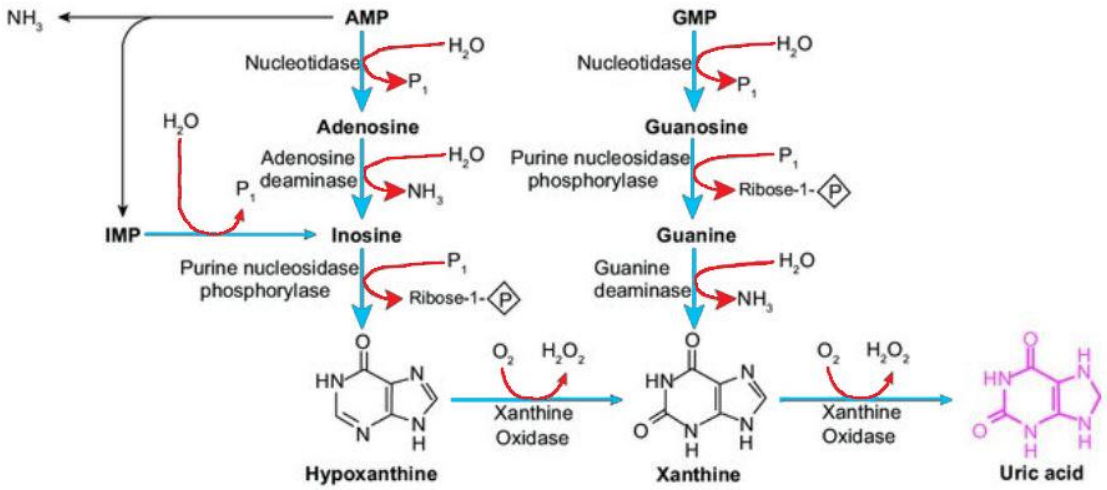

Figure 3.4. Pathway for the enzymatic degradation of purines in humans. Reproduced with permission from (Berry and Hare, 2004).

GDA, a homologue of *Drosophila dihydropterin deaminase (CG18143)* which encodes an enzyme responsible for the hydrolytic deamination of guanine, i.e. conversion of guanine to xanthine (Kim et al., 2009, Takikawa et al., 1983). Xanthine is again oxidised by xanthine oxidase to form the final product, uric acid. Therefore, we knocked down *CG18143* in *Drosophila* MTs to determine its involvement in oxalate stone formation.

3.2.1.10 Na^+/H^+ exchanger regulatory factor (*NHERF1)*- homologue of Drosophila *Sip1 (CG10939)*

NHERF1 was first characterised in rabbit border membrane as an essential cofactor for cyclic AMP inhibition of Na^+/H^+ exchanger (Weinman et al., 1989, Murtazina et al., 2007). Mutation of *NHERF1* is associated with different diseases such as imbalance in renal phosphate absorption (Giral et al., 2012), hypercalciuria (Levi and Bruesegem, 2008), osteoporosis tumour growth (Pan et al., 2006) and uric acid stones formation (Cunningham et al., 2007). Intriguingly, targeted deletion of NHERF1 in mouse elevates intestinal deposition of calcium and also triggers calcium oxalate and uric acid crystal formation (Shenolikar, 2002). Hence, to better understand the role of NHERF1 in *Drosophil*a kidney, I selectively knocked down *Sip1*(Drosophila homologue of human *NHERF1*) in stellate cells to observe the impact on stones formation. The detailed characterisation of Sip1 gene is presented in **Chapter 5**.

3.3 Results

3.3.1 Determination of the dose of NaOx

A preliminary study was performed to determine the minimum dose of NaOx to induce CaOx crystals in *Drosophila* MTs. Different dosage of NaOx (0.1%, 0.2%. 0.5% and 1%) were fed to *Canton-S* (wild-type strain of *D. melanogaster)* and the total stones accumulated within MTs were quantified at day 1, day 2 and day 4. For this MTs were dissected and imaged using a polarised light microscope to visualise the birefringent crystals of CaOx.

Astonishingly, CaOx crystals appear as early as within 2 hours when viewed under the microscope. Monohydrate CaOx crystals (clear or jewel-like gloss; six-sided prisms or various forms) are more common than the typical dihydrate CaOx crystals. Various forms of monohydrate CaOx crystals shapes were also identified. Free crystals were extensive, with many incorporated in casts. Their size is estimated to vary approximately between 5 and 20μm. Most crystals were identified within the 'enlarged initial (distal) segment' of the anterior MTs of flies of either sex, where the calcium is stored in concretions. **Figure 3.5** indicates a representative image of CaOx crystal deposition in the MTs.

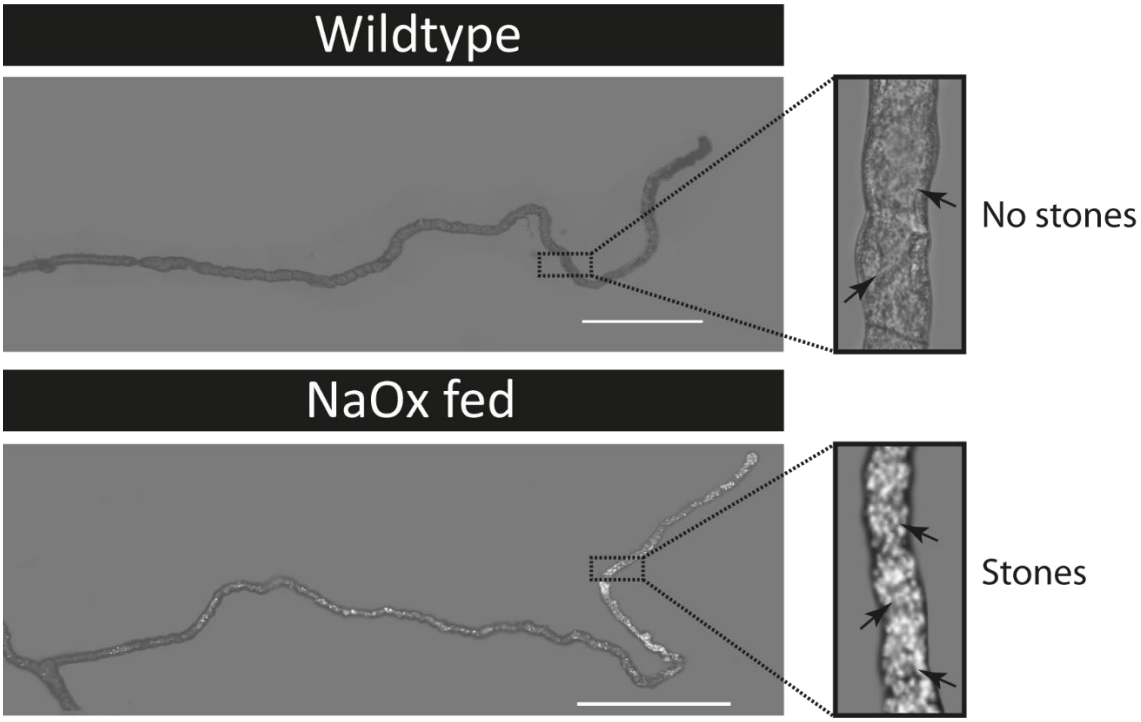

Figure 3.5. Oxalate nephrolithiasis in *Drosophila* renal tubules. A. tubules dissected from adult fly fed in a normal diet. B. tubules from the adult fly fed with NaOx. Scale: 500 μm.

To optimise NaOx concentration, crystal-inducing period, and the quantity of crystal formation in anterior and posterior tubules, male flies were fed with different concentrations of NaOx for 1,2 and 4 days. The details are shown in **Figure 3.6**. The mean stone formation time in anterior tubules is high as compared to posterior tubules at days 1, 2 and 4. Interestingly in anterior tubules, the accumulation of stones increased with feeding time, e.g. 0.2% NaOx fed flies at day 1 had 13.09±2.61% stones; on day 2, 19.46±0.85% and on day 4 23.84±5.29. Similarly, at a particular day (either day 1, day 2 or day 4), the quantity of stones accumulated increased with the concentration of NaOx, i.e. 1% fed flies have a higher quantity of stones compared to 0.5% NaOx fed flies followed by 0.2% and 0.1% NaOx fed flies. However, we did not observe consistent results in posterior tubules. For example, the total quantity of stones accumulated in day 1 is significantly higher compared to flies dissected in day 2, fed with the same dose (0.2%) of NaOx. Hence, the quantity of stones formed by feeding male flies with 0.2% for 2 days was found to be sensitised background in which only impact (positive or negative) on stone formation would be readily detectable. Hence, this dose was used throughout the experiment.

	Day 1		Day 2		Day 4	
	Anterior	Posterior	Anterior	Posterior	Anterior	Posterior
Control	0.0±0.0	0.0±0.0	0.65±0.62	0.087±1.73	0.19±0.09	0.62±0.45
NaOx						
0.1%	0.09±0.08	1.24±1.52	2.11±0.92	0.47±0.31	18.78±3.32	15.49±2.26
0.2%	13.09±2.61	8.65±1.03	19.46±0.85	2.34±1.04	23.84±5.29	16.45±4.29
0.5%	18.49±4.74	11.41±3.18	23.64±2.91	18.33±8.25	24.47±6.07	11.54±2.57
1%	32.40±4.43	12.75±2.62	26.91±2.89	8.82±1.90	41.59±6.67	6.12±2.58

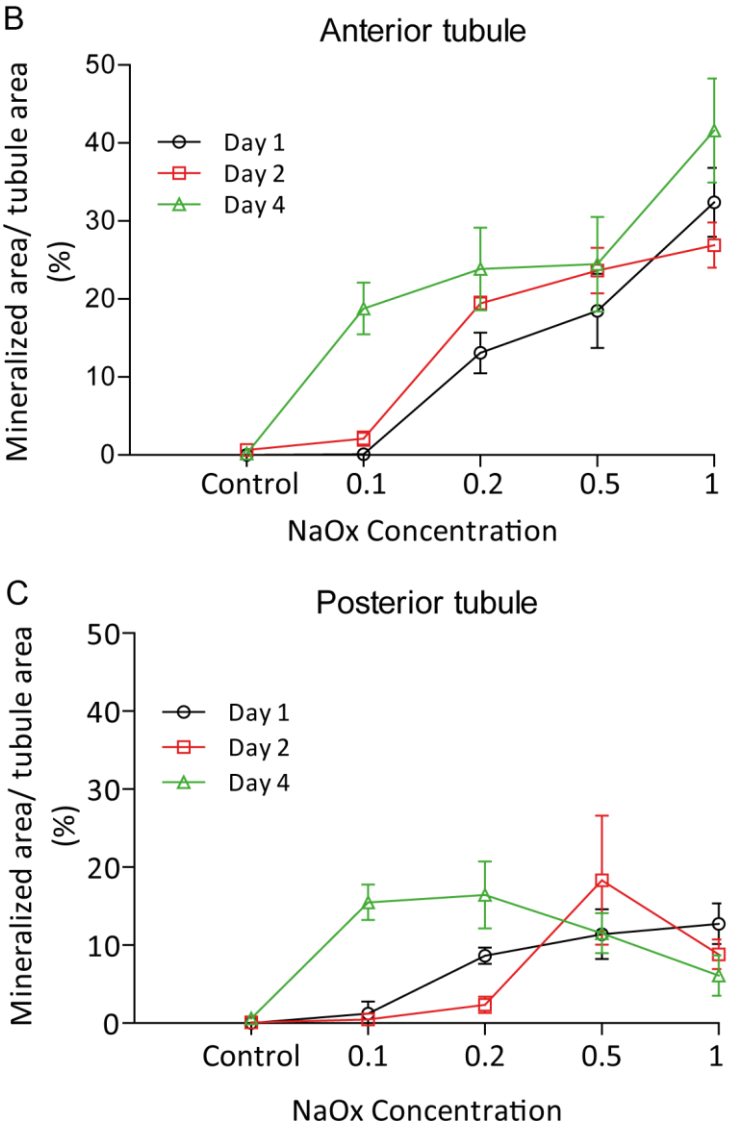

Figure 3.6. The extent of crystals formation in male adult *Drosophila* MTs fed on NaOx. A. The total quantity of stones accumulated in anterior and posterior tubules after feeding with different doses of NaOx for different days represented in table and graphs. (B-C) Line graph representing the total stones accumulated in the anterior and posterior tubules after feeding flies with 0.2% NaoX for 2 days. Values were expressed as mean ± SEM, N = 10 tubules for each condition.

3.3.2 Genes knockdown results in an alteration in the accumulation of oxalate stones within the *Drosophila* Malpighian tubules

Seeking a *Drosophila* model for the urinary stone disease, we examined the consequences of knockdown of homologues of human genes (**Error! Reference s ource not found.**) implicated in kidney stone formation. All parental lines (*Capa-R-GAL4*/+ and *UAS- GeneX RNAi*/+) and knockdown lines (*CapaR-GAL4>UAS-RNAi*) were fed with 0.2% NaOx and the mineralised concretion in adult *Drosophila* MTs after 48 hours quantified. The Representative images of the parental lines and knockdown conditions are shown in **Figure 3.7.**

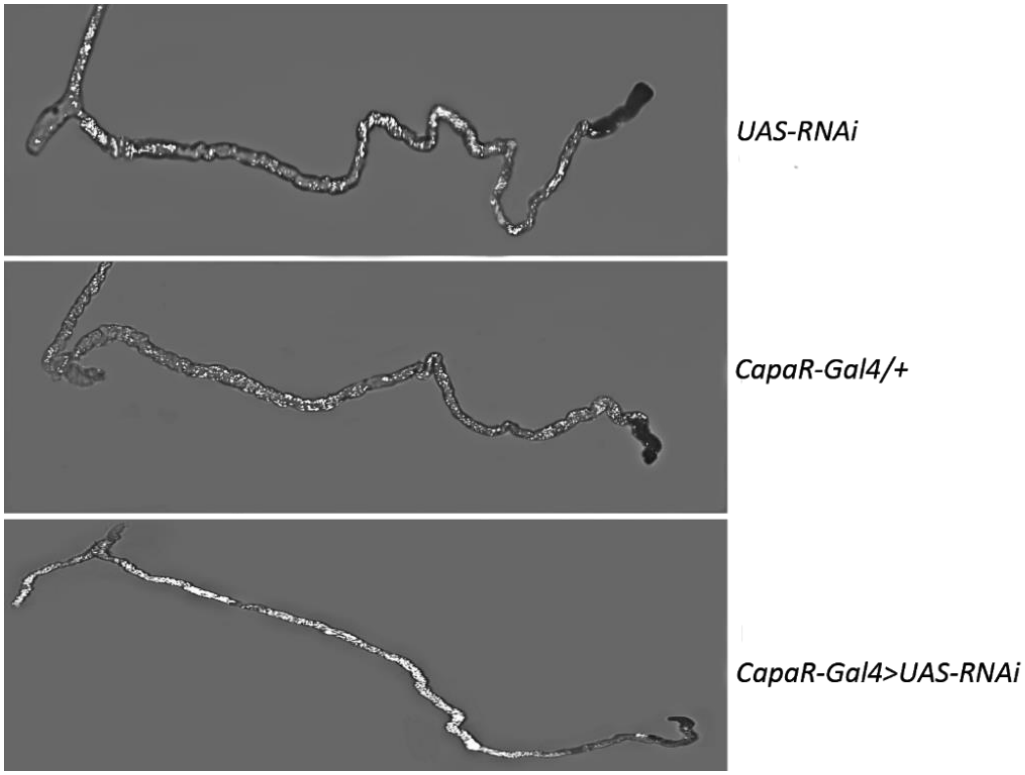

Figure 3.7. Representative images of tubules from control flies (CapaR *GAL4*/+ and UAS-RNAi/+) and gene knockdown flies (CapaR *GAL4*>UAS-RNAi/+) fed with 0.2% NaOx for 2 days. White concretions are birefringent crystals accumulated intraluminally.

Under light microscopy examination, concretions were birefringent intraluminal contents within the MTs and had the appearance of small stones. Upon dissection, they also looked like small stones, given their physical appearance, we refer to these as fly stones composed of oxalate. Throughout the

experiment, UAS-RNAi> Capa R *GAL4* was regarded as a knockdown group and *UAS-RNAi*/+ and CapaR-*GAL4*/+ were regarded as control groups. From a screen of twenty independent RNAi lines, we did not observe the significant change in the quantity of stone accumulation in twelve RNAi lines, as compared to the parental controls. The list of the genes is enlisted in **Figure 3.8**.

Gene ID	Source	UAS-RNAi/+	CapaR-*GAL4*/+	UAS-RNAi> Capa R *GAL4*	Statistics
CAH1 (CG7820)	VDRC	69.17±3.447	21.20±3.479	24.04±4.584	NS
SPoCK (CG32451)	VDRC	52.91±2.863	21.20±3.479	44.26±3.232	NS
Wtrw (CG31284)	VDRC	55.08±3.049	21.91±4.680	35.07±1.887	NS
UAT (CG11374)	BDSC	62.07±2.137	21.91±4.680	35.60±3.302	NS
Cin (CG2945)	VDRC	28.74±3.275	21.91±4.680	23.16±3.176	NS
Dihydropterin deaminsase (CG18143)	BDSC	49.69±4.226	21.91±4.680	51.10±2.177	NS
Dihydropterin deaminsase (CG18143)	VDRC	55.07±2.835	21.20±3.479	29.82±3.366	NS
MOCS1 (CG33048)	BDSC	50.09±3.337	21.91±4.680	55.20±2.354	NS

B

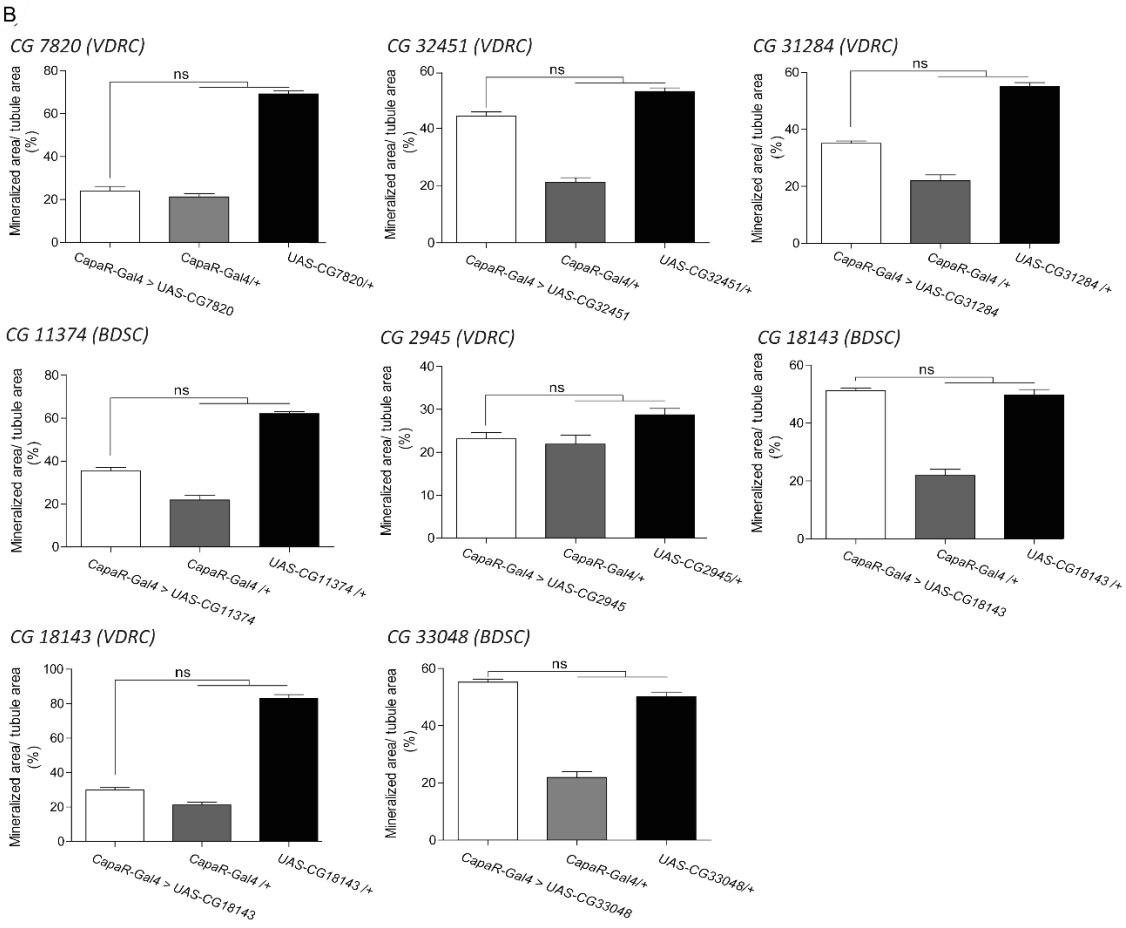

Figure 3.8. List of RNAi lines which on knockdown did not show significant aggregation or decrease in stone quantity.. A. Table enlisting a list of genes which on knockdown did not have a significant effect in the quantity of stones accumulation compared to parental control conditions. B. The data shown in

the table are represented in the bar graph. Data are presented as mean ± SEM. N=10 MTs. One-way ANOVA followed by Dunnett's test. N.S. stands for non-significant. BDSC: Bloomington Drosophila Stock Centre, VDRS: Vienna Drosophila research centre.

However, in the remaining eight RNAis, I observed a significant high/low quantity of stones upon knockdown as compared to parental controls. The list of genes are *Waterwitch (Wtrw)*, *Serine Pyruvate Amino Transferase (Spat)*, *Cinnamon (Cin)*, *Na^+-dependent inorganic Phosphate Co-transporter (NaPi-T)*, *Sarcoplasmic Calcium-binding Protein 2 (Scp2)* and *Secretory Pathway Ca^{2+}/Mn^{2+}-ATPase (SPoCK)* and is enlisted in **Figure 3.9**. Remaining two are described in **Chapter 4, Chapter 5** and **Chapter 6**. Further, gene silencing efficiency for all the shortlisted genes was quantified by qPCR and represented in **Figure 3.10**. Among all the genes enlisted in **Figure 3.9**, Spat (CG3926 from VDRC) did not show any significant knockdown compared to parental controls; hence, the result is not mentioned in **Figure 3.10**.

A

Gene ID	Source	UAS-RNAi/+	CapaR-*GAL4*/+	UAS-RNAi> Capa R *GAL4*	Statistics
Cin (CG2945)	BDSC	25.22±3.429	21.91±4.680	43.53±1.614	***
Spat (CG3926)	BDSC	45.20±4.464	21.20±3.479	67.44±2.385	***
Wtrw (CG31284)	BDSC	38.51±1.915	22.71±4.824	64.11±2.348	***
SPoCK (CG32451)	BDSC	32.12±3.208	21.20±3.479	50.82±3.389	***
Spat (CG3926)	VDRC	61.68±7.778	21.91±4.680	13.38±1.942	***
Scp2 (CG14904)	VDRC	26.47±3.447	22.71±4.824	40.90±4.715	***

B

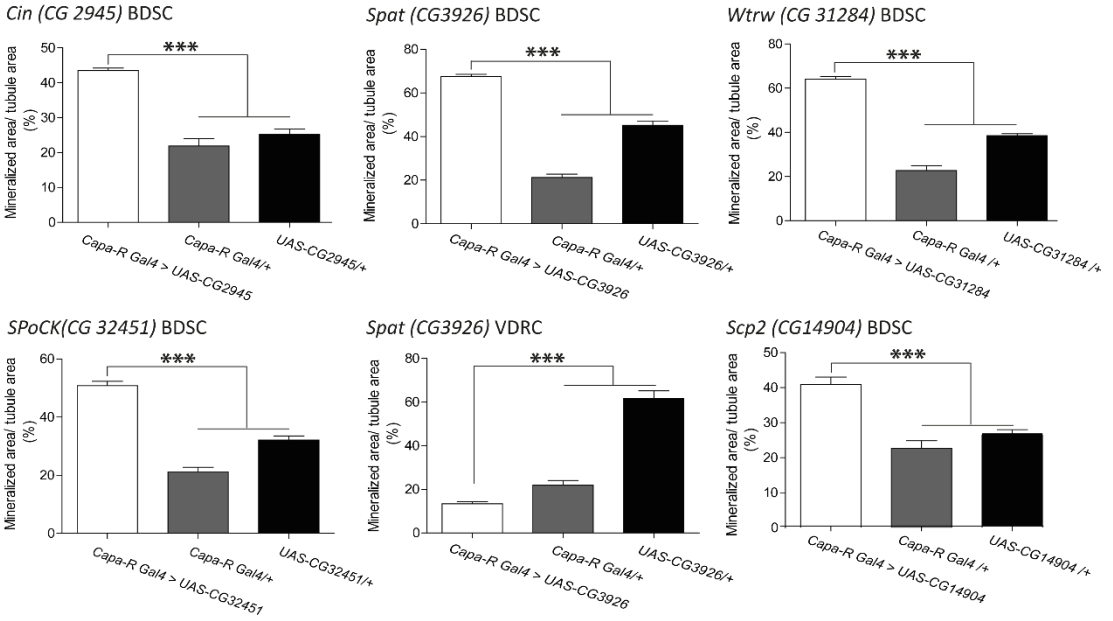

Figure 3.9. Silencing/Downregulating candidate genes expression alters/impacts the concretion formation in a fly model for oxalate kidney stone formation. A. Table enlisting the list of a gene which on knockdown resulted in a significant alteration in stone accumulation compared to parental controls. B. Measuring the areas of the tubule lumen occupied by mineralised concretions in control flies (*CapaR GAL4*/+, *UAS-RNAi*/+) and knockdown flies (*CapaR GAL4>UAS-RNAi*)fed with 0.2% NaOx for 2 days. Data are presented as mean ± SEM. ***p<0.05, **p<0.01, *p<0.001 one-way *ANOVA* with Dunnett's test, N = 10.

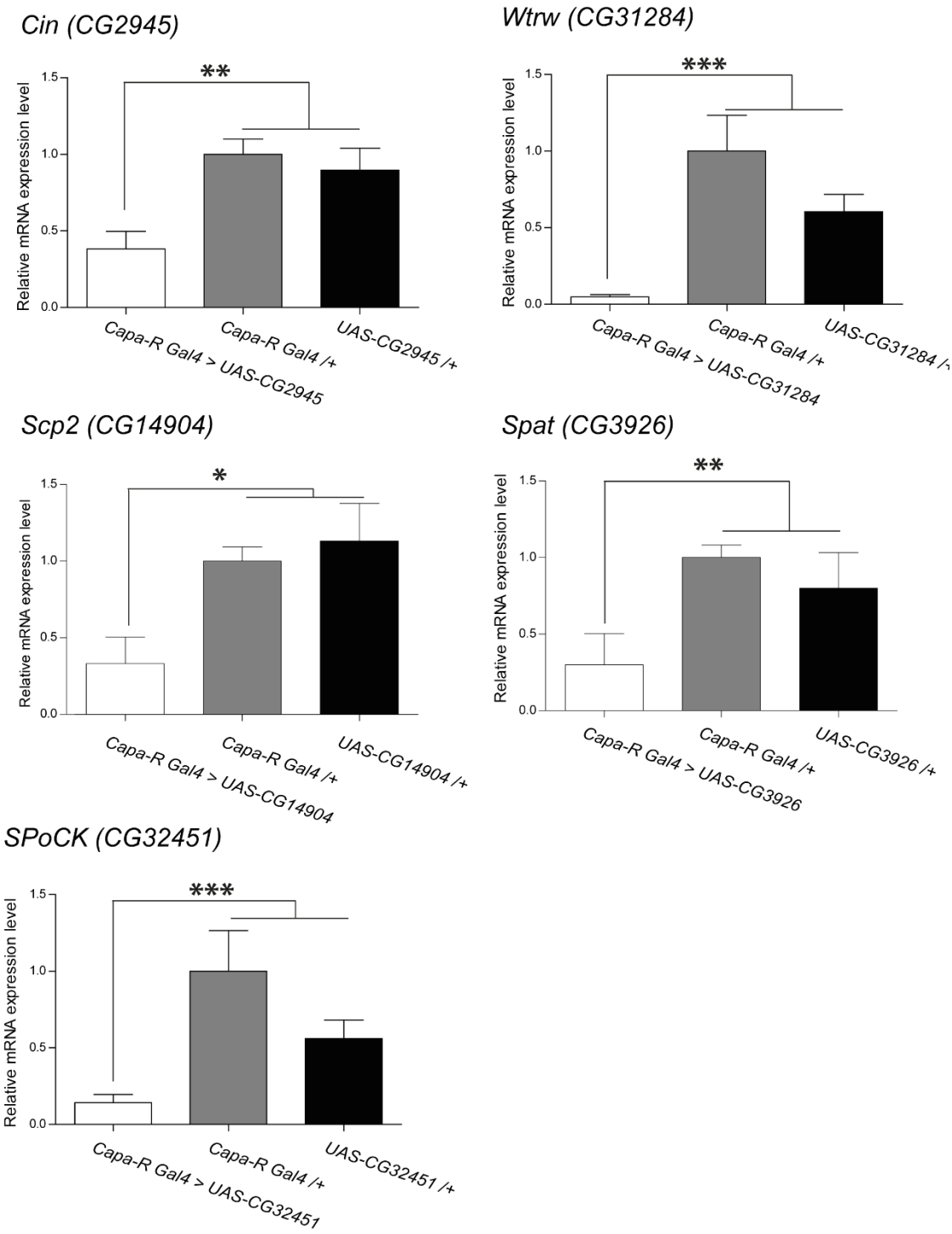

Figure 3.10. Validation of gene expression in principal cells of MTs in Gene knockdown MTs. The expression of Gene X was significantly reduced in *CapaR GAL4>UAS-Gene RNAi* compared to parental lines (*CapaR GAL4/+*, *UAS-RNAi/+)*. Data are presented as fold change, N=3, ***p <0.05, ** p <0.01, *** p <0.001 one-way ANOVA followed by Dunnett's test .

3.3.2.1 Discussion

Despite possible limitations of *D. melanogaster* as a pre-clinical model for nephrolithiasis, we hypothesised that it could have value as a screening platform for identifying genes which could increase or decrease calcium oxalate calculus formation. Previous studies have validated the use of *Drosophila* for the screening of the genes and the compounds for the treatment of the diseases (Chi et al., 2015, Hirata et al., 2012). Hence we used flies as an amenable genetic model for the study. However, it is important to consider the physiological nature of concretion accumulated within the tubules. Dube et al. demonstrated that flies mainly formed concretions in the anterior MTs and postulated that this was meant to regulate calcium; tubular calcium excretion was thought to be a normal homeostatic function in the wild-type fly (Cabrero et al., 2014, Dube et al., 2000). These concretions were visible as small calcium-containing spherules/spherites (Hirata et al., 2012, Miller et al., 2013). In our model, similarly, appearing concretions are induced by feeding flies with stones inducing lithogenic agent (NaOx).

This screening platform relies on the dietary administration of sodium oxalate in parental control and knockdown RNAi flies (candidate genes knockdown) to observe changes in intraluminal calculus quantity via imaging and quantification (Hirata et al., 2012). The assay performed in *D. melanogaster* provides a highly promising *in vivo* screening platform for the identification of the genes involved in stone formation. The results of our study were consistent with data from rats and humans. It is flexible and scalable to screen hundreds of candidate genes at a minimal cost. However, it might take too much time if crosses are not maintained regularly. The use of birefringent signals to quantitate stone accumulation is a validated and innovative system that is cost-effective and does not require any additional processing or staining. It also suggests that other birefringent calculi, such as uric acid calculi are also amenable to this type of screen.

This screening platform provides several avenues of opportunity to narrow down large numbers of potentially overlooked candidate genes with possible clinical applications for further evaluation. This permitted us to select the genes which had human homologues and might have some impact on kidney

stone formation. Another key point for the selection of the genes was the use of the RNAi lines which were efficiently knocked down in *Drosophila* MTs principal cells. Screening of 20 different RNAi lines led to the identification of eight major genes that have a significant impact in stone formation and were referred to as candidate "hits". The list of hits is; *Waterwitch (Wtrw)*, *Serine Pyruvate Amino Transferase (Spat)*, *Cinnamon (Cin)*, *Na^+-dependent inorganic Phosphate Co-transporter (NaPi-T)*, *Sarcoplasmic Calcium-binding Protein 2 (Scp2)* and *Secretory Pathway Ca^{2+}/Mn^{2+}-ATPase (SPoCK)*. Two genes from this initial screen were further studied for their impact on stone formation. Still, we cannot exclude the genes which were not hits, because although no change in stone formation was seen in the RNAi lines, I had not performed qPCR on genes that had not shown an effect. Hence, the effect may be due to poor RNAi lines. However, positives resulting from the screen and with confirmed qPCR knockdown are likely to be genuine positives.

The observed effects of hits in these experiments raise intriguing questions about the potential for these genes to be used as a strategy to prevent and or treat pre-existing human calcium oxalate stone disease. In patients at risk for calcium oxalate stone formation, these genes could through competitive inhibition, prevent calcium oxalate binding. In humans, it has been noted that PH1 occurs due to the mutation and polymorphism of the *AGXT* gene (Cochat et al., 2010). The *Drosophila* homologue of *AGXT* is *spat*, which functions in catalysing the conversion of glyoxylate to glycine using L-alanine as the amino donor (Lüneburg et al., 2014). It might play a distinct role in the determination of oxalate concentration. In addition to this, it has been noted that *rosy* and maroon like mutants (homologues to *XDH* genes) suffer from the whole-body accumulation of xanthine and the formation of xanthine concretion within the Malpighian tubules (Dow and Romero, 2010, Miller et al., 2013). Defects of *XDH* causes Xanthinuria. In nonneuronal tissues, the encoded protein is also required for molybdenum cofactor (Moco) biosynthesis. Moco contains the element molybdenum, which is essential for the function of several enzymes, including XDH. Another gene cinnamon, a homologue of human gephyrin, is a conserved evolutionary gene in mammals and multicellular fungi. Recent work (Wittle AE et al.) in *Drosophila Moco* gene *cinnamon* (*cin*), which encodes a multidomain protein, CIN, shows significant similarity to different proteins encoded by

prokaryotic Moco genes (Wittle et al., 1999). Lack of Moco biosynthesis results in the loss of all Moco dependent enzyme activities, finally leading to death in affected patients. Hence gephyrin might have a vital role in nephrolithiasis.

Furthermore, a recent study has shown that other genes namely, Calcium Binding protein (*Scp2; CG14904*), Sodium Phosphate symport (*NaPi-T; CG10207*), Calcium pump (*SPoCK*) and Trp like calcium channel water witch (*CG31284*), which are expressed in the initial segment of tubules might play an important role in nephrolithiasis (Chintapalli et al., 2012b). *SPoCK* has the major role in Ca^{2+} /Mn^{2+} ATPase in the tubules along with the peroxisomal biogenesis. Ca^{2+} can enter to the specialised peroxisome through Trp like plasma membrane channel along with *SPoCK* (Southall et al., 2006); phosphate is supplied through Na^{+}/phosphate cotransporter; *Napi-T*, the membrane is polarised by V-ATPase (with protons provided by a highly enriched isoform of carbonic anhydrase). Calcium is enriched by *Scp2*, a specialised calcium-binding protein (Gao et al., 2006). This screening platform provides several avenues of opportunity to narrow down large numbers of potentially overlooked candidate genes with possible clinical applications for further evaluation.

Our study has several advantages yet is not without limitations. We have applied a novel animal model, which readily provided a large number of test subjects. In addition, the results of our study were consistent with data from rats and humans. The translation of our obtained results using the proposed model to humans is difficult because human stones are composed of different stones causing agents like phosphate, oxalate or uric acid. There are two main concerns. One is that the absorption, metabolism, and excretion of a given substance using an invertebrate model can be different from those of mammals, and consequently, the results may not be comparable. The second aspect is related to the composition of fluids in MTs of flies and the urine composition of mammals.

The percentage of candidate hits (40 %) that resulted in significantly alteration in stone accumulation compared to the control conditions was unexpected. Similarly, the total stones accumulated in UAS-RNAi/+ were significantly high compared to the UAS-Gal4/+ hence, further investigation is required to address this question. That means these RNAi lines might have some other factors

silenced which might be the major influencing factor of kidney stones. However, re-screening was not performed using different approaches. This is a flaw in the study design; it would have prompted more screens of the library with no true termination point. Further, the stones accumulated in the knockdown lines of CG3926 (Spat) is opposite between two lines of different origins, i.e. BDSC and VDRC. However, on verification with qPCR, I did not observe any significant knockdown in VDRC origin RNAi lines. Hence further investigation would be important to determine the reason behind it. Upon completion of the first pass of the genes screen, the set of genes discovered led to focused studies on a single gene. Discovery of a gene with an essential role in stone formation validated the capacity of the screen, which was the main goal of the study.

3.4 Conclusion

The reverse genetic screening provides a useful insight into the function of genes which modulate oxalate stone formation in the MTs. We examined the role of phosphate, urate and calcium transporters in initiating fly stone formation using a genetic approach to knock down genes expressed in MTs principal cells. Ion transporters and channels are particularly prevalent in having an impact/effect on oxalate stone formation in *Drosophila* MTs. Knockdown of four homologues genes resulted in upregulation in stone formation while downregulation of one of the genes resulted in a decrease in stone accumulation. Thus, this finding suggests that characterisation of the candidate genes identified in our screen will help to reveal molecular mechanisms that modulate stone formation in many different organisms.

Chapter 4 Characterisation of the role of temperature and age in kidney stone formation

4.1 Summary

In **Chapter 3,** I discussed different factors (such as genetics, environmental, socio-economic, dietary intake, lifestyle) as the key contributors promoting renal stones. In this chapter, the impact of environmental factors on mineralisation is characterised. Although many studies have been conducted in the human/mouse model to understand the impact of temperature and age in renal stone development, the stage of and nature of the stones developed remains predominantly unknown. The frequent association of renal stones with temperature and age highlights their role in the occurrence and relapse of the disease, which is the critical focus of this investigation. The introduction to this chapter describes current understanding regarding the role of environmental factors in initiating the mineralisation process. The results presented in this chapter help to establish *Drosophila melanogaster* as a model for phosphate stone studies. For this, flies were reared at a different temperature, altering the temperature weekly and quantifying stones over an extended time frame. To further test the role of phosphate transporters, *NaPi-T* and *Picot*, in driving the creation of stones, flies were reared for 21 days, and the alteration in expression with age was observed. Colorimetric analysis of the stones in 21 days old *Drosophila* Malpighian tubules (MTs) revealed high enrichment of phosphate, which is also one of the major constituents in human kidney stones. Additionally, when the expression of *NaPi-T* was silenced, surprisingly significant growth of stones was observed. Taken together, investigation based on physiological, genetic, biochemical and pharmacological assays validate a critical role of temperature and age in the process of nucleation, which eventually leads to the stone deposition. In conclusion, the findings of the present study potentially suggest a novel mechanism for renal stone growth involving temperature and age.

4.2 Introduction

Kidney stone deposition is a multi-faceted process often associated with genetics, environmental and physiological behaviours (Hirata et al., 2012, Miller et al., 2013); such as human feeding behaviour, age, the altitude of residence, hydration levels, urinary volume and the urine pH (Worcester and Coe, 2010, Dow and Romero, 2010). Ageing and geographical variation are significant risk factors contributing to the development of kidney stones. Ageing is the outcome of the interaction of the plethora of genetic and environmental factors and biochemical pathways. As we age, we accumulate cellular damage at the molecular levels, accompanied by a decrease in the efficiency of our body, causing various metabolic and physiological disorders (Ortega and Farley, 2015). Furthermore, environmental factors like region of residence, seasonal variance and global climate change also increase the rate of kidney stone disease. In the broad consensus, the average global temperature has been increasing over the past few decades and also is mirrored by the rate of hospitalised patients due to stones. Hence, an in-depth study of the involvement of the demographic and regional variations in the incidence of kidney stones may provide clues to their aetiology and prevention.

4.2.1 Kidney stone prevalence with age

Recent investigations suggest that ageing is one of the main factors initiating kidney stones (Taylor et al., 2004, Scales Jr et al., 2012). Although little is known about the effect, it is identified that the rate of stone creation varies among different age groups mainly depending on the composition of the stones. For example, cystine stones initiate in the first and second decades of life; calcium stones form in between the third and fifth decades of life; while uric acid stones usually start after the age of 50 (Lancina Martin et al., 2004). However, children and adolescents show a low incidence of stones of all compositions (Knoll et al., 2011).

Kidney stones cause a higher rate of morbidity in older adults as compared to the younger population because older adults have are high risk to other multiple comorbidities including hypertension, diabetes mellitus and metabolic syndrome (MeS), coronary artery disease, obesity, and excessive meat

consumption (Kaur, 2014). Recent studies have shown that 10.6% of men and 18.4% of women develop their first calculus before they turn the age of 20 (Lancina et al., 2004) and these outcomes are believed to be the consequences of changes in lifestyle and diet (Krambeck et al., 2013).

Further, the elderly population over 60 years of age are most prone to stone disease associated with complications of infection due to the increased frequency of urinary tract infection and concomitant urological diseases. It is estimated that, in this age group, the risk of attaining the disease is 20% in men and 5–10% in women (Knoll et al., 2011). A cross-sectional study conducted across different states in the United States of America (USA) has pointed out that the incidence of mineralisation increases with age until the age of 70 and then decreases after that (Soucie et al., 1994, Cramer and Forrest, 2006). Another study conducted in Iran, Japan and USA has reported that the incidence rate among different age group alters with age of the population. The peak age of occurrence was similar among these three countries, ranging from 40 to 49 years, except for Japanese women for whom the peak incidence occurred between the age of 50 to 59 years (Romero et al., 2010).

Studies have shown that the prevalence rate increased with age in Germany, Iceland, Iran, Italy, Greece, Turkey, and the USA, although there is a sharp decrease in prevalence in Italians, age > 60 years, living in Milan (Stamatelou et al., 2003, Amato et al., 2004, Hesse et al., 2003, Trinchieri, 2008). In South-Korea, prevalence rate declines with an increase in the age of men; however the result is opposite in women (hoe Kim et al., 2002). In the USA, a study during 1976 through 1980 showed that frequency decreases in women over age 59 and men over age 69, but by 1991 prevalence rates continued increasing as the population got older among all age groups (Stamatelou et al., 2003).

4.2.2 Kidney stone prevalence with gender

Gender specifically, males are more susceptible to suffer from kidney stone as compared to women (Parmar, 2004), with lifetime occurrence rate up to 50%. According to the USA National Health and Nutrition Examination Survey (NHANES), the susceptibility ratio of men to women is 3:1, prevalence was 7.1% in women and 10.6% in men, however, in other western countries is 4.3% in

women and 6.9% in men (Lin et al., 2014). Similarly, the sex ratio ranges from 2.5:1 in Japan to 1.15:1 in Iran (Safarinejad, 2007, Fujita, 1979). Nevertheless, there is an age range in some countries where this ratio is reversed. Studies suggest that women have lower urinary calcium, oxalate and uric acid concentrations, but have higher concentrations of citrate than men, which might be the cause for reduced frequency of stone formation (Vega Carbó et al., 2009). However, over the years this rate has increased for females, which could be due to other risk factors associated with a lifestyle such as a diet intake and obesity (Lancina et al., 2004) **Figure 4.1**.

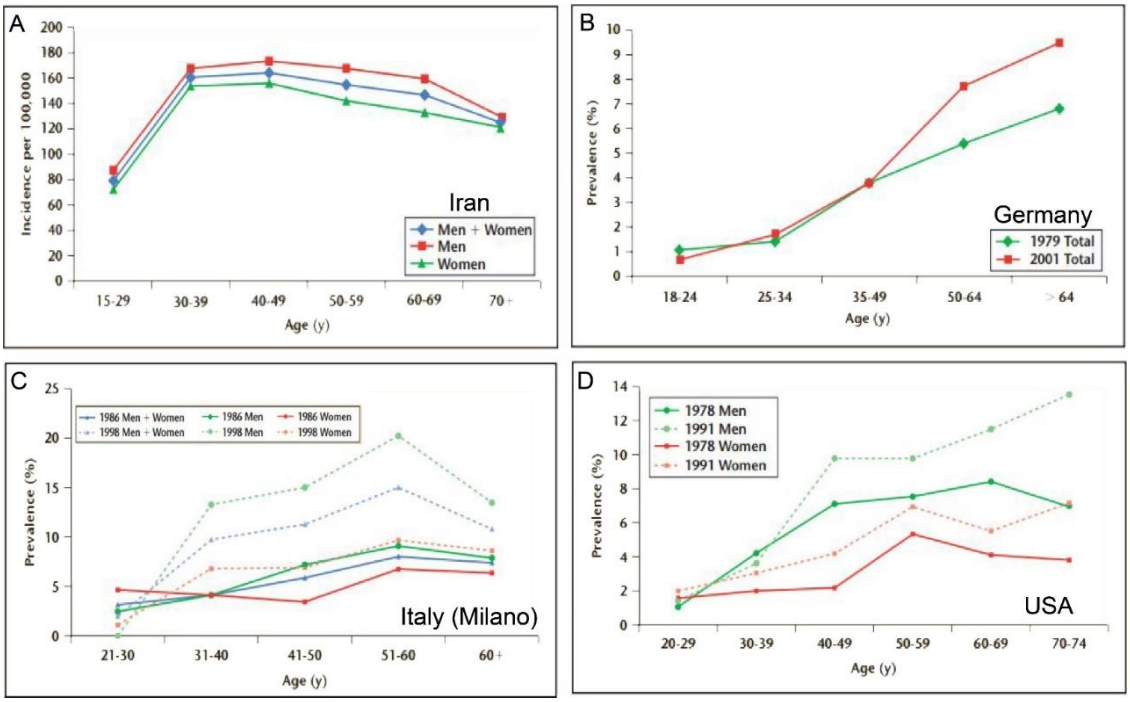

Figure 4.1. Kidney stone prevalence by age group. (A) Rise-and-fall pattern is observed for reported incidence rates in Iran during 2005. (B) Prevalence of stones increases with age in Germans. (C) Prevalence rate increases along with age among those living in Milan, but a prevalence decreases after 60 years of age. (D) Prevalence in men and women demonstrates a rise-and-fall pattern as the population ages in the USA. Adapted from (Romero et al., 2010).

4.2.3 Kidney stone prevalence with geographical location

Geographical variation is another influential factor responsible for alteration in the accumulation of renal stones. The prevalence in a given population not only depends on the geographical area but also differs depending on the racial composition and socioeconomic status of the community (Trinchieri, 2008).

Evidence attained from different geographical regions in the USA, Europe and Asia demonstrates that people residing in warmer areas have a high prevalence of renal stones as compared to people residing in colder areas **Figure 4.2** (Dirks et al., 2006, Soucie et al., 1994, Brikowski et al., 2008).

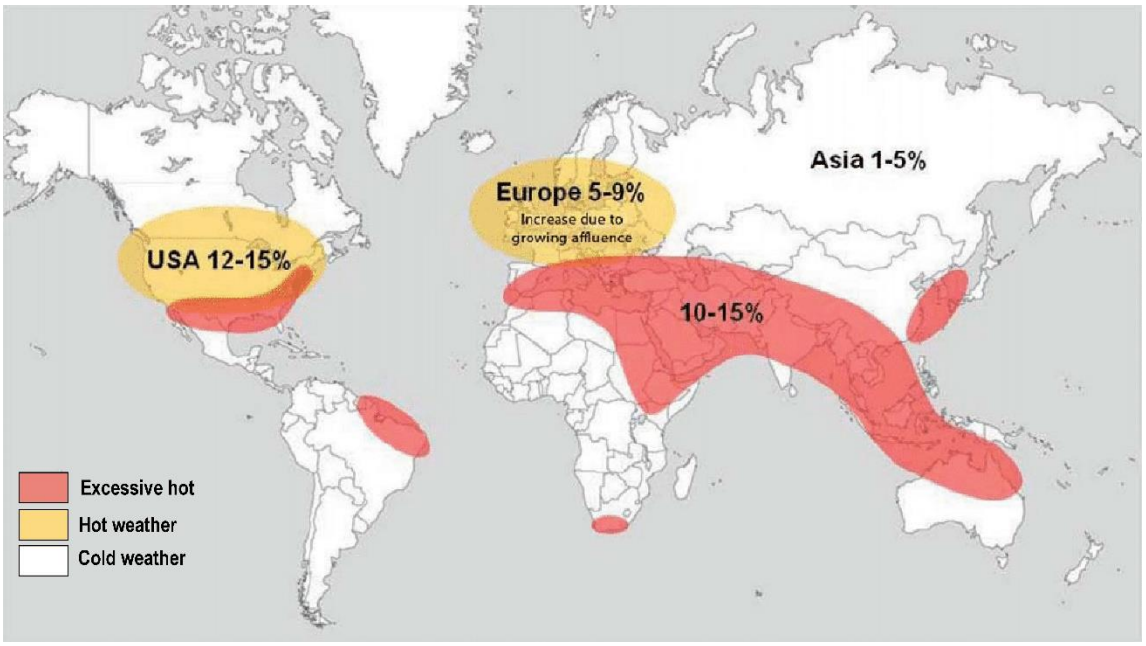

Figure 4.2. The predicted kidney stone risk areas around the globe. The stone belt (red) extends all the way around the world and is characterised by the urinary stone prevalence of 10 to 15%. Climate simulations for the USA indicate that the stone belt will move northwards in the coming decades. Adapted from (Fisang et al., 2015).

The probability of conceiving stones varies considerably in different parts of the world. It affects 10–15% of the population in parts of Asia, 5–9% in Europe, and 12-15% in North America (Silva et al., 2011). The risk of developing kidney stone among adults is more significant in the western hemisphere (9.5% in Europe, 12% in Canada, 13–15% in the USA) as compared to the adults living in the eastern hemisphere (5.1%) (López and Hoppe, 2010). South western Asia represents a high-risk environment for stones (5 times higher) (Evans and Costabile, 2005) as compared to other regions of the world. The highest risk has been reported in the United Arab Emirates (UAE), Kuwait and Saudi Arabia (20.1%) (Robertson, 2012).

4.2.4 Kidney stone prevalence with temperature

There is an increasing incidence of nephrolithiasis in the tropics, especially during the summer, where the risk is aggravated by low urine volume (Trinchieri, 2008). It is known that elevated temperature causes increase in heat-induced sweating which further, leads to a state of dehydration causing reduced urine volume and increase in diuretic concentrations, which thereby facilitates the crystallisation of the urinary compositions, thus triggering the accumulation of stones (Silva et al., 2011).

Previous studies hypothesise that dry climate increases the development of renal calculi, mainly due to dehydration (Khan et al., 2016, Clark et al., 2016). Further, it is known that the incidence of nephrolithiasis is higher in countries with a warm climate, mainly the North American and Afro-Asian stone belts, probably due to low urinary output and low fluid intake (López and Hoppe, 2010). In the United Kingdom, a similar study was conducted to find the relation between seasonal variation in temperature with mineralisation process, where researchers analysed urine samples for 24-hours from 246 male patients with a history of kidney stones (Fakheri and Goldfarb, 2011). Further analysis demonstrated statistically significant changes in the quantity of stones in summer as compared to winter. However, no change was observed in urine pH or volume in this UK study.

A similar study was conducted in Finland throughout a year, and the results were analysed by measuring the serum level of 25-hydroxyvitamin D, urinary calcium, and urinary oxalate (Juuti and Heinonen, 1979). It is known that sunshine activates vitamin D and therefore increases the concentration of serum 25-hydroxyvitamin D, thereby elevating urinary calcium levels in summer (Lin et al., 2014). Moreover, the levels of 25-hydroxyvitamin D were higher throughout the year in hypercalciuric stone-formers than normocalciuric stone-formers. All the changes observed correlated temporally with an increase in sunlight measured by units of ultraviolet light. Further, seasonal variation was also evaluated in Kuwait by quantifying the number of patients visiting in the hospitals due to renal colic; the authors found 980 cases of colic in the summer versus only 524 cases in the winter (Fakheri and Goldfarb, 2011).

Studies conducted across the USA found that the rate of stone prevalence increased from north to south and west to east (**Figure 4.3**). The north-to-south trend correlates well with temperature variation, but the role of climate in the west-to-east trend is much more ambiguous (Brikowski et al., 2008). These reports were further supported by other researches across the USA. In addition to that, another study has shown/examined the relation between stone prevalence and specific risk factors such as mean temperature, sunlight index, and beverage consumption. For males, sunlight exposure caused more stones as compared to variation in mean annual temperature or beverage consumption. For women, beverage consumption, average temperature, and sunlight index explained regional variation more or less equally (Soucie et al., 1996).

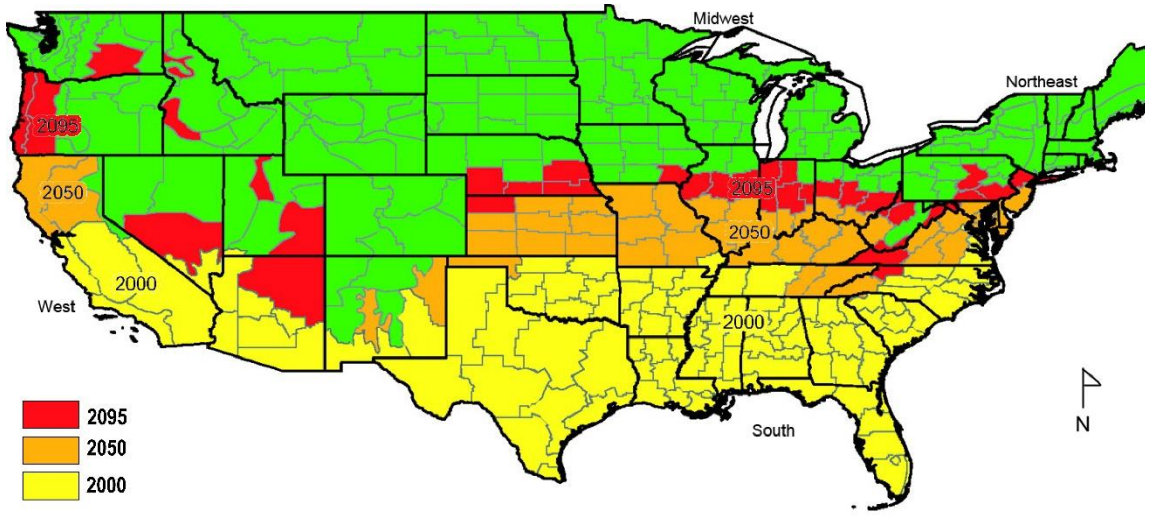

Figure 4.3. Predicted growth in the high-risk stone area (stone belt; risk ratio ≥1.2) vs time, for 2000 (yellow), 2050 (orange), and 2095 (red); linear model. At 2000, 41% of the population is within a high-risk zone, 56% in 2050, and 70% in 2095, based on the year 2000 population distribution. Reproduced with permission from (Brikowski et al., 2008)

Subsequently, the first prospective study in healthy human population showed that the mean time to develop symptomatic urinary calculi was 93 days after continuous exposure to hot temperature (Evans and Costabile, 2005). Furthermore, consistent results were attained analysing the duration of symptoms (stones) occurrence in the European immigrants moving to Israel (Frank et al., 1959) and also with military desert deployments (Blacklock,

1965). Similarly, professional cooks exposed to intense heat for a long time have a high prevalence of renal stones; and likewise, the workers exposed to the extensive heat in the glass industry (Atan et al., 2005).

Overall, these data provide a comprehensive picture to forecast the relationship between geographic variability and weather in the creation and development of renal stones. Based on these observations, we derive two primary outcomes:

a. Kidney stone growth increases with a rise in environmental temperature.

b. The incidence of mineralisation increases with age.

4.3 Aims:

Evidence shows that many factors may influence nephrolithiasis, either as protective or risk factors (Scales Jr et al., 2012). To further elucidate the possible mechanisms behind temperature and age-induced nephrolithiasis, we undertook a study to observe the trend of the mineralisation process using *Drosophila* as a model organism. Besides all the benefits of using *Drosophila* in molecular research as enumerated in **section 1.6**. *Drosophila* can be readily switched from one temperature to another, which allows researchers to make a rapid observation of the effect of environmental alteration in stone production. Specifically, we studied variation by rearing and switching flies between high and low temperature or vice versa. Further, we altered the temperature every week to observe the change in the pattern of stone formation. Through quantification and analysis of the data, we provide clear evidence that temperature variation correlates with renal stones accumulation. Thus, *Drosophila* can be used to model the impact of the environment on stone formation.

4.4 Results:

4.4.1 Rise in temperature accelerates *Drosophila* stone development

To investigate the functional role of temperature in stone development newly emerged wild-type flies (Canton S) were collected from stock tubes and reared at different temperatures: 18°C, 22°C, 26°C and 29°C. All the experimental flies reared at temperatures as mentioned earlier were dissected on day 7, day 14 and day 21 and the total stones accumulated within MTs were quantified. Under light microscopic examination, the intraluminally accumulated dark content had the physical and visual appearance of small stones (hardness of stones could be felt by touching with fingers), suggesting the presence of stones within the MTs. Given their characteristics, these abundant concretions were referred as fly stones **Figure 4.4**.

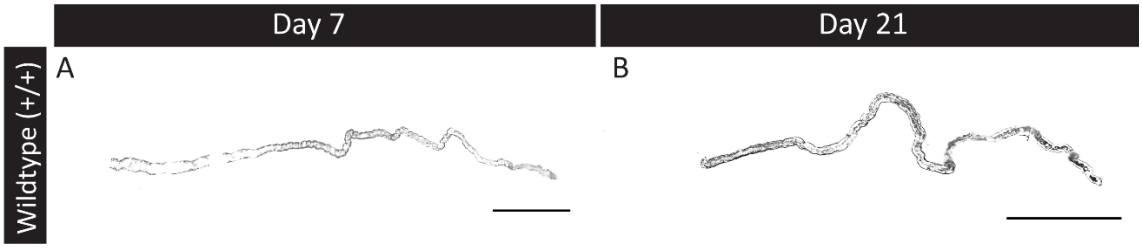

Figure 4.4. Representative tubule from control flies reared at 29°C, for (A) day 7 and (B) day 21. Stones are dark intraluminal contents. Scale bars: 500 µm.

Interestingly in mammals, sexual dimorphism is evident in kidney stone growth (Ling et al., 1998, Stamatelou et al., 2003). Hence, in this study, the stones in flies of either sex were quantified to observe the difference in stone accumulation in between male and female flies. The amount of concretions accumulated in MTs of female flies at 18°C, 22°C, 26°C and 29°C on day 7, day 14 and day 21, was quantified using a comparative analysis method. At day 7 and day 14 there was no significant difference in the quantity of stones accumulated among all the groups (flies reared at 18°C, 22°C, 26°C and 29°C). On day 21, flies reared at 18°C, 22°C, 26°C and 29°C exhibited 13.33 ± 0.81 %, 23.45 ± 2.61 %, 24.86 ± 1.92 %, 27.04 ± 1.08 % stones respectively which was significantly higher as compared to stones accumulated at day 14 (**Table 4.1,**

A) (flies reared at 18˚C, 22˚C, 26˚C and 29˚C exhibited 0.86 ± 0.13 %, 0.96 ± 0.29%, 1.52 ± 0.17% and 2.01 ± 0.1% respectively). However, there was no significant difference in the quantity of stones between flies reared at 22˚C, 26˚C and 29˚C. Furthermore, male flies also showed a similar response to that of female flies (**Table 4.1, B**).

A. Female Anterior

Temp	18˚C	22˚C	26˚C	29˚C
Days	**Mean ± SEM**	**Mean ± SEM**	**Mean ± SEM**	**Mean ± SEM**
7	0.867 ± 0.304	0.901 ± 0.130	1.733 ± 0.225	2.354 ± 0.203
14	0.866 ± 0.136	0.962 ± 0.296	1.529 ± 0.178	2.015 ± 0.513
21	13.337 ± 0.812	24.866 ± 1.923	23.456 ± 2.614	27.040 ± 1.077
28	21.444 ± 1.450	21.408 ± 1.025	25.020 ± 1.803	25.860 ± 1.268

B. Male Anterior

Temp	18˚C	22˚C	26˚C	29˚C
Days	**Mean ± SEM**	**Mean ± SEM**	**Mean ± SEM**	**Mean ± SEM**
7	1.646 ± 0.456	0.876 ± 0.085	1.355 ± 0.418	0.370 ± 0.158
14	1.677 ± 0.302	1.329 ± 0.167	0.880 ± 0.131	0.901 ± 0.105
21	15.632 ± 1.368	20.127 ± 2.284	20.793 ± 1.655	21.553 ± 0.999
28	20.995 ± 1.489	20.115 ± 1.070	20.733 ± 2.178	20.234 ± 1.654

Table 4.1. Temperature and age-specific occurrence of kidney stones among female and male flies. The total luminal area occupied by mineralised concretions in (A) female and (B) male flies. At day 21, flies reared at 29˚C produce significantly more concretions compared to flies reared at 18˚C in both the cases. However, at day 7 and day 14, there was no significant difference in the quantity of accumulated stones in between 18˚C, 22˚C, 26˚C and 29˚C reared flies. Both female and male flies show a similar response to the temperature). Data shown are the mean ± SEM, N=10.

In summary, the results indicate a clear positive correlation between temperature and renal stone accumulation in flies of either sex. Thus, these data are consistent with a similar study conducted in a human model (Fakheri and Goldfarb, 2011, Romero et al., 2010), thereby validating *Drosophila* as a useful model for such studies.

4.4.2 The incidence of kidney stone increases with age

Next, the influence of age in kidney stone accumulation was examined. For this, all the flies were reared for 21 days, and accumulated stones were quantified every week. It was observed that the stone formation increased with age, irrespective of the gender and temperature they were reared (**Figure 4.5**). Among all the groups, 21-day old female flies reared at 29˚C, has 27.04 ± 1.07% stones which are 12-fold high as compared to the stones accumulated in 14-day old flies. A similar result was also observed between 21 days and 14 days old female flies, reared at 18˚C, 22˚C and 26˚C. Interestingly, the impact of age on stone formation was similar in male flies, thereby confirming that stones formation increases with age.

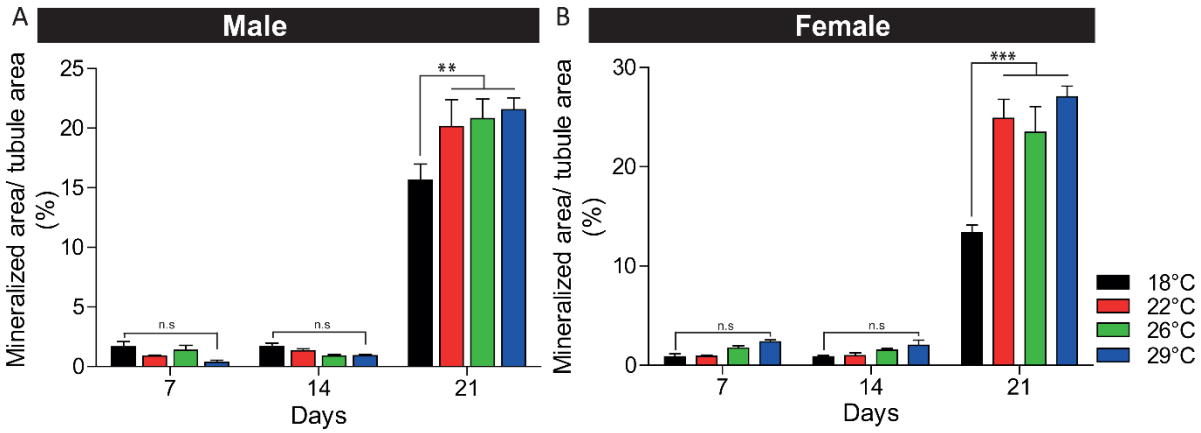

Figure 4.5. Data are replotted from Error! Reference source not found. **to d raw attention to the effect of age on kidney stone formation**. In both (A) Female and (B) male flies, development of kidney stone increases with age, 21 days old flies have a significantly higher amount of stones accumulate as compared to day 7 or day 14 old flies. Data are presented as mean± SEM, N=10. *p <0.05, two-way ANOVA.

In summary, based on the observations above, we can conclude that the rate of renal stone accumulation is directly proportional to the age.

4.4.3 Alteration in the stone formation rate in response to changing of temperature

In our previous results, temperature specific alteration in stones development was demonstrated, where the maximum effect was observed in flies reared at 29°C, and the minimum in flies reared at 18°C. Hence, to further determine an impact of alteration in temperature and exposure time in stone production, flies were reared at 18°C and 29°C and then switched to an alternate temperature weekly (day 7, day 14 and day 21). The quantity of accumulated amount of stones measured for each temperature and age combinations. The experimental procedure is shown in **Figure 4.6**.

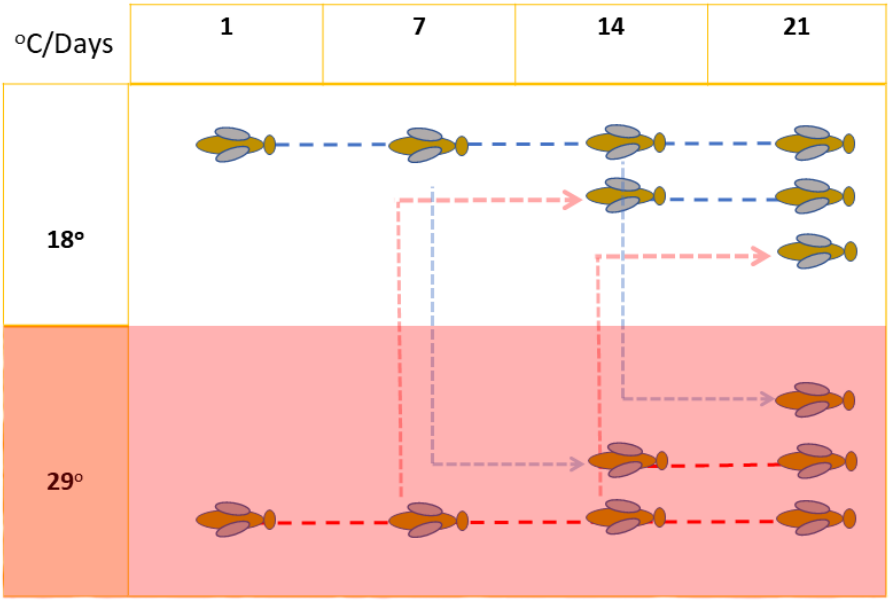

Figure 4.6. Workflow for fly maintenance and temperature switching

Wild-type flies were reared at 18°C and 29°C, and at age 1, 2 and 3-week they were switched from one temperature to other. First, it was confirmed that flies, aged 21 days, have an increased amount of stones compared to 7- and 14-days old flies. Interestingly, it was also shown that at day 21, female flies kept at 18°C have significantly fewer stones as compared to flies switched from 18°C to 29°C at day 7 and day 14 (**Figure 4.7 A**). Similarly, flies raised at 18°C and changed to 29°C, at day 7 exhibited significantly higher levels of renal stones than flies switched from 18°C to 29°C at day 14. This was expected as

rearing flies at higher temperature should accelerate the rate of stone formation.

The relation of the temperature switching with accumulated stones was further analysed by reverse-switching flies from 29˚C to 18˚C, at day 7 and day 14. By contrast, flies reared at 29˚C for 21 days accumulated significantly more stones as compared to flies switched from 29˚C to 18˚C, at day 7 and day (**Figure 4.7, B**).

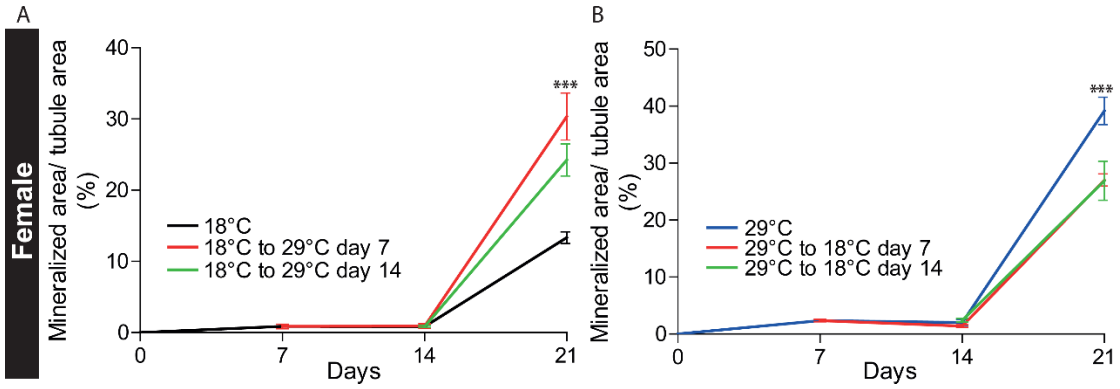

Figure 4.7. Disproportion in renal stone formation in response to switching of temperature in female flies. A. Quantification of the total stones accumulated in female flies reared at (A) 18˚C and switched to 29˚C, at day 7 and 14 and (B) at 29˚C and switched to 18˚C, at day 7 and 14. Data shown are the mean ± SEM, N=8, tubules. For 18˚C reared and switched flies 18˚C was regarded as a control and 29˚C reared and switched flies 29˚C was regarded as control. ***p <0.001, two-way ANOVA.

Further, the same analysis was concurrently performed in male flies to observe a potential variation in stone accumulation. Surprisingly, 21-days-old males reared at 18˚C did not show any significant stones compared to males switched from 18˚C to 29˚C, at day 7 or 14. By contrast, 21-day-old males kept at 29˚C showed a higher quantity of stones compared to males switched from 29 ˚C to 18˚C, at days 7 or 14, **Figure 4.8**.

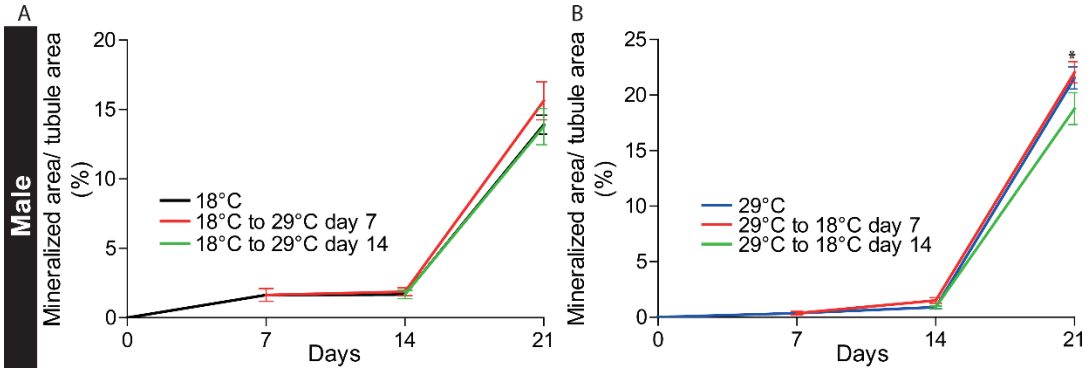

Figure 4.8. Renal stone formation in male flies in response to a temperature switch. (A) Quantification of stone in flies reared at 18˚C and then switched to 29˚C, at day 7 and 14, or (B) reared at 29˚C and then switched to 18˚C, at day 7 and 14. Data shown are the mean ± SEM, N=8. For 18˚C reared and switched flies 18˚C was regarded as control and 29˚C reared and switched flies 29˚C was regarded as control. *p <0.05, two-way ANOVA .

Taken together, these results demonstrate that the incidence of a renal stone depends upon the age of flies and the temperature of their current habitation, with past exposed temperature having no detectable effect. Hence, it can be proposed that flies reared at low temperature has reduced the quantity of stones entirely as a consequence of less accumulation of ageing related damage. In reciprocal switches from 29˚C to 18˚C, the stones were significantly higher in flies reared at 29˚C for a more extended period. Throughout the experiments, female flies subjected to temperature switching analysis showed consistent results as compared to male flies. Further, it is known that female flies have higher tubule calcium content compared to male flies (Chintapalli et al., 2012, Dube et al., 2000), which is required for egg production. Hence, a significantly enhanced accumulation was observed in female as compared to male flies.

4.4.4 Intraluminally accumulated stones are composed of Phosphate

Next, the chemical composition of the intraluminally accumulated stones was analysed using a colorometric assay. The intensity of the colour of the tubule sample was plotted based on the absorbance at 620 nm as a function of phosphate concentration in the sample (**Figure 4.9**). The resultant linear

regression equation for the male flies was: Abs=0.1133+0.001754 (R^2=0.9424) and for female was Abs=0.1103+0.001701 (R^2=0.9084).

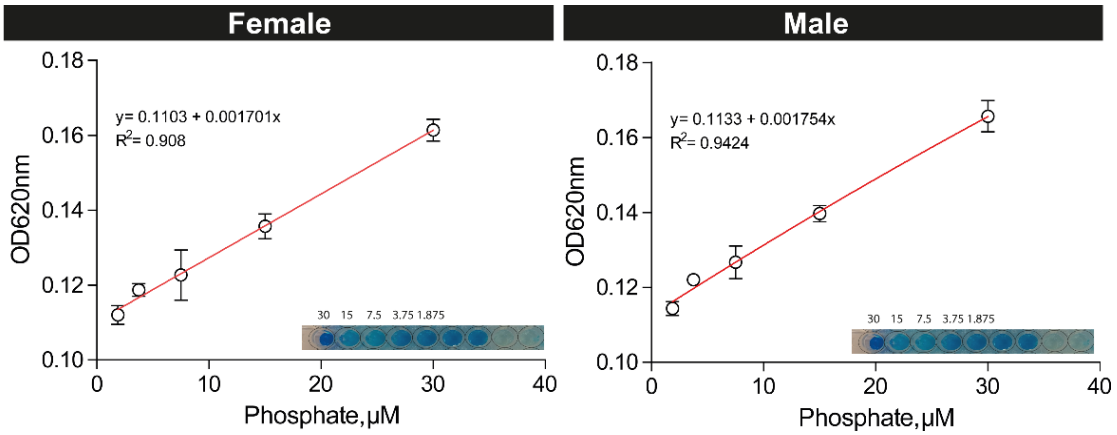

Figure 4.9. Calibration curves corresponding to phosphate concentration in MTs of 21 days old female and male flies. The blue colour intensity in the control and samples can be observed directly by naked eyes.; dark blue=high concentration.

To examine the selectivity of this system towards the phosphate detection in MTs of 7- and 21-days old flies, the phosphate concentration was quantified in MTs of both age group flies. The results are displayed in **Figure 4.10**. As expected, the total concentrations of phosphate in MTs of 21 days old flies were significantly higher compared to 7 days old flies, independently of the gender (~3-fold increase in both males and females).

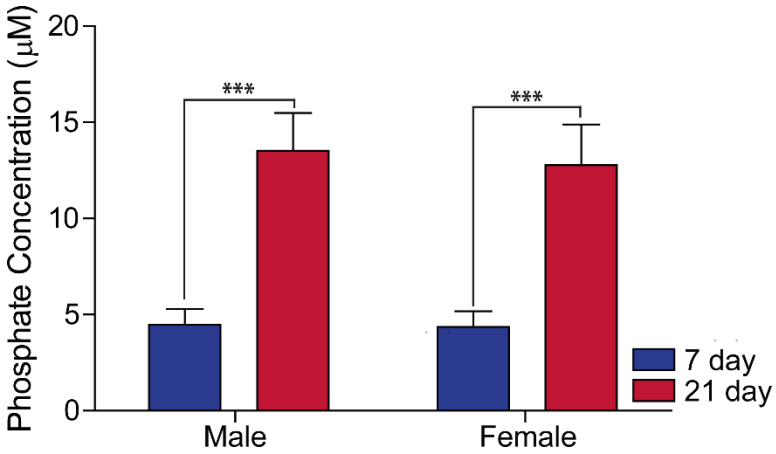

Figure 4.10. Intraluminal phosphate concentration increases with age. The total phosphate concentration in anterior MTs was quantified at day 7 and day 21. 21 days old flies have significantly higher phosphate quantity as compared to 7-day old flies. Data are expressed as mean ± SEM (n = 60). ***p<0.001, *students t*-test.

Taken together, these results unambiguously demonstrate the presence of phosphate stones within MTs and elevation in the quantity of phosphate stones along with age.

4.4.5 Age-dependent variation in expression of *NaPi-T* and *Picot*

On the basis of the above-mentioned colorimetric result, it is hypothesised that phosphate stones might be formed due to high transport of phosphate intraluminally in MTs. Hence to better understand the phenomena, the alteration in the expression of genes involved in the transport of the phosphate across the membrane in MTs was observed in 7- and 21-day old flies. In *Drosophila*, two essential phosphate transporter genes (*NaPi-T* and *Picot*) have been reported to be highly expressed in MTs (**section 4.6**), whose function is to regulate phosphate movement across the cell membrane (Chintapalli et al., 2012a, Overend, 2010).

In this model, the expression level of *NaPi-T* and *Picot* was compared with age (7 and 21-days old flies) using qRT-PCR. Observations indicate significant downregulation (55%) in the expression of *NaPi-T* in 21-day-old flies as compared to 7-day-old flies. Additionally, modest upregulation in the expression levels of *Picot* was observed in 21-days-old MTs as compared to 7-day-old MTs (**Figure 4.11**).

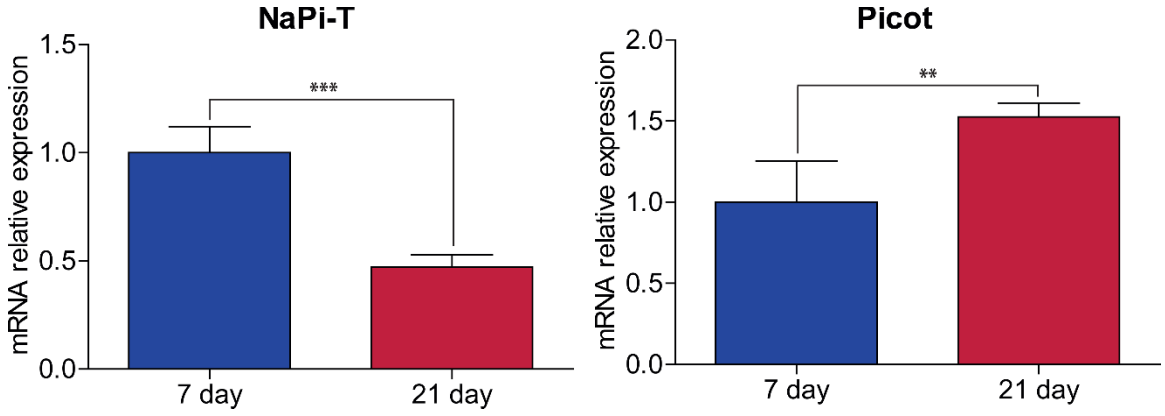

Figure 4.11. Effect of age in *NaPi-T* and *Picot* genes expression in MTs. A. *NaPi-T* B. *Picot*. The experiment was conducted in three biological replicates. Data are expressed as the mean of mRNA relative expression ± SEM, N=3. **p<0.01, ***p<0.001, *students t*-test.

4.4.6 Knockdown of *NaPi-T* increases phosphate concentration within the MTs

NaPi-T is the *Drosophila* orthologue of human sodium phosphate specific Transporter-II predominantly expressed in MTs. It is located on the apical membrane of the tubular cells and facilitates the excretion of phosphate across the cell membrane into the lumen (detail **Chapter 6**). Based on previously published data in other organisms, it can be postulated that by inhibiting transport genes function using RNA interference technology, phosphate should be sequestered away from the tubule lumen where it would otherwise be excreted and should, therefore, be accumulated in higher levels. So, in order to verify the effect of *NaPi-T* in the modulation of the quantity of phosphate, genetic and biochemical assays were performed.

For this, initially, an expression of *NaPi-T* was silenced in the MTs principal cells using *CapaR-GAL4*. It is found that the expression of mRNA levels of *NaPi-T* was reduced by 75% (**Figure 4.12**).

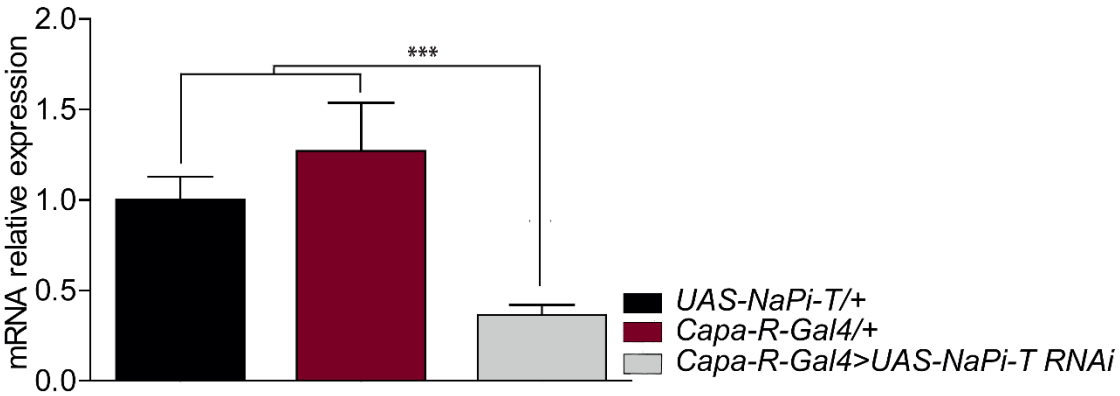

Figure 4.12. Validation of knockdown of *NaPi-T* expression in principal cells of MTs. The relative expression shows a significant downregulation of *Capa-R-GAL4>UAS-NaPi-T RNAi* compared to parental control lines. Data are expressed as mean ± SEM, n=3. *p<0.05, one-way ANOVA followed by Dunnett's test.

As shown in **Chapter 3** it is observed that RNAi inhibition of *NaPi-T* resulted in increased tubular phosphate concentration as compared to the controls. In addition to that, the stones in this model were physically and visually alike to

phosphate stones. Hence it is assured that the stones accumulated within the MTs are composed of phosphate. Further, the chemical composition of the stones was determined using the colorimetric assay kit. We found that ubiquitous knockdown of *NaPi-T* in principal cells (*CapaR-GAL4>UAS-NaPi-T* RNAi) induces significantly higher (~200-fold increase) phosphate concentration compared to controls, in both males and females (**Figure 4.13**).

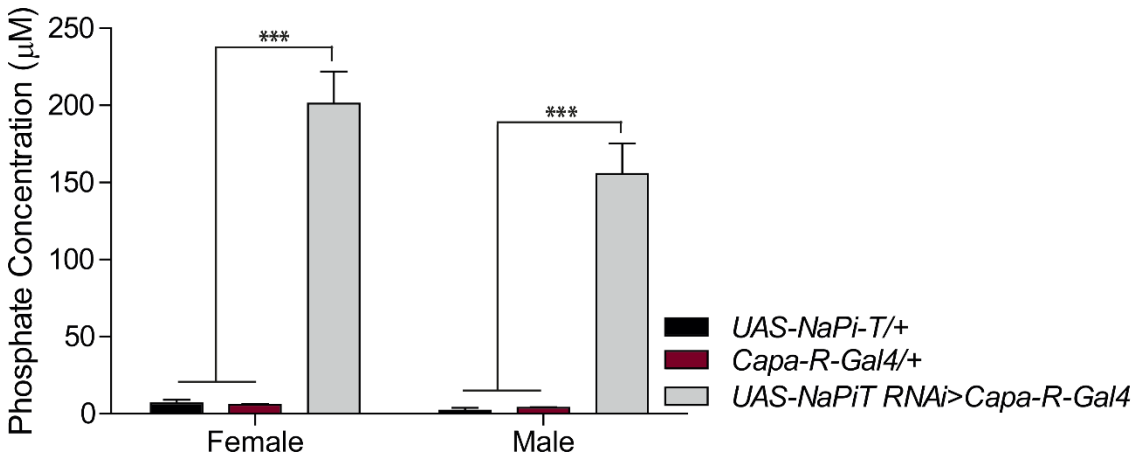

Figure 4.13. Downregulation of *NaPi-T* expression elevates tubule phosphate concentration. *CapaR>NaPi-T RNAi* exhibits a significant increase in the phosphate levels in MTs in both female and male flies compared to controls. Data are expressed as the mean ± SEM, N = 60). ***p<0.001, one-way ANOVA followed by Dunnett's test.

Our results demonstrate the importance of *NaPi-T* in the maintenance of intraluminal phosphate concentration. Taken together, these results chemically validate the previous findings assuring that inhibition of the function of *NaPi-T* causes formation of phosphate stones.

4.5 Discussion

Understanding the diverse causes that give rise to renal stones and the development of effective medical management to cure the disease is a long-standing challenge (Moe, 2006). A significant barrier for such management includes a rudimentary understanding of the detailed mechanisms initiating stones accumulation (detail in **section 1.4.4**).

In this study, the time and duration of stone accumulation concerning gender and temperature are well documented, which allows calculating the pattern of

stones formation. Previous human studies in the US have shown that locations with high temperature have a high prevalence of renal stones (Soucie et al., 1994). A consistent result was obtained in the European immigrants to Israel (Frank et al., 1959) as well with the military desert deployments (Blacklock, 1965). Similarly, professional cooks exposed to intense heat for a long time have a high prevalence of renal stones, and similar results have been observed with workers exposed to the intense heat of the glass industry (Atan et al., 2005).

The temperature switch experiment revealed that accumulation of stone surges at high temperature and decreases with lowering temperature. However, once the stones are generated, they reside forever without disintegration. We present strong evidence that stone formation was elevated when flies were switched from 18°C to 29°C compared to flies permanently reared at 18°C. In reciprocal switches from 29°C to 18°C conditions, stones level remained unaffected in switched flies. Long-term 18°C reared flies; therefore, either impeded the female's ability to respond to 29°C or ageing related damage could not accumulate (Mair et al., 2003).

Additionally, previous studies have observed that flies reared at 29°C age earlier and accumulate ageing-related damage compared to flies reared at 18°C, 22°C or 26°C. It is generally accepted that anterior tubule of *Drosophila* store a high amount of calcium as a phosphate-rich mineral concentration in large initial segments (Dube et al., 2000). Furthermore, anterior tubules are enriched with genes implicated in calcium and phosphate transport (Chintapalli et al., 2012, Wessing and Eichelberg, 1979). Hence; all the studies were carried out using anterior tubules of *D. melanogaster*.

However, the primary aim of our experiment was to determine the change in the stone accumulation with age. Hence, to be consistent throughout the experiment (among all the age groups and temperature reared flies), the stones within MTs were quantified every week. Overall, these results extend the findings that the process is dependent on the duration of the current exposure temperature, and once the stones start accumulating they remain accumulated for more time. Further, this observation was validated by biochemical assays which revealed that the stones within MTs were indeed

composed of phosphate and the phosphate concentration increases with age, which thereby might bind with calcium forming the calcium phosphate crystals (Ratkalkar and Kleinman, 2011). The details about the formation mechanism of calcium phosphate and calcium oxalate crystals are well documented in **section 1.4.5.1**.

Our physiological and biochemical experiments revealed that there are two alternative scenarios to explain the elevation of intraluminal phosphate; a. Role of phosphate transporters, b. Phosphate storage in the form of concretions within the tubule (Chintapalli et al., 2012a, Bergwitz et al., 2012). *H. Sapiens* has three types of membrane-bound phosphate transporters: type I: *SLC17A1-9, type II: NPT2a*, *NPT2b*, and *NPT2c*, and type III: *Pit1* and *Pit2; which* are thought to be exclusively transporting phosphate across the membrane (Levi and Bruesegem, 2008). However, in *Drosophila* MTs, *NaPi-T* and *Picot* are the knows major players involved in elevating intraluminal concentration that contributes to the kidney disease (Villa-Bellosta et al., 2009, Chintapalli et al., 2012). In humans (Blaine et al., 2015, Virkki et al., 2007) and rat studies (Villa-Bellosta et al., 2009), it has been shown that the sodium phosphate cotransporters are positioned in the apical membrane of renal proximal tubule cells, to move phosphate from lumen to the cell interior (Curthoys and Moe, 2014b). The qPCR results described suggest that *NaPi-T* and *Picot* act as contributors to the accumulation of phosphate stones. However, the mechanism behind an influence of temperature in the change of body physiological function to contribute stones accumulation remains unclear and requires further study.

In humans, the primary driving force is a transporter, Na^+/K^+-ATPase generating an electrochemical gradient for apical phosphate entry (Virkki et al., 2007). Mutation of the phosphate transporters causes high accumulation of sodium and phosphate intraluminally. Hence, it is hypothesised that a similar mechanism is also conserved in the flies resulting in aggregation of renal stones. However, *Picot* is present in the basolateral membrane in *Drosophila* tubules (Overend et al., 2015) and is required to transport sodium inside the vesicles to maintain phosphate concentration inside the cell interior (unpublished results; Dow/Davies lab). It is hypothesised that, with age, *Picot* expression increases,

thereby elevating the concentration of inward flow of phosphate within the tubule.

In conclusion, our analysis demonstrates that high temperature and age causes accumulation of phosphate crystals due to change in expression of phosphate transporters. Furthermore, these data complement previous work (Hirata et al., 2012, Chi et al., 2015) to establish *Drosophila melanogaster* as one of the best models to study the renal stone formation and highlights its importance in the field of biomedicine. Further research focused on the relationship between age, temperature, and renal stone formation may reveal new possibilities for the management of renal and unrevealing possible new efficient therapies and cures for this condition.

4.6 Supplementary data

NaPi-T

	Adult Male		Adult Female		Larval	
Tissue	**FPKM**	**Enrichment**	**FPKM**	**Enrichment**	**FPKM**	**Enrichment**
Head	0.2	0.0	0.1	0.0		
Eye	0.2	0.0	0.1	0.0		
Brain / CNS	0.2	0.0	0.3	0.0	0.5	0.0
Thoracico abdominal ganglion	0.9	0.0	0.8	0.1		
Crop	0.5	0.0	1.0	0.1		
Midgut	1.9	0.1	0.4	0.1	0.5	0.0
Hindgut	0.9	0.0	1.0	0.1	2.4	0.1
Malpighian Tubules	1004	35	917	115	615	28
Fat body					3.3	0.2
Salivary gland	2.1	0.1	0.3	0.0	0.2	0.0
Heart						
Trachea					1.4	0.1
Ovary			0.3	0.0		
Virgin Spermatheca			0.0	0.0		
Mated Spermatheca			0.2	0.0		
Testis	1.3	0.0				
Accessory glands	0.1	0.0				
Carcass	7.9	0.3	6.2	0.8	0.7	0.0
Rectal pad	0.2	0.0	0.4	0.1		

Picot

	Adult Male		Adult Female		Larval	
Tissue	**FPKM**	**Enrichment**	**FPKM**	**Enrichment**	**FPKM**	**Enrichment**
Head	42	1.0	40	1.5		
Eye	33	0.8	29	1.1		
Brain / CNS	24	0.6	26	1.0	19	0.9
Thoracico abdominal ganglion	40	1.0	44	1.6		
Crop	4.9	0.1	7.5	0.3		
Midgut	125	3.0	107	3.9	18	0.9
Hindgut	677	16	656	24	112	5.4
Malpighian Tubules	215	5.2	261	9.6	154	7.4
Fat body					2.0	0.1
Salivary gland	18	0.4	28	1.0	7.7	0.4
Heart						
Trachea					20	1.0
Ovary			10	0.4		
Virgin Spermatheca			94	3.4		
Mated Spermatheca			113	4.2		
Testis	20	0.5				
Accessory glands	18	0.4				
Carcass	20	0.5	19	0.7	6.3	0.3
Rectal pad	24	0.6	56	2.1		

Supplementary Tables. Expression of *NaPi-T* and *Picot* in *Drosophila* adult (male and female) and larval MTs. Data is obtained from RNA-seq analysis, FPKM (Fragments Per Kilobase Million). Adapted from FlyAtlas2 (Leader et al., 2017).

Chapter 5 Role of *Sip1* in Uric acid stones formation in *Drosophila* MTs

5.1 Summary

In **Chapter 3**, different genes expressed in MTs that are putatively involved in renal stone formation were identified. In this chapter, the role of *Sip1* (SRY-interacting protein 1) gene, a homologue of human *NHERF1* (Sodium-Hydrogen Exchanger Regulatory Factor-1) in *Drosophila* MTs, and its impact on nephrolithiasis were determined. The introduction of this chapter describes the uric acid stones formation pathway. Further, we emphasise the characterisation of mammalian *NHERF1* and its importance in uric acid stones formation. Previous studies have demonstrated that targeted deletion of *NHERF1* augmented intestinal deposition of calcium, thereby elevating calcium oxalate and uric acid stone formation. *Drosophila Sip1* is strongly expressed in MTs and is the primary focus of this study. Mutation or tubule knockdown of the *Sip1* gene led to abundant uric acid stone formation in MTs, which was validated by physical, chemical and pharmacological studies. Further, the localisation of SIP1 protein and its partner proteins Moesin and NHE2 were demonstrated in stellate cells. In MTs, exchange of Na^+/H^+ is mediated by *NHE2* and has a specialised role in ion transport in MTs. It is proposed that *NHEs* transport H^+ into the lumen using the inward Na^+ chemical gradient, thereby decreasing luminal [Na^+] and increasing luminal [H^+] resulting in a lower pH that favours precipitation of urate as uric acid crystals. Taken together, our results further increase the understanding of the molecular mechanisms of kidney stone formation in *Drosophila*, which may be beneficial for mammalian studies leading to the identification of novel approaches to human renal stone treatment.

5.2 Introduction

Urate, the anionic form of uric acid (Nuki, 2012), plays an essential role in many biological functions, including maintenance of vascular endothelial cell integrity and defence against neurological and autoimmune diseases through various physiological and biochemical pathways (El Ridi and Tallima, 2017). In the normal physiological condition of the human body, uric acid predominates at neutral pH and is present both intracellularly in all the body fluids (Bobulescu and Moe, 2012). The enzyme urate oxidase (UO or uricase) has been lost with evolution in higher primates like humans, suggesting the importance of uric acid in survival and reproductive functions of the normal body (Álvarez-Lario and Macarrón-Vicente, 2010, Riches et al., 2009). However, in mammals, uric acid is excreted in the urine, as an end product of purine metabolism. Continuous accumulation of uric acid in the body causes various noxious effects like gout and kidney stone (Moe, 2006).

Uric acid stones are the third most common class of kidney stones, accounting for around 10% prevalence among the total global population (Curhan, 2007). Uric acid stones were first isolated in 1776 from urinary calculi by Karl Wilhelm Scheele. He initially called the substance lithic acid and later proved it to be one of the major components present in human urine (Fink et al., 2003). Similarly, in 1798 George Pearson isolated uric acid from 200 urinary calculi specimens and characterised them physically and chemically as uric acid (Pearson, 1798). In 1875 Ludwig Medicus proposed the first structure of uric acid, without definitive evidence. The first total synthesis of uric acid was performed in 1895 by the 1902 Nobel laureate Emil Fischer (Hall et al., 2016), proving the accuracy of Medicus' proposed structure. It has a molecular formula of $C_5H_4N_4O_3$ (168.112 g/mol). Since then, different forms of uric acid crystals have been recognized as noticeable components in these pathological deposits (Atsmon, 1963, Mandel and Mandel, 1989), including anhydrous uric acid (UA) (Ringertz, 1965, Ringertz, 1966), uric acid dihydrate (UAD), uric acid monohydrate (UAM), the structure of which was only recently reported, as well as the ionized forms monosodium urate monohydrate (MSU) and ammonium acid urate.

5.2.1 Physiology of purines and Uric acid

In human, uric acid is a necessary product in the purine metabolism pathway. Xanthine oxidase (XO), the mediator enzyme, converts hypoxanthine to xanthine and xanthine to uric acid, **Figure 5.1**. In most mammals, uric acid is an intermediate product, as it undergoes oxidation by hepatic uricase to the more soluble allantoin. However, multiple cumulative mutations result in non-functional uricase in higher primates, including humans. Thus urate is an end product of purine metabolism in humans (Riches et al., 2009). Allantoin is a highly soluble compound without any known adverse effects on health (Maiuolo et al., 2016). XO inhibitors are effective in reducing new/de novo uric acid formation, but the accumulation of xanthine may result in acute xanthine nephropathy (LaRosa et al., 2007).

The sources of purines in the human body are (a) de novo synthesis, (b) cellular RNA from the normal turnover of cells, and (c) exogenous, i.e., from external sources like dietary intake (Maiuolo et al., 2016, Lane and Fan, 2015). Under standard conditions, endogenous uric acid production is about 300–400 mg per day. The role of exogenous purines is variable though it usually contributes less than 50% of total uric acid production. Elimination of uric acid is achieved via the gastrointestinal tract (30%) and the kidneys (70%). About 90% of uric acid is freely filtered; the remaining 10% is protein-bound urates. The filtered load undergoes several cycles of absorption and secretion by the kidney for a final fractional excretion rate of about 10% (Kamel et al., 2005).

Alkaline supplementation is one of the most effective treatments for existing uric acid stone. If the urine pH is upheld at 6.5 or higher (which often requires 90 to 120 mEq of supplemental alkali per day), uric acid stones dissolve within the human body. Slightly lower doses may be used to avoid new uric acid stone formation (Kanbara et al., 2010). An XO inhibitor is a second-line choice if the patient has noticeable hyperuricosuria or is unable to maintain a urine pH higher than 6.5. Several drugs such as benzbromarone, losartan, probenecid and salicylic acid have a uricosuric property and thus increase the risk of renal stones formation by influencing the renal handling of uric acid. Recent molecular identification and functional analysis of urate-specific transporters have provided important new insights (Enomoto et al., 2002, Lipkowitz et al.,

2001, Leal-Pinto et al., 2002). This is of interest not just to better elucidate the complex renal handling of uric acid, but also for understanding the genetic mechanism behind uric acid stone formation using *Drosophila* renal tubules (Sorensen and Chandhoke, 2002, Johri et al., 2010).

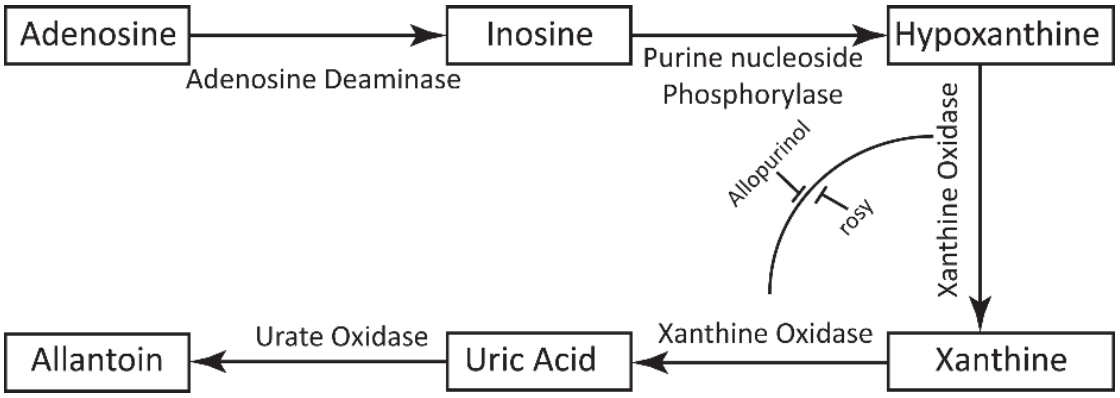

Figure 5.1. Uric acid biosynthesis pathway. Uric acid is the end product of purine metabolism catalysed by different enzymes, including Xanthine Oxidase. Adapted from (Berry and Hare, 2004).

5.2.2 Pathophysiology of uric acid stone formation

The pathogenesis of uric acid stone formation is only moderately understood, therefore limiting the prevention and therapeutic approach of the disease. Persistent acidic urine, hyperuricosuria and excretion of low urinary volume, are the most prevalent risk factors of uric acid nephrolithiasis in humans (Moe, 2006). Among all, urinary pH is the main determining factor of uric acid manifestation and precipitation. If the acidic pH level in urine gets too high, then the uric acid crystals may not dissolve, resulting in accumulation of a high quantity of uric acid stones (Coe and Coe, 1983). Alternatively, if urinary pH becomes alkaline, uric acid stones solubilise and do not precipitate.

Despite recent findings suggesting that defects in renal tubular ammonia production and secretion can at least partially explain low urinary pH, the pathophysiology of the disease has not been entirely explained (Gianfrancesco et al., 2003, Weiner and Verlander, 2017). Hence, this is of interest not just to

better elucidate the complex renal handling of uric acid, but also for our understanding of some rare forms of familiar nephrolithiasis associated with hypouricemia due to a high fractional excretion of uric acid.

5.2.3 *NHERF1* in mammals

The cause of uric acid stone development has been the subject to several recent investigations, and attention has centred on genetic approaches for determination of causative factor of the disease (Riches et al., 2009, Vasudevan et al., 2017). Despite the accessibility of various precursor pathways and genes proposed to have an essential role in nephrolithiasis, very few genes have been characterised and linked with kidney stone formation. In mammals, targeted deletion of Na^+/H^+ Exchanger Regulatory Factor (*NHERF1*) results in uric acid stone formation (Cunningham et al., 2007). Additionally, *NHERF1*$^{(-/-)}$ mutant mice (male and female) have increased urinary excretion of phosphate, calcium, and uric acid associated with interstitial deposition of calcium in the papilla of the kidney (Weinman et al., 2006).

The sodium-hydrogen exchanger regulatory factor 1 (*NHERF1*) is one of the four related scaffolding proteins (*NHERF1- NHERF4*), which regulates sodium hydrogen exchanger *NHE3* in rabbit kidney epithelial and mainly in the apical surface of epithelial cells (Weinman et al., 2006, Ardura and Friedman, 2011, Voltz et al., 2001). Scaffold proteins allow the formation of protein complexes, interacting with a wide variety of cellular targets. The association of multiple target proteins is facilitated by the presence of postsynaptic density protein; *Drosophila* disc large tumour suppressor zonulaoccludens1 protein (PDZ) modular protein-protein interaction modules (Cortese et al., 2008). These domains interact with specific carboxyl-terminal motifs on target proteins. Moreover, the scaffolding function can be enhanced by oligomerisation with other PDZ domains.

NHERF1 is encoded by the *SLC9A3R1* gene, which contains six exons and is localised in human chromosome 17q25.1. It contains 358 amino acids and is characterised by the presence of two PDZ domains, PDZ1 (11-97 amino acids) and PDZ2 (150-237 amino acids); these two domains resemble 74% to each other and carboxyterminal Ezrin–Radixin–Moesin (*ERM*) binding region, **Figure**

5.2 (Morales et al., 2004). Human NHERF1 presents 84% similar identity to rabbit protein co-factor Na^+/H^+ exchanger regulatory factor (NHERF) and 48% identity to human Tyrosine Kinase Activator Protein 1(TKA-1). NHERF is involved in the regulation of rabbit renal brush border Na^+/H^+ ion exchanger (Weinman et al., 1995). NHERF1 align very well over their entire lengths, while the sequence of TKA-1 diverges after G261 in NHERF1, and PDZ1 together with PDZ2 are found in nearly identical versions in both protein cofactor and TKA-1 (Fouassier et al., 2001, Kreimann et al., 2007, Weinman et al., 2006). Studies have shown that loss of heterozygosity for NHERF1 results in breast cancer, suggesting its potential role as a tumour suppressor (Le Dai et al., 2004, Pan et al., 2006). Additionally, there is evidence from breast tumour cell lines that overexpression or mislocalization of ezrin is correlated with invasiveness (Sarrió et al., 2006).

NHERF1 is enriched in epithelial cells microvilli in various organs of the human body such as kidney, intestine, liver and placenta. Microvilli are specialised cell surface structures present in polarised epithelial cells and are enriched in members of the ERM family protein (Berryman et al., 1993, Amieva et al., 1994). ERM proteins organise protein complexes that link the membrane to the cytoskeleton. The structure of ERM proteins comprises an amino (N)-terminal FERM (band 4.1, ERM) domain and a short carboxy (C)-terminal domain. ERM proteins bind to transmembrane or membrane-associated proteins with the FERM domain and interact, with their C-terminal domains, with actin of the cytoskeleton (Morales et al., 2007).

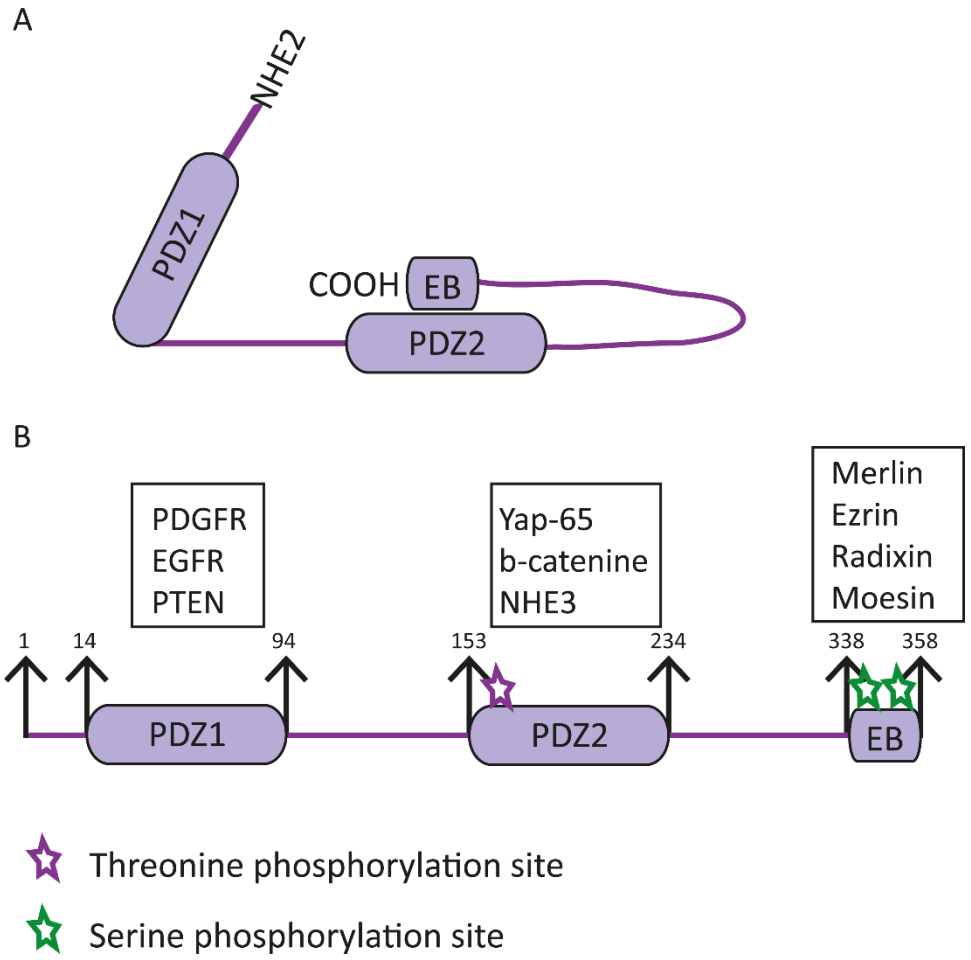

Figure 5.2. Domain structure of human NHERF1. (A) Intramolecular structure of NHERF1 conformation; (B) The amino acid positions of differently truncated domains, including phosphorylation sites: phosphorylation is on Thr156, and Ser 339-340 disturb self-association, favouring PDZ-ligands interaction. Adapted from (Centonze et al., 2018).

An observation in the Dow lab (Southall and Giannakou, unpublished) suggested that stones were abundant in a P-element insertional mutant for NHERF. In **Chapter 3**, I confirmed this finding; here I established that these stones are of uric acid and these findings can be further studied in the context of mammalian studies.

5.2.4 *NHERF1* and kidney stones

Recent studies have shown that mutations in *NHERF1* resulted in phosphaturia in human (Vaquero et al., 2017, Karim et al., 2008), where three out of seven patients who had lower TMP/GFR (tubular maximal reabsorption of phosphate/ glomerular filtration rate) values, lower serum phosphate concentrations, and

higher serum 1,25-dihydroxy vitamin D concentrations than controls were identified with the *NHERF1* mutation. Although the *NHERF1* mutation causes stones, the mechanism behind it is not precise. Furthermore, *NHERF1* mutant mice or inhibition of the activity of *NHERF1* in cells have impaired transport activity and expression of *NPT2a* in the apical membrane. Phosphorylation of *NHERF1* by PTH is important in the internalisation of sodium-phosphate cotransporter-IIa (*NPT2a*) (Weinman et al., 2007). However, the actual mechanism behind the abnormalities of phosphate transport in humans due to *NHERF1* mutations is not known because the expression of the mutant *NHERF1* cDNA does not affect phosphate transport. In addition, it will be important to determine whether these mutations directly modulate the transport activity and expression of *NPT2c* as well as *NPT2a* and whether there are secondary effects on sodium-potassium–ATPase, which is also regulated by PTH through an *NHERF1*-dependent pathway and may regulate sodium phosphate cotransport by means of decreased generation of the sodium gradient.

Recent studies indicate that *NHERF1* also interacts with mouse urate transporter 1 to regulate uric acid transport in the proximal renal tubule and that NHERF1-knockout mice have increased uric acid excretion (Cunningham et al., 2007). A further study has also indicated a potential interaction between NHERF1 and the renal-proximal-tubule sodium sulfate transporter NaSi-1, but it is not known whether NHERF1-knockout mice have increased urinary sulfate excretion (Gisler et al., 2008). It is important to know whether the subjects with *NHERF1* mutations also abnormalities in uric acid or sulphate excretion since these are highly relevant to nephrolithiasis.

To overcome this issue and to know much about the role of *NHERF1* in the kidney stones formation, we proposed to use *Drosophila* as a model organism in advancing the understanding of the mechanism by which mineralisation occurs by mutation and knockdown of the *NHERF1* homologue, *Drosophila Sip1*.

5.2.5 *Drosophila* homologue of *NHERF1*

A Blast search of the human protein RefSeq database using *Drosophila* SIP1 sequence reported that the closest homologue of SIP1 is human EBP50/NHERF1

and NHERF2 (Altschul et al., 1990). *Drosophila* SIP1 is more identical to NHERF1 as it has 57% resemblance and 81 % similarity to NHERF1 PDZ domain1, however, NHERF2 is only 45% identical and 60% similar. Moreover, a reciprocal blast search was performed using human NHERF1/EBP50 against *Drosophila* protein database, which showed a similar alignment. Furthermore, a sequence alignment of *Drosophila* SIP1 PDZ domains was compared to PDZ1 and PDZ2 domains of human, rat mouse and *C. elegans*. Additionally, it is found that the EB domain or C-terminal end of NHERF1, which binds with mammalian ERM protein is also conserved in *Drosophila* SIP1. Similarly, EB domain of *Drosophila* SIP1 and human NHERF1 has 23% identity (61% similarity) and 28% identity (67% similarity) with NHERF2 (**Figure 5.3**) (Hughes et al., 2010). The high degree of similarity in PDZ domains and EB domains strongly suggests that *Sip1* is a *Drosophila* orthologue to human EBP50/NHERF1 and that they adopt similar structures. Further, RNA-seq analysis obtained from FlyAtlas2 has shown that *Sip1* is up-regulated in male and female adult tubules, midgut and hindgut. Further, it is also highly enriched in male accessory glands and rectal pads **Table 5.1**.

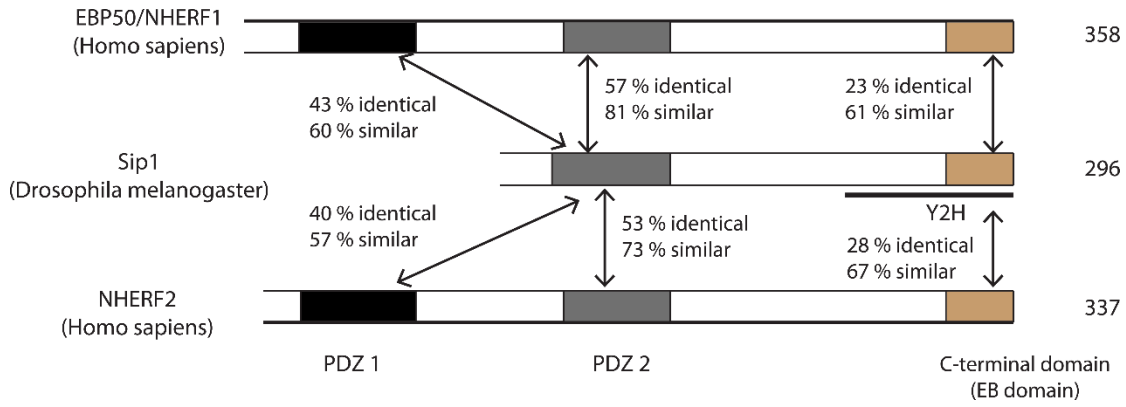

Figure 5.3. A comparative analysis of the composition of *Drosophila* SIP1 (NP_524712) protein with human EBP50/NHERF1 (NP_004243) and NHERF2 (NP_001123484) proteins. *Drosophila* N-terminal contains only a single PDZ domain which is more similar to NHERF1 as compared to NHERF2. The percentage identity and percentage similarity are indicated by vertical arrows. The C-terminal FERM-binding domain also appears to be conserved in *Drosophila*. The interacting domain as determined by overlapping clones from the two-hybrid interaction of SIP1 and Moesin is indicated by the dark horizontal line (Y2H). Adapted from (Hughes et al., 2010).

	Adult Male		Adult Female		Larval	
Tissue	**FPKM**	**Enrichment**	**FPKM**	**Enrichment**	**FPKM**	**Enrichment**
Head	18	1.3	16	1.4		
Eye	6.7	0.5	6.6	0.6		
Brain / CNS	0.5	0.0	0.7	0.1	13	0.6
Thoracicoabdominal ganglion	1.9	0.1	2.7	0.2		
Crop	26	1.9	29	2.6		
Midgut	12	0.9	4.8	0.4	19	0.8
Hindgut	34	2.5	37	3.3	24	1.1
Malpighian Tubules	26	1.9	27	2.4	10	0.4
Fat body					3.6	0.2
Salivary gland	46	3.3	34	3.0	43	1.8
Heart						
Trachea					35	1.5
Ovary			16	1.4		
Virgin Spermatheca			37	3.3		
Mated Spermatheca			46	4.0		
Testis	9.0	0.7				
Accessory glands	145	11				
Carcass	15	1.1	14	1.3	42	1.8
Rectal pad	85	6.2	79	7.0		

Table 5.1. **Expression of *Sip1* in *Drosophila* adult male and female and larval tissues obtained from RNA-Seq analysis.** FPKM (Fragments Per Kilobase Million). Adapted from Fly Atlas2 (Leader et al., 2017).

5.3 Results

5.3.1 Mutation of *Sip1* induces stones accumulation

Mutation of *Sip1* results in the formation of a very high number of small birefringent stones in both male and female MTs compared to wild-type tubules of either sex (**Figure 5.4, A-F**). Quantification of the mineralised area covered between 70-80% of both anterior and posterior tubule area of male and female flies (**Figure 5.4, G-H**). The anterior tubules have an enlarged initial segment (Wessing and Eichelberg, 1978, Sözen et al., 1997), which handles most of the organism's excess calcium (Dube et al., 2000); however, this region did not develop birefringent stones in *Sip1* mutants, and the stone burden was similar in anterior and posterior tubules (**Figure 5.4**), suggesting that these calculi were not calcium-based.

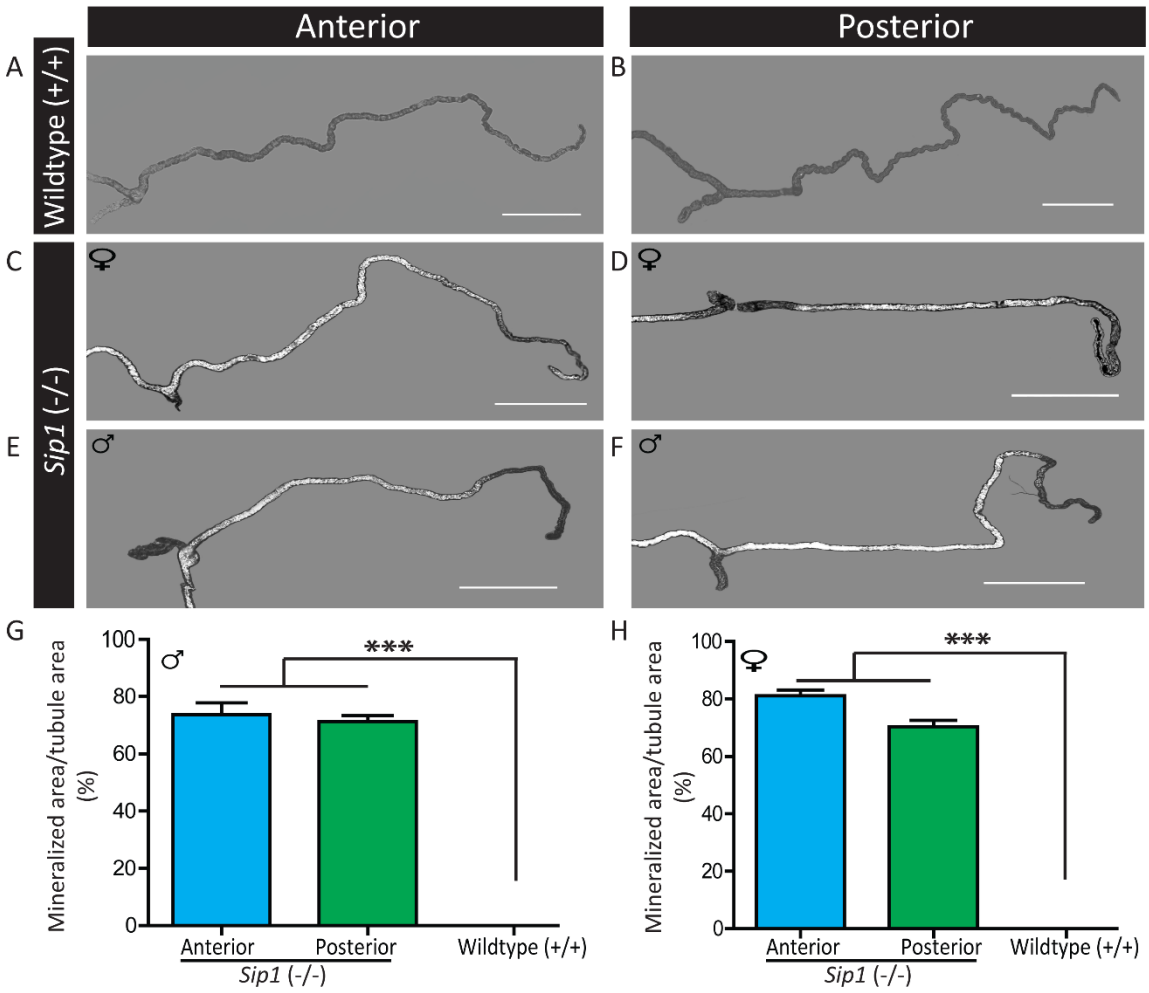

Figure 5.4. Quantification of intraluminal stones in *Sip1* mutant flies. (A-F) Representative polarised microscopy images of wildtype $^{(+/+)}$ and *Sip1* mutant $^{(-/-)}$. MTs are showing intraluminal accumulation of birefringent stones. Bars represent the percentage of total stones in the anterior and posterior MTs of male (G) and female (H) *Sip1* mutant flies compared to wildtype MTs are represented in bar graphs. Data are presented as mean ± SEM, N=5. ***p<0.001, one-way ANOVA followed by Dunnett's test. In panels A-F, scale bars represent 500 µm.

5.3.2 Cell-specific knockdown of *Sip1* promotes lithiasis

We next investigated whether renal, cell-specific knockdown of *Sip1* in tubule specific cells (Principal and Stellate cells) under control of the appropriate *GAL4* driver lines resulted in the same phenotype. The Bloomington *UAS-Sip1 RNAi* line produced a significant knockdown (>70%) in overall tubule expression of *Sip1* when driven in stellate cells (**Figure 5.5, A**), but no knockdown when driven in principal cells (data not shown), suggesting that *Sip1* is expressed uniquely in the stellate cells. Accordingly, specific knockdown of the *Sip1* gene in tubule

principal cells using CapaR-*GAL4* driver line did not result in an increase in stone burden (**Figure 5.5, B)**, while stellate cells specific knockdown of the *Sip1* gene (ClCa-*GAL4*>UAS-*Sip1* RNAi) showed, as expected, marked increase of birefringent stones compared to parental control lines (ClC-a-*GAL4*/+, UAS-*Sip1* RNAi/+) (**Figure 5.5, C**), indicating a novel role of *Sip1* in tubule stellate cells in mediating stone formation. Taken together, these results suggest that RNAi knockdown of *Sip1* in SCs promoted the accumulation of stones.

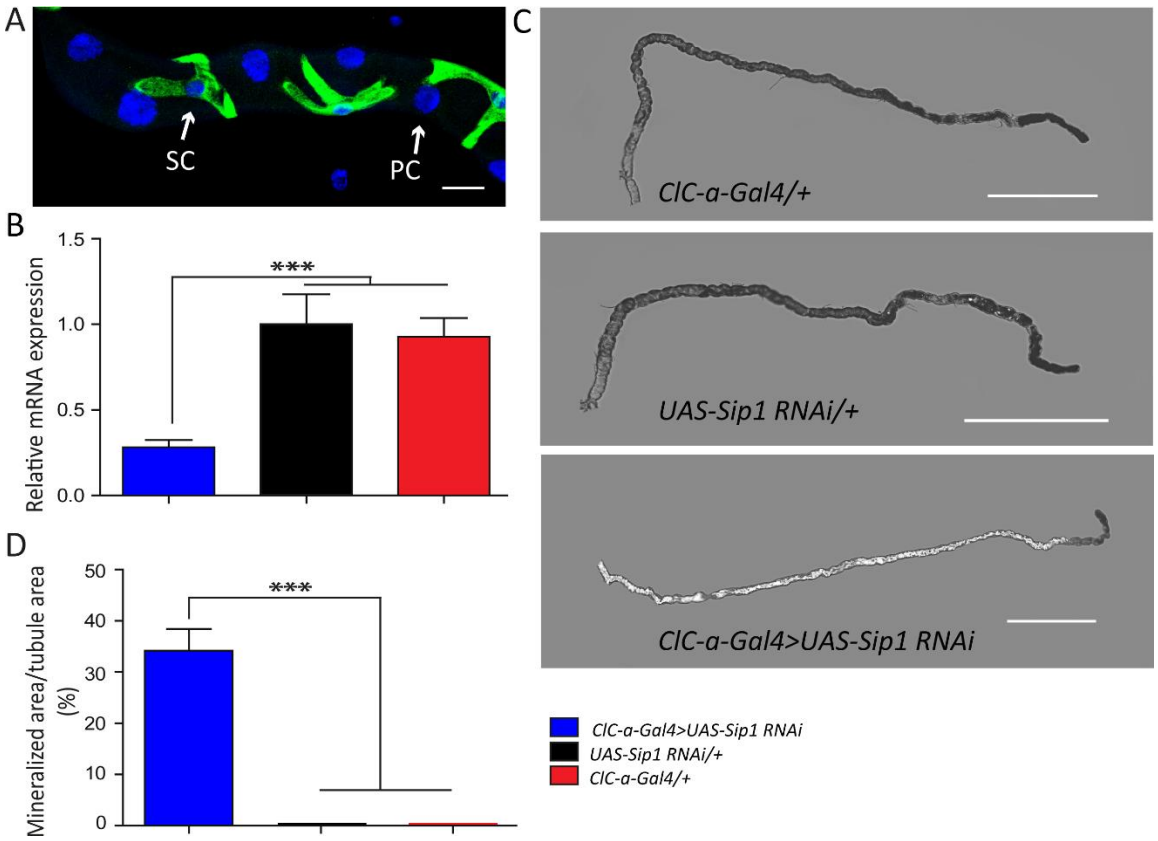

Figure 5.5. Quantification of stones accumulated in *Sip1* knockdown MTs. (A-B) The expression of *Sip1* was significantly decreased in *ClCa-GAL4>UAS-Sip1* flies as compared to parental lines. (C) Representative polarised microscopy images of *ClCa-GAL4>UAS-Sip1 RNAi* knockdown flies compared to parental controls, *ClC-a-GAL4*/+ and *UAS-Sip1 RNAi*/+. (D) Quantification of stones accumulated in knockdown and control conditions. Bar diagrams were constructed by considering the accumulated stones at time 0 as 100%. Data are presented as mean ± SEM, N=5, *p<0.05, one-way *ANOVA* followed by Dunnet's test. In panels C, scale bars represent 500 µm.

5.3.3 Modulation of pH affects stone solubility

To determine the chemical nature of the observed stones, we incubated *Sip1* mutant tubules under acidic or alkaline load by altering pH by 1 pH unit from 5 to 10. At pH 5 and pH 6, no change in the quantity of stones after 30 minutes was noted. However, we found that at pH 7 the total accumulated stones started to dissolve significantly within 20 min and this process occurred faster with increased pH of the bathing solution, where 90% of the stones were dissolved within 10 min at pH 10 (**Figure 5.6, A**).

To precisely determine at which pH stones start dissolving, the pH of the bathing solution was altered by 0.1 pH unit ranging between pH 6 and pH 7. So, placing tubules under acidic or basic load, we found that intraluminal stones start dissolving significantly at pH 6.7 and above (**Figure 5.6, B-C**). Chemically, the dissociation constant (pKa) for uric acid is 5.35 to 5.5 (Sakhaee and Maalouf, 2008, Martillo et al., 2014), where uric acid precipitates out of acidic solution. Thus, at a normal *Drosophila* physiologic pH of 7.4 (Schneider medium), most uric acid is in de-protonated form. However, in the urine, the pH of the solution might vary dependent on the concentration of uric acid in the sample. The risk of uric acid crystallisation increases with a progressive fall in urine pH and decreases with an increase of pH. Therefore, these results provide strong evidence that the stones accumulated in *Sip1* mutant MTs share similar chemical behaviour with uric acid stones.

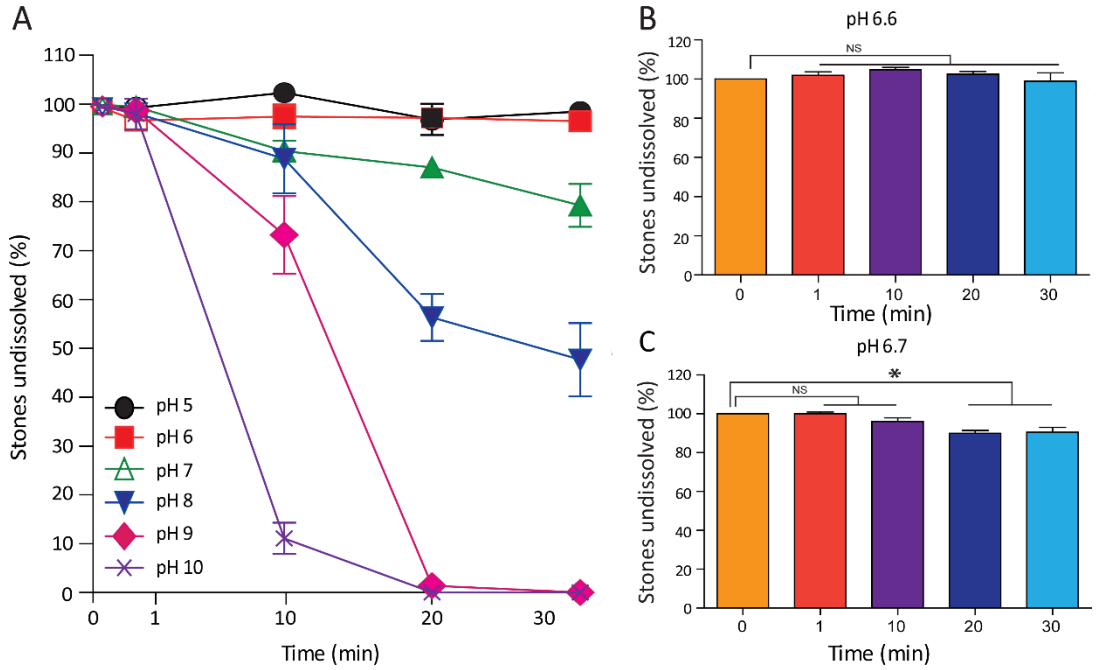

Figure 5.6. pH modulates solubility of tubule stones. (A) Graph represents the percentage of undissolved stones corresponding to the pH change of the bathing solution. (B-C) Bar diagram represents the pH (pH 6.6 to 6.7) at which stones start dissolving over a 30 min period. Data are expressed as mean ± SEM, N=5. *p<0.05, which one-way ANOVA followed by Dunnett's test, N.S. stands for non-significant.

5.3.4 Inhibition of the function of Xanthine Oxidase leads to the disappearance of the stones of *Sip1* mutant tubules

The biochemical pathway of uric acid formation shows that uric acid is the end product of purine metabolism, **Figure 5.1**. The pathway includes Xanthine Oxidase (XO) which is responsible for converting hypoxanthine to xanthine; and xanthine to uric acid. Allopurinol inhibits the function of XO, thereby blocking the biosynthesis of uric acid (Parks and Granger, 1986) resulting in a concomitant increase of hypoxanthine and xanthine concentration (Pacher et al., 2006). Similarly, XO gene mutant fly, *rosy* (*ry*) mutant (Dow and Romero, 2010), has an elevated the level of hypoxanthine and xanthine due to inhibition of the formation of uric acid.

To confirm the presence of uric acid in MTs of *Sip1* mutant flies, flies were fed with allopurinol. Feeding allopurinol allows us to assess the presence of uric acid stones in the *Sip1* mutant. On a normal diet, *Sip1* mutant flies accumulate stones throughout the lumen of MTs. However, wild-type and *rosy* mutant flies

(with no XO enzyme activity) do not produce uric acid stones (**Figure 5.7, A;C;E;G**). Wild-type, *Sip1* mutant and *rosy* mutant flies were fed with allopurinol containing diet which led to the disappearance of birefringent crystals in the tubules (**Figure 5.7**, **B;D;F;H**). The allopurinol fed flies phenocopy xanthine oxidase mutants (*ry* flies), in which they show a complete absence of birefringent urate stones (**Figure 5.7, H**). Thus, pharmacological inhibition of XO by feeding with allopurinol leads to the disappearance of stones, confirming that the intraluminally accumulated stones are uric acid stones.

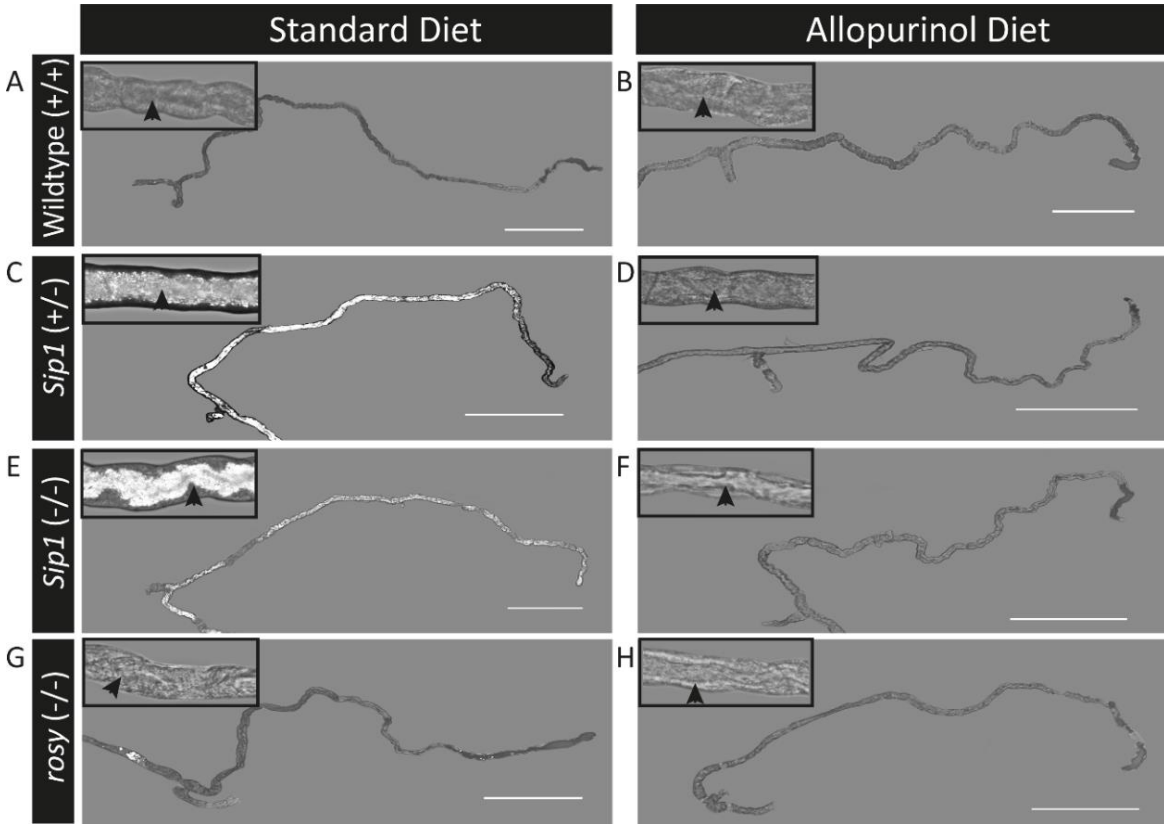

Figure 5.7. Pharmacological evidence and quantification of uric acid stones. Representative images of MTs from different genotypes (wildtype, *Sip1*$^{(-/-)}$, *Sip1*$^{(+/-)}$ and *rosy* $^{(-/-)}$) in normal or allopurinol diet. In all cases, flies fed with allopurinol did not accumulate stones. In panels B-G, scale bars represent 500 µm.

5.3.5 Uric acid is accumulated in *Sip1* knockdown tubules

I next quantified the concentration of the uric acid in the MTs of wild-type, Sip1 mutant and Stellate cell-specific Sip1 knockdown flies. The total concentration of uric acid in the MTs of Sip1 mutant flies was 8.5-fold higher compared to wild-type flies (**Figure 5.8, A**). Similarly, in *Sip1* RNAi lines (*ClC-a-GAL4>UAS-Sip1 RNA*i)

a 3-fold increase in the quantity of uric acid compared to the parental controls was measured (*ClC-a-GAL4*/+ and *UAS-Sip1 RNAi*/+) (**Figure 5.8**, **B**). Taken altogether, these results unambiguously demonstrate the presence of uric acid stones within MTs of *Sip1* mutant and *Sip1* knockdown flies, and that *Sip1* gene expression in the stellate cells mediates proper tubular lumen pH.

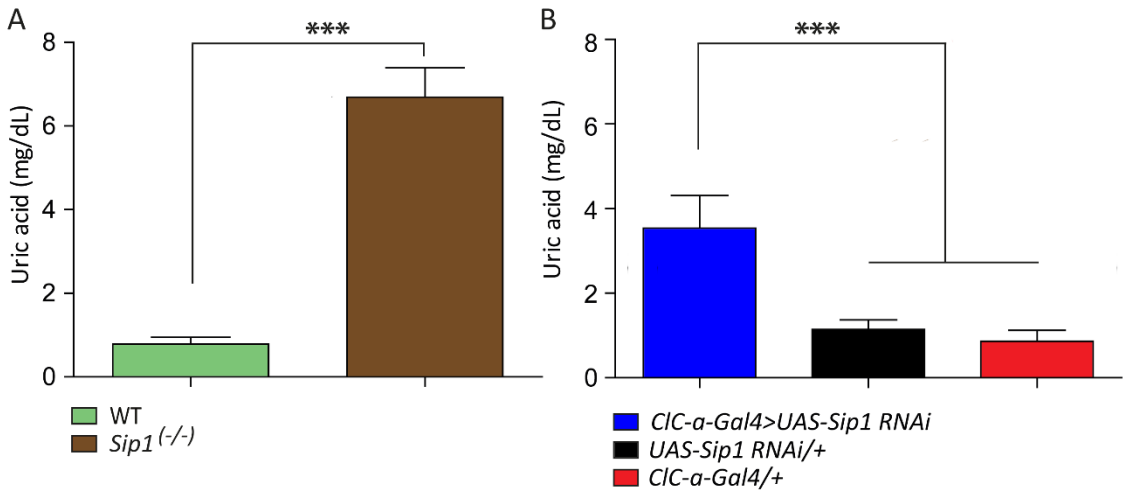

Figure 5.8. Concentration of Uric acid in *Sip1* mutant and knockdown flies. (A) Uric acid level in *Sip1* mutant MTs is significantly higher compared to control tubules. (B) Uric acid concentration is high in *Sip1* knockdown flies (*ClCa-GAL4>UAS-Sip1 RNAi*) compared to parental lines. Data are presented as mean ± SEM, N=5. ***p<0.001, student t-test (A), one-way ANOVA followed by Dunnett's test (B).

5.3.6 *Sip1* and *Moesin* localise to the apical membrane of tubule stellate cells

SIP1 encodes a protein that functions as a scaffold linking the plasma membrane and cytoskeletal linker proteins encoded by Moesin (Hughes et al., 2010) where SIP1 and Moesin interact with each other to maintain epithelial integrity via phosphorylation (Hughes et al., 2010, Ponuwei, 2016). We tested the co-localisation of these proteins in MTs using polyclonal antibodies raised against both SIP1 and Moesin. Immunocytochemistry showed specific labelling of SIP1 (**Figure 5.9, A**) and Moesin (**Figure 5.9**, **B**) of only stellate cells within the tubule of wild-type flies. Thus, confocal microscopy revealed that the location was on the apical membrane as showed by immunostaining apical to the DAPI-

stained nuclei. As expected, no immunostaining was observed in tubules from Sip1 and Moesin mutant flies (**Figure 5.9**), confirming the specificity of their respective antibodies and the clear expression of SIP1 and Moesin to the same tubule cell type.

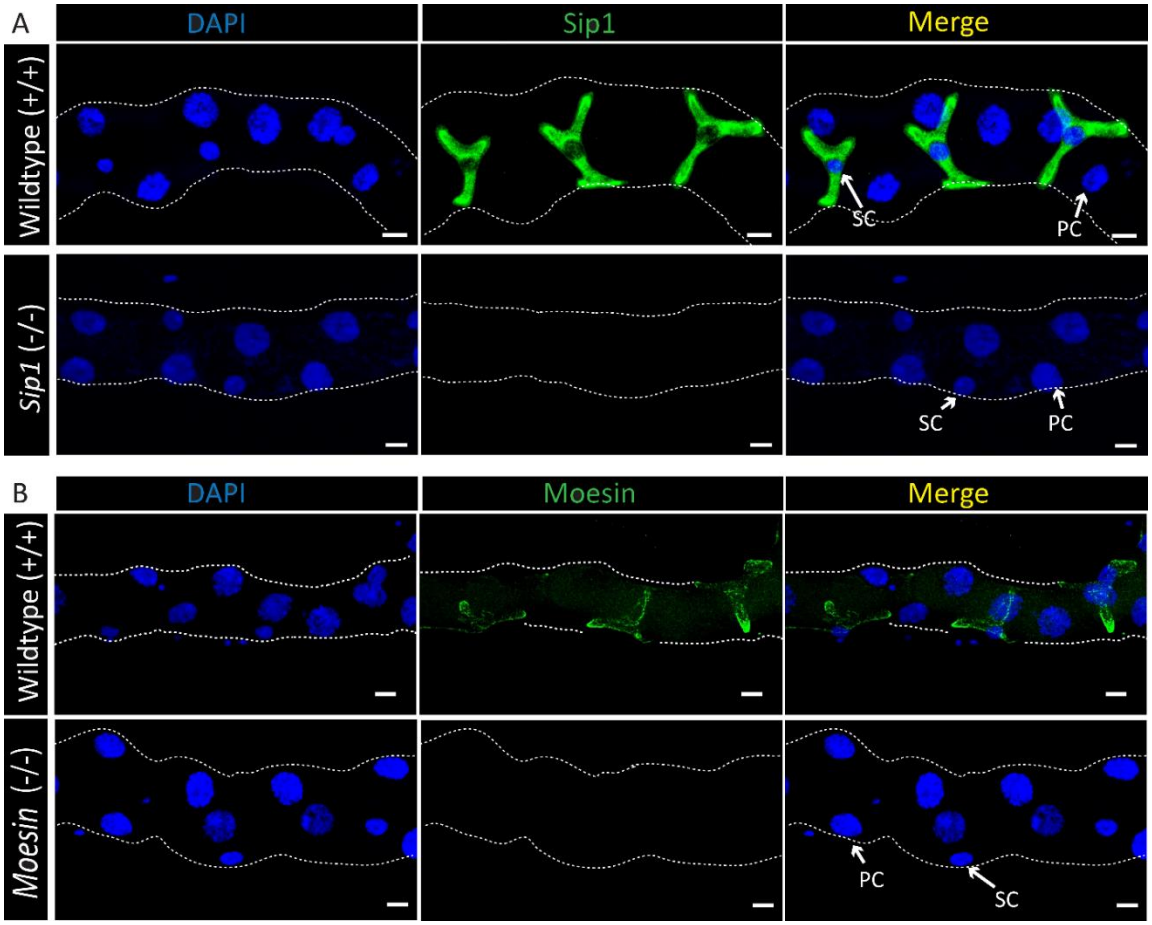

Figure 5.9. Expression of SIP1 and Moesin proteins in MT stellate cells. (**A**) Sip1 (***B***) Moesin. Both proteins are specifically expressed in MT SCs of wild-type fly while no expression was seen in *Sip1* and *Moesin* mutant flies respectively. DAPI (blue), Sip1/Moesin (Green), Merged (yellow); Scale bar represents 10 µm.

5.3.7 SIP1 colocalises with Na^+/H^+ Exchanger NHE2 and Moesin in stellate cells

The function of NHEs was first characterised in isolated cortical brush-border membrane vesicles showing Na^+-driven H^+ movement and H^+-driven Na^+ movement across the membrane (Murer et al., 1998). Further, computational modelling of the hydrophobic-hydrophilic nature and predicted structure of NHEs has also shown an interaction between NHEs with NHERF1 (Orlowski and Grinstein, 2004). It is known that SIP1 is a scaffold protein required for the

regulation of several transmembrane receptors and ion transporters (Vaquero et al., 2017, Hughes et al., 2010), so we hypothesised that SIP1 could regulate the activity of alkali-metal/proton exchanger (NHE) protein family in *Drosophila* tubules.

NHEs play an important role in the transport of Na^+ and H^+ across the membrane (Giannakou and Dow, 2001) as well as maintenance of cellular and epithelial integrity. *D. melanogaster* has three NHE genes - *NHE1*, NHE2, and *NHE3*, which are expressed in multiple tissues, **Figure 5.10** (Giannakou and Dow, 2001) but NHE2 seems to be tubule SCs specific, **Figure 5.11** (Day et al., 2008).

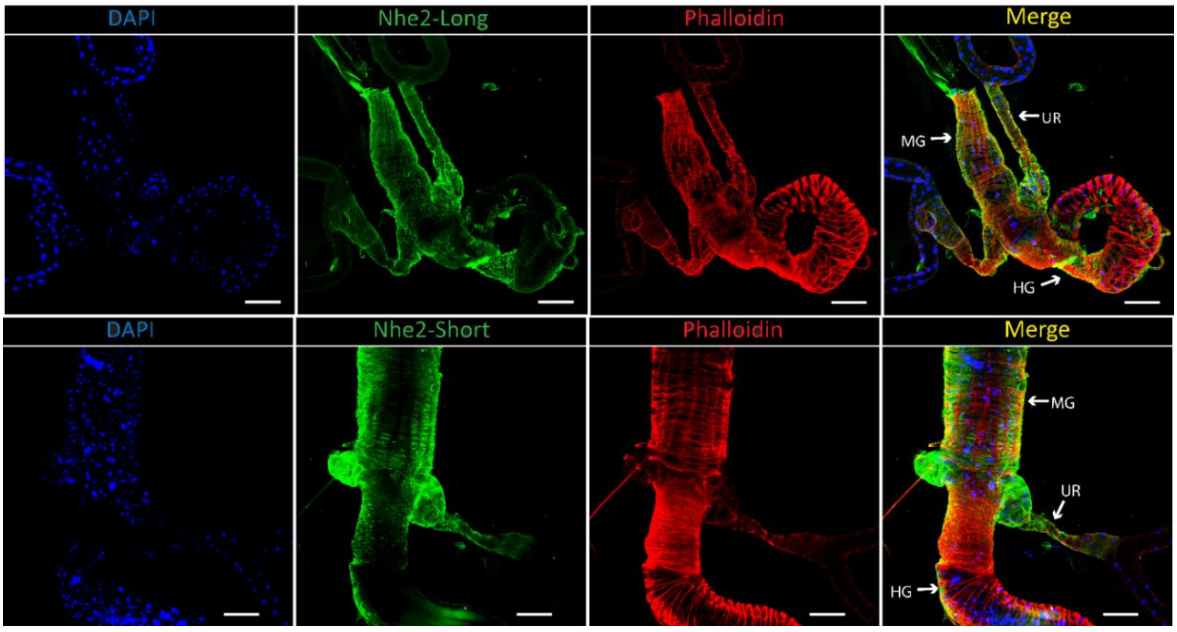

Figure 5.10. Expression pattern of NHE2-long and NHE2-short in different tissues of adult *Drosophila melanogaster*. Expression of NHE2-long and NHE2-short isoforms in Midgut (MG), Hindgut (HG), Ureter (UR). DAPI (blue), NHE2-long and -short (Green), Phalloidin (Red) and Merged (yellow). Scale bar represents 10 µm.

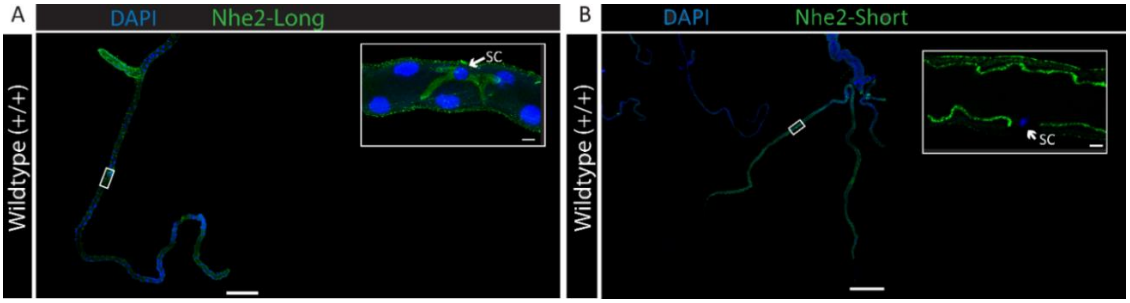

Figure 5.11. Expression of NHE2 (Long and Short isoform). (A) *NHE2-long* is expressed in MT stellate cells, scale bar: 500 µm. DAPI (blue), NHE2-long (Green). (C) Expression of NHE2-Short isoform in the apical membrane of the tubule, scale bar: 500 µm. DAPI (blue), NHE2-short (Green).

Interestingly, we found that the NHE2-long isoform also has clear localisation in stellate cells of wild-type MTs; whilst the NHE2-short antibody labels the apical membrane of tubule principal cells (**Figure 5.12, A-B**). Further, when Moesin was specifically knocked down by *Moesin* RNAi in MT SCs, no birefringent crystals were observed in *Moesin* RNAi lines (*ClC-a-GAL4>UAS-Moesin RNAi*) compared to parental controls (ClC-a-*GAL4*/+ and UAS-Moesin RNAi/+) suggesting the absence of the role of Moesin alone in the formation of uric acid stones (data not shown).

Consistent with the co-localisation of SIP1, Moesin and NHE2 proteins, we investigated a putative functional relationship between these proteins. To achieve this, we use an immunocytochemistry approach using anti-NHE2 long and anti-NHE2 short rabbit polyclonal antibodies to stain tubules of *Sip1* and *Moesin* mutant flies. Interestingly, no immunostaining using both NHE antibodies were observed in tubules from *Sip1* and *Moesin* mutant flies, suggesting that both SIP1 and Moesin and NHE proteins are part of a scaffold linking the plasma membrane and cytoskeletal of tubule stellate cells (**Figure 5.12, A-B**).

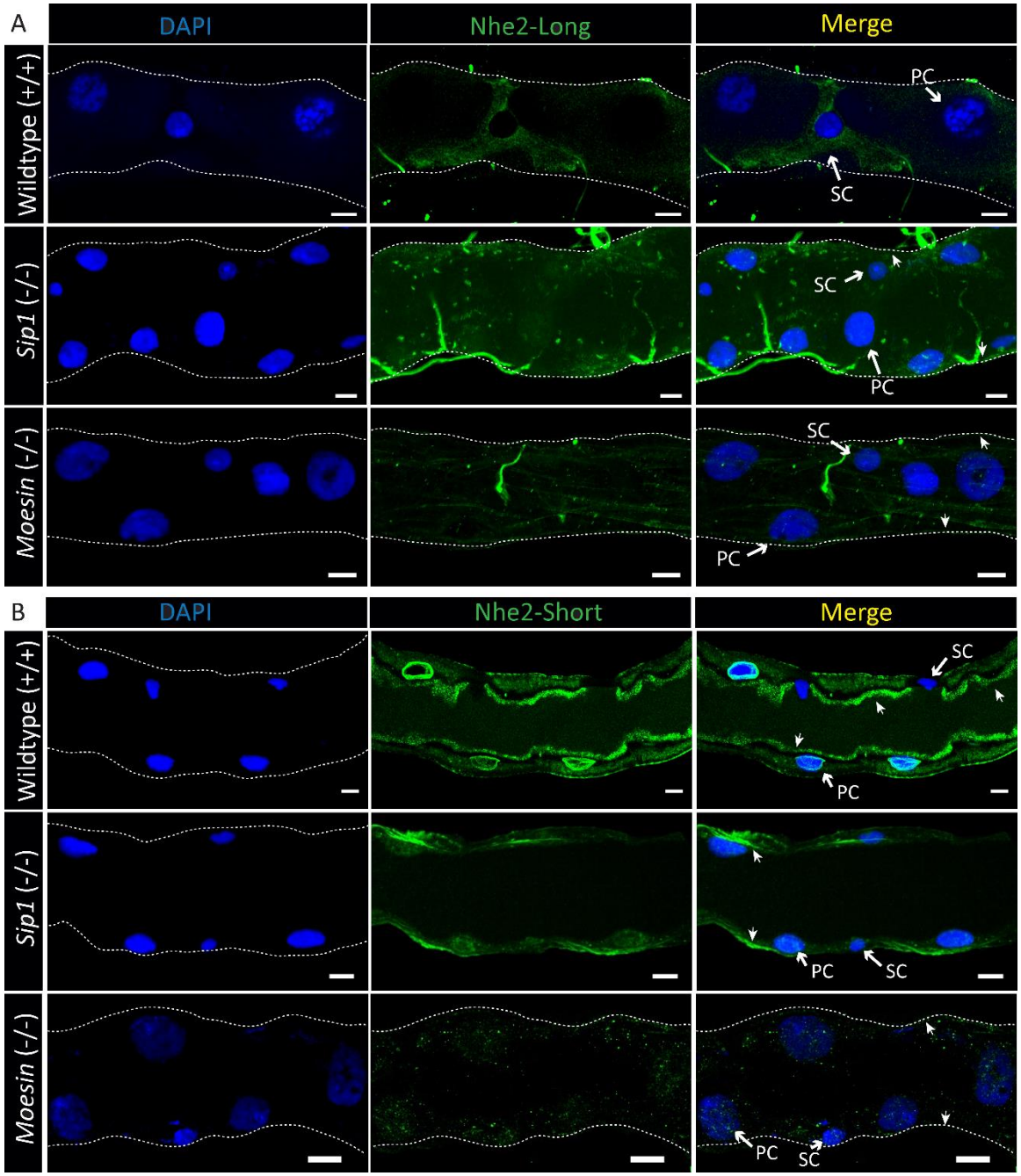

Figure 5.12. Expression of NHE2-long and NHE2-short isoforms of wild-type, *Sip1* mutant and *Moesin* mutant flies. (A) NHE2-long isoform is expressed in the MT stellate cells of wildType fly. DAPI (blue), NHE2-long (Green) and merged image (Yellow). (B) NHE2-short isoform has clear localisation in the apical membrane of MT PCs. DAPI (blue), NHE2-short (Green) and merged image (Yellow). Scale bar represents 20 µm.

5.4 Interaction between SIP1, Moesin and NHE2

Consistent with the co-localisation of SIP1, Moesin and NHE2 proteins to the stellate cells, we investigated a putative functional relationship between these proteins. To achieve this, we use an immunocytochemistry approach using anti-

NHE2 long and anti-NHE2 short rabbit polyclonal antibodies to stain tubules of Sip1 and Moesin mutant flies. Interestingly, no immunostaining using both NHE antibodies were observed in tubules from Sip1 and Moesin mutant flies, suggesting that both SIP1 and Moesin and NHE proteins are part of a scaffold linking the plasma membrane and cytoskeletal of tubule stellate cells.

Interestingly, co-immunoprecipitation (co-IP) studies between SIP1 and Moesin in pupae and in Drosophila S2 cells suggested that SIP1 regulates Moesin activity, possibly by acting as a scaffold that links these proteins together, leading to phosphorylation of Moesin thereby forming a SIP1-Moesin complex. Therefore, to investigate the potential physical interaction between these three proteins SIP1, Moesin and NHE2, we performed co-IP experiments using Drosophila S2 cells transfected with a Sip1 construct or MTs overexpressing the Sip1 gene specifically to the stellate cells (ClC-a-*GAL4*>UAS-Sip1). Essentially, we immobilised Sip1 antibody to the support in order to precipitate SIP1 target protein along with the binding partners/protein complex, which we detected by SDS-PAGE and western blot analysis. Unfortunately, we were unable to demonstrate a direct interaction between SIP1, Moesin and NHE2 proteins from both S2 cells or tubules lysate using the Co-IP technique .

5.5 Discussion

Mammalian NHERF1 was first characterised in rabbit border membrane as an essential cofactor for cyclic AMP inhibition of Na^+/H^+ exchanger (Weinman et al., 1989, Murtazina et al., 2007). Here, the role of the *Drosophila* orthologue *NHERF1, Sip1,* in mediating uric acid stone formation in *Drosophila* MTs was characterised by biochemical, pharmacological and genetic assays. Insects, like birds, are considered to have uricotelic excretory systems, in which waste nitrogen is dumped as uric acid, in order to conserve water, and so uric acid calculi are constitutive in most terrestrial insects (Dow, 2012). However, adult *Drosophila* tubules express very high levels of urate oxidase (uricase) (Wallrath et al., 1990), and so urate crystals are not normally abundant. In this context, the extreme accumulations observed here in Sip1 mutants are remarkable.

Mutation and specific knockdown of *Sip1* in MT SCs resulted in the significant deposition of birefringent stones in the lumen of the tubule. Our experiments

provide evidence that these stones are uric acid stones based on the results obtained from physical appearance and biochemical experiments (Dow and Romero, 2010). To analyse the chemical nature of the stones, we performed pH-based solubility experiments which is the traditional method to determine the solubility of the stones and threshold pH value of 6.7 was determined. The results demonstrate similarity in characteristic between the accumulated stones and uric acid stones. Previous experiments have demonstrated that uric acid crystallisation and precipitation mainly depends on two major factors; uric acid concentration and uric acid solubility. However, the solubility of uric acid is more dependent on pH because of hyperuricosuria and low urinary volume (Pak et al., 2005, Pak et al., 2001). Uric acid is a weak organic acid with a first pKa of 5.5, resulting in the loss of 1 proton from uric acid and formation of anionic urate (Finlayson and Smith, 1974). The second pKa value is 10.3, but it has no physiological significance in human stones formation (Shekarriz and Stoller, 2002). Hence, at the normal body physiological pH, i.e. 7.4 uric acid is in de-protonated and more soluble form. In urine, however, the pH can vary over a wide range, which determines the concentration of uric acid. The risk of uric acid supersaturation increases with a progressive fall in urine pH. At a pH 5.3, 50% of uric acid will be in its poorly soluble form (Sakhaee et al., 1983). This scenario is much less likely then crystallisation due to an acid urine pH. The solubility of de-protonated urate also depends on its cation. Our results also show that increment of pH of the bathing solution leads to an increase in the solubility of the stones confirming the stones accumulated intraluminally are indeed uric acid stones.

Xanthine oxidase catalyses the final step of purine degradation resulting in the formation of uric acid. Allopurinol, a Xanthine oxidase inhibitor, is used as a drug for the treatment of gout by inhibition of uric acid synthesis. Allopurinol, when fed to wild-type *Drosophila*, phenocopied the *rosy* mutant by inhibiting XO and caused accumulation of xanthine and hypoxanthine stones. Allopurinol is a prodrug which is converted to oxypurinol by the enzymatic reaction of XO. Oxypurinol is an inhibitor of XO which replaces the hydroxyl ligand of the molybdenum ion at the active site of XO and thus very effectively prevents the conversion of hypoxanthine to xanthine and xanthine to uric acid. Accordingly, *Sip1* mutant flies fed with allopurinol did not develop stones within the MTs,

which further illustrates that the stones accumulated within the MTs of the *Sip1* mutant flies are uric acid stones.

What mediates precipitation of uric acid stones in the tubule? In mammals, interaction between SIP1 and urate transporters has been suggested (Cunningham et al., 2007); our results suggest SIP1 connects plasma membrane proteins such as NHE2, with members of the ERM (Ezrin, Radixin, Moesin) family, thereby regulating lumen acidification (Vaquero et al., 2017, Hughes et al., 2010). In mammals, ERM protein complex interacts with the plasma membrane and actin cytoskeleton (Hirao et al., 1996, Weinman et al., 1995) within specific domains to systematise the plasma membrane (Hanzel et al., 1991) and thereby providing a regulated linkage between the plasma membrane and the actin cytoskeleton. Recent genetic and biochemical studies have shown that NHERF1/SIP1 plays an essential role in the activation of ERM proteins in mammals (Brône and Eggermont, 2005) and also in *D. melanogaster* (Hughes et al., 2010). Intriguingly, targeted deletion of *NHERF*1 in mouse elevates intestinal deposition of calcium and also triggers calcium oxalate and uric acid crystal formation (Shenolikar, 2002). However, loss of ERM proteins results in mislocalization of *NHERF*1 in mouse (Saotome et al., 2004). In *D. melanogaster,* Moesin is the sole representative of the ERM family (Roch et al., 2010). SIP1 promotes Moesin function by affecting interaction with Slik Kinase; genetic and functional interactions between SIP1, Moesin and Slik kinase has been shown in *Drosophila* pupae and cultured S2 cells (Hughes et al., 2010). We demonstrated the expression of SIP1 and Moesin in the MT SCs, potentially suggesting an interaction in SCs.

Na^+/H^+ exchangers (NHEs) are a part of integral membrane proteins which comprises multiple transmembrane domains and a large cytosolic carboxyl-terminal domain (Yoshida et al., 2016). Studies in the mammalian model have shown that NHERF1 phosphorylates NHEs, thereby affecting their activity and microenvironment acidification (Centonze et al., 2018). Interestingly, rabbit NHERF1 is involved in the regulation of the renal brush border NHEs (Giral et al., 2012). Also, the computational modelling of the hydrophobic-hydrophilic nature and predicted structure of NHEs has also shown the interaction between NHEs with NHERF1 (Orlowski and Grinstein, 2004). Previous studies have shown that

the null allele of *NHE2* catalyses the influx of Na^+ and efflux of intracellular H^+ (Ulmschneider et al., 2016). Mutation of *NHE2* decreases pH but does not change larval tissue morphology (Grillo-Hill et al., 2015). Previous findings augmented by our Immunocytochemistry experiments reveal that NHE2-long is localised to MT SCs but are not expressed in *Sip1* and *Moesin* mutant MTs. Thus, as all three proteins SIP1, Moesin, and NHEs are localised explicitly in MT SCs, there may be a functional interaction in the SCs.

Collectively, our experimental results allow a model for the formation of uric acid stones in the MTs of *D. melanogaster* with the support of other studies which have shown the genetic interaction between *Sip1* and *Moesin* as well as co-immunoprecipitation experiments in mammals and S2 cells (Hughes et al., 2010, Giral et al., 2012). Additionally, Reczek et al. have shown the interaction between NHERF1 and ERM proteins in the mammalian model (Reczek et al., 1997) by co-immunoprecipitation experiments with extracts of purified placental microvilli. Previous studies have also shown the interaction between NHERF1 with NHEs by co-immunoprecipitation experiments, **Figure 5.13**, (Weinman et al., 2000, Bhattacharya et al., 2012). It is proposed that NHEs bind multiple members of the NHERF family of multiple PDZ domain proteins, potentially via the physical linkage of NHE (Donowitz et al., 2013, Orlowski and Grinstein, 2004). Support for this model comes from the co-localisation of SIP1, Moesin, and NHE2.

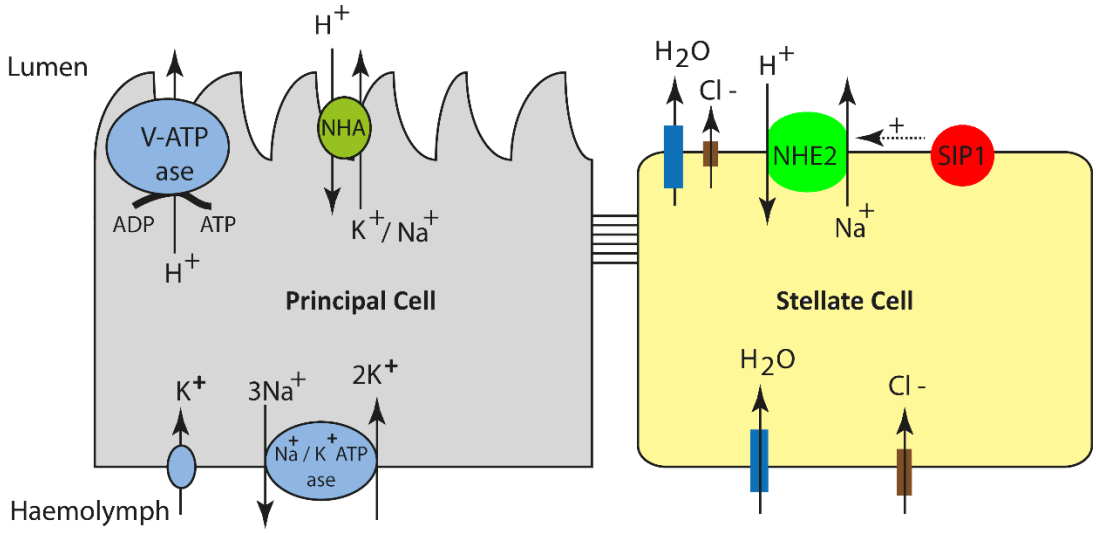

Figure 5.13. Model illustrating the role of SIP1 protein in uric acid stone formation in *Drosophila* tubules. (A) Hydrogen ion transport across the membrane in *Drosophila* MTs. Moesin-Sip1 complex interacts with NHE2 and activates the transport of Na^+ and H^+ (B) Mutation of *Sip1* disrupts the interaction between SIP1 and NHE2 thereby inactivating the function of NHE2 and leading to high accumulation of H^+ ions intraluminally and tubular lumen acidification, mediating uric acid stones formation.

5.6 Conclusion

In summary, the results presented in chapter 5 indicate that *Drosophila Sip1*, an ortholog of human *NHERF1,* plays an essential role in the prevention of uric acid stone formation. Our study further reflects the conservation of the function of a homologous gene pair, *NHERF1* from mammals to *Drosophila*. Mutation of *Sip1* results in a decrease of intraluminal pH (acidic) resulting in high accumulation of birefringent crystals in MTs. The physical, chemical and pharmacological assays unambiguously suggest that the accumulated stones were uric acid stones. We hypothesise that the Sip1 mutants display such a phenotype by interacting with proton pump transporter thereby amplifying accumulation of intraluminal H^+ ion. We further exhibited that the increase of uric acid is deleterious and also showed involvement of proton exchangers NHEs, particularly NHE2 for the increment of acidic environment intraluminally. Our results also highlight the importance of Moesin, which plays a crucial role in interaction with NHE2, specifically in the stellate cells. A critical question that remains to be answered regarding the interaction between SIP1, Moesin and NHE2 and how their activities are regulated in MTs. Results from the previous studies and our localisation assays help us to predict that SIP1-Moesin forms a complex which

bind with NHE2 for a normal physiological function. However, mutation of *Sip1* potentially alters the phenomena resulting in high accumulation of H^+ thereby increasing luminal H^+ ion, and making lumen of the tubule acidic, favourable for the precipitation of uric acid.

Chapter 6 Role of *Napi-T* in Phosphate stones formation

6.1 Summary

Recent genetic studies in different model organisms have successfully identified the role of physio-chemical factors and significant heritability of the genes in renal stone formation. Genetic screening in *Drosophila melanogaster*, as described in Chapter 3, has successfully identified a list of genes which might be involved in renal stone formation. Mutation of renal phosphate transporters has been characterised to be associated with several pathological states, including the renal stone formation and recurrence. In the introduction of this chapter, we explain about the phosphate transporter families in mammals and our current understandings of their physiological role. Further, we explain the function of phosphate transporters and their involvement in renal tubular handling of lithogenic substrates such as calcium, oxalate and phosphate. In the results section, we describe the impact of silencing of the sodium-phosphate co-transporter, *NaPi-T* in *Drosophila* Malpighian tubules, which is the focus of the study. Additionally, we analysed the physiological and chemical properties of the stones, which suggested that knockdown of *NaPi-T* results in accumulation of phosphate stones. There is no clear human homologue of *Drosophila NaPi-T*; hence, further experiments to elucidate how *NaPi-T* regulates the transport of phosphate across the membrane and identification of the human homologue of *NaPi-T* is required. Finally, in the discussion section, our results are linked with previous findings to demonstrate the influential role of sodium-phosphate transporters in phosphate stone formation. Taken together, in this chapter I discuss the role of physiological, genetic and pharmacological interventions to alter phosphate concentration within MTs to confirm a critical role of *NaPi-T* in the process of nucleation which eventually leads to stone formation. In conclusion, the findings of the present study open a novel perspective in the identification of the role of *NaPi-T* in the formation of renal phosphate stones.

6.2 Introduction

Over the past few decades, considerable research advancement has been achieved in understanding the vital role of various minerals in the human physiological and metabolic process (Tomlekova et al., 2017). Among them, phosphorus is one of the essential elements. In the human body, it is absorbed in the form of inorganic phosphate ($H_2PO_4^-$ or HPO_4^{2-}); abbreviated as P_i, through the small intestine; and is expended for normal human physiological function, cell metabolism (energetics and signalling) and maintenance of the body structural integrity (phospholipid membrane and skeletal tissue) (Takeda et al., 2004a). It is known to be involved in fuel storage and critical energy transformations in the body (Bonora et al., 2012). In addition to this, it is required for other essential functions like maintenance of nucleic acid and nucleoprotein complexes, signal transduction pathways, delivery of oxygen to tissues (Krebs and Beavo, 1979, Hubbard and Till, 2000), muscle contraction, lipid metabolism, neuronal function and integrity of the bones (Crook and Swaminathan, 1996, Takeda et al., 2004b). All the functions mentioned above are achieved by maintaining a balance between dietary phosphate intake and phosphate excretion in the form of sweat, urine and faeces.

6.2.1 Phosphate balance in the human body

Phosphorus is transported intracellularly from the extracellular environment via secondary transporters (Virkki et al., 2007), in the form of negatively charged inorganic phosphates. In the healthy person under a normal dietary condition, around 80-90% of Pi is present in bone (approximately 10 g/100 g dry fat-free tissue), mainly complexed with calcium, in the form of hydroxyapatite (Hansen et al., 1976). The remaining 10-20 % is present in skeletal muscles and extracellular fluids, where the phosphate comprises about 0.1- 0.3 % of wet weight. The average serum Pi changes with age, i.e. highest during the neonatal period (1.88-2.4 mM) and gradually decreases with age reaching 0.85-1.44 mM during the adult age (Pettifor, 2008).

In the human body, intracellular Pi level is widely distributed with significant functions in vital cellular processes, cell metabolism, growth and pathological changes. In mammals, it is also involved in the regulation of extracellular

mineralisation processes (formation of complexes of phosphate with calcium). To maintain balance and control between mineralisation and cellular delivery, the extracellular phosphate levels and the total body phosphate content are firmly regulated by some hormones, including parathyroid hormone (PTH), 1,25-dihydroxy vitamin D (1,25(OH)2D), and fibroblast growth factor 23 (FGF23) (Sterling and Nemere, 2005). When phosphate concentration increases (as a result of high phosphate intake or a reduced glomerular filtration rate [GFR]), it inhibits secretion of parathyroid hormone (PTH) (which also decreases renal phosphate reabsorption) and increases secretion of FGF-23 (Prasad and Bhadauria, 2013). However, when phosphate concentration decreases, it stimulates the synthesis of 1,25(OH)2D, the active form of vitamin D **Figure 6.1**.

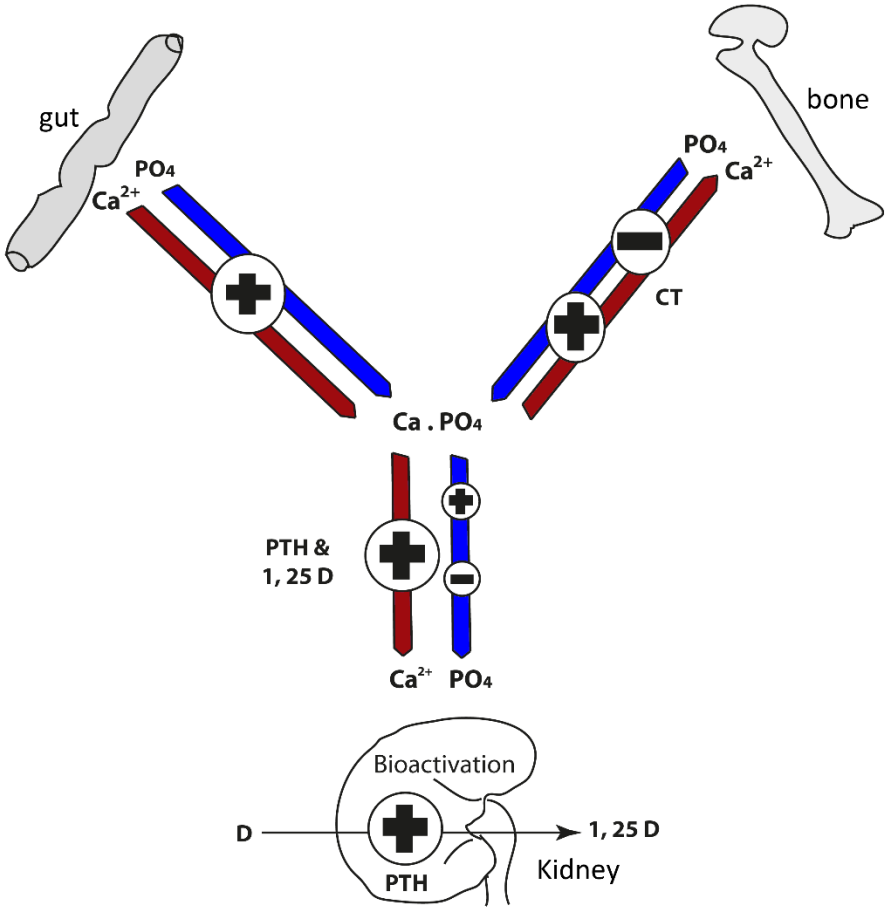

Figure 6.1: Phosphate Homeostasis in the human body. Phosphate homeostasis involving different organs and various regulators such as PTH and 1, 25 D. Adapted from:(Forster et al., 2013).

Reabsorption of phosphate filtered by the glomerulus occurs almost exclusively in the proximal renal tubule by an active hormonally regulated process. The

amount of reabsorbed phosphate is a crucial determining factor of the total plasma phosphate concentration. Mis-regulation of phosphate homeostasis or phosphate deficiency results in clinical symptoms like muscle weakness, impaired leukocyte function, central nervous system dysfunction, and abnormal bone mineralisation resulting in osteomalacia (Solanki, 2013). Considering these diverse pathological conditions, tight regulatory control over Pi concentration and maintenance of metabolic and endocrine phosphate effects is therefore very pivotal for the routine maintenance of human health.

6.2.2 Renal phosphate co-transporters

Sodium phosphate co-transporters are expressed in various parts of the human body (**Figure 6.2**) and are identified for their functions in human clinical physiology and disease processes (Prié et al., 2009). Under normal circumstances, the negative electrochemical potential across the cell membrane prevents the entry of anionic phosphate into the cell cytosol by simple diffusion. Hence, the availability of phosphate being the rate-limiting factor, an efficient phosphate transport system across the prevailing electrochemical gradient is vital for the maintenance of various normal physiological functions (Werner and Kinne, 2001). Transport of phosphate across the apical membrane of the proximal tubule epithelia requires Na^+, i.e. inward phosphate transport across the apical membrane depends on the outward electrochemical gradient of Na^+ (Hammerman, 1986).

Previous studies have demonstrated that phosphate concentration in the human body is mediated by at least three different sodium-dependent phosphate transporters; type-I (SLC17 family), type-II (SLC34 family) and type-III (SLC20 family) (Miyaji et al., 2013, Crouthamel et al., 2013). All three types of Pi transporters are multispanning membrane proteins, assigned to the solute carrier series (SLC) or proteins. Despite having similarity in the basic structure, these phosphate transporters differ in their affinity to the phosphate distribution in the tissues and physiological regulations. Their specific role in human health and disease has not been defined clearly; hence in this chapter, we discuss the importance of phosphate transporters in the maintenance of human physiology and pathophysiology (**Figure 6.2**).

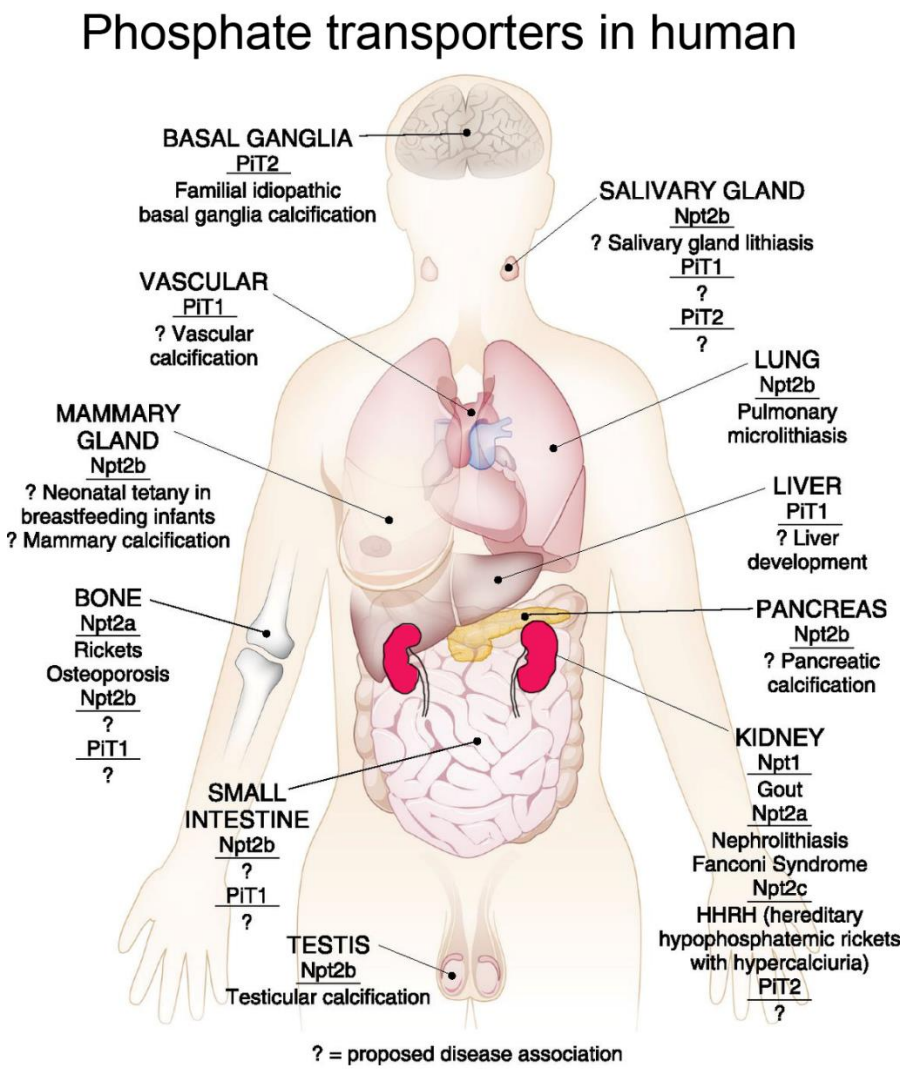

Figure 6.2. Distribution of Phosphate transporters in the body and diseases associated with its dysfunction. The figure shows the locations of sodium phosphate cotransporters and the transporters represented underlined. Proposed but unidentified associations are represented by a question mark. Reproduced with permission from (Lederer and Miyamoto, 2012).

6.2.3 Phosphate co-transporters and stone formation

The role of sodium phosphate co-transporters in the deterioration of the human physiology and the occurrence of kidney stone formation has been poorly studied. To bring new insight into the understanding of the formation of the disease due to the substantial contribution of phosphate co-transporters studies are conducted in different animal models to overcome, at least in part, the vast knowledge gap on the genetics of phosphate stone formation.

Studies in mice and human models have indicated that impaired expression of phosphate transporters led to renal stones (Han et al., 2015, Vasudevan et al., 2017). It has been known that hypercalciuric rats, fed with a low phosphate diet, form fewer kidney stones due to a decrease in urinary phosphate excretion. Similarly, studies in humans have emphasised that subjects with renal phosphate loss, develop kidney stones composed of calcium phosphate and calcium oxalate (Letavernier and Daudon, 2018, Ratkalkar and Kleinman, 2011).

Furthermore, deficiency in renal phosphate reabsorption could trigger the formation of renal stones thereby increasing the concentration of calcium and phosphate ions in the loop of Henle. In this segment, water retrieval from the lumen increases phosphate and calcium concentrations which thereby favours initiation of the stone's formation. Examination of renal-biopsy specimens obtained from different human samples suffering from renal stones suggests that calcium phosphate crystals form on the basement membrane of the thin loop of Henle and migrate through the epithelium to the papilla, where they form calcium phosphate stones (Evan et al., 2014, Yu et al., 2018).

Several studies in human have shown that total phosphate concentrations in serum and urine can be used to calculate the maximum tubular reabsorption of phosphate (TMP) normalised for the GFR (the TMP/GFR value). The TMP/GFR value less than <0.70 mmol per litre value shows impaired renal phosphate reabsorption (Bech et al., 2013). In the study conducted in 207 subjects with the case of calcium oxalate stones, it was reported that 20% of the subjects with normal parathyroid function had decreased TMP/GFR value (Wang et al., 2013). The associated mild hypophosphatemia results in increased 1,25-dihydroxy vitamin D production, which increases intestinal phosphate and calcium absorption. The combination of hypercalciuria from the increased intestinal calcium absorption and the hyperphosphaturia favours the formation of calcium phosphate complex resulting in kidney stone formation.

Therefore, these studies show the potential role of mutations in the renal sodium phosphate transporters and with the mutations of proteins interacting with sodium phosphate may also play a vital role in renal phosphate stone formation.

6.2.4 Inorganic phosphate stones in *Drosophila* Malpighian Tubules

Compared to mice and human models, little is known about the mutational effects of phosphate cotransporters in invertebrates like *Drosophila*. Over the past decade, various studies have shown that some human sodium phosphate cotransporters have homologues/analogues in *Drosophila melanogaster* (Bergwitz et al., 2013). Presence of homologues makes *Drosophila* an attractive model to understand the impact of sodium phosphate cotransporters in human physiology and metabolic disorders. In *Drosophila* two types of concretions have been identified, a. Type I concretions: they are composed of calcium, magnesium, Pi and bicarbonate, and are present in the initial segment of the anterior tubule. The number of types I concretions in the initial segment increases in parallel with the increase in calcium in the *Drosophila* diet. b. Type II concretions: they are composed of potassium, calcium and magnesium, and are found in the transitional segment of the anterior tubule (Wessing and Eichelberg, 1979, Wessing and Zierold, 1999, Wessing et al., 1992). It has been suggested that excess ions such as iron may be stored in the concretions as a storage/deposit. The concretions would, therefore, be a way of isolating materials which are toxic in excess, by confining them to the tubules (**Figure 6.3**). Alternatively, the concretions may be a useful store centre of ions, which can then be re-directed as needed to sustain biological processes, such as oogenesis in the ovaries.

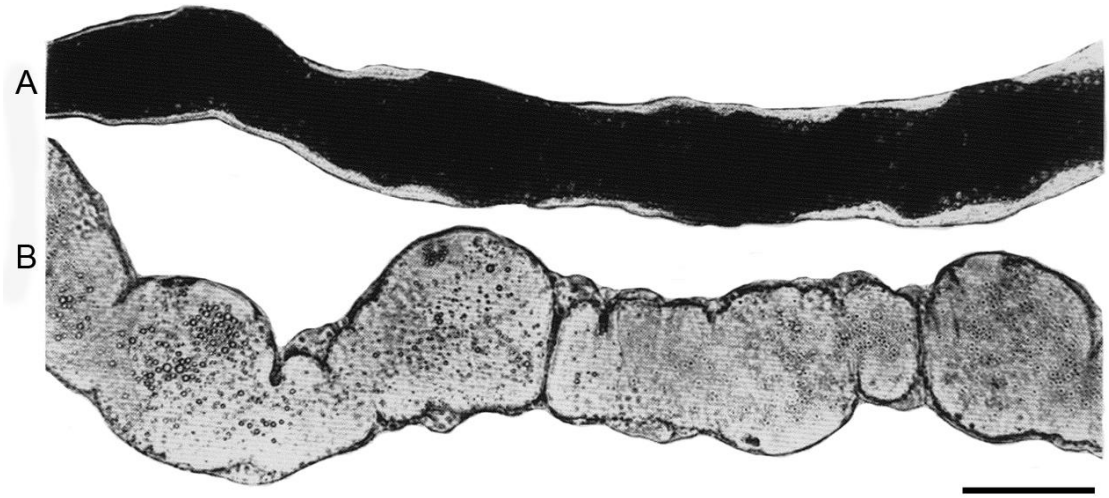

Figure 6.3. Light microscopy of anterior Malpighian tubules, distal segments of *Drosophila melanogaster*. a) Normal diet. The lumen is filled with type-I concretions. b) 72 hours after feeding with 5g/kg carbonic anhydrase inhibitor (hydrochlorothiazide). This carbonic anhydrase inhibitor prevents the formation of phosphate stones. Bar=100 nm. Reproduced with permission from (Wessing and Zierold, 1999).

6.2.5 Inorganic phosphate transporters in *Drosophila*

A recent study has provided evidence that the anterior tubules of *Drosophila* store calcium as phosphate-rich mineral concretions in the enlarged initial segments (Chintapalli et al., 2012) and transport Ca^{2+} at a high rate (Dube et al., 2000). The tubule transcriptome of the anterior tubule is enriched by the genes implicated in the transport of calcium and phosphate and for peroxisomal biogenesis, resulting in the formation of spherites. Calcium is enriched in the specialised peroxisome by entry through trp-like plasma membrane channel and phosphate is provided by Na^+/phosphate cotransporter, *NaPi-T*. In *Drosophila* MTs, *NaPi-T* is one of the major phosphate cotransporters which elevates intraluminal concentration that contributes to the disease (Villa-Bellosta et al., 2009, Chintapalli et al., 2012). In human studies, it has been shown that the sodium phosphate cotransporters are positioned in the apical membrane of renal proximal tubule cells, to move phosphate from lumen to the cell interior (Curthoys and Moe, 2014b). The primary driving force is *Na^+K^+-ATPase* generating an electrochemical gradient for apical phosphate entry (Virkki et al., 2007). Mutation of the phosphate cotransporters causes high accumulation of sodium

and phosphate intraluminally. Hence, we hypothesise that a similar mechanism is also conserved in the flies resulting in aggregation of the stones.

To better understand the significance of *NaPi-T* in renal stones formation we genetically inhibited *NaPi-T*, which markedly increased the accumulation of stones within the fly MTs. These findings were corroborated by colorimetric analysis, which helped us to elucidate that the stones were composed of phosphate and helped us to quantify the total phosphate content within MTs. Further, we compared the binding capacity of the intraluminal calcium by measuring the total quantity of phosphate stones alone and in combination with sodium oxalate. It is known that oxalate and phosphate bind with calcium to form calcium oxalate/calcium phosphate stones, hence measuring phosphate in *NaPi-T* knockdown flies helps to recognise the role of phosphate transporters in phosphate stones formation.

Herein, we hypothesise that *NaPi-T* plays an essential role in the formation of kidney stones. Our data support the idea that *NaPi-T* facilitates phosphate stones formation and represents a possible target for developing preventive and therapeutic strategies against kidney stone formation.

6.3 Results

6.3.1 The orientation of the tubules and gender alters *Drosophila* stone formation

Male and female tubules have markedly distinct expression profiles of various classes of genes. According to the transcriptomes, there is also renal asymmetry with anterior and posterior tubules in both male and female flies (Chintapalli et al., 2012). To determine whether kidney stone formation varies between gender and orientation of the tubules we dissected seven days old wildtype flies and quantified the stones. Upon dissection, the intraluminal concretions looked like small stones, and their hardness could be felt between ones' fingers. Under light microscopic analysis, concretions were visible as dark intraluminal contents within the MTs and had the appearance of small stones **Figure 6.4**. Given their dark physical appearance under light microscopic examination, we suggest these abundant concretions as fly stones composed of phosphate, based on their

similar location of formation to those described by Wessing (Wessing and Zierold, 1999, Wessing et al., 1992) and Southall (Southall et al., 2006).

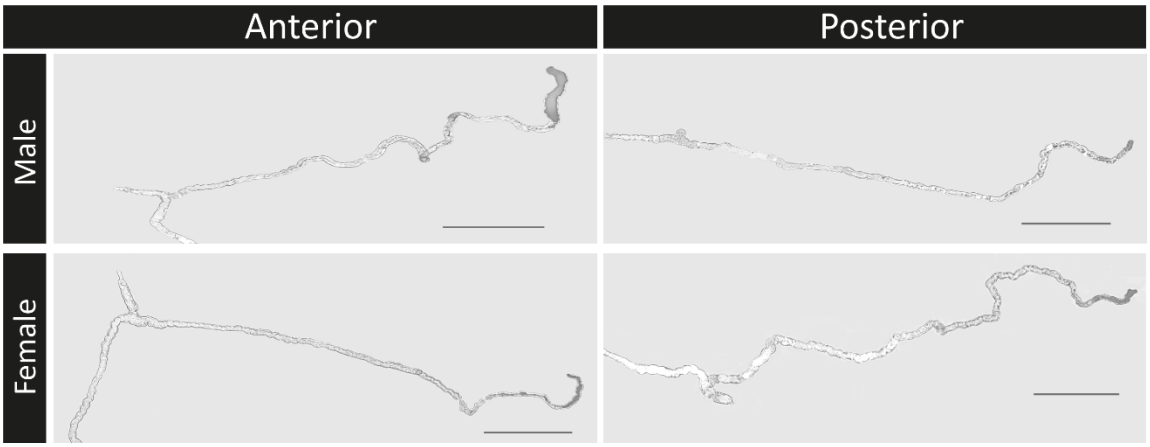

Figure 6.4. Representative tubule images of control flies of both the sexes. Visually, anterior tubules have prominent concretions in an initial segment as compared to the posterior tubules. Bar=500 µm.

Next, using Image-J software, I quantified the total concretion content within both the tubules of male and female flies. The total stone content in anterior tubules of female flies is significantly higher (~2-fold) as compared to a posterior tubule. However, we did not observe any significant difference in the total quantity of stones in between anterior and posterior tubules of male flies **Figure 6.5**.

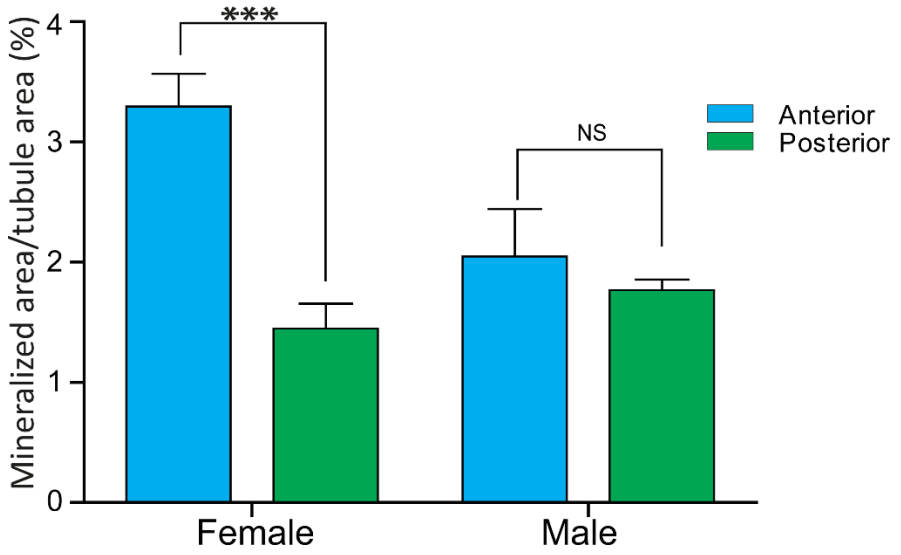

Figure 6.5. Measurement of the total luminal area of the tubules occupied by concretions. Anterior tubules accumulate significantly more concretions as compared to posterior tubules, but no difference was observed in the quantity of concretions content between anterior and posterior tubules in male flies. Similarly, the quantity of stones accumulated in female MTs is significantly high compared to male MTs. Data are expressed as mean ± SEM, N=3. ***p<0.001, two-way ANOVA.

6.3.2 Intraluminally accumulated crystals are composed of Phosphate

To analyse the chemical nature of these fly stones, we performed a colorimetric assay and confirmed that these stones are composed of phosphate. The intensity of the colour of the sample was plotted based on the absorbance at 620nm as a function of phosphate concentration in the sample. The colour intensity in 30 µM standard solution was high as compared to the 1.875 µm standard solution (the inset of **Figure 6.6**), which could be observed directly with the naked eye. The resultant linear regression equation for the female flies was: Abs= 0.03031+0.01670x (R^2=0.9860) and for male was Abs=0.0007857+0.01691x (R^2=0.9903).

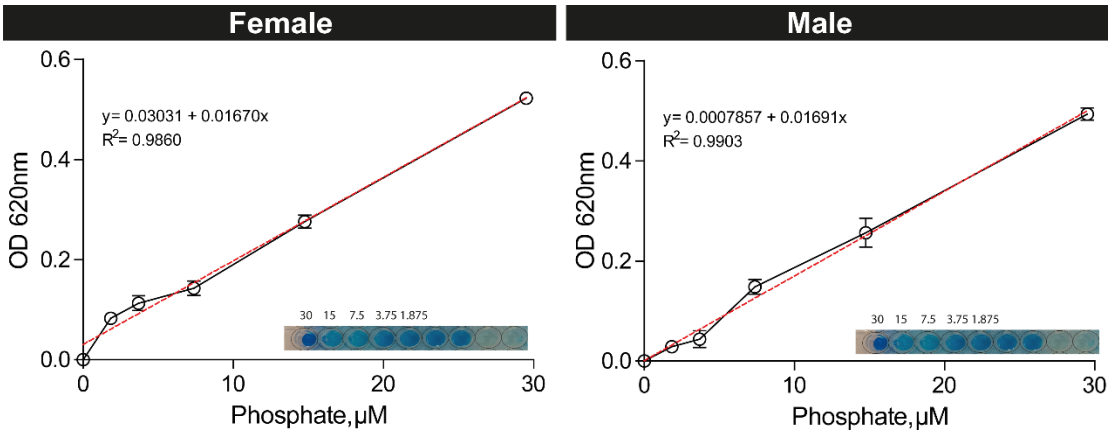

Figure 6.6. The calibration curve corresponding to Phosphate concentration in MTs of female and male flies. Inset: the corresponding photograph of the coloured products for reaction with different phosphate concentrations; dark blue= high concentration.

To examine the selectivity of this system towards the phosphate detection on the basis of gender and tubule orientation, we measured phosphate concentration in both anterior and posterior tubules of flies of both sexes. The results are displayed in **Figure 6.7**. The total phosphate concentration in the anterior MTs of female flies is ~6-fold higher than in posterior tubules. Similarly, the total phosphate concentration in the anterior MTs of male flies is ~2-fold higher than posterior tubules. The results obtained herein clearly supports our quantification results, suggesting that anterior tubules have more stone content, compared to the posterior tubules.

As previously known, female flies have more calcium content as compared to male. Hence excess intraluminal calcium can bind with phosphate forming calcium phosphate stones in high rate in female flies as compared to males (Chintapalli et al., 2012, Davies and Terhzaz, 2009). Additionally, most of the calcium transporters are expressed more in anterior tubules than the posterior tubules. Therefore, the presence of high phosphate stones in anterior female tubules suggests that stone formation is gender and tubule specific.

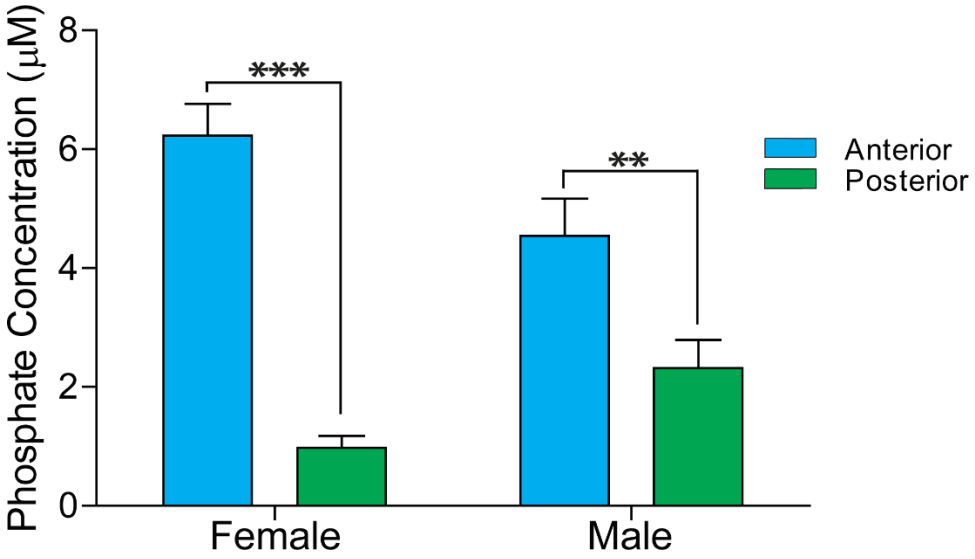

Figure 6.7. Intraluminal phosphate concentration is enriched in anterior tubules. The total phosphate concentration in anterior tubules is significantly high in both male and female flies as compared to posterior tubules. Similarly, female MTs has a significantly high accumulation of phosphate compared to male MTs. Data are expressed as mean ± SEM, N=3. **p<0.01, ***p<0.001 *two-way ANOVA*.

6.3.3 Cell-specific knockdown of *NaPi-T* promotes lithiasis within the *Drosophila* MTs

Seeking *Drosophila* genes (orthologues of human genes), for urinary stone formation, we examined the consequences of cell-specific knockdown of *Napi-T* in principal tubule cells under the control of *CapaR-GAL4* in adult *Drosophila* MTs. In our fly model, we observed that RNAi inhibition of *NaPi-T* (*CapaR-Gla4>UAS-Napi-T RNAi*) conferred a significant increase of the tubular luminal space occupied by fly stones as compared to parental lines (*CapaR-Gal/+*, *UAS-NaPi-T RNAi/+*), highlighting the critical role of *NaPi-T* in the kidney stone formation process. In female flies, the total quantity of stones accumulated in the knockdown condition was significantly higher (~1.5 fold) in both the tubules as compared to the parental lines **Figure 6.8**, **A**. A similar result was observed in male anterior tubules, where the total stones in knockdown flies was significantly higher as compared to parental lines **Figure 6.8, B**. However, there was no significant accumulation of crystals in male posterior tubules of knockdown flies as compared to parental lines.

The Vienna *UAS-NaPi-T RNAi* line produced a significant (>65%) silencing of *NaPi-T* in principal cells **Figure 6.9**. The RNAi knockdown efficiency was confirmed by qPCR. Taken together, our result shows that *NaPi-T* suppression leads to the accumulation of phosphate crystals. These results in *Drosophila* recapitulate the findings and demonstrate the conserved role for *NaPi-T* in enhancing stones formation in the fly tubular lumen.

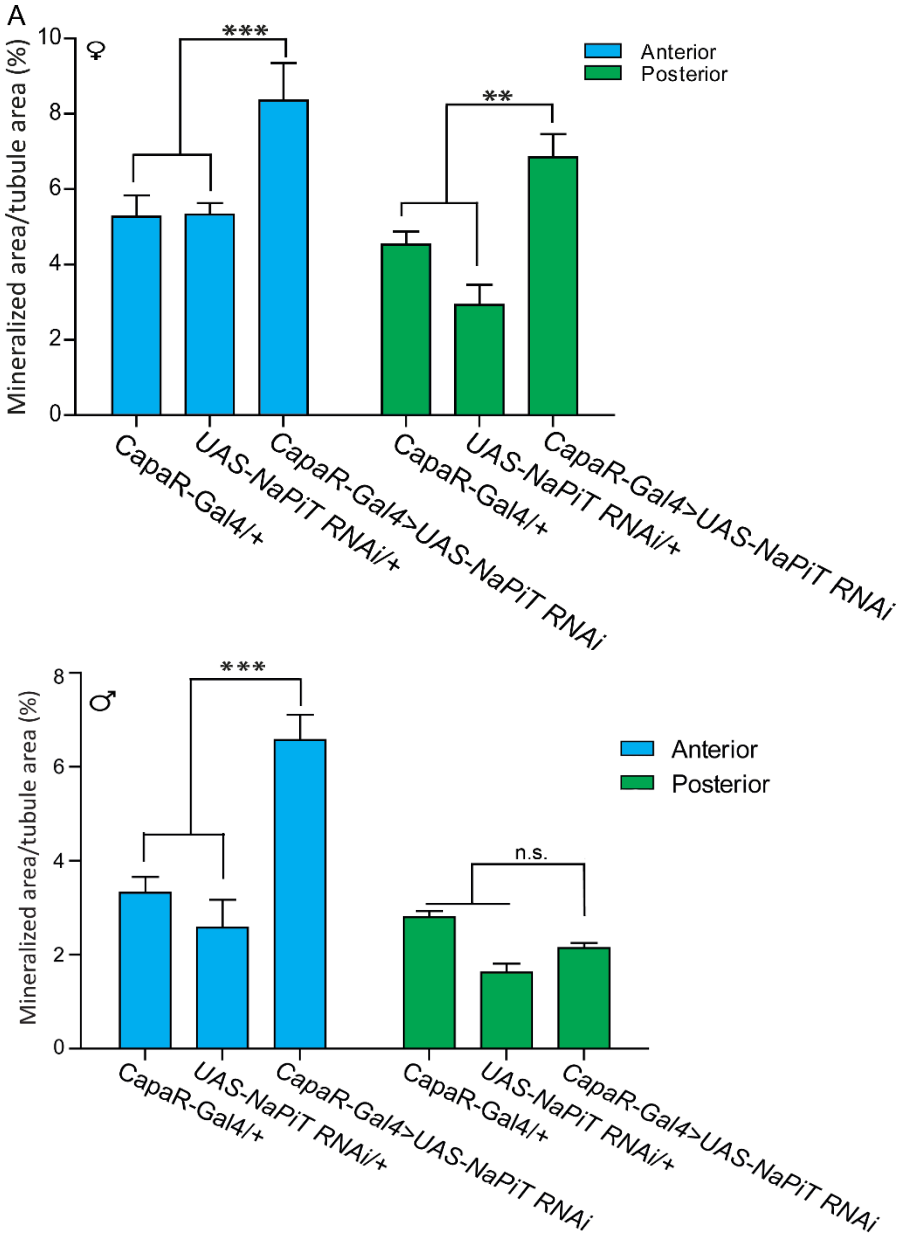

Figure 6.8. Knockdown of NaPi-T increases the quantity of stones in anterior tubules of both male and female flies. A. With silencing of *NaPi-T*, the quantity of stones increases dramatically in *CapaR-GAL4>UAS-NaPi-T RNAi* group as compared to the control groups, i.e. *CapaR-GAL4 /+*, *NaPi-T RNAi/+* in both the anterior and posterior tubules of female flies. B. However, in male flies, knockdown of *NaPi-T* increases the total quantity of stones in the anterior tubule of *CapaR-GAL4>UAS-NaPi-T RNAi* compared to parental lines, (*CapaR-GAL4 /+*, NaPi-T RNAi/+) but no significant difference was observed in posterior tubules. Data are represented in a bar graph as mean ± SEM, N=5. **p <0.01, ***p <0.001. two-way ANOVA.

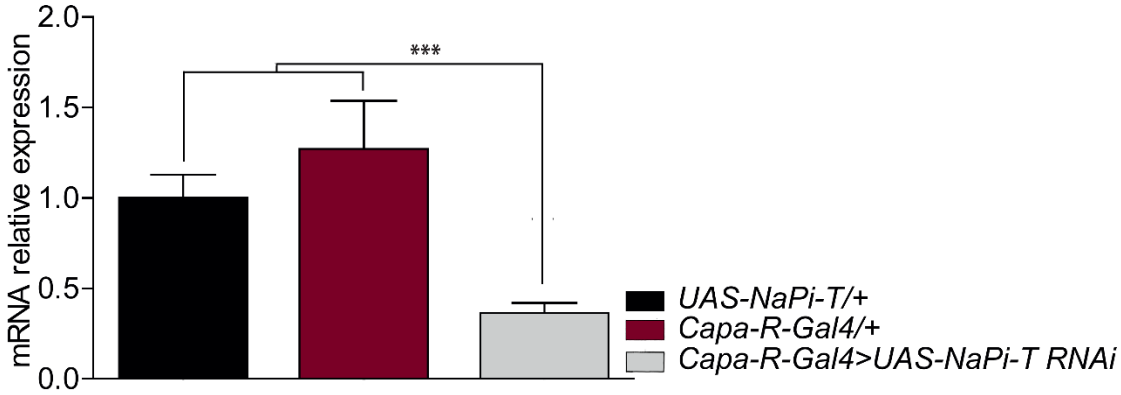

Figure 6.9. Downregulation of *NaPi-T* expression in the fly lines. Expression of *NaPi-T* was significantly reduced in *CapaR-GAL4* driven *UAS-NaPi-T RNAi* fly line as compared with the parental *UAS-NaPi-T RNAi*/+ and *CapaR-GAL4*/+ enhancer trap lines. Data are represented in a bar graph as mean ± SEM, N=3. ***p<0.001, One-way *ANOVA* followed by Dunnett's test.

6.3.4 Calcium phosphate crystallisation with and without oxalate

Biochemical studies have shown that human kidney stones are composed of multiple calcium oxalate monohydrate (COM) crystals encasing a calcium phosphate nucleation. Further, it has been known that amorphous calcium phosphate is a rapidly forming precursor to the formation of calcium phosphate minerals in vivo (Lotsari et al., 2018). Investigation on the events of nucleation mechanism of the crystals has revealed that amorphous calcium phosphate plays a crucial role in the nucleation of calcium oxalate stones by promoting the aggregation of amorphous calcium oxalate precursors at early induction times (Ruiz-Agudo et al., 2017). Hence, I hypothesised that the existence of amorphous calcium phosphate complexes and their coaggregation with amorphous calcium oxalate might be a critical initial step in the mechanism leading to the formation of stones.

In our model, I quantified phosphate stones in the MTs of *NaPi-T* knockdown flies and parental lines, with and without feeding with oxalate to observe any interaction between CaOx and phosphate stone formation. This analysis demonstrated that the quantity of phosphate stones in female MTs decreased significantly after feeding with oxalate in all three conditions **Figure 6.10, A**. However, we did not observe consistent results in male flies (**Figure 6.10, B**). The sex dimorphic results were expected, given that female flies have higher calcium content compared to males. Throughout the experiment, opaque stones

were scored by brightfield, whereas birefringent oxalate stones were determined by polarisation microscopy. The most important causes of these differences in compositional distributions is related to the conversion of phosphate stones to oxalate stones. These results suggest that stones within MTs of *NaPi-T* knockdown flies are indeed composed of phosphate. Hence, once flies are fed with oxalate, calcium binds with oxalate forming oxalate stones, thereby decreasing phosphate stone concentration and increasing concentration of oxalate stones. Taken together, these data demonstrate a role of *NaPi-T* in modulating oxalate stone formation.

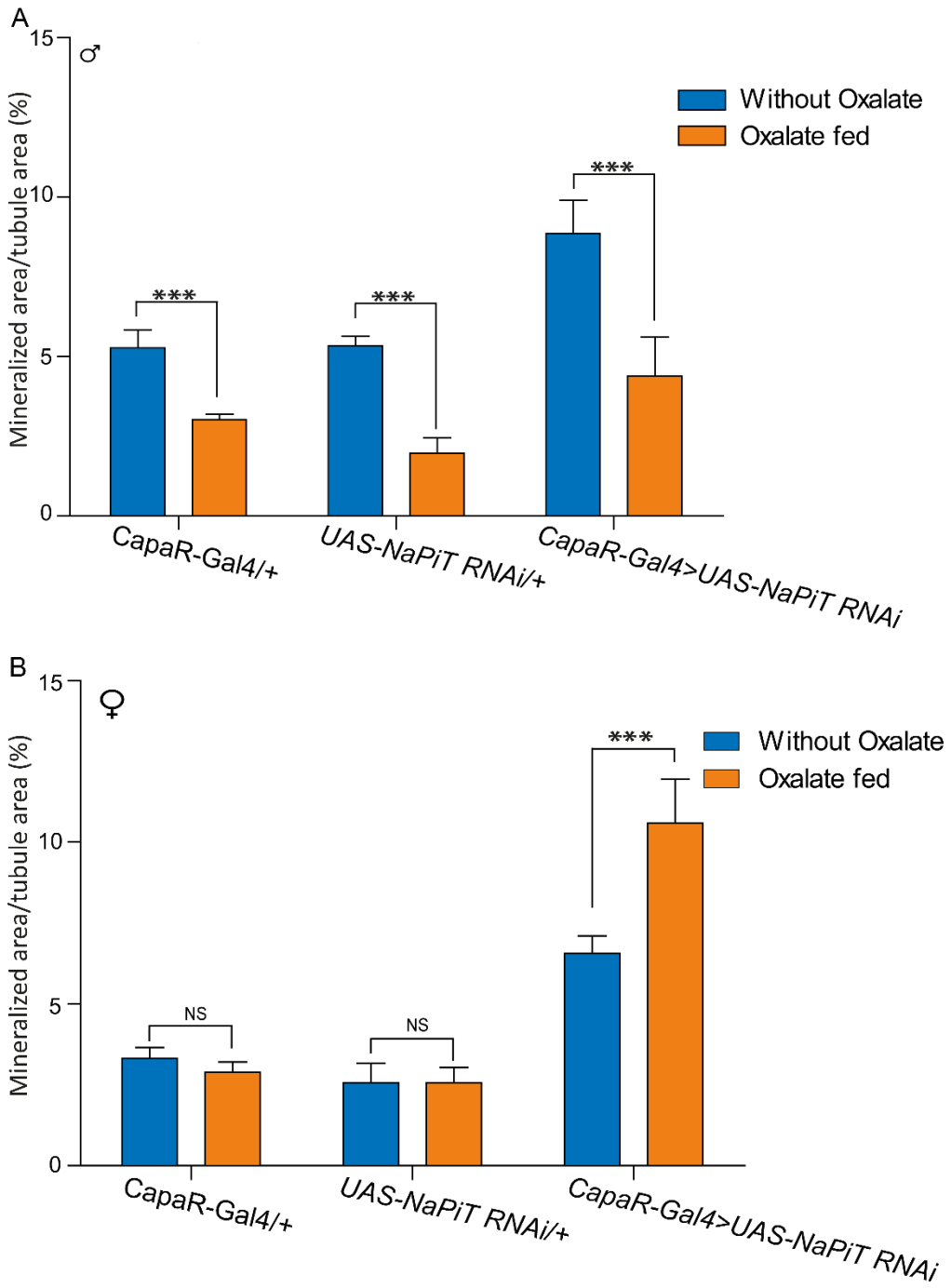

Figure 6.10. Phosphate stones accumulation is altered by oxalate stones formation (A) Typical tubule images are taken from *CapaR-GAL4/+*, *UAS-NaPi-T RNAi/+* and *CapaR-GAL4>UAS-NaPi-T RNAi*, male flies after feeding them with sodium oxalate. (B) The images were taken from *CapaR-GAL4/+*, *UAS-NaPi-T RNAi/+* and *CapaR-GAL4>UAS-NaPi-T RNAi*, female flies before and after feeding them with sodium oxalate, and the stones being accumulated in both the conditions was quantified. The extent of stones formation was quantified as the percentage of the tubule lumen occupied by mineralised material. Data are represented in a bar graph as mean ± SEM, N=5. ***p <0.001, two-way ANOVA.

6.4 Discussion

Over the past few decades, a breakthrough has not been achieved in the discovery of novel drugs for the treatment of kidney stones due to an incomplete understanding of the mechanisms of the disease and the lack of suitable model system. Among various causes of kidney stone, genetics has been one of the significant instigating factors (Dow and Romero, 2010, Hirata et al., 2012). In this section, we discuss the role of putative inorganic phosphate co-transporter *NaPi-T* in the MTs and its involvement in kidney stone formation.

Several previous studies have predicted that the accumulation of stones is caused due to monogenic (Griffin, 2004) or polygenic mutation (Braun et al., 2016, Sayer, 2017). High throughput screening of the genes by next-generation sequencing has revealed that 15% of renal stones form due to monogenic causes (Halbritter et al., 2015). Homozygous and compound heterozygous mutations were found in the autosomal recessive genes including *ATP6V1B1*, *ATP6V0A4*, *CLDN16*, *SLC3A1*, *CYP24A1*, *SLC12A1*, and *AGXT*. Heterozygous variants were described in putatively dominantly-inherited disease genes including *ADCY10*, *SLC4A1*, *SLC9A3R1*, *SLC34A1*, and *VDR* (Schlingmann et al., 2016). Presence of evidence showing the role of phosphate co-transporters in kidney stone formation highlights the potential role of phosphate co-transports in the calcification process (Wagner et al., 2017) (Reed et al., 2002) The consistent presence of the sodium-phosphate co-transporters in the transport of sodium and phosphate across the kidney in higher organism encourages us to investigate the role of phosphate transporters in invertebrates like *Drosophila*, to understand the detailed mechanism of phosphate stone formation.

The regulation, transport and storage of minerals such as phosphate and calcium are essential processes in all cells and tissues. Phosphate is the third most abundant anion in the body required for the proper mineralisation and biological function. Hindrances in the balance between absorption and excretion of circulating phosphate in the body is a result in either hypo or hyper phosphatemic states (Prié et al., 2002, Prié et al., 2009). Further, hypophosphatemia leads to bone mineralisation and also may result in cardiac dysfunction, whereas hyperphosphatemia is linked to hyperparathyroidism and reduced life expectancy (Jüppner, 2007). In humans, phosphate transporters are

associated with various diseases, including kidney stone formation. In this study, stones formation was studied in the *Drosophila* Malpighian tubule utilising a background of inhibition of *NaPi-T* in principal cells.

We have shown that stones are formed naturally in the anterior tubules and postulated that this is the way that tubules maintain phosphate balance in wild-type flies with the normal homeostatic function. The concretions were small visible spherules with a dark black appearance. The physical and visual appearance of the concretions in our model was similar to that observed by Wessing and his colleagues in previous studies (Wessing and Zierold, 1999, Wessing et al., 1992). We believe that these concretions mix with each other in forming the larger mineralised particles. Further, we used quantitative and chemical analysis which confirmed that these stones were composed of phosphate. We believe that our result represents two distinct phenomena (a). Female flies significantly accumulate more stone as compared to male flies (b). *Drosophila* stones are highly formed in the initial segment of the anterior tubules.

Sodium phosphate cotransporters play a crucial role in the reabsorption of Pi from the proximal tubule with minimal contribution of the distal segments. Several Na-dependent Pi co-transporters from the SLC34 and SLC20 families of solute carriers, *NaPi-IIa* (*SLC34A1*) (Custer et al., 1994), *NaPi-IIc* (*SLC34A3*) (Segawa et al., 2002), and *PiT2* (*SLC20A2*) (Villa-Bellosta et al., 2009) are expressed in the brush border membrane (BBM) of proximal tubular cells. Among them, *NaPi-IIa* deficient mice are hypophosphatemia due to increased urinary excretion of Pi despite a substantial upregulation of *NaPi-IIc* (Beck et al., 1998). These findings, together with the lack of phenotype of *NaPi-IIc* deficient mice regarding Pi balance (Shenolikar et al., 2002), indicate that *NaPi-IIa* is the major phosphate cotransporter in the kidney. Knockout of both *NaPi-IIa* (Chau et al., 2003) and *NaPi-IIc* (Segawa et al., 2002) results in hypercalcemia and hypercalciuria. In the absence of apparent orthologs of different phosphate transports of human in flies, it is difficult to understand the ancestral gene function. Here, inhibition of the function of *NaPi-T* resulted in the rapid accumulation of the concretions, centred in the initial segment of the Malpighian tubules. The physical appearance of the stones was similar to

phosphate stones. Further, the result was validated chemically which demonstrated the accumulation of phosphate crystals in anterior tubules of *NaPi-T* knockdown flies suggesting the role of *NaPi-T* in the modulation of phosphate concretion formation.

The mechanisms of stone accumulation due to the involvement of sodium phosphate transporters in basically unknown. One of the possible mechanisms elucidating mineralisation is the formation of the vesicles, i.e. matrix vesicle (MV)-mediated mineralisation which may involve these transporters (Anderson et al., 1997). Based on these findings, phosphate transporters especially, *PiT1/2* may mediate transport of P_i into the osteoblasts/chondrocytes to initiate mineralisation via the MV route. MVs are small cellular vesicles which bud off from mineralised tissue cells and within which mineral can be observed (Anderson et al., 1975). Previous observations made in fly Malpighian tubules have reported that calcium phosphate stones are stored in the form of spherites within the peroxisomes of the tubules (Southall et al., 2006, Wessing and Zierold, 1999, Chintapalli et al., 2012).

Further, calcium is admitted to specialised peroxisomes by trp-like membrane transporters, and phosphate is provided by *NaPi-T* (Chintapalli et al., 2012). Calcium is stabilised in the peroxisome by binding with phosphate forming the calcium phosphate crystals. Hence, the demonstration of the development mechanism of phosphate stones due to knockdown of *NaPi-T* reflects a conserved role of sodium phosphate transporters in kidney stones formation. Our results in *Drosophila* reiterate these findings and demonstrate a conserved mechanism of calcification in the fly tubular lumen.

To test whether all the calcium within the tubule binds with phosphate forming phosphate stones, we fed flies with oxalate diet and measured the quantity of phosphate stones before and after feeding with oxalate. The central role for the phosphate or oxalate stone formation is the quantity of calcium content in the body. Ca^{2+} homeostasis in the body is maintained through the interchange of calcium in between intestines, bone, and kidney (Sayer, 2017). Ca^{2+} present in the diet is absorbed via the intestine into the blood, which subsequently is filtered by the glomerulus, and then reabsorbed along the nephron or stored in bone for the long term. However, the excess calcium which is not reabsorbed by

the nephrons will be excreted by the kidney, demonstrating the role of the kidney in the maintenance of calcium balance in the body. An inappropriate excretion of calcium in the urine also termed as hypercalciuria contributes to the development of osteoporosis and kidney stone formation (Coe et al., 2016, Asplin et al., 2006).

It is known that ~10% of all kidney stones are calcium-phosphate stones (Timio et al., 2003). These findings demonstrated that short-term dietary changes could result in hypercalciuria and phosphaturia, which are important risk factors for stone formation (Ferraro et al., 2016). We show that flies develop fewer phosphate stones after feeding flies with oxalate. Nucleation analysis of calcium oxalate crystals in the previous study has shown that stable clusters are formed with the composition of $[Ca\text{-}(HPO_4)_{1+x}\cdot nH2O]^{2x}$. In the presence of phosphate, the existence of negative Ca-P complexes, $[Ca\text{-}(HPO_4)_{1+x}\cdot nH2O]^{2x-}$, will promote the aggregation of positive CaOx clusters, $[Ca_2Ox\cdot H_2O]^{2+}$ by electrostatic attraction and form the CaP-CaOx coaggregation structure. In the meantime, some calcium ions released from slow condensation of $[Ca_2Ox\cdot H_2O]^{2+}$ clusters forms complex with more HPO_4^{2-} and persuades hydrolysis $H_2PO_4^{-}$, resulting in a slow pH decrease during the induction period (Lei et al., 2018). The coaggregation effect from Ca-P promotes the formation of large calcium oxalate complexes, which promote the formation of CaOx perinuclei, increasing the size of spherical thereby forming stable nuclei (Xie et al., 2015). Once the circular structure is formed various CaOx clusters aggregating around the Ca-P sphere provide multiple sites for subsequent nucleation and growth, resulting in multiple calcium oxalate crystals encapsulating the calcium phosphate phase. This is similar to a Ca−Ox renal stone. The agglomerate structure of multiple CaOx crystals aggregating around the calcium phosphate crystals results in a simulated kidney stone which is too large to pass the urinary tract.

These results confirm that *Drosophila* can be used as a model to study phosphate stone formation mechanism. This approach is particularly valuable because there are very few studies conducted to observe the interaction between phosphate and oxalate stones. Many forces are at work balancing the absorption and secretion of Pi or Ca^{2+} from the kidney, and a better understanding of the interplay can lead to new therapeutic strategies. This manipulation of the

function of NaPi-T could be leveraged as a therapeutic target for the prevention of many forms of stones formation. Our findings in *Drosophila* may appear near translation to human physiology. However, an in-depth study of the mechanism of the formation of Pi in flies. To date, no evidence supports the use of *NaPi-T* in kidney stones formation. Future studies should aim at understanding the underlying molecular effects of low-salt and high-K^+ diet on the progression of age-related bone loss and the development of kidney stones.

6.5 Conclusion

Knowing the vital role of Pi in various physiological processes, considerable advances have been made in our understanding of the various mechanisms involved in Pi homeostasis. The pathophysiology underlying renal stone formation is a complex process due to the influence of genes in polygenic and monogenic forms. Understanding the kidney stone disease has evolved dramatically over the past century, eliciting an appreciation for the participatory role of proteins, including transporters channels and receptors.

The work in this chapter reports on the function of *NaPi-T* in renal phosphate stone formation mainly in the anterior tubule of female flies, which supports the findings of previous mammalian studies. While these studies provide important new data on *NaPi-T* function, to date, the mechanism of how *NaPi-T* knockdown causes kidney stone is still unknown. Based on the physiological and chemical analysis of the observed stone, we hypothesise that *NaPi-T* is involved in renal phosphate stone formation in flies. However, the results do not provide the conclusive data regarding the mechanism of phosphate stone formation due to mutation of phosphate cotransporters. In the future, an in-depth understanding of the role of *NaPi-T* and further studies into the mechanism, opening an avenue for the identification of new therapeutic targets and approaches to treatment is required.

Chapter 7 Conclusion and Future work

7.1 Summary

This chapter interconnects the outcomes obtained in each chapter and helps to derive the final conclusion of this thesis. These include the summary of results obtained from different chapters of my PhD, followed by the problems faced during the experiments and most importantly, the follow-up projects which can be done in future. In brief, this thesis entitled "**Identifying Genetic Loci for Metabolic Disorders Affecting the Renal Tract**" is devoted to the understanding of the role of genes and environmental condition in management and prevention of the kidney stones. Further, the significant consequence of this study is the validation of the use of *Drosophila melanogaster* as a physiological model for kidney stone studies. Our work also complements previous work by identifying a genetic means to modulate fly mineralisation.

7.2 Introduction

Nephrolithiasis is the process of aggregation of the crystals in the urinary tract resulting in stone formation. It is a common and complex metabolic disorder effecting the, quality of life and an economic burden on the individual and the health system of the country. Various intrinsic and extrinsic factors contribute to the formation of kidney stones. Among intrinsic factors are race, sex, and genetics (**detail section 1.4.2**) (Stamatelou et al., 2003). However, the pathophysiology of nephrolithiasis remains poorly understood, and there have been very few advances in the treatment of the disease in the last decades. Thus, finding the cause and pathophysiology underlying nephrolithiasis will help to reduce the consequences and complications of the disease thereby reducing the cost of treatment by establishing preventative measures in addition to patient education (Curhan, 2007).

Even though the prevalence of nephrolithiasis is increasing, our understanding of the pathophysiology has not kept the same pace, and new therapeutic approaches have not emerged. Genetic factors play an essential role in the

aetiology of urolithiasis as a polygenic (common) or monogenic (rare) (Mahdieh and Rabbani, 2013). Hence, knowledge about the stones and early diagnosis are essential to achieve the goals of reducing patient suffering and economic burdens. Therefore, efforts have been made in this thesis to continue research to be directed to unveiling the underlying pathophysiology of kidney stone formation.

7.3 Results

The conclusion obtained from each chapter are enlisted below:

Chapter 1: The first chapter of this thesis discusses various causes of kidney stones, and reason how genetic, environmental, and metabolic factors act singly or in concert to trigger stone formation. Similarly, it also explains the significance of different model organisms that elucidate the pathophysiology of CaOx stone formation in combination with clinical research in the hope for advancing the field and leading to the development of new therapeutic approaches that have the potential to reduce the morbidity, mortality, and cost associated with this disease. Further, this chapter elucidates the use of *Drosophila melanogaster* as an invertebrate model in understanding mineralisation.

Chapter 2: Chapter 2 discusses different experimental protocols and materials used during this thesis and summarises the rearing conditions of *Drosophila melanogaster* for different experiments. Appropriate references for methods used are listed where applicable.

Chapter 3: Evidence presented in the third chapter of this thesis helps us to understand of the role of genetics in kidney stone crystallisation. In this chapter, I explained about the screening of different potential genes to understand the mechanisms behind its involvement in CaOx nephrolithiasis. Among twenty independent RNAi or mutant panel of flies screened, only eight RNAi lines showed significant variation in accumulation of CaOx stones compared to parental lines. The knockdown flies cause an increase or decrease in intraluminal oxalate concentration as compared to the control conditions. These

genes were identified as hits and the following chapters of this thesis discuss the role of some of these genes in stone formation.

Chapter 4: Experimental outcomes of chapter 4 demonstrate the role of age and temperature in the stone formation. In this chapter, I found that an elevation in the temperature of residence increases the incidence of nephrolithiasis, furthermore the higher the age of the flies the greater the risk of stone formation. Analysing the results, I found that change in stone accumulation was due to a change in expression of phosphate transporters *NaPi-T* and *Picot* which causes accumulation of phosphate within the lumen of tubules. This led to a state where an excess of intraluminal calcium binds with phosphate causing higher sodium phosphate concentrations, which facilitates the crystallisation of substances in urine triggering stone formation.

In chapter 5 and 6 I discuss monogenic forms of kidney stone formation. Genes play an important role in the aetiology of nephrolithiasis. There are two forms of genetic involvement, the common polygenic and the rare monogenic forms. Clinical recognition of the monogenic hereditary forms of nephrolithiasis can be challenging, due to their rarity, broad spectrum of disease, expression time and overlap with calcium oxalate nephrolithiasis.

Chapter 5: Evidence presented in chapter 5 of this thesis characterises the novel role of *Drosophila SRY interacting protein1 (Sip1)*, in renal stone formation. *Sip1* was selectively knocked down in Stellate Cells (SCs) resulting in stone formation within MTs which physically and chemically was similar to uric acid stones. The outcome was validated by physiological, chemical, pharmacological and genetic analyses including the development of a chemical approach to quantify uric acid accumulation in MTs. In addition to that, localisation of SIP1, Moesin, and NHE2 in wild-type, *Sip1* mutant, and *Moesin* mutant flies, showed that *Sip1* functions with *Moesin* and *NHE2* to promote the increase of H+ into the lumen using an inward Na^+ chemical gradient thereby decreasing luminal [Na^+] and increasing luminal [H^+], resulting in a favourable environment for uric acid stone formation.

Chapter 6: In chapter 6, I discuss the role of *NaPi-T* in phosphate stones formation in MTs. I found that knockdown of *NaPi-T* in MTs results in the accumulation of phosphate stones. Based on the results I hypothesise that the

intracellular stones of inorganic phosphate are maintained by *NaPi-T,* which on downregulation causes accumulation of phosphate concretions intraluminally larger than predicted. The result was further verified by physiological and chemical assays. However, future research is required in order to know details about the role of phosphate transporter in phosphate balance.

7.4 Limitations of the study

Chapter 1:

1. Throughout the experiment, I used *Drosophila* as a model organism. There are advantages of the *Drosophila* system that should be noted, namely, (1) The low cost of maintaining *Drosophila* colonies, (2) the rapid deployment of new transgenic lines, and (3) the ability to test hypotheses in lower-species in vivo systems before embarking on studies in higher organisms. The key limitation is that the insect renal system is aglomerular, and thus the composition of the final tubular fluid is based entirely on active secretion rather than ultrafiltration followed by a combination of reabsorption and secretion. The absence of a filtration structure is explained by the physical relationship between the blood supply and the tubules: the tubules freely float in the hemocoel (blood-filled body cavity) rather than having a vascular system that hugs the tubules, as in the mammalian renal system.

Chapter 3:

1. In this chapter, the genes were selected based on the previous results from published articles. This limits the unbiased selection and identification of the group of genes represented in the screening list.

2. Although nephrolithiasis is roughly 50% heritable, the presence of a family history usually does not affect treatment since most stone disease is regarded as polygenic, i.e. not attributable to a single gene. However, in this investigation, I only focused on the monogenic cause (2% of stones). Hence, the orientation of research towards polygenic cause of stones formation might demonstrate the clinical outcome. This intriguing

possibility holds the potential to change the management paradigm in stone prevention and understanding of the complex trait with environmental and polygenic determinants.

3. The successful identification of the role of 8 genes in stone formation in *Drosophila* was restricted by the investigative techniques utilised. RNAi is a useful molecular tool when combined with the *UAS/GAL4* system, but it also has shortcomings. During the screening of the genes, I could not get high knockdown of the gene in RNAi lines. Hence, I was not assured whether renal stones are related to that particular gene activity or not. Although every effort was made to get an RNAi flies which are gene-specific and may still cause an off-target silencing effect on other genes when inserted into the *Drosophila* genome and expressed, the results of these experiments do not exclude the effects of off-target silencing on other genes, which could be assessed by further microarray studies on each *UAS-RNAi* fly-line. Despite these limitations, the sensitised background offers a screen platform in a whole panel of RNAi lines and this cover the *Drosophila* genome without selection bias.

Chapter 4

1. In humans, the mechanism for pathogenesis causing stone disease is attributed to heat-induced sweating, loss of water and ions. Loss of extracellular fluid leads to an increase in serum osmolarity that in turn leads to change in hormones, leading to an increase in urinary concentration thereby reducing the urinary volume and causing kidney stones. As urine volume decreases the concentration of relatively insoluble salts such as calcium oxalate or phosphate increases thereby reaching an upper limit of solubility, hence the salts precipitate out of the solution forming solid crystals developing stones. The results observed in this chapter were consistent with a study performed in male flies irrespective of the days of exposure but not in the female flies. Further, I did not consider evaluating any changes in the loss of ions in the MTs in male and female flies. It should be predicted that, as in humans, *Drosophila* tubules should secrete less fluid under heat or desiccation

stress. This would be relatively easy to test. Similarly, the role of humidity was never explored throughout the study. Hence the understanding of the mechanism of how humidity affects the urinary volume and urinary concentration of ions should be studied.

Chapter 5

1. This thesis is the first study to use *Drosophila* as a model organism for uric acid stone formation. Mutation of *Sip1* and stellate cell-specific knockdown caused an accumulation of uric acid stones. The results were verified by molecular assays; however, if I had performed a metabolomic assay comparing mutant lines and control flies, the result so obtained could have verified the change in expression of the genes and also have helped to discover other candidate genes.

2. The Sip1, Moesin and NHE2 antibodies designed show specific expression in immunostaining. However, when the same antibody was used during co-immunoprecipitation and Western blotting, I did not observe a specific band size. The putative antigenic areas were checked on flybase.org, but I could not see any specificity. The antigenic region, which was most likely to produce a specific, working antibody was not functioning which limited our study to perform co-immunoprecipitation. Throughout the experiment, we minimised non-specific binding by using the lowest antibody concentration possible, and by using antibody solutions which had been preabsorbed on other tissues, which had little effect on the number of proteins identified during Western blotting.

Chapter 6

1. In the results, I found that knockdown of *NaPi-T* results in higher accumulation of intraluminal oxalate concentration compared to parental lines. The results were validated by physiological and chemical analysis. However, limited success was achieved in collecting the secreted fluid. Collection of the intraluminal fluid and analysing of the concentration of ions in knockdown and parental lines would have given an idea about the

roles of different factors which influence the stone concentration, such as pH, hormones, and subcellular compartmentalisation.

2. Human studies have shown that many enzymes of key metabolic pathways are regulated by phosphate; these pathways include those for anaerobic glycolysis, gluconeogenesis, mitochondrial metabolism, glutamine, purine and nucleic acid metabolism. Although I performed chemical analysis to validate presence of phosphate but did not perform any immunostaining experiments to validate its localisation in the organs/cells.

   Further, previous articles have shown successful targeting localisation of phosphate transporters only in mammals. Whether these mammalian pharmacological agents block homologueous genes in *Drosophila* is not yet known, but they could prove to be a useful way of controlling the efficacy of transporter function without interfering with transcription or translation.

7.5 Future work

Many aspects of the work described in this thesis would benefit from further investigation. These studies could not only help to find new genes involved in kidney stone formation but could also increase our understanding of the mechanism behind the stone formation. Further ways of extending the data include additional characterisation of the nature of the gene to determine whether the genes investigated would be successful kidney stone targets. Despite advances, there are still vast areas in nephrolithiasis that are poorly understood or even unexplored. To further the progression of research and clinical management of kidney stones, multilevel translational approaches are needed.

1. Improved laboratory studies and animal and cell culture models are needed, and greater effort needs to be made to identify candidate loci and genes. The metabolomic studies are beneficial and a powerful method in the biological fields, in the normal as well as in the disease states. The expression of the genes identified in this thesis can be tested

in mammalian samples which could validate our findings in higher organisms.

2. In chapter 3, I performed extensive research by knocking down the genes (**section 3.3.2**) and introducing calcium oxalate stones by feeding with NaOx, but there remain many unanswered and unexplored areas of this disease. E.g. is it the only gene involved in calcium oxalate stone origination? Is there an influence of any other lithogenic agents other than NaOx in the accumulation of the stones? The availability and use of the other lithogenic agents would have strengthened our observation. The mode of inheritance of idiopathic nephrolithiasis has been discussed for decades and is usually regarded polygenic. Previous articles have shown that most rare genetic causes of stones bear their metabolic signatures, and as such should be recognised and diagnosed based on clinical findings and stepwise metabolic testing using metabolomics, proteomics or transcriptomic analysis.

3. In chapter 3, I believe that the stones are accumulated in the tubules because of two distinct phenomena; one being of pathological, ectopic, and exuberant calcification while the former is a normal, physiologic process. The pathologic fly stone is the foundation upon which our model is built. Studies have shown that mutation or specific knockdown of the gene should have some impact on the life span of the flies. It is assumed that this excessive intraluminal stone accumulation might be harmful to the fly. The reduced lifespan appears to be due to the presence of excessive, enlarged, ectopic, and consistently obstructive fly stones. Hence performing lifespan extension would help in identification for the role of gene or genes which modulates both stone formation and survivorship independent of one another.

4. In our temperature vs kidney stone formation experiment (chapter 4), I have found causal links between age and ambient temperature with stone prevalence are surprisingly sparse and complicated by other variables. Given the preponderance of evidence from different human study across the globe, it seems undeniable that climate, whether it is through temperature, humidity, or sunlight, has at least some role in the

development of urinary calculi. Hence, maintenance of constant humidity throughout the experiment in all the conditions would provide an accurate correlation between temperature in kidney stone formation.

5. In chapter 5 our experimental results allow a model for the formation of uric acid stones in the MTs of *D. melanogaster*. Previous results, been shown the genetic interaction between Sip1 and Moesin through co-immunoprecipitation experiments in mammals and S2 cells. However, I was not able to show the interaction between SIP1, Moesin and NHE2 using co-immunoprecipitation due to non-specific binding of antibodies. Hence, purchase of a commercially available antibody to validate our result which would be a milestone for an understanding of the formation of uric acid stones.

6. To have new insights about causal genes of nephrolithiasis, technology and skills should be coupled for the faster screening of the genes with standardised and precise clinical methods. The work presented in this thesis hopefully represents another step along the path to understanding the genetic principles that determine the role of genetic and environmental factors in kidney stone formation and the mechanisms behind the process.

Bibliography

ACHESON, L. S., WIESNER, G. L., ZYZANSKI, S. J., GOODWIN, M. A. & STANGE, K. C. 2000. Family history-taking in community family practice: implications for genetic screening. *Genetics in Medicine,* 2**,** 180-185.

ADAM, M., ARDINGER, H., PAGON, R., WALLACE, S., BEAN, L., STEPHENS, K. & AMEMIYA, A. Primary Hyperoxaluria Type 1--GeneReviews®. [Internet]. Seattle (WA): University of Washington, Seattle; 1993-2019.

ADAMS, M. D., CELNIKER, S. E., HOLT, R. A., EVANS, C. A., GOCAYNE, J. D., AMANATIDES, P. G., SCHERER, S. E., LI, P. W., HOSKINS, R. A. & GALLE, R. F. 2000. The genome sequence of Drosophila melanogaster. *Science,* 287**,** 2185-2195.

AGGARWAL, K. P., NARULA, S., KAKKAR, M. & TANDON, C. 2013. Nephrolithiasis: molecular mechanism of renal stone formation and the critical role played by modulators. *BioMed research international,* 2013,1-21.

AGGARWAL, R., SRIVASTAVA, A., JAIN, S. K., SUD, R. & SINGH, R. 2017. Renal stones: A clinical review. *EMJ Urol,* 5**,** 98-103.

AKOUDAD, S., SZKLO, M., MCADAMS, M. A., FULOP, T., ANDERSON, C. A., CORESH, J. & KÖTTGEN, A. 2010. Correlates of kidney stone disease differ by race in a multi-ethnic middle-aged population: the ARIC study. *Preventive medicine,* 51**,** 416-420.

AKUM, B. F., CHEN, M., GUNDERSON, S. I., RIEFLER, G. M., SCERRI-HANSEN, M. M. & FIRESTEIN, B. L. 2004. Cypin regulates dendrite patterning in hippocampal neurons by promoting microtubule assembly. *Nature neuroscience,* 7**,** 145-152.

ALELIGN, T. & PETROS, B. 2018. Kidney stone disease: an update on current concepts. *Advances in urology,* 2018, 1-12.

ALHUZAIM, O. N., ALMOHAREB, O. M. & SHERBEENI, S. M. 2015. Carbonic Anhydrase II Deficiency in a Saudi Woman. *Clinical Medicine Insights: Case Reports,* 8**,** 7-10.

ALI, S. N., DAYARATHNA, T. K., ALI, A. N., OSUMAH, T., AHMED, M., COOPER, T. T., POWER, N. E., ZHANG, D., KIM, D. & KIM, R. 2018. Drosophila melanogaster as a function-based high-throughput screening model for antinephrolithiasis agents in kidney stone patients. *Disease models & mechanisms,* 11**,** 1-11.

ALTSCHUL, S. F., GISH, W., MILLER, W., MYERS, E. W. & LIPMAN, D. J. 1990. Basic local alignment search tool. *Journal of molecular biology,* 215**,** 403-410.

ÁLVAREZ-LARIO, B. & MACARRÓN-VICENTE, J. 2010. Uric acid and evolution. *Rheumatology,* 49**,** 2010-2015.

AMATO, M., LUSINI, M. & NELLI, F. 2004. Epidemiology of nephrolithiasis today. *Urologia internationalis,* 72**,** 1-5.

AMIEVA, M., TURUMEN, O., VAHERI, A., LOUVARD, D. & ARPIN, M. 1994. Radixin ls a Component of Hepatocyte Microvilli in Situ. *Exp. Cell Res,* 210**,** 140-144.

ANDERSON, H. C., CECIL, R. & SAJDERA, S. W. 1975. Calcification of rachitic rat cartilage in vitro by extracellular matrix vesicles. *The American journal of pathology,* 79**,** 237-254.

ANDERSON, H. C., HSU, H. H., MORRIS, D. C., FEDDE, K. N. & WHYTE, M. P. 1997. Matrix vesicles in osteomalacic hypophosphatasia bone contain

apatite-like mineral crystals. *The American journal of pathology,* 151**,** 1555–1561.

ANDRUS, S., GERSHOFF, S., FARAGALLA, F. & PRIEN, E. 1960. Production of calcium oxalate renal calculi in vitamin B6-deficient rats: study of the influence of urine pH. *Laboratory Investigation,* 9**,** 7-27.

ARDURA, J. A. & FRIEDMAN, P. A. 2011. Regulation of G protein-coupled receptor function by Na+/H+ exchange regulatory factors. *Pharmacological reviews,* 63**,** 882-900.

ASPLIN, J., DONAHUE, S., KINDER, J. & COE, F. 2006. Urine calcium excretion predicts bone loss in idiopathic hypercalciuria. *Kidney international,* 70**,** 1463-1467.

ATAN, L., ANDREONI, C., ORTIZ, V., SILVA, E. K., PITTA, R., ATAN, F. & SROUGI, M. 2005. High kidney stone risk in men working in steel industry at hot temperatures. *Urology,* 65**,** 858-861.

ATSMON, A. 1963. *Uric acid lithiasis*, *The American Journal of Medicine*; 1963, 880-892.

BACIC, D., LEHIR, M., BIBER, J., KAISSLING, B., MURER, H. & WAGNER, C. 2006. The renal Na+/phosphate cotransporter NaPi-IIa is internalized via the receptor-mediated endocytic route in response to parathyroid hormone. *Kidney international,* 69**,** 495-503.

BACKOV, R., LEE, C. M., KHAN, S. R., MINGOTAUD, C., FANUCCI, G. E. & TALHAM, D. R. 2000. Calcium oxalate monohydrate precipitation at phosphatidylglycerol Langmuir monolayers. *Langmuir,* 16**,** 6013-6019.

BAGGA, H. S., CHI, T., MILLER, J. & STOLLER, M. L. 2013. New insights into the pathogenesis of renal calculi. *Urologic Clinics of North America,* 40**,** 1-12.

BARBAS, C., GARCıA, A., SAAVEDRA, L. & MUROS, M. 2002. Urinary analysis of nephrolithiasis markers. *Journal of Chromatography B,* 781**,** 433-455.

BASAVARAJ, D. R., BIYANI, C. S., BROWNING, A. J. & CARTLEDGE, J. J. 2007. The role of urinary kidney stone inhibitors and promoters in the pathogenesis of calcium containing renal stones. *EAU-EBU update series,* 5**,** 126-136.

BECH, A., BLANS, M., RAAIJMAKERS, M., MULKENS, C., TELTING, D. & DE BOER, H. 2013. Hypophosphatemia on the intensive care unit: individualized phosphate replacement based on serum levels and distribution volume. *J Crit Care,* 28**,** 838-43.

BECK, L., KARAPLIS, A. C., AMIZUKA, N., HEWSON, A. S., OZAWA, H. & TENENHOUSE, H. S. 1998. Targeted inactivation of Npt2 in mice leads to severe renal phosphate wasting, hypercalciuria, and skeletal abnormalities. *Proceedings of the National Academy of Sciences,* 95**,** 5372-5377.

BECKER, M. A., PUIG, J. G., MATEOS, F. A., JIMENEZ, M. L., KIM, M. & SIMMONDS, H. A. 1988. Inherited superactivity of phosphoribosylpyrophosphate synthetase: association of uric acid overproduction and sensorineural deafness. *The American journal of medicine,* 85**,** 383-390.

BERGWITZ, C., RASMUSSEN, M. D., DEROBERTIS, C., WEE, M. J., SINHA, S., CHEN, H. H., HUANG, J. & PERRIMON, N. 2012. Roles of major facilitator superfamily transporters in phosphate response in Drosophila. *PloS one,* 7**,** e31730.

BERGWITZ, C., WEE, M. J., SINHA, S., HUANG, J., DEROBERTIS, C., MENSAH, L. B., COHEN, J., FRIEDMAN, A., KULKARNI, M., HU, Y., VINAYAGAM, A., SCHNALL-LEVIN, M., BERGER, B., PERKINS, L. A., MOHR, S. E. &

PERRIMON, N. 2013. Genetic determinants of phosphate response in Drosophila. *PloS one,* 8**,** e56753-e56753.

BERRY, C. E. & HARE, J. M. 2004. Xanthine oxidoreductase and cardiovascular disease: molecular mechanisms and pathophysiological implications. *The Journal of physiology,* 555**,** 589-606.

BERRYMAN, M., FRANCK, Z. & BRETSCHER, A. 1993. Ezrin is concentrated in the apical microvilli of a wide variety of epithelial cells whereas moesin is found primarily in endothelial cells. *Journal of cell science,* 105**,** 1025-1043.

BHATTACHARYA, R., WANG, E., DUTTA, S. K., VOHRA, P. K., GUANGQI, E., PRAKASH, Y. & MUKHOPADHYAY, D. 2012. NHERF-2 maintains endothelial homeostasis. *Blood***,** blood-2011-11-392563.

BIBER, J., CUSTER, M., WERNER, A., KAISSLING, B. & MURER, H. 1993. Localization of NaPi-1, a Na/Pi cotransporter, in rabbit kidney proximal tubules. *Pflügers Archiv,* 424**,** 210-215.

BLACKLOCK, N. 1965. The pattern of urolithiasis in the Royal Navy. *Journal of the Royal Naval Medical Service,* 51**,** 99-111.

BLAINE, J., CHONCHOL, M. & LEVI, M. 2015. Renal control of calcium, phosphate, and magnesium homeostasis. *Clinical Journal of the American Society of Nephrology,* 10**,** 1257-1272.

BOBULESCU, I. A. & MOE, O. W. 2012. Renal transport of uric acid: evolving concepts and uncertainties. *Advances in chronic kidney disease,* 19**,** 358-371.

BOEVE, E., DENG, G., CAO, L., STIJNEN, T. & SCHRÖDER, F. 1996. Experimental nephrolithiasis in rats: the effect of ethylene glycol and vitamin D3 on the induction of renal calcium oxalate crystals. *Scanning microscopy,* 10**,** 591-601.

BONORA, M., PATERGNANI, S., RIMESSI, A., DE MARCHI, E., SUSKI, J. M., BONONI, A., GIORGI, C., MARCHI, S., MISSIROLI, S., POLETTI, F., WIECKOWSKI, M. R. & PINTON, P. 2012. ATP synthesis and storage. *Purinergic signalling,* 8**,** 343-357.

BONVINI, S. J., BIRRELL, M. A., GRACE, M. S., MAHER, S. A., ADCOCK, J. J., WORTLEY, M. A., DUBUIS, E., CHING, Y.-M., FORD, A. P. & SHALA, F. 2016. Transient receptor potential cation channel, subfamily V, member 4 and airway sensory afferent activation: Role of adenosine triphosphate. *Journal of Allergy and Clinical Immunology,* 138**,** 249-261.

BORGHI, L., MESCHI, T., SCHIANCHI, T., BRIGANTI, A., GUERRA, A., ALLEGRI, F. & NOVARINI, A. 1999. Urine volume: stone risk factor and preventive measure. *Nephron,* 81**,** 31-37.

BRAND, A. H. & PERRIMON, N. 1993. Targeted gene expression as a means of altering cell fates and generating dominant phenotypes. *Development,* 118**,** 401-415.

BRANDSTATTER, A., LAMINA, C., KIECHL, S., HUNT, S. C., COASSIN, S., PAULWEBER, B., KRAMER, F., SUMMERER, M., WILLEIT, J., KEDENKO, L., ADAMS, T. D. & KRONENBERG, F. 2010. Sex and age interaction with genetic association of atherogenic uric acid concentrations. *Atherosclerosis,* 210**,** 474-8.

BRAUN, D. A., LAWSON, J. A., GEE, H. Y., HALBRITTER, J., SHRIL, S., TAN, W., STEIN, D., WASSNER, A. J., FERGUSON, M. A. & GUCEV, Z. 2016. Prevalence of monogenic causes in pediatric patients with nephrolithiasis or nephrocalcinosis. *Clinical Journal of the American Society of Nephrology***,** CJN. 07540715.

BREUER, R., MATTHEISEN, M., FRANK, J., KRUMM, B., TREUTLEIN, J., KASSEM, L., STROHMAIER, J., HERMS, S., MÜHLEISEN, T. W. & DEGENHARDT, F. 2018. Detecting significant genotype–phenotype association rules in bipolar disorder: market research meets complex genetics. *International journal of bipolar disorders,* 6**,** 1-24.

BRIKOWSKI, T. H., LOTAN, Y. & PEARLE, M. S. 2008. Climate-related increase in the prevalence of urolithiasis in the United States. *Proceedings of the National Academy of Sciences*, 105 (28) 9841-9846.

BRÖER, S., SCHUSTER, A., WAGNER, C., BRÖER, A., FORSTER, I., BIBER, J., MURER, H., WERNER, A., LANG, F. & BUSCH, A. 1998. Chloride conductance and P i transport are separate functions induced by the expression of NaPi-1 in Xenopus oocytes. *The Journal of membrane biology,* 164**,** 71-77.

BRÔNE, B. & EGGERMONT, J. 2005. PDZ proteins retain and regulate membrane transporters in polarized epithelial cell membranes. *American Journal of Physiology-Cell Physiology,* 288**,** C20-C29.

BROWN, G., OTERO, L., LEGRIS, M. & BROWN, R. 1994. Pyruvate dehydrogenase deficiency. *Journal of Medical Genetics,* 31**,** 875-879.

BRUMBY, A. M. & RICHARDSON, H. E. 2005. Using Drosophila melanogaster to map human cancer pathways. *Nature Reviews Cancer,* 5**,** 626-639.

BUSCH, A. E., SCHUSTER, A., WALDEGGER, S., WAGNER, C. A., ZEMPEL, G., BROER, S., BIBER, J., MURER, H. & LANG, F. 1996. Expression of a renal type I sodium/phosphate transporter (NaPi-1) induces a conductance in Xenopus oocytes permeable for organic and inorganic anions. *Proceedings of the National Academy of Sciences,* 93**,** 5347-5351.

BUSHINSKY, D. A., ASPLIN, J. R., GRYNPAS, M. D., EVAN, A. P., PARKER, W. R., ALEXANDER, K. M. & COE, F. L. 2002. Calcium oxalate stone formation in genetic hypercalciuric stone-forming rats. *Kidney international,* 61**,** 975-987.

BUSHINSKY, D. A. & FAVUS, M. 1988. Mechanism of hypercalciuria in genetic hypercalciuric rats. Inherited defect in intestinal calcium transport. *The Journal of clinical investigation,* 82**,** 1585-1591.

BUSHINSKY, D. A., GRYNPAS, M. D., NILSSON, E. L., NAKAGAWA, Y. & COE, F. L. 1995. Stone formation in genetic hypercalciuric rats. *Kidney international,* 48**,** 1705-1713.

BUSHINSKY, D. A., PARKER, W. R. & ASPLIN, J. R. 2000. Calcium phosphate supersaturation regulates stone formation in genetic hypercalciuric stone-forming rats. *Kidney international,* 57**,** 550-560.

CABRERO, P., TERHZAZ, S., ROMERO, M. F., DAVIES, S. A., BLUMENTHAL, E. M. & DOW, J. A. 2014. Chloride channels in stellate cells are essential for uniquely high secretion rates in neuropeptide-stimulated Drosophila diuresis. *Proceedings of the National Academy of Sciences,* 111**,** 14301-14306.

CAMPBELL, M. F., WEIN, A. J. & KAVOUSSI, L. R. 2007. *Campbell-Walsh urology: editor-in-chief, Alan J. Wein; editors, Louis R. Kavoussi...[et al.].* *Urology,* 14:148–53.

CAPUANO, P., RADANOVIC, T., WAGNER, C. A., BACIC, D., KATO, S., UCHIYAMA, Y., ST.-ARNOUD, R., MURER, H. & BIBER, J. R. 2005. Intestinal and renal adaptation to a low-Pi diet of type II NaPi cotransporters in vitamin D receptor-and 1αOHase-deficient mice. *American Journal of Physiology-Cell Physiology,* 288**,** C429-C434.

CARPENTER, T. O. 2018. Primary disorders of phosphate metabolism. *Endotext [Internet]*. MDText. com, Inc; 2000-. 2018 Oct 23.

CENTONZE, M., SAPONARO, C. & MANGIA, A. 2018. NHERF1 Between Promises and Hopes: Overview on Cancer and Prospective Openings. *Translational oncology,* 11, 374-390.

CHAU, H., EL-MAADAWY, S., MCKEE, M. D. & TENENHOUSE, H. S. 2003. Renal calcification in mice homozygous for the disrupted type IIa Na/Pi cotransporter gene Npt2. *Journal of Bone and Mineral Research,* 18, 644-657.

CHAUDHARY, A., SINGLA, S. & TANDON, C. 2010. In vitro evaluation of Terminalia arjuna on calcium phosphate and calcium oxalate crystallization. *Indian journal of pharmaceutical sciences,* 72, 340-345.

CHAUHAN, C., JOSHI, M. & VAIDYA, A. 2009. Growth inhibition of struvite crystals in the presence of herbal extract Commiphora wightii. *Journal of Materials Science: Materials in Medicine,* 20, S85-92.

CHEN, H. & FIRESTEIN, B. L. 2007. RhoA regulates dendrite branching in hippocampal neurons by decreasing cypin protein levels. *Journal of Neuroscience,* 27, 8378-8386.

CHEN, M., LUCAS, K. G., AKUM, B. F., BALASINGAM, G., STAWICKI, T. M., PROVOST, J. M., RIEFLER, G. M., JORNSTEN, R. J. & FIRESTEIN, B. L. 2005. A novel role for snapin in dendrite patterning: interaction with cypin. *Molecular biology of the cell,* 16, 5103-5114.

CHEN, Y.-H., LIU, H.-P., CHEN, H.-Y., TSAI, F.-J., CHANG, C.-H., LEE, Y.-J., LIN, W.-Y. & CHEN, W.-C. 2011. Ethylene glycol induces calcium oxalate crystal deposition in Malpighian tubules: a Drosophila model for nephrolithiasis/urolithiasis. Kidney international, 80, 369-377.

CHI, T., KIM, M. S., LANG, S., BOSE, N., KAHN, A., FLECHNER, L., BLASCHKO, S. D., ZEE, T., MUTELIEFU, G. & BOND, N. 2015. A Drosophila model identifies a critical role for zinc in mineralization for kidney stone disease. *PloS one,* 10, e0124150.

CHIAL, H. 2008. Rare genetic disorders: learning about genetic disease through gene mapping, SNPs, and microarray data. *Nature education,* 1, 192.

CHIEN, S., REITER, L. T., BIER, E. & GRIBSKOV, M. 2002. Homophila: human disease gene cognates in Drosophila. *Nucleic acids research,* 30, 149-151.

CHINTAPALLI, V. R., TERHZAZ, S., WANG, J., AL BRATTY, M., WATSON, D. G., HERZYK, P., DAVIES, S. A. & DOW, J. A. 2012b. Functional correlates of positional and gender-specific renal asymmetry in Drosophila. *PloS one,* 7, e32577-e32577.

CHINTAPALLI, V. R., WANG, J. & DOW, J. A. 2007. Using FlyAtlas to identify better Drosophila melanogaster models of human disease. *Nature genetics,* 39, 715-720.

CHUNG, V. Y., KONIETZNY, R., CHARLES, P., KESSLER, B., FISCHER, R. & TURNEY, B. W. 2016. Proteomic changes in response to crystal formation in Drosophila Malpighian tubules. *Fly,* 10, 91-100.

CLARK, W. F., SONTROP, J. M., HUANG, S.-H., MOIST, L., BOUBY, N. & BANKIR, L. 2016. Hydration and chronic kidney disease progression: a critical review of the evidence. *American journal of nephrology,* 43, 281-292.

CLINE, T. W. 1978. Two closely linked mutations in Drosophila melanogaster that are lethal to opposite sexes and interact with daughterless. *Genetics,* 90, 683-697.

COCHAT, P., DELORAINE, A., ROTILY, M., OLIVE, F., LIPONSKI, I., DERIES, N., NÉPHROLOGIE, S. D. & PÉDIATRIQUE, T. S. D. N. 1995b. Epidemiology of

primary hyperoxaluria type 1. *Nephrology Dialysis Transplantation,* 10**,** 3-7.
COCHAT, P., PICHAULT, V., BACCHETTA, J., DUBOURG, L., SABOT, J.-F., SABAN, C., DAUDON, M. & LIUTKUS, A. 2010. Nephrolithiasis related to inborn metabolic diseases. *Pediatric Nephrology,* 25**,** 415-424.
COE, F. L. & COE, F. 1983. Uric acid and calcium oxalate nephrolithiasis. *Kidney international,* 24**,** 392-403.
COE, F. L., EVAN, A. & WORCESTER, E. 2005. Kidney stone disease. *The Journal of clinical investigation,* 115**,** 2598-2608.
COE, F. L., PARKS, J. H. & ASPLIN, J. R. 1992. The pathogenesis and treatment of kidney stones. *New England Journal of Medicine,* 327**,** 1141-1152.
COE, F. L., WORCESTER, E. M. & EVAN, A. P. 2016. Idiopathic hypercalciuria and formation of calcium renal stones. *Nat Rev Nephrol,* 12**,** 519-33.
COLLINS, J. F., BAI, L. & GHISHAN, F. K. 2004. The SLC20 family of proteins: dual functions as sodium-phosphate cotransporters and viral receptors. *Pflügers Archiv,* 447**,** 647-652.
CORTESE, M. S., UVERSKY, V. N. & DUNKER, A. K. 2008. Intrinsic disorder in scaffold proteins: getting more from less. *Progress in biophysics and molecular biology,* 98**,** 85-106.
CRAMER, J. S. & FORREST, K. 2006. Renal lithiasis: addressing the risks of austere desert deployments. *Aviation, space, and environmental medicine,* 77**,** 649-653.
CROCKER, A. & SEHGAL, A. 2008. Octopamine regulates sleep in Drosophila through protein kinase A-dependent mechanisms. *Journal of Neuroscience,* 28**,** 9377-9385.
CROOK, M. & SWAMINATHAN, R. 1996. Disorders of plasma phosphate and indications for its measurement. *Annals of clinical biochemistry,* 33**,** 376-396.
CROUTHAMEL, M. H., LAU, W. L., LEAF, E. M., CHAVKIN, N. W., WALLINGFORD, M. C., PETERSON, D. F., LI, X., LIU, Y., CHIN, M. T., LEVI, M. & GIACHELLI, C. M. 2013. Sodium-dependent phosphate cotransporters and phosphate-induced calcification of vascular smooth muscle cells: redundant roles for PiT-1 and PiT-2. *Arteriosclerosis, thrombosis, and vascular biology,* 33**,** 2625-2632.
CUNNINGHAM, R., BRAZIE, M., KANUMURU, S., XIAOFEI, E., BISWAS, R., WANG, F., STEPLOCK, D., WADE, J. B., ANZAI, N. & ENDOU, H. 2007. Sodium-hydrogen exchanger regulatory factor-1 interacts with mouse urate transporter 1 to regulate renal proximal tubule uric acid transport. *Journal of the American Society of Nephrology,* 18**,** 1419-1425.
CURHAN, G. C. 2007. Epidemiology of stone disease. *Urologic Clinics of North America,* 34**,** 287-293.
CURHAN, G. C., WILLETT, W. C., RIMM, E. B. & STAMPFER, M. J. 1997. Family history and risk of kidney stones. *Journal of the American Society of Nephrology,* 8**,** 1568-1573.
CURTHOYS, N. P. & MOE, O. W. 2014a. Proximal tubule function and response to acidosis. *Clinical journal of the American Society of Nephrology : CJASN,* 9**,** 1627-1638.
CURTHOYS, N. P. & MOE, O. W. 2014b. Proximal tubule function and response to acidosis. *Clinical Journal of the American Society of Nephrology,* 9**,** 1627-1638.
CURTIS, A. R., FEY, C., MORRIS, C. M., BINDOFF, L. A., INCE, P. G., CHINNERY, P. F., COULTHARD, A., JACKSON, M. J., JACKSON, A. P. & MCHALE, D. P.

2001. Mutation in the gene encoding ferritin light polypeptide causes dominant adult-onset basal ganglia disease. *Nature genetics,* 28**,** 350-354.

CUSTER, M., LOTSCHER, M., BIBER, J., MURER, H. & KAISSLING, B. 1994. Expression of Na-P (i) cotransport in rat kidney: localization by RT-PCR and immunohistochemistry. *American Journal of Physiology-Renal Physiology,* 266**,** F767-F774.

DAL MORO, F., MANCINI, M., TAVOLINI, I. M., DE MARCO, V. & BASSI, P. 2005. Cellular and molecular gateways to urolithiasis: a new insight. *Urologia internationalis,* 74**,** 193-197.

DANPURE, C. J. 2005. Molecular etiology of primary hyperoxaluria type 1: new directions for treatment. *American journal of nephrology,* 25**,** 303-310.

DAUDON, M., BAZIN, D. & LETAVERNIER, E. 2015. Randall's plaque as the origin of calcium oxalate kidney stones. *Urolithiasis,* 43**,** 5-11.

DAUDON, M., COHEN-SOLAL, F., BARBEY, F., GAGNADOUX, M.-F., KNEBELMANN, B. & JUNGERS, P. 2003. Cystine crystal volume determination: a useful tool in the management of cystinuric patients. *Urological research,* 31**,** 207-211.

DAUDON, M., FROCHOT, V., BAZIN, D. & JUNGERS, P. 2018. Drug-induced kidney stones and crystalline nephropathy: pathophysiology, prevention and treatment. *Drugs,* 78**,** 163-201.

DAUDON, M. & JUNGERS, P. 2004. Clinical value of crystalluria and quantitative morphoconstitutional analysis of urinary calculi. *Nephron Physiology,* 98**,** p31-p36.

DAVIES, S.-A. & DOW, J. A. 2009. Modulation of epithelial innate immunity by autocrine production of nitric oxide. *General and comparative endocrinology,* 162**,** 113-121.

DAVIES, S. A. & TERHZAZ, S. 2009. Organellar calcium signalling mechanisms in Drosophila epithelial function. *Journal of Experimental Biology,* 212**,** 387-400.

DAWSON, C. H. & TOMSON, C. R. 2012. Kidney stone disease: pathophysiology, investigation and medical treatment. *Clinical Medicine,* 12**,** 467-471.

DAWSON, P. A., RUSSELL, C. S., LEE, S., MCLEAY, S. C., VAN DONGEN, J. M., COWLEY, D. M., CLARKE, L. A. & MARKOVICH, D. 2010. Urolithiasis and hepatotoxicity are linked to the anion transporter Sat1 in mice. *The Journal of clinical investigation,* 120**,** 706-712.

DAY, J. P., WAN, S., ALLAN, A. K., KEAN, L., DAVIES, S. A., GRAY, J. V. & DOW, J. A. 2008. Identification of two partners from the bacterial Kef exchanger family for the apical plasma membrane V-ATPase of Metazoa. *Journal of cell science,* 121**,** 2612-2619.

DEHGHAN, A., KÖTTGEN, A., YANG, Q., HWANG, S.-J., KAO, W. L., RIVADENEIRA, F., BOERWINKLE, E., LEVY, D., HOFMAN, A. & ASTOR, B. C. 2008. Association of three genetic loci with uric acid concentration and risk of gout: a genome-wide association study. *The Lancet,* 372**,** 1953-1961.

DENSTEDT, J. D. & FULLER, A. 2012. Epidemiology of stone disease in North America. *Urolithiasis.* 5(4), 205–214.

DENT, C. & PHILPOT, G. 1954. Xanthinuria: An inborn error (or deviation) of metabolism. *The Lancet,* 263**,** 182-185.

DI PIETRO, V., PERRUZZA, I., AMORINI, A. M., BALDUCCI, A., CECCARELLI, L., LAZZARINO, G., BARSOTTI, P., GIARDINA, B. & TAVAZZI, B. 2007. Clinical, biochemical and molecular diagnosis of a compound homozygote for the

254 bp deletion–8 bp insertion of the APRT gene suffering from severe renal failure. *Clinical biochemistry,* 40**,** 73-80.

DIETZL, G., CHEN, D., SCHNORRER, F., SU, K.-C., BARINOVA, Y., FELLNER, M., GASSER, B., KINSEY, K., OPPEL, S. & SCHEIBLAUER, S. 2007. A genome-wide transgenic RNAi library for conditional gene inactivation in Drosophila. *Nature,* 448**,** 151-156.

DIMASI, J. A., HANSEN, R. W. & GRABOWSKI, H. G. 2003. The price of innovation: new estimates of drug development costs. *Journal of health economics,* 22**,** 151-185.

DIRKS, J., REMUZZI, G., HORTON, S., SCHIEPPATI, A. & RIZVI, S. A. H. 2006. Diseases of the kidney and the urinary system. *Disease control priorities in developing countries,* 2**,** 695-706.

DONOWITZ, M., TSE, C. M. & FUSTER, D. 2013. SLC9/NHE gene family, a plasma membrane and organellar family of Na+/H+ exchangers. *Molecular aspects of medicine,* 34**,** 236-251.

DOW, J., DAVIES, S. A., GUO, Y., GRAHAM, S., FINBOW, M. E. & KAISER, K. 1997. Molecular genetic analysis of V-ATPase function in Drosophila melanogaster. *Journal of Experimental Biology,* 200**,** 237-245.

DOW, J. A. & DAVIES, S. A. 2001. The Drosophila melanogaster malpighian tubule. *Advances in Insect Physiology,* 28**,** 1-83.

DOW, J. A. & DAVIES, S. A. 2003. Integrative physiology and functional genomics of epithelial function in a genetic model organism. *Physiological Reviews,* 83**,** 687-729.

DOW, J. A., MADDRELL, S. H., GORTZ, A., SKAER, N. J., BROGAN, S. & KAISER, K. 1994. The malpighian tubules of Drosophila melanogaster: a novel phenotype for studies of fluid secretion and its control. *J Exp Biol,* 197**,** 421-8.

DOW, J. A. & ROMERO, M. F. 2010. Drosophila provides rapid modeling of renal development, function, and disease. *American Journal of Physiology-Renal Physiology,* 299**,** F1237-F1244.

DOW, J. A. T. 2012. Excretion and salt and water regulation. *In:* SIMPSON, S. J. & DOUGLAS, A. E. (eds.) *The insects: structure & function / R.F. Chapman.* Cambridge, UK: Cambridge University Press, 2012, 546-587.

DRYSDALE, R. A., CONSORTIUM, F., CROSBY, M. A. & CONSORTIUM, F. 2005. FlyBase: genes and gene models. *Nucleic acids research,* 33**,** D390-D395.

DU TOIT, P., VAN ASWEGEN, C., STEINMANN, C., KLUE, L. & DU PLESSIS, D. 1997. Does urokinase play a role in renal stone formation? *Medical hypotheses,* 49**,** 57-59.

DUBE, K., MCDONALD, D. & O'DONNELL, M. 2000. Calcium transport by isolated anterior and posterior Malpighian tubules of Drosophila melanogaster: roles of sequestration and secretion. *Journal of insect physiology,* 46**,** 1449-1460.

DURSUN, M., OTUNCTEMUR, A. & OZBEK, E. 2015. Kidney stones and ceftriaxone. *European Medical Journal of Urology,* 3**,** 68-74.

EDVARDSSON, V. O., INDRIDASON, O. S., HARALDSSON, G., KJARTANSSON, O. & PALSSON, R. 2013. Temporal trends in the incidence of kidney stone disease. *Kidney international,* 83**,** 146-152.

EICHENLAUB-RITTER, U. 1996. Parental age-related aneuploidy in human germ cells and offspring: A story of past and present. *Environmental and molecular mutagenesis,* 28**,** 211-236.

EL RIDI, R. & TALLIMA, H. 2017. Physiological functions and pathogenic potential of uric acid: A review. *Journal of advanced research,* 8**,** 487-493.

ENOMOTO, A., KIMURA, H., CHAIROUNGDUA, A., SHIGETA, Y., JUTABHA, P., CHA, S. H., HOSOYAMADA, M., TAKEDA, M., SEKINE, T. & IGARASHI, T. 2002. Molecular identification of a renal urate–anion exchanger that regulates blood urate levels. *Nature,* 417**,** 447-452.

ETTINGER, B., TANG, A., CITRON, J. T., LIVERMORE, B. & WILLIAMS, T. 1986. Randomized trial of allopurinol in the prevention of calcium oxalate calculi. *New England Journal of Medicine,* 315**,** 1386-1389.

EVAN, A., LINGEMAN, J., COE, F. & WORCESTER, E. 2006. Randall's plaque: pathogenesis and role in calcium oxalate nephrolithiasis. *Kidney international,* 69**,** 1313-1318.

EVAN, A. P. 2010. Physiopathology and etiology of stone formation in the kidney and the urinary tract. *Pediatric Nephrology,* 25**,** 831-841.

EVAN, A. P., LINGEMAN, J. E., COE, F. L., PARKS, J. H., BLEDSOE, S. B., SHAO, Y., SOMMER, A. J., PATERSON, R. F., KUO, R. L. & GRYNPAS, M. 2003. Randall's plaque of patients with nephrolithiasis begins in basement membranes of thin loops of Henle. *The Journal of clinical investigation,* 111**,** 607-616.

EVAN, A. P., LINGEMAN, J. E., WORCESTER, E. M., SOMMER, A. J., PHILLIPS, C. L., WILLIAMS, J. C. & COE, F. L. 2014. Contrasting histopathology and crystal deposits in kidneys of idiopathic stone formers who produce hydroxy apatite, brushite, or calcium oxalate stones. *Anatomical record (Hoboken, N.J. : 2007),* 297**,** 731-748.

EVAN, A. P., WORCESTER, E. M., COE, F. L., WILLIAMS, J. & LINGEMAN, J. E. 2015. Mechanisms of human kidney stone formation. *Urolithiasis,* 43**,** 19-32.

EVANS, J. M., ALLAN, A. K., DAVIES, S. A. & DOW, J. A. 2005. Sulphonylurea sensitivity and enriched expression implicate inward rectifier K+ channels in Drosophila melanogaster renal function. *Journal of Experimental Biology,* 208**,** 3771-3783.

EVANS, K. & COSTABILE, R. A. 2005. Time to development of symptomatic urinary calculi in a high risk environment. *The Journal of urology,* 173**,** 858-861.

FAKHERI, R. J. & GOLDFARB, D. S. 2011. Ambient temperature as a contributor to kidney stone formation: implications of global warming. *Kidney international,* 79**,** 1178-1185.

FELIUBADALÓ, L., ARBONÉS, M. L., MAÑAS, S., CHILLARÓN, J., VISA, J., RODÉS, M., ROUSAUD, F., ZORZANO, A., PALACÍN, M. & NUNES, V. 2003. Slc7a9-deficient mice develop cystinuria non-I and cystine urolithiasis. *Human molecular genetics,* 12**,** 2097-2108.

FERNÁNDEZ-BOO, S., VILLALBA, A. & CAO, A. 2016. Protein expression profiling in haemocytes and plasma of the M anila clam R uditapes philippinarum in response to infection with P erkinsus olseni. *Journal of fish diseases,* 39**,** 1369-1385.

FERRARO, P. M., MANDEL, E. I., CURHAN, G. C., GAMBARO, G. & TAYLOR, E. N. 2016. Dietary Protein and Potassium, Diet–Dependent Net Acid Load, and Risk of Incident Kidney Stones. *Clinical Journal of the American Society of Nephrology***,** 11(10),1834-1844.

FINK, D. A., SOURS, R. E. & SWIFT, J. A. 2003. Modulated uric acid crystal growth in the presence of acridine dyes. *Chemistry of materials,* 15**,** 2718-2723.

FINLAYSON, B. 1978. Physicochemical aspects of urolithiasis. *Kidney international,* 13**,** 344-360.

FINLAYSON, B. & SMITH, A. 1974. Stability of first dissociable proton of uric acid. *Journal of Chemical and Engineering Data,* 19, 94-97.

FISANG, C., ANDING, R., MÜLLER, S. C., LATZ, S. & LAUBE, N. 2015. Urolithiasis—an interdisciplinary diagnostic, therapeutic and secondary preventive challenge. *Deutsches Ärzteblatt International,* 112, 83-91.

FISCHER, A. 2007. Human primary immunodeficiency diseases. *Immunity,* 27, 835-845.

FORSTER, I. C., HERNANDO, N., BIBER, J. & MURER, H. 2013. Phosphate transporters of the SLC20 and SLC34 families. *Molecular aspects of medicine,* 34, 386-395.

FOUASSIER, L., DUAN, C., FERANCHAK, A. P., YUN, C. C., SUTHERLAND, E., SIMON, F., FITZ, J. G. & DOCTOR, R. B. 2001. Ezrin-radixin-moesin–binding phosphoprotein 50 is expressed at the apical membrane of rat liver epithelia. *Hepatology,* 33, 166-176.

FRANK, M., DE VRIES, A., ATSMON, A., LAZEBNIK, J. & KOCHWA, S. 1959. Epidemiological investigation of urolithiasis in Israel. *Journal of Urology,* 81, 497-505.

FUJITA, K. 1979. Epidemiology of Urinary Stone Colic 1606595. *Eur. Urol,* 5, 26-28.

GAO, Y., GILLEN, C. M. & WHEATLY, M. G. 2006. Molecular characterization of the sarcoplasmic calcium-binding protein (SCP) from crayfish Procambarus clarkii. *Comparative Biochemistry and Physiology Part B: Biochemistry and Molecular Biology,* 144, 478-487.

GARROD, A. E. & HARRIS, H. 1909. Inborn errors of metabolism.*American Journal of Obsetrics and Gynecology*, 90, 1024-1034.

GEES, M., COLSOUL, B. & NILIUS, B. 2010. The role of transient receptor potential cation channels in Ca2+ signaling. *Cold Spring Harbor perspectives in biology,* 2 (10), a003962.

GERSHOFF, S. & ANDRUS, S. 1961. Dietary magnesium, calcium, and vitamin B6 and experimental nephropathies in rats: calcium oxalate calculi, apatite nephrocalcinosis. *The Journal of Nutrition,* 73, 308-316.

GIANFRANCESCO, F., ESPOSITO, T., OMBRA, M. N., FORABOSCO, P., MANINCHEDDA, G., FATTORINI, M., CASULA, S., VACCARGIU, S., CASU, G. & CARDIA, F. 2003. Identification of a novel gene and a common variant associated with uric acid nephrolithiasis in a Sardinian genetic isolate. *The American Journal of Human Genetics,* 72, 1479-1491.

GIANNAKOU, M. E. & DOW, J. A. 2001. Characterization of the Drosophila melanogaster alkali-metal/proton exchanger (NHE) gene family. *Journal of Experimental Biology,* 204, 3703-3716.

GIANNOSSI, M. L. & SUMMA, V. 2012. A review of pathological biomineral analysis techniques and classification schemes. *An introduction to the study of mineralogy*. 123-146.

GIRAL, H., CRANSTON, D., LANZANO, L., CALDAS, Y., SUTHERLAND, E., RACHELSON, J., DOBRINSKIKH, E., WEINMAN, E. J., DOCTOR, R. B. & GRATTON, E. 2012. NHE3 regulatory factor 1 (NHERF1) modulates intestinal sodium-dependent phosphate transporter (NaPi-2b) expression in apical microvilli. *Journal of Biological Chemistry,* 287, 35047-35056.

GISLER, S. M., KITTANAKOM, S., FUSTER, D., WONG, V., BERTIC, M., RADANOVIC, T., HALL, R. A., MURER, H., BIBER, J. & MARKOVICH, D. 2008. Monitoring protein-protein interactions between the mammalian integral membrane transporters and PDZ-interacting partners using a modified split-ubiquitin

membrane yeast two-hybrid system. *Molecular & cellular proteomics,* 7, 1362-1377.
GOLDFARB, D. S. 2014. The search for monogenic causes of kidney stones. Am Soc Nephrol, 26(3), 507-510.
GRIFFIN, D. 2004. A review of the heritability of idiopathic nephrolithiasis. *Journal of clinical pathology,* 57, 793-796.
GRIFFITH, D. P. 1978. Struvite stones. *Kidney international,* 13, 372-382.
GRILLO-HILL, B. K., CHOI, C., JIMENEZ-VIDAL, M. & BARBER, D. L. 2015. Increased H+ efflux is sufficient to induce dysplasia and necessary for viability with oncogene expression. *Elife,* 4, e03270.
HALBERG, K. A., TERHZAZ, S., CABRERO, P., DAVIES, S. A. & DOW, J. A. 2015. Tracing the evolutionary origins of insect renal function. *Nature communications,* 6, 6800.
HALBRITTER, J., BAUM, M., HYNES, A. M., RICE, S. J., THWAITES, D. T., GUCEV, Z. S., FISHER, B., SPANEAS, L., PORATH, J. D. & BRAUN, D. A. 2015. Fourteen monogenic genes account for 15% of nephrolithiasis/nephrocalcinosis. *Journal of the American Society of Nephrology,* 26, 543-551.
HALL, V. M., COX, K. A., SOURS, R. E. & SWIFT, J. A. 2016. Urochrome Pigment in Uric Acid Crystals. *Chemistry of Materials,* 28, 3862-3869.
HAMMERMAN, M. R. 1986. Phosphate transport across renal proximal tubular cell membranes. *Am J Physiol,* 251, F385-98.
HAN, H., SEGAL, A. M., SEIFTER, J. L. & DWYER, J. T. 2015. Nutritional Management of Kidney Stones (Nephrolithiasis). *Clinical nutrition research,* 4, 137-152.
HANSEN, N. M., FELIX, R., BISAZ, S. & FLEISCH, H. 1976. Aggregation of hydroxyapatite crystals. *Biochimica et Biophysica Acta (BBA)-General Subjects,* 451, 549-559.
HANZEL, D., REGGIO, H., BRETSCHER, A., FORTE, J. & MANGEAT, P. 1991. The secretion-stimulated 80K phosphoprotein of parietal cells is ezrin, and has properties of a membrane cytoskeletal linker in the induced apical microvilli. *The EMBO Journal,* 10, 2363-2373.
HAYES, J. M. 2015. An examination of the modifiable technical factors of ESWL on effective and efficient urinary stone fragmentation.
HEDIGER, M. A., JOHNSON, R. J., MIYAZAKI, H. & ENDOU, H. 2005. Molecular physiology of urate transport. *Physiology,* 20, 125-133.
HELPS, C., MURER, H. & MCGIVAN, J. 1995. Cloning, sequence analysis and expression of the cDNA encoding a sodium-dependent phosphate transporter from the bovine renal epithelial cell line NBL-1. *Eur J Biochem,* 228, 927-30.
HERMANN, A. & COX, J. A. 1995. Sarcoplasmic calcium-binding protein. *Comparative Biochemistry and Physiology Part B: Biochemistry and Molecular Biology,* 111, 337-345.
HESSE, A., BRÄNDLE, E., WILBERT, D., KÖHRMANN, K.-U. & ALKEN, P. 2003. Study on the prevalence and incidence of urolithiasis in Germany comparing the years 1979 vs. 2000. *European urology,* 44, 709-713.
HIRAO, M., SATO, N., KONDO, T., YONEMURA, S., MONDEN, M., SASAKI, T., TAKAI, Y. & TSUKITA, S. 1996. Regulation mechanism of ERM (ezrin/radixin/moesin) protein/plasma membrane association: possible involvement of phosphatidylinositol turnover and Rho-dependent signaling pathway. *The Journal of cell biology,* 135, 37-51.

HIRATA, T., CABRERO, P., BERKHOLZ, D. S., BONDESON, D. P., RITMAN, E. L., THOMPSON, J. R., DOW, J. A. & ROMERO, M. F. 2012. In vivo Drosophilia genetic model for calcium oxalate nephrolithiasis. *American Journal of Physiology-Renal Physiology,* 303**,** F1555-F1562.

HOAG, H. M., MARTEL, J., GAUTHIER, C. & TENENHOUSE, H. S. 1999. Effects of Npt2 gene ablation and low-phosphate diet on renal Na(+)/phosphate cotransport and cotransporter gene expression. *J Clin Invest,* 104**,** 679-86.

HOBANI, Y. H. 2012. *Metabolomic analyses of Drosophila models for human renal disease*. University of Glasgow.

HOE KIM, H., JO, M. K., KWAK, C., PARK, S. K., YOO, K.-Y., KANG, D. & LEE, C. 2002. Prevalence and epidemiologic characteristics of urolithiasis in Seoul, Korea. *Urology,* 59**,** 517-521.

HOENDEROP, J. G., VAN LEEUWEN, J. P., VAN DER EERDEN, B. C., KERSTEN, F. F., VAN DER KEMP, A. W., MERILLAT, A. M., WAARSING, J. H., ROSSIER, B. C., VALLON, V., HUMMLER, E. & BINDELS, R. J. 2003. Renal Ca2+ wasting, hyperabsorption, and reduced bone thickness in mice lacking TRPV5. *J Clin Invest,* 112**,** 1906-14.

HRUSKA, K. A., MATHEW, S., LUND, R., QIU, P. & PRATT, R. 2008. Hyperphosphatemia of chronic kidney disease. *Kidney international,* 74**,** 148-157.

HUBBARD, S. R. & TILL, J. H. 2000. Protein tyrosine kinase structure and function. *Annual review of biochemistry,* 69**,** 373-398.

HUGHES, S. C., FORMSTECHER, E. & FEHON, R. G. 2010. Sip1, the Drosophila orthologue of EBP50/NHERF1, functions with the sterile 20 family kinase Slik to regulate Moesin activity. *J Cell Sci,* 123**,** 1099-1107.

ICHIDA, K., AMAYA, Y., KAMATANI, N., NISHINO, T., HOSOYA, T. & SAKAI, O. 1997. Identification of two mutations in human xanthine dehydrogenase gene responsible for classical type I xanthinuria. *The Journal of clinical investigation,* 99**,** 2391-2397.

ICHIDA, K., IBRAHIM AYDIN, H., HOSOYAMADA, M., KALKANOGLU, H. S., DURSUN, A., OHNO, I., COSKUN, T., TOKATLI, A., SHIBASAKI, T. & HOSOYA, T. 2006. A Turkish case with molybdenum cofactor deficiency. *Nucleosides, Nucleotides and Nucleic Acids,* 25**,** 1087-1091.

ICHIDA, K., MATSUMURA, T., SAKUMA, R., HOSOYA, T. & NISHINO, T. 2001. Mutation of human molybdenum cofactor sulfurase gene is responsible for classical xanthinuria type II. *Biochemical and biophysical research communications,* 282**,** 1194-1200.

IHARADA, M., MIYAJI, T., FUJIMOTO, T., HIASA, M., ANZAI, N., OMOTE, H. & MORIYAMA, Y. 2010. Type 1 sodium dependent phosphate transporter (SLC17A1 protein) is a Cl--dependent urate exporter. *Journal of Biological Chemistry***,** jbc. M110. 122721.

IKURA, M., OSAWA, M. & AMES, J. B. 2002. The role of calcium-binding proteins in the control of transcription: structure to function. *Bioessays,* 24**,** 625-636.

JIANG, Z., ASPLIN, J. R., EVAN, A. P., RAJENDRAN, V. M., VELAZQUEZ, H., NOTTOLI, T. P., BINDER, H. J. & ARONSON, P. S. 2006. Calcium oxalate urolithiasis in mice lacking anion transporter Slc26a6. *Nature genetics,* 38**,** 474-478.

JIMENEZ-SANCHEZ, G., CHILDS, B. & VALLE, D. 2001. Human disease genes. *Nature,* 409**,** 853-855.

JOHNSON, C. M., WILSON, D. M., O'FALLON, W. M., MALEK, R. S. & KURLAND, L. T. 1979. Renal stone epidemiology: a 25-year study in Rochester, Minnesota. *Kidney international,* 16**,** 624-631.

JOHRI, N., COOPER, B., ROBERTSON, W., CHOONG, S., RICKARDS, D. & UNWIN, R. 2010. An update and practical guide to renal stone management. *Nephron Clinical Practice,* 116**,** c159-c171.

JOSEPH, K., PAREKH, B. B. & JOSHI, M. 2005. Inhibition of growth of urinary type calcium hydrogen phosphate dihydrate crystals by tartaric acid and tamarind. *Current Science,* 88**,** 1232-1238.

JOSEPH, S. & DAVID, W. R. 2001. Molecular cloning: a laboratory manual. *The Quarterly Review of Biology,* 76**,** 348-349.

JÜPPNER, H. 2007. Novel regulators of phosphate homeostasis and bone metabolism. *Therapeutic Apheresis and Dialysis,* 11**,** S3-S22.

JUUTI, M. & HEINONEN, O. P. 1979. Incidence of urolithiasis leading to hospitalization in Finland. *Acta medica scandinavica,* 206**,** 397-403.

KAMEL, K., CHEEMA-DHADLI, S., SHAFIEE, M., DAVIDS, M. & HALPERIN, M. 2005. Recurrent uric acid stones. *Qjm,* 98**,** 57-68.

KANBARA, A., HAKODA, M. & SEYAMA, I. 2010. Urine alkalization facilitates uric acid excretion. *Nutrition journal,* 9**,** 45-50.

KANEKO, I., YAMAMOTO, H., IKUTA, K., TATSUMI, S., SEGAWA, H. & MIYAMOTO, K.-I. 2017. Transcriptional Regulation of Sodium-Phosphate Cotransporter Gene Expression. *Molecular, Genetic, and Nutritional Aspects of Major and Trace Minerals*. Elsevier.

KARIM, Z., GÉRARD, B., BAKOUH, N., ALILI, R., LEROY, C., BECK, L., SILVE, C., PLANELLES, G., URENA-TORRES, P. & GRANDCHAMP, B. 2008. NHERF1 mutations and responsiveness of renal parathyroid hormone. *New England Journal of Medicine,* 359**,** 1128-1135.

KAUR, J. 2014. A comprehensive review on metabolic syndrome. *Cardiology research and practice,* 2014, 943162.

KAVANAUGH, M. P. & KABAT, D. 1996. Identification and characterization of a widely expressed phosphate transporter/retrovirus receptor family. *Kidney international,* 49**,** 959-963.

KENNERDELL, J. R. & CARTHEW, R. W. 2000. Heritable gene silencing in Drosophila using double-stranded RNA. *Nature biotechnology,* 18**,** 896.

KHAN, S. 1997. Animal models of kidney stone formation: an analysis. *World journal of urology,* 15**,** 236-243.

KHAN, S., FINLAYSON, B. & HACKETT, R. 1979. Histologic study of the early events in oxalate induced intranephronic calculosis. *Investigative urology,* 17**,** 199-202.

KHAN, S., GLENTON, P. & BYER, K. 2006. Modeling of hyperoxaluric calcium oxalate nephrolithiasis: experimental induction of hyperoxaluria by hydroxy-L-proline. *Kidney international,* 70**,** 914-923.

KHAN, S. R. 1991. Pathogenesis of oxalate urolithiasis: lessons from experimental studies with rats. *American journal of kidney diseases,* 17**,** 398-401.

KHAN, S. R. 2013. Animal models of calcium oxalate kidney stone formation. *Animal Models for the Study of Human Disease*. Elsevier, 2013, 483-498.

KHAN, S. R. 2014. Reactive oxygen species, inflammation and calcium oxalate nephrolithiasis. *Translational andrology and urology,* 3**,** 256-276.

KHAN, S. R., BYER, K. J., THAMILSELVAN, S., HACKETT, R. L., MCCORMACK, W. T., BENSON, N. A., VAUGHN, K. L. & ERDOS, G. W. 1999. Crystal-cell

interaction and apoptosis in oxalate-associated injury of renal epithelial cells. *Journal of the American Society of Nephrology: JASN,* 10, S457-63.
KHAN, S. R. & GLENTON, P. A. 2010. Experimental induction of calcium oxalate nephrolithiasis in mice. *The Journal of urology,* 184, 1189-1196.
KHAN, S. R. & HACKETT, R. L. 1987. Urolithogenesis of mixed foreign body stones. *The Journal of urology,* 138, 1321-1328.
KHAN, S. R., PEARLE, M. S., ROBERTSON, W. G., GAMBARO, G., CANALES, B. K., DOIZI, S., TRAXER, O. & TISELIUS, H.-G. 2016. Kidney stones. *Nature Reviews Disease Primers,* 2, 16008-16016.
KHAN, S. R., SHEVOCK, P. N. & HACKETT, R. L. 1992. Acute hyperoxaluria, renal injury and calcium oxalate urolithiasis. *The Journal of urology,* 147, 226-230.
KIBERD, B. 2006. The chronic kidney disease epidemic: stepping back and looking forward. *Journal of the American Society of Nephrology,* 17, 2967-2973.
KIM, J., PARK, S. I., AHN, C., KIM, H. & YIM, J. 2009. Guanine deaminase functions as dihydropterin deaminase in the biosynthesis of aurodrosopterin, a minor red eye pigment of Drosophila. *Journal of Biological Chemistry,* 284, 23426-23435.
KNAUF, F. & PREISIG, P. A. 2011. Drosophila: a fruitful model for calcium oxalate nephrolithiasis&quest. *Kidney international,* 80, 327-329.
KNOLL, T. 2010. Epidemiology, pathogenesis, and pathophysiology of urolithiasis. *European Urology Supplements,* 9, 802-806.
KNOLL, T., SCHUBERT, A. B., FAHLENKAMP, D., LEUSMANN, D. B., WENDT-NORDAHL, G. & SCHUBERT, G. 2011. Urolithiasis through the ages: data on more than 200,000 urinary stone analyses. *The Journal of urology,* 185, 1304-1311.
KNORR, B. A., LIPKOWITZ, M., POTTER, B., MASUR, S. & ABRAMSON, R. 1994. Isolation and immunolocalization of a rat renal cortical membrane urate transporter. *Journal of Biological Chemistry,* 269, 6759-6764.
KOK, D. J. & KHAN, S. R. 1994. Calcium oxalate nephrolithiasis, a free or fixed particle disease. *Kidney international,* 46, 847-854.
KOVACS, C. 2000. Calcium and Phosphate Metabolism and Related Disorders During Pregnancy and Lactation, *Endotext,* 2000 South Dartmouth (MA): MDText.com, Inc..
KOVSHILOVSKAYA, B., CHI, T., MILLER, J. & STOLLER, M. L. 2012. Systemic implications of urinary stone disease. *Translational andrology and urology,* 1, 89-96.
KRAMBECK, A. E., LIESKE, J. C., LI, X., BERGSTRALH, E. J., MELTON III, L. J. & RULE, A. D. 2013. Effect of age on the clinical presentation of incident symptomatic urolithiasis in the general population. *The Journal of urology,* 189, 158-164.
KREBS, E. G. & BEAVO, J. A. 1979. Phosphorylation-dephosphorylation of enzymes. *Annual review of biochemistry,* 48, 923-959.
KREIMANN, E., MORALES, F., DE ORBETA-CRUZ, J., TAKAHASHI, Y., ADAMS, H., LIU, T., MCCREA, P. & GEORGESCU, M. 2007. Cortical stabilization of ß-catenin contributes to NHERF1/EBP50 tumor suppressor function. *Oncogene,* 26, 5290-5299.
KRIEGER, N. S., STATHOPOULOS, V. M. & BUSHINSKY, D. A. 1996. Increased sensitivity to 1, 25 (OH) 2D3 in bone from genetic hypercalciuric rats. *American Journal of Physiology-Cell Physiology,* 271, C130-C135.
KUZMITS, R., SEYFRIED, H., WOLF, A. & MÜLLER, M. 1980. Evaluation of serum guanase in hepatic diseases. *Enzyme,* 25, 148-152.

LAGE, M. D., PITTMAN, A. M., RONCADOR, A., CELLINI, B. & TUCKER, C. L. 2014. Allele-specific characterization of alanine: glyoxylate aminotransferase variants associated with primary hyperoxaluria. *PLoS One,* 9**,** e94338.

LANCINA, J. M., NOVÁS, S. C., RODRÍGUEZ-RIVERA, J. G., RUIBAL, M. M., BLANCO, A. D., FERNÁNDEZ, E. R., BARBAGELATA, A. L. & GONZÁLEZ, M. M. 2004. Age of onset of urolithiasis: relation to clinical and metabolic risk factors. *Archivos espanoles de urologia,* 57**,** 119-125.

LANCINA MARTIN, J. A., NOVAS CASTRO, S., RODRIGUEZ-RIVERA GARCIA, J., RUIBAL MOLDES, M., BLANCO DIEZ, A., FERNANDEZ ROSADO, E., BARBAGELATA LOPEZ, A. & GONZALEZ MARTIN, M. 2004. [Age of onset of urolithiasis: relation to clinical and metabolic risk factors]. *Arch Esp Urol,* 57**,** 119-25.

LANE, A. N. & FAN, T. W.-M. 2015. Regulation of mammalian nucleotide metabolism and biosynthesis. *Nucleic acids research,* 43**,** 2466-2485.

LAROSA, C., MCMULLEN, L., BAKDASH, S., ELLIS, D., KRISHNAMURTI, L., WU, H.-Y. & MORITZ, M. L. 2007. Acute renal failure from xanthine nephropathy during management of acute leukemia. *Pediatric Nephrology,* 22**,** 132-135.

LE DAI, J., WANG, L., SAHIN, A. A., BROEMELING, L. D., SCHUTTE, M. & PAN, Y. 2004. NHERF (Na+/H+ exchanger regulatory factor) gene mutations in human breast cancer. *Oncogene,* 23**,** 8681-8687.

LEADER, D. P., KRAUSE, S. A., PANDIT, A., DAVIES, S. A. & DOW, J. A. T. 2017. FlyAtlas 2: a new version of the Drosophila melanogaster expression atlas with RNA-Seq, miRNA-Seq and sex-specific data. *Nucleic acids research,* 46**,** D809-D815.

LEAL-PINTO, E., COHEN, B. E., LIPKOWITZ, M. S. & ABRAMSON, R. G. 2002. Functional analysis and molecular model of the human urate transporter/channel, hUAT. *American Journal of Physiology-Renal Physiology,* 283**,** F150-F163.

LEDERER, E. & MIYAMOTO, K.-I. 2012. Clinical consequences of mutations in sodium phosphate cotransporters. *Clinical Journal of the American Society of Nephrology***,** CJN. 09090911, 7(7), 1179-87.

LEI, Y., SONG, B., SAAKES, M., VAN DER WEIJDEN, R. D. & BUISMAN, C. J. N. 2018. Interaction of calcium, phosphorus and natural organic matter in electrochemical recovery of phosphate. *Water Res,* 142**,** 10-17.

LEMAITRE, B., RONSSERAY, S. & COEN, D. 1993. Maternal repression of the P element promoter in the germline of Drosophila melanogaster: a model for the P cytotype. *Genetics,* 135**,** 149-160.

LETAVERNIER, E. & DAUDON, M. 2018. Vitamin D, Hypercalciuria and Kidney Stones. *Nutrients,* 10**,** 366-376.

LEVARTOVSKY, D., LAGZIEL, A., SPERLING, O., LIBERMAN, U., YARON, M., HOSOYA, T., ICHIDA, K. & PERETZ, H. 2000. XDH gene mutation is the underlying cause of classical xanthinuria: a second report. *Kidney international,* 57**,** 2215-2220.

LEVI, M. & BRUESEGEM, S. 2008. Renal phosphate–transporter regulatory proteins and nephrolithiasis. *The New England journal of medicine,* 359**,** 1171-1173.

LEWIS, E. B. 1978. A gene complex controlling segmentation in Drosophila. *Genes, Development and Cancer*. Springer, 276, 205-217.

LI, X.-Q., TEMBE, V., HORWITZ, G. M., BUSHINSKY, D. A. & FAVUS, M. J. 1993. Increased intestinal vitamin D receptor in genetic hypercalciuric rats. A

cause of intestinal calcium hyperabsorption. *The Journal of clinical investigation,* 91, 661-667.

LIAO, B.-Y. & ZHANG, J. 2008. Null mutations in human and mouse orthologs frequently result in different phenotypes. *Proceedings of the National Academy of Sciences,* 105, 6987-6992.

LIEBELT, A. G. 1998. Unique Features of Anatomy, Histology, and Ultrastructure Kidney, Mouse. *Urinary system.* Springer, 1998, 24-44.

LIEBMAN, M. & AL-WAHSH, I. A. 2011. Probiotics and other key determinants of dietary oxalate absorption. *Advances in Nutrition,* 2, 254-260.

LIEBOW, A., LI, X., RACIE, T., HETTINGER, J., BETTENCOURT, B. R., NAJAFIAN, N., HASLETT, P., FITZGERALD, K., HOLMES, R. P. & ERBE, D. 2017. An investigational RNAi therapeutic targeting glycolate oxidase reduces oxalate production in models of primary hyperoxaluria. *Journal of the American Society of Nephrology,* 28, 494-503.

LIESKE, J. C., RULE, A. D., KRAMBECK, A. E., WILLIAMS, J. C., BERGSTRALH, E. J., MEHTA, R. A. & MOYER, T. P. 2014. Stone composition as a function of age and sex. *Clinical journal of the American Society of Nephrology,* 9, 2141-2146.

LIESKE, J. C., SPARGO, B. H. & TOBACK, F. G. 1992. Endocytosis of calcium oxalate crystals and proliferation of renal tubular epithelial cells in a patient with type 1 primary hyperoxaluria. *The Journal of urology,* 148, 1517-1519.

LIN, K.-J., LIN, P.-H., CHU, S.-H., CHEN, H.-W., WANG, T.-M., CHIANG, Y.-J., LIU, K.-L. & WANG, H.-H. 2014. The impact of climate factors on the prevalence of urolithiasis in Northern Taiwan. *Biomedical journal,* 37, 24-30.

LING, G. V., RUBY, A. L., JOHNSON, D. L., THURMOND, M. & FRANTI, C. E. 1998. Renal calculi in dogs and cats: prevalence, mineral type, breed, age, and gender interrelationships (1981–1993). *Journal of veterinary internal medicine,* 12, 11-21.

LIPKOWITZ, M. S., LEAL-PINTO, E., COHEN, B. E. & ABRAMSON, R. G. 2002. Galectin 9 is the sugar-regulated urate transporter/channel UAT. *Glycoconjugate journal,* 19, 491-498.

LIPKOWITZ, M. S., LEAL-PINTO, E., RAPPOPORT, J. Z., NAJFELD, V. & ABRAMSON, R. G. 2001. Functional reconstitution, membrane targeting, genomic structure, and chromosomal localization of a human urate transporter. *The Journal of clinical investigation,* 107, 1103-1115.

LOFFING, J., LOFFING-CUENI, D., VALDERRABANO, V., KLAUSLI, L., HEBERT, S. C., ROSSIER, B. C., HOENDEROP, J. G., BINDELS, R. J. & KAISSLING, B. 2001. Distribution of transcellular calcium and sodium transport pathways along mouse distal nephron. *Am J Physiol Renal Physiol,* 281, F1021-7.

LÓPEZ, M. & HOPPE, B. 2010. History, epidemiology and regional diversities of urolithiasis. *Pediatric nephrology,* 25, 49-59.

LOTSARI, A., RAJASEKHARAN, A. K., HALVARSSON, M. & ANDERSSON, M. 2018. Transformation of amorphous calcium phosphate to bone-like apatite. *Nature communications,* 9, 4170-4170.

LÜNEBURG, N., LIEB, W., ZELLER, T., CHEN, M.-H., MAAS, R., CARTER, A. M., XANTHAKIS, V., GLAZER, N. L., SCHWEDHELM, E. & SESHADRI, S. 2014. Genome-Wide Association Study of l-Arginine and Dimethylarginines Reveals Novel Metabolic Pathway for Symmetric Dimethylarginine. *Circulation: Cardiovascular Genetics*, CIRCGENETICS. 7(6), 864-72.

LVOVS, D., FAVOROVA, O. & FAVOROV, A. 2012. A polygenic approach to the study of polygenic diseases. *Acta Naturae (англоязычная версия),* 4 (3):59-71.

MACPHERSON, M. R., POLLOCK, V. P., BRODERICK, K. E., KEAN, L., O'CONNELL, F. C., DOW, J. & DAVIES, S. A. 2001. Model organisms: new insights into ion channel and transporter function. L-type calcium channels regulate epithelial fluid transport in Drosophila melanogaster. *American journal of physiology. Cell physiology,* 280, C394-407.

MAGAGNIN, S., WERNER, A., MARKOVICH, D., SORRIBAS, V., STANGE, G., BIBER, J. & MURER, H. 1993. Expression cloning of human and rat renal cortex Na/Pi cotransport. *Proc Natl Acad Sci U S A,* 90, 5979-83.

MAHDIEH, N. & RABBANI, B. 2013. An overview of mutation detection methods in genetic disorders. *Iranian journal of pediatrics,* 23, 375-388.

MAIR, W., GOYMER, P., PLETCHER, S. D. & PARTRIDGE, L. 2003. Demography of dietary restriction and death in Drosophila. *Science,* 301, 1731-1733.

MAIUOLO, J., OPPEDISANO, F., GRATTERI, S., MUSCOLI, C. & MOLLACE, V. 2016. Regulation of uric acid metabolism and excretion. *International journal of cardiology,* 213, 8-14.

MANDEL, N. S. & MANDEL, G. S. 1989. Urinary tract stone disease in the United States veteran population. II. Geographical analysis of variations in composition. *The Journal of urology,* 142, 1516-1521.

MANOLI, I. & VENDITTI, C. 2016. Disorders of branched chain amino acid metabolism. *Translational science of rare diseases,* 1, 91-110.

MARSHALL, V., WHITE, R., SAINTONGE, M. C. D., TRESIDDER, G. & BLANDY, J. 1975. The natural history of renal and ureteric calculi. *British journal of urology,* 47, 117-124.

MARTILLO, M. A., NAZZAL, L. & CRITTENDEN, D. B. 2014. The crystallization of monosodium urate. *Current rheumatology reports,* 16, 400-410.

MARTIN, S. G., DOBI, K. C. & ST JOHNSTON, D. 2001. A rapid method to map mutations in Drosophila. *Genome biology,* 2,1-13.

MARTÍNEZ, P. R., COLORADO, S. R. & DEL BARCO, L. E. 2007. Urolitiasis y embarazo. *Ginecologia y Obstetricia de Mexico,* 75, 357-363.

MARTINS, A. M. 1999. Inborn errors of metabolism: a clinical overview. *Sao Paulo Medical Journal,* 117, 251-265.

MATTHIES, A., RAJAGOPALAN, K., MENDEL, R. R. & LEIMKÜHLER, S. 2004. Evidence for the physiological role of a rhodanese-like protein for the biosynthesis of the molybdenum cofactor in humans. *Proceedings of the National Academy of Sciences,* 101, 5946-5951.

MBOGE, M., MAHON, B., MCKENNA, R. & FROST, S. 2018. Carbonic anhydrases: role in pH control and cancer. *Metabolites,* 8, 19-50.

MCCLELLAN, J. & KING, M.-C. 2010. Genetic heterogeneity in human disease. *Cell,* 141, 210-217.

MCGETTIGAN, J., MCLENNAN, R., BRODERICK, K., KEAN, L., ALLAN, A., CABRERO, P., REGULSKI, M., POLLOCK, V., GOULD, G. & DAVIES, S.-A. 2005. Insect renal tubules constitute a cell-autonomous immune system that protects the organism against bacterial infection. *Insect biochemistry and molecular biology,* 35, 741-754.

MENETON, P., ICHIKAWA, I., INAGAMI, T. & SCHNERMANN, J. R. 2000. Renal physiology of the mouse. *American Journal of Physiology-Renal Physiology,* 278, F339-F351.

MENTE, A., D'A. HONEY, R. J., MCLAUGHLIN, J. R., BULL, S. B. & LOGAN, A. G. 2007. Ethnic differences in relative risk of idiopathic calcium nephrolithiasis in North America. *The Journal of urology,* 178, 1992-1997.

MERRIMAN, T. R. 2015. An update on the genetic architecture of hyperuricemia and gout. *Arthritis Res Ther,* 17, 98-121.

MICARONI, M. 2010. The role of calcium in intracellular trafficking. *Current molecular medicine,* 10, 763-773.

MILLER, J., CHI, T., KAPAHI, P., KAHN, A. J., KIM, M. S., HIRATA, T., ROMERO, M. F., DOW, J. A. & STOLLER, M. L. 2013. Drosophila melanogaster as an emerging translational model of human nephrolithiasis. *The Journal of urology,* 190, 1648-1656.

MITCHELL, K. J. 2012. What is complex about complex disorders? *Genome biology,* 13, 237-248.

MIYAJI, T., KAWASAKI, T., TOGAWA, N., OMOTE, H. & MORIYAMA, Y. 2013. Type 1 sodium-dependent phosphate transporter acts as a membrane potential-driven urate exporter. *Curr Mol Pharmacol,* 6, 88-94.

MIYAMOTO, K., TATSUMI, S., MORITA, K. & TAKEDA, E. 1998. Does the parathyroid'see'phosphate? *Nephrology, dialysis, transplantation: official publication of the European Dialysis and Transplant Association-European Renal Association,* 13, 2727-2729.

MO, L., HUANG, H.-Y., ZHU, X.-H., SHAPIRO, E., HASTY, D. L. & WU, X.-R. 2004. Tamm-Horsfall protein is a critical renal defense factor protecting against calcium oxalate crystal formation. *Kidney international,* 66, 1159-1166.

MO, L., LIAW, L., EVAN, A. P., SOMMER, A. J., LIESKE, J. C. & WU, X.-R. 2007. Renal calcinosis and stone formation in mice lacking osteopontin, Tamm-Horsfall protein, or both. *American Journal of Physiology-Renal Physiology,* 293, F1935-F1943.

MOE, O. W. 2006. Uric acid nephrolithiasis: proton titration of an essential molecule? *Current opinion in nephrology and hypertension,* 15, 366-373.

MONICO, C. G., WEINSTEIN, A., JIANG, Z., ROHLINGER, A. L., COGAL, A. G., BJORNSON, B. B., OLSON, J. B., BERGSTRALH, E. J., MILLINER, D. S. & ARONSON, P. S. 2008. Phenotypic and functional analysis of human SLC26A6 variants in patients with familial hyperoxaluria and calcium oxalate nephrolithiasis. *American Journal of Kidney Diseases,* 52, 1096-1103.

MORALES, F. C., TAKAHASHI, Y., KREIMANN, E. L. & GEORGESCU, M.-M. 2004. Ezrin–radixin–moesin (ERM)-binding phosphoprotein 50 organizes ERM proteins at the apical membrane of polarized epithelia. *Proceedings of the National Academy of Sciences,* 101, 17705-17710.

MORALES, F. C., TAKAHASHI, Y., MOMIN, S., ADAMS, H., CHEN, X. & GEORGESCU, M.-M. 2007. NHERF1/EBP50 head-to-tail intramolecular interaction masks association with PDZ domain ligands. *Molecular and cellular biology,* 27, 2527-2537.

MORGAN, T. H. & BRIDGES, C. B. 1916. *Sex-linked inheritance in Drosophila*, Carnegie institution of Washington, 10(2), 117–147.

MURER, H., HERNANDO, N., FORSTER, I. & BIBER, J. R. 2000. Proximal tubular phosphate reabsorption: molecular mechanisms. *Physiological reviews,* 80, 1373-1409.

MURER, H., HOPFER, U. & KINNE, R. 1998. Sodium/proton antiport in brush-border-membrane vesicles isolated from rat small intestine and kidney. 1976. *Journal of the American Society of Nephrology,* 9, 143-150.

MURTAZINA, R., KOVBASNJUK, O., ZACHOS, N. C., LI, X., CHEN, Y., HUBBARD, A., HOGEMA, B. M., STEPLOCK, D., SEIDLER, U. & HOQUE, K. M. 2007. Tissue-specific regulation of sodium/proton exchanger isoform 3 activity in Na+/H+ exchanger regulatory factor 1 (NHERF1) null mice cAMP inhibition is differentially dependent on NHERF1 and exchange protein directly activated by cAMP in ileum versus proximal tubule. *Journal of Biological Chemistry,* 282**,** 25141-25151.

NIE, M., BAL, M. S., YANG, Z., LIU, J., RIVERA, C., WENZEL, A., BECK, B. B., SAKHAEE, K., MARCIANO, D. K. & WOLF, M. T. 2016. Mucin-1 Increases Renal TRPV5 Activity In Vitro, and Urinary Level Associates with Calcium Nephrolithiasis in Patients. *J Am Soc Nephrol,* 27**,** 3447-3458.

NITA, M. & GRZYBOWSKI, A. 2016. The role of the reactive oxygen species and oxidative stress in the pathomechanism of the age-related ocular diseases and other pathologies of the anterior and posterior eye segments in adults. *Oxidative Medicine and Cellular Longevity,* 2016, 1-23.

NUKI, G. 2012. Uricase therapy of gout. *Gout & Other Crystal Arthropathies.* Elsevier, 2012, 66-71.

NÜSSLEIN-VOLHARD, C. & WIESCHAUS, E. 1980. Mutations affecting segment number and polarity in Drosophila. *Nature,* 287**,** 795-801.

NYGAARD, P., BESTED, S. M., ANDERSEN, K. A. & SAXILD, H. H. 2000. Bacillus subtilis guanine deaminase is encoded by the yknA gene and is induced during growth with purines as the nitrogen source. *Microbiology,* 146**,** 3061-3069.

O'DONNELL, M. J. & MADDRELL, S. 1995. Fluid reabsorption and ion transport by the lower Malpighian tubules of adult female Drosophila. *Journal of Experimental Biology,* 198**,** 1647-1653.

OGAWA, Y., YAMAGUCHI, K. & MOROZUMI, M. 1990. Effects of magnesium salts in preventing experimental oxalate urolithiasis in rats. *The Journal of urology,* 144**,** 385-389.

OKADA, A., NOMURA, S., HIGASHIBATA, Y., HIROSE, M., GAO, B., YOSHIMURA, M., ITOH, Y., YASUI, T., TOZAWA, K. & KOHRI, K. 2007. Successful formation of calcium oxalate crystal deposition in mouse kidney by intraabdominal glyoxylate injection. *Urological research,* 35**,** 89-99.

OKUNADE, G. W., MILLER, M. L., AZHAR, M., ANDRINGA, A., SANFORD, L. P., DOETSCHMAN, T., PRASAD, V. & SHULL, G. E. 2007. Loss of the Atp2c1 secretory pathway Ca2+-ATPase (SPCA1) in mice causes Golgi stress, apoptosis, and midgestational death in homozygous embryos and squamous cell tumors in adult heterozygotes. *Journal of Biological Chemistry,* 282**,** 26517-26527.

ORDOVAS, J. M. 2008. Genotype–phenotype associations: modulation by diet and obesity. *Obesity,* 16**,** S40-S46.

ORLOWSKI, J. & GRINSTEIN, S. 2004. Diversity of the mammalian sodium/proton exchanger SLC9 gene family. *Pflügers Archiv,* 447**,** 549-565.

ORTEGA, J. D. & FARLEY, C. T. 2015. Effects of aging on mechanical efficiency and muscle activation during level and uphill walking. *Journal of Electromyography and Kinesiology,* 25**,** 193-198.

OVEREND, G. 2010. *Drosophila as a model for the Anopheles Malpighian tubule.* University of Glasgow.

OVEREND, G., CABRERO, P., HALBERG, K. A., RANFORD-CARTWRIGHT, L. C., WOODS, D. J., DAVIES, S. A. & DOW, J. A. 2015. A comprehensive transcriptomic view of renal function in the malaria vector, Anopheles gambiae. *Insect biochemistry and molecular biology,* 67**,** 47-58.

PACHER, P., NIVOROZHKIN, A. & SZABÓ, C. 2006. Therapeutic effects of xanthine oxidase inhibitors: renaissance half a century after the discovery of allopurinol. *Pharmacological reviews,* 58**,** 87-114.

PAK, C. Y., MOE, O. W., SAKHAEE, K., PETERSON, R. D. & POINDEXTER, J. R. 2005. Physicochemical metabolic characteristics for calcium oxalate stone formation in patients with gouty diathesis. *The Journal of urology,* 173**,** 1606-1609.

PAK, C. Y., SAKHAEE, K., PETERSON, R. D., POINDEXTER, J. R. & FRAWLEY, W. H. 2001. Biochemical profile of idiopathic uric acid nephrolithiasis. *Kidney international,* 60**,** 757-761.

PAN, Y., WANG, L. & LE DAI, J. 2006. Suppression of breast cancer cell growth by Na+/H+ exchanger regulatory factor 1 (NHERF1). *Breast Cancer Research,* 8**,** R63-R73.

PARK, C., HA, Y.-S., KIM, Y.-J., YUN, S.-J., LEE, S.-C. & KIM, W.-J. 2010. Comparison of metabolic risk factors in urolithiasis patients according to family history. *Korean journal of urology,* 51**,** 50-53.

PARKS, D. A. & GRANGER, D. N. 1986. Xanthine oxidase: biochemistry, distribution and physiology. *Acta physiologica Scandinavica. Supplementum,* 548**,** 87-99.

PARMAR, M. S. 2004. Kidney stones. *BMJ: British Medical Journal,* 328**,** 1420.

PATEL, K. P., O'BRIEN, T. W., SUBRAMONY, S. H., SHUSTER, J. & STACPOOLE, P. W. 2012. The spectrum of pyruvate dehydrogenase complex deficiency: clinical, biochemical and genetic features in 371 patients. *Molecular genetics and metabolism,* 106**,** 385-394.

PEARSON, G. 1798. II. Experiments and observations, tending to show the composition and properties of urinary concretions. *Philosophical Transactions of the Royal Society of London,* 88**,** 15-46.

PENG, J.-B., SUZUKI, Y., GYIMESI, G. & HEDIGER, M. A. 2018. TRPV5 and TRPV6 Calcium-Selective Channels. *Calcium Entry Channels in Non-Excitable Cells*. CRC Press/Taylor & Francis, 2018. Chapter 13..

PETTIFOR, J. M. 2008. What's new in hypophosphataemic rickets? *European journal of pediatrics,* 167**,** 493-499.

PISTON, D. W. & RIZZO, M. A. 2008. FRET by fluorescence polarization microscopy. *Methods in cell biology,* 85**,** 415-430.

PONUWEI, G. A. 2016. A glimpse of the ERM proteins. *Journal of biomedical science,* 23**,** 35-42.

PRASAD, N. & BHADAURIA, D. 2013. Renal phosphate handling: Physiology. *Indian journal of endocrinology and metabolism,* 17**,** 620-627.

PRIÉ, D., HUART, V., BAKOUH, N., PLANELLES, G., DELLIS, O., GÉRARD, B., HULIN, P., BENQUÉ-BLANCHET, F., SILVE, C. & GRANDCHAMP, B. 2002. Nephrolithiasis and osteoporosis associated with hypophosphatemia caused by mutations in the type 2a sodium–phosphate cotransporter. *New England Journal of Medicine,* 347**,** 983-991.

PRIÉ, D., TORRES, P. U. & FRIEDLANDER, G. 2009. Latest findings in phosphate homeostasis. *Kidney international,* 75**,** 882-889.

PUSHKIN, A., ABULADZE, N., GROSS, E., NEWMAN, D., TATISHCHEV, S., LEE, I., FEDOTOFF, O., BONDAR, G., AZIMOV, R. & NGYUEN, M. 2004. Molecular mechanism of kNBC1–carbonic anhydrase II interaction in proximal tubule cells. *The Journal of physiology,* 559**,** 55-65.

QASEEM, A., DALLAS, P., FORCIEA, M. A., STARKEY, M. & DENBERG, T. D. 2014. Dietary and pharmacologic management to prevent recurrent

nephrolithiasis in adults: a clinical practice guideline from the American College of Physicians. *Annals of internal medicine,* 161, 659-667.
RATKALKAR, V. N. & KLEINMAN, J. G. 2011. Mechanisms of Stone Formation. *Clinical reviews in bone and mineral metabolism,* 9, 187-197.
RECZEK, D., BERRYMAN, M. & BRETSCHER, A. 1997. Identification of EBP50: A PDZ-containing phosphoprotein that associates with members of the ezrin-radixin-moesin family. *The Journal of cell biology,* 139, 169-179.
REDDY, S. T., WANG, C.-Y., SAKHAEE, K., BRINKLEY, L. & PAK, C. Y. 2002. Effect of low-carbohydrate high-protein diets on acid-base balance, stone-forming propensity, and calcium metabolism. *American Journal of Kidney Diseases,* 40, 265-274.
REED, B. Y., GITOMER, W. L., HELLER, H. J., HSU, M. C., LEMKE, M., PADALINO, P. & PAK, C. Y. 2002. Identification and characterization of a gene with base substitutions associated with the absorptive hypercalciuria phenotype and low spinal bone density. *The Journal of Clinical Endocrinology & Metabolism,* 87, 1476-1485.
REILLY, R. F., PEIXOTO, A. J. & DESIR, G. V. 2010. The evidence-based use of thiazide diuretics in hypertension and nephrolithiasis. *Clinical Journal of the American Society of Nephrology,* 5, 1893-1903.
REISS, J. 2000. Genetics of molybdenum cofactor deficiency. *Human genetics,* 106, 157-163.
REISS, J., COHEN, N., DORCHE, C., MANDEL, H., MENDEL, R. R., STALLMEYER, B., ZABOT, M.-T. & DIERKS, T. 1998. Mutations in a polycistronic nuclear gene associated with molybdenum cofactor deficiency. *Nature genetics,* 20, 706-711.
REISS, J. & HAHNEWALD, R. 2011. Molybdenum cofactor deficiency: mutations in GPHN, MOCS1, and MOCS2. *Human mutation,* 32, 10-18.
REITER, L. T., POTOCKI, L., CHIEN, S., GRIBSKOV, M. & BIER, E. 2001. A systematic analysis of human disease-associated gene sequences in Drosophila melanogaster. *Genome research,* 11, 1114-1125.
RENKEMA, K. Y., NIJENHUIS, T., VAN DER EERDEN, B. C., VAN DER KEMP, A. W., WEINANS, H., VAN LEEUWEN, J. P., BINDELS, R. J. & HOENDEROP, J. G. 2005. Hypervitaminosis D mediates compensatory Ca2+ hyperabsorption in TRPV5 knockout mice. *Journal of the American Society of Nephrology,* 16, 3188-3195.
RESNICK, M., PRIDGEN, D. B. & GOODMAN, H. O. 1968. Genetic predisposition to formation of calcium oxalate renal calculi. *New England Journal of Medicine,* 278, 1313-1318.
REYES, L., ALMAGUER, M., CASTRO, T. & VALDIVIA, J. 2002. Clinico-epidemiologic study of urolithiasis in a Caribbean urban area. *Nefrologia: publicacion oficial de la Sociedad Espanola Nefrologia,* 22, 239-244.
RICHES, P. L., WRIGHT, A. F. & RALSTON, S. H. 2009. Recent insights into the pathogenesis of hyperuricaemia and gout. *Human molecular genetics,* 18, R177-R184.
RINGERTZ, H. 1965. Optical and crystallographic data of uric acid and its dihydrate. *Acta Crystallographica,* 19, 286-287.
RINGERTZ, H. 1966. The molecular and crystal structure of uric acid. *Acta Crystallographica,* 20, 397-403.
ROBERTSON, W. & PEACOCK, M. 1980. The cause of idiopathic calcium stone disease: hypercalciuria or hyperoxaluria? *Nephron,* 26, 105-110.
ROBERTSON, W. G. 2012. Stone formation in the Middle Eastern Gulf States: a review. *Arab journal of urology,* 10, 265-272.

ROCH, F., POLESELLO, C., ROUBINET, C., MARTIN, M., ROY, C., VALENTI, P., CARRENO, S., MANGEAT, P. & PAYRE, F. 2010. Differential roles of PtdIns (4, 5) P2 and phosphorylation in moesin activation during Drosophila development. *J Cell Sci,* 123, 2058-2067.

ROMERO, M. F., HENRY, D., NELSON, S., HARTE, P. J., DILLON, A. K. & SCIORTINO, C. M. 2000. Cloning and Characterization of a Na+-driven Anion Exchanger (NDAE1) A NEW BICARBONATE TRANSPORTER. *Journal of Biological Chemistry,* 275, 24552-24559.

ROMERO, V., AKPINAR, H. & ASSIMOS, D. G. 2010. Kidney stones: a global picture of prevalence, incidence, and associated risk factors. *Reviews in urology,* 12, e86-96.

ROPERS, H.-H. 2010. Single gene disorders come into focus-again. *Dialogues in clinical neuroscience,* 12, 95-102.

RUBIN, G. M. & SPRADLING, A. C. 1982. Genetic transformation of Drosophila with transposable element vectors. *Science,* 218, 348-353.

RUBIN, G. M. & SPRADLING, A. C. 1983. Vectors for P element-mediated gene transfer in Drosophila. *Nucleic acids research,* 11, 6341-6351.

RUBINSTEIN, Y. R., GROFT, S. C., BARTEK, R., BROWN, K., CHRISTENSEN, R. A., COLLIER, E., FARBER, A., FARMER, J., FERGUSON, J. H. & FORREST, C. B. 2010. Creating a global rare disease patient registry linked to a rare diseases biorepository database: Rare Disease-HUB (RD-HUB). *Contemporary clinical trials,* 31, 394-404.

RUIZ-AGUDO, E., BURGOS-CARA, A., RUIZ-AGUDO, C., IBAÑEZ-VELASCO, A., CÖLFEN, H. & RODRIGUEZ-NAVARRO, C. 2017. A non-classical view on calcium oxalate precipitation and the role of citrate. *Nature communications,* 8, 768-768.

RUMSBY, G., SHARMA, A., CREGEEN, D. P. & SOLOMON, L. R. 2001. Primary hyperoxaluria type 2 without l-glycericaciduria: is the disease under-diagnosed? *Nephrology Dialysis Transplantation,* 16, 1697-1699.

RUSHTON, H. & SPECTOR, M. 1982. Effects of magnesium deficiency on intratubular calcium oxalate formation and crystalluria in hyperoxaluric rats. *The Journal of urology,* 127, 598-604.

RYDER, E. & RUSSELL, S. 2003. Transposable elements as tools for genomics and genetics in Drosophila. *Briefings in Functional Genomics,* 2, 57-71.

SAFARINEJAD, M. R. 2007. Adult urolithiasis in a population-based study in Iran: prevalence, incidence, and associated risk factors. *Urological research,* 35, 73-82.

SAINT-MARC, C. & DAIGNAN-FORNIER, B. 2004. GUD1 (YDL238c) encodes Saccharomyces cerevisiae guanine deaminase, an enzyme expressed during post-diauxic growth. *Yeast,* 21, 1359-1363.

SAKHAEE, K. 2009. Pharmacology of stone disease. *Adv Chronic Kidney Dis,* 16, 30-8.

SAKHAEE, K. & MAALOUF, N. M. Metabolic syndrome and uric acid nephrolithiasis. Seminars in nephrology, 2008. Elsevier, 174-180.

SAKHAEE, K., MAALOUF, N. M. & SINNOTT, B. 2012. Kidney stones 2012: pathogenesis, diagnosis, and management. *The Journal of Clinical Endocrinology & Metabolism,* 97, 1847-1860.

SAKHAEE, K., NICAR, M., HILL, K., PAK, C. Y. & SAKHAEE, K. 1983. Contrasting effects of potassium citrate and sodium citrate therapies on urinary chemistries and crystallization of stone-forming salts. *Kidney international,* 24, 348-352.

SALEM, M. S. Z. 2016. Pathogenetics. An introductory review. *Egyptian Journal of Medical Human Genetics,* 17, 1-23.

SANDS, J. M. & LAYTON, H. E. The physiology of urinary concentration: an update. Seminars in nephrology, 2009. Elsevier, 178-195.

SAOTOME, I., CURTO, M. & MCCLATCHEY, A. I. 2004. Ezrin is essential for epithelial organization and villus morphogenesis in the developing intestine. *Developmental cell,* 6, 855-864.

SARRIÓ, D., RODRÍGUEZ-PINILLA, S. M., DOTOR, A., CALERO, F., HARDISSON, D. & PALACIOS, J. 2006. Abnormal ezrin localization is associated with clinicopathological features in invasive breast carcinomas. *Breast cancer research and treatment,* 98, 71-79.

SAYER, J. A. 2017. Progress in Understanding the Genetics of Calcium-Containing Nephrolithiasis. *Journal of the American Society of Nephrology : JASN,* 28, 748-759.

SCALES JR, C. D., SMITH, A. C., HANLEY, J. M., SAIGAL, C. S. & PROJECT, U. D. I. A. 2012. Prevalence of kidney stones in the United States. *European urology,* 62, 160-165.

SCHLINGMANN, K. P., RUMINSKA, J., KAUFMANN, M., DURSUN, I., PATTI, M., KRANZ, B., PRONICKA, E., CIARA, E., AKCAY, T. & BULUS, D. 2016. Autosomal-recessive mutations in SLC34A1 encoding sodium-phosphate cotransporter 2A cause idiopathic infantile hypercalcemia. *Journal of the American Society of Nephrology,* 27, 604-614.

SCHMIDT-NIELSEN, B. & SANDS, J. 2001. Urea excretion in white rats and kangaroo rats as influenced by excitement and by diet. *J Am Soc Nephrol,* 12, 856-864.

SCHMITTGEN, T. D. & LIVAK, K. J. 2008. Analyzing real-time PCR data by the comparative CT method. *Nature protocols,* 3, 1101-1108.

SCRIVER, C. R. 2008. Garrod's Croonian Lectures (1908) and the charter 'Inborn Errors of Metabolism': albinism, alkaptonuria, cystinuria, and pentosuria at age 100 in 2008. *Journal of inherited metabolic disease,* 31, 580-598.

SEGAWA, H., KANEKO, I., TAKAHASHI, A., KUWAHATA, M., ITO, M., OHKIDO, I., TATSUMI, S. & MIYAMOTO, K.-I. 2002. Growth-related renal type II Na/Pi cotransporter. *Journal of Biological Chemistry,* 277(22), 19665-72.

SELVAM, R. & DEVARAJ, S. 1997. Oxalate binding protein from the kidney of rat and human mitochondria: studies on properties. *Indian journal of biochemistry & biophysics,* 34, 470-478.

SELVAM, R. & KALAISELVI, P. 2003. Oxalate binding proteins in calcium oxalate nephrolithiasis. *Urological research,* 31, 242-256.

SENTRY, J. & KAISER, K. 1995. Progress inDrosophila genome manipulation. *Transgenic research,* 4, 155-162.

SHAFIEE JR, M. A. 2012. *Urinary Composition and Stone Formation.*

SHAH, G. N., BONAPACE, G., HU, P. Y., STRISCIUGLIO, P. & SLY, W. S. 2004. Carbonic anhydrase II deficiency syndrome (osteopetrosis with renal tubular acidosis and brain calcification): Novel mutations in CA2 identified by direct sequencing expand the opportunity for genotype-phenotype correlation. *Human mutation,* 24, 272-272.

SHEKARRIZ, B. & STOLLER, M. L. 2002. Uric acid nephrolithiasis: current concepts and controversies. *The Journal of urology,* 168, 1307-1314.

SHENOLIKAR, S. 2002. Targeted disruption of the mouse gene encoding a PDZ domain containing protein adaptor, NHERF-1, promotes Npt2 internalization and renal phosphate wasting. *Proc Natl Acad Sci USA,* 99, 11470-11475.

SHENOLIKAR, S., VOLTZ, J., MINKOFF, C., WADE, J. & WEINMAN, E. 2002. Targeted disruption of the mouse NHERF-1 gene promotes internalization of proximal tubule sodium-phosphate cotransporter type IIa and renal phosphate wasting. *Proceedings of the National Academy of Sciences,* 99**,** 11470-11475.

SHIOTA, G., FUKADA, J., ITO, T., TSUKIZAWA, M., YAMADA, M. & SATO, M. 1989. Clinical significance of serum guanase activity in various liver diseases. *Jpn J Med,* 28**,** 22-4.

SHULL, G. E., MILLER, M. L. & PRASAD, V. 2011. Secretory pathway stress responses as possible mechanisms of disease involving Golgi Ca2+ pump dysfunction. *Biofactors,* 37**,** 150-158.

SILVA, S. F. R. D., SILVA, S. L. D., CAMPOS, H. D. H., DAHER, E. D. F. & SILVA, C. A. B. D. 2011. Demographic, clinical and laboratory data of patients with urinary lithiasis in Fortaleza, Ceará. *Jornal Brasileiro de Nefrologia,* 33**,** 295-299.

SINGH, S. R., LIU, W. & HOU, S. X. 2007. The adult Drosophila malpighian tubules are maintained by multipotent stem cells. *Cell stem cell,* 1**,** 191-203.

SLY, W. S., HEWETT-EMMETT, D., WHYTE, M. P., YU, Y.-S. & TASHIAN, R. E. 1983. Carbonic anhydrase II deficiency identified as the primary defect in the autosomal recessive syndrome of osteopetrosis with renal tubular acidosis and cerebral calcification. *Proceedings of the National Academy of Sciences,* 80**,** 2752-2756.

SOFOLA, O., SUNDRAM, V., NG, F., KLEYNER, Y., MORALES, J., BOTAS, J., JACKSON, F. R. & NELSON, D. L. 2008. The Drosophila FMRP and LARK RNA-binding proteins function together to regulate eye development and circadian behavior. *Journal of Neuroscience,* 28**,** 10200-10205.

SOLANKI, S. 2013. *Sodium-phosphate co-transporter PiT1 is required for mineralization of ATDC5 chondrogenic cultures.* McGill University.

SORENSEN, C. M. & CHANDHOKE, P. S. 2002. Hyperuricosuric calcium nephrolithiasis. *Endocrinology and metabolism clinics of North America,* 31**,** 915-925.

SORENSEN, M. D. 2014. Calcium intake and urinary stone disease. *Translational andrology and urology,* 3**,** 235-240.

SORRIBAS, V., LOTSCHER, M., LOFFING, J., BIBER, J., KAISSLING, B., MURER, H. & LEVI, M. 1996. Cellular mechanisms of the age-related decrease in renal phosphate reabsorption. *Kidney Int,* 50**,** 855-63.

SORRIBAS, V., MARKOVICH, D., HAYES, G., STANGE, G., FORGO, J., BIBER, J. & MURER, H. 1994. Cloning of a Na/Pi cotransporter from opossum kidney cells. *J Biol Chem,* 269**,** 6615-21.

SOUCIE, J. M., COATES, R. J., MCCLELLAN, W., AUSTIN, H. & THUN, M. 1996. Relation between geographic variability in kidney stones prevalence and risk factors for stones. *American journal of epidemiology,* 143**,** 487-495.

SOUCIE, J. M., THUN, M. J., COATES, R. J., MCCLELLAN, W. & AUSTIN, H. 1994. Demographic and geographic variability of kidney stones in the United States. *Kidney international,* 46**,** 893-899.

SOUTHALL, T. D., TERHZAZ, S., CABRERO, P., CHINTAPALLI, V. R., EVANS, J. M., DOW, J. A. & DAVIES, S.-A. 2006. Novel subcellular locations and functions for secretory pathway Ca2+/Mn2+-ATPases. *Physiological genomics,* 26**,** 35-45.

SÖZEN, M. A., ARMSTRONG, J. D., YANG, M., KAISER, K. & DOW, J. A. 1997. Functional domains are specified to single-cell resolution in a Drosophila

epithelium. *Proceedings of the National Academy of Sciences,* 94, 5207-5212.
SPRADLING, A. C. & RUBIN, G. M. 1982. Transposition of cloned P elements into Drosophila germ line chromosomes. *Science,* 218, 341-347.
STAMATELOU, K. K., FRANCIS, M. E., JONES, C. A., NYBERG JR, L. M. & CURHAN, G. C. 2003. Time trends in reported prevalence of kidney stones in the United States: 1976–19941. *Kidney international,* 63, 1817-1823.
STARK, K., REINHARD, W., GRASSL, M., ERDMANN, J., SCHUNKERT, H., ILLIG, T. & HENGSTENBERG, C. 2009. Common polymorphisms influencing serum uric acid levels contribute to susceptibility to gout, but not to coronary artery disease. *PloS one,* 4, e7729.
STERLING, T. M. & NEMERE, I. 2005. 1,25-dihydroxyvitamin D3 stimulates vesicular transport within 5 s in polarized intestinal epithelial cells. *J Endocrinol,* 185, 81-91.
SULLIVAN, D. T. & SULLIVAN, M. C. 1975. Transport defects as the physiological basis for eye color mutants of Drosophila melanogaster. *Biochemical genetics,* 13, 603-613.
SUMMERS, J. & MASON, W. S. 1982. Replication of the genome of a hepatitis B-like virus by reverse transcription of an RNA intermediate. *Cell,* 29, 403-415.
SUPURAN, C. T., SCOZZAFAVA, A. & CASINI, A. 2003. Carbonic anhydrase inhibitors. *Medicinal research reviews,* 23, 146-189.
SUTHERLAND, J. W., PARKS, J. H. & COE, F. L. 1985. Recurrence after a single renal stone in a community practice. *Miner Electrolyte Metab,* 11, 267-9.
SUZUKI, Y., LANDOWSKI, C. P. & HEDIGER, M. A. 2008. Mechanisms and regulation of epithelial Ca2+ absorption in health and disease. *Annu Rev Physiol,* 70, 257-71.
TAGUCHI, K., OKADA, A., HAMAMOTO, S., IWATSUKI, S., NAIKI, T., ANDO, R., MIZUNO, K., TOZAWA, K., KOHRI, K. & YASUI, T. 2015. Proinflammatory and metabolic changes facilitate renal crystal deposition in an obese mouse model of metabolic syndrome. *The Journal of urology,* 194, 1787-1796.
TAKEDA, E., TAKETANI, Y., SAWADA, N., SATO, T. & YAMAMOTO, H. 2004a. The regulation and function of phosphate in the human body. *Biofactors,* 21, 345-55.
TAKEDA, E., YAMAMOTO, H., NASHIKI, K., SATO, T., ARAI, H. & TAKETANI, Y. 2004b. Inorganic phosphate homeostasis and the role of dietary phosphorus. *Journal of cellular and molecular medicine,* 8, 191-200.
TAKIKAWA, S.-I., TSUSUÉ, M. & GYURE, W. L. 1983. Characterization of a dihydropterin deaminase from Drosophila melanogaster. *Insect Biochemistry,* 13, 361-368.
TAWASHI, R., COUSINEAU, M. & SHARKAWI, M. 1980. Calcium oxalate crystal formation in the kidneys of rats injected with 4-hydroxy-L-proline. *Urological research,* 8, 121-127.
TAYLOR, E. N., STAMPFER, M. J. & CURHAN, G. C. 2004. Dietary factors and the risk of incident kidney stones in men: new insights after 14 years of follow-up. *Journal of the American Society of Nephrology,* 15, 3225-3232.
TELONIS-SCOTT, M., KOPP, A., WAYNE, M. L., NUZHDIN, S. V. & MCINTYRE, L. M. 2009. Sex-specific splicing in Drosophila: widespread occurrence, tissue specificity and evolutionary conservation. *Genetics,* 181, 421-434.
TERHZAZ, S., CABRERO, P., ROBBEN, J. H., RADFORD, J. C., HUDSON, B. D., MILLIGAN, G., DOW, J. A. & DAVIES, S.-A. 2012. Mechanism and function

of Drosophila capa GPCR: a desiccation stress-responsive receptor with functional homology to human neuromedinU receptor. *PLoS One,* 7**,** e29897.

TERHZAZ, S., O'CONNELL, F. C., POLLOCK, V. P., KEAN, L., DAVIES, S. A., VEENSTRA, J. A. & DOW, J. A. 1999. Isolation and characterization of a leucokinin-like peptide of Drosophila melanogaster. *Journal of Experimental Biology,* 202**,** 3667-3676.

THAMILSELVAN, S., HACKETT, R. L. & KHAN, S. R. 1997. Lipid peroxidation in ethylene glycol induced hyperoxaluria and calcium oxalate nephrolithiasis. *The Journal of urology,* 157**,** 1059-1063.

TIMIO, F., KERRY, S. M., ANSON, K. M., EASTWOOD, J. B. & CAPPUCCIO, F. P. 2003. Calcium urolithiasis, blood pressure and salt intake. *Blood pressure,* 12**,** 122-127.

TIMMER, R. T. & GUNN, R. B. 2000. The molecular basis for Na-dependent phosphate transport in human erythrocytes and K562 cells. *J Gen Physiol,* 116**,** 363-78.

TOMLEKOVA, N. B., WHITE, P. J., THOMPSON, J. A., PENCHEV, E. A. & NIELEN, S. 2017. Mutation increasing beta-carotene concentrations does not adversely affect concentrations of essential mineral elements in pepper fruit. *PLoS One,* 12**,** e0172180.

TORRES, R. J., PRIOR, C. & PUIG, J. G. 2007. Efficacy and safety of allopurinol in patients with hypoxanthine-guanine phosphoribosyltransferase deficiency. *Metabolism,* 56**,** 1179-1186.

TRINCHIERI, A. 2008. Epidemiology of urolithiasis: an update. *Clinical cases in mineral and bone metabolism,* 5**,** 101-106.

TSAI, C.-H., CHEN, Y.-C., CHEN, L.-D., PAN, T.-C., HO, C.-Y., LAI, M.-T., TSAI, F.-J. & CHEN, W.-C. 2008. A traditional Chinese herbal antilithic formula, Wulingsan, effectively prevents the renal deposition of calcium oxalate crystal in ethylene glycol-fed rats. *Urological Research,* 36**,** 17-24.

TSUJIHATA, M. 2008. Mechanism of calcium oxalate renal stone formation and renal tubular cell injury. *International Journal of Urology,* 15**,** 115-120.

TÜRK, C., KNOLL, T., PETRIK, A., SARICA, K., SEITZ, C., STRAUB, M. & TRAXER, O. 2010. Guía clínica sobre la urolitiasis. *European Association of Urology***,** 448-460.

TURNEY, B. W., REYNARD, J. M., NOBLE, J. G. & KEOGHANE, S. R. 2012. Trends in urological stone disease. *BJU international,* 109**,** 1082-1087.

TZOU, D. T., TAGUCHI, K., CHI, T. & STOLLER, M. L. 2016a. Animal models of urinary stone disease. *International Journal of Surgery,* 36**,** 596-606.

UCKERT, W., WILLIMSKY, G., PEDERSEN, F. S., BLANKENSTEIN, T. & PEDERSEN, L. 1998. RNA levels of human retrovirus receptors Pit1 and Pit2 do not correlate with infectibility by three retroviral vector pseudotypes. *Human gene therapy,* 9**,** 2619-2627.

ULMSCHNEIDER, B., GRILLO-HILL, B. K., BENITEZ, M., AZIMOVA, D. R., BARBER, D. L. & NYSTUL, T. G. 2016. Increased intracellular pH is necessary for adult epithelial and embryonic stem cell differentiation. *J Cell Biol,* 215**,** 345-355.

VAIDYANATHAN, K., NARAYANAN, M. & VASUDEVAN, D. 2011. Organic acidurias: an updated review. *Indian Journal of Clinical Biochemistry,* 26**,** 319-325.

VAQUERO, J., HO-BOULDOIRES, T. N., CLAPÉRON, A. & FOUASSIER, L. 2017. Role of the PDZ-scaffold protein NHERF1/EBP50 in cancer biology: from signaling regulation to clinical relevance. *Oncogene,* 36**,** 3067-3079.

VASUDEVAN, V., SAMSON, P., SMITH, A. D. & OKEKE, Z. 2017. The genetic framework for development of nephrolithiasis. *Asian journal of urology,* 4**,** 18-26.

VEGA CARBÓ, M. E., GONZÁLEZ CARRODEGUAS, M. C. & CASTRO ABREU, I. 2009. CARACTERÍSTICAS CLÍNICO-EPIDEMIOLÓGICAS DE LA LITIASIS RENAL COMUNIDAD MANZANILLO 2006-2007. *Revista Habanera de Ciencias Médicas,* 8**,** 52-64.

VILLA-BELLOSTA, R., RAVERA, S., SORRIBAS, V., STANGE, G., LEVI, M., MURER, H., BIBER, J. R. & FORSTER, I. C. 2009. The Na+-Pi cotransporter PiT-2 (SLC20A2) is expressed in the apical membrane of rat renal proximal tubules and regulated by dietary Pi. *American Journal of Physiology-Renal Physiology,* 296**,** F691-F699.

VIRKKI, L. V., BIBER, J., MURER, H. & FORSTER, I. C. 2007. Phosphate transporters: a tale of two solute carrier families. *American Journal of Physiology-Renal Physiology,* 293**,** F643-F654.

VOLTZ, J. W., WEINMAN, E. J. & SHENOLIKAR, S. 2001. Expanding the role of NHERF, a PDZ-domain containing protein adapter, to growth regulation. *Oncogene,* 20**,** 6309-6314.

WAGNER, C. A., RUBIO-ALIAGA, I. & HERNANDO, N. 2017. Renal phosphate handling and inherited disorders of phosphate reabsorption: an update. *Pediatric Nephrology***,** 1-11.

WALLRATH, L. L., BURNETT, J. B. & FRIEDMAN, T. B. 1990. Molecular characterization of the *Drosophila melanogaster* urate oxidase gene, an ecdysone-repressible gene expressed only in the Malpighian tubules. *Mol Cell Biol,* 10**,** 5114-27.

WANG, J., KEAN, L., YANG, J., ALLAN, A. K., DAVIES, S. A., HERZYK, P. & DOW, J. A. 2004. Function-informed transcriptome analysis of Drosophila renal tubule. *Genome biology,* 5**,** 1-21.

WANG, M., YOU, L., LI, H., LIN, Y., ZHANG, Z., HAO, C. & CHEN, J. 2013. Association of circulating fibroblast growth factor-23 with renal phosphate excretion among hemodialysis patients with residual renal function. *Clinical journal of the American Society of Nephrology : CJASN,* 8**,** 116-125.

WANG, X., WU, Y. & ZHOU, B. 2009. Dietary zinc absorption is mediated by ZnT1 in Drosophila melanogaster. *The FASEB Journal,* 23**,** 2650-2661.

WEINER, I. D. & VERLANDER, J. W. 2017. Ammonia transporters and their role in acid-base balance. *Physiological reviews,* 97**,** 465-494.

WEINMAN, E. J., BISWAS, R. S., PENG, Q., SHEN, L., TURNER, C. L., XIAOFEI, E., STEPLOCK, D., SHENOLIKAR, S. & CUNNINGHAM, R. 2007. Parathyroid hormone inhibits renal phosphate transport by phosphorylation of serine 77 of sodium-hydrogen exchanger regulatory factor–1. *The Journal of clinical investigation,* 117**,** 3412-3420.

WEINMAN, E. J., DUBINSKY, W. & SHENOLIKAR, S. 1989. Regulation of the renal Na+-H+ exchanger by protein phosphorylation. *Kidney international,* 36**,** 519-525.

WEINMAN, E. J., HALL, R. A., FRIEDMAN, P. A., LIU-CHEN, L.-Y. & SHENOLIKAR, S. 2006a. The association of NHERF adaptor proteins with G protein–coupled receptors and receptor tyrosine kinases. *Annu. Rev. Physiol.,* 68**,** 491-505.

WEINMAN, E. J., MOHANLAL, V., STOYCHEFF, N., WANG, F., STEPLOCK, D., SHENOLIKAR, S. & CUNNINGHAM, R. 2006b. Longitudinal study of urinary

excretion of phosphate, calcium, and uric acid in mutant NHERF-1 null mice. *American Journal of Physiology-Renal Physiology,* 290, F838-F843.

WEINMAN, E. J., STEPLOCK, D., DONOWITZ, M. & SHENOLIKAR, S. 2000. NHERF associations with sodium− hydrogen exchanger isoform 3 (NHE3) and ezrin are essential for cAMP-mediated phosphorylation and inhibition of NHE3. *Biochemistry,* 39, 6123-6129.

WEINMAN, E. J., STEPLOCK, D., WANG, Y. & SHENOLIKAR, S. 1995. Characterization of a protein cofactor that mediates protein kinase A regulation of the renal brush border membrane Na (+)-H+ exchanger. *The Journal of clinical investigation,* 95, 2143-2149.

WEINSTEIN, D. A., SOMERS, M. J. & WOLFSDORF, J. I. 2001. Decreased urinary citrate excretion in type 1a glycogen storage disease. *The Journal of pediatrics,* 138, 378-382.

WEISS, M. J., COLE, D., RAY, K., WHYTE, M. P., LAFFERTY, M. A., MULIVOR, R. A. & HARRIS, H. 1988. A missense mutation in the human liver/bone/kidney alkaline phosphatase gene causing a lethal form of hypophosphatasia. *Proceedings of the National Academy of Sciences,* 85, 7666-7669.

WELLS, C. C., CHANDRASHEKAR, K. B., JYOTHIRMAYI, G. N., TAHILIANI, V., SABATINO, J. C. & JUNCOS, L. A. 2012. Kidney Stones. *Clinician Reviews,* 22, 31-37.

WERNER, A. & KINNE, R. K. 2001. Evolution of the Na-Pi cotransport systems. *American Journal of Physiology-Regulatory, Integrative and Comparative Physiology,* 280, R301-R312.

WERNER, A., MOORE, M., MANTEI, N., BIBER, J., SEMENZA, G. & MURER, H. 1991. Cloning and expression of cDNA for a Na/Pi cotransport system of kidney cortex. *Proceedings of the National Academy of Sciences,* 88, 9608-9612.

WESSING, A. & EICHELBERG, D. 1978. Malpighian tubules, rectal papillae and excretion. *In:* ASHBURNER, A. & WRIGHT, T. R. F. (eds.) *The genetics and biology of Drosophila.* London: Academic Press, 197, 421-428.

WESSING, A. & ZIEROLD, K. 1999. The formation of type-I concretions in Drosophila Malpighian tubules studied by electron microscopy and X-ray microanalysis. *Journal of insect physiology,* 45, 39-44.

WESSING, A., ZIEROLD, K. & HEVERT, F. 1992. Two types of concretions in Drosophila Malpighian tubules as revealed by X-ray microanalysis: a study on urine formation. *Journal of insect physiology,* 38, 543-554.

WESSON, J. A., JOHNSON, R. J., MAZZALI, M., BESHENSKY, A. M., STIETZ, S., GIACHELLI, C., LIAW, L., ALPERS, C. E., COUSER, W. G. & KLEINMAN, J. G. 2003. Osteopontin is a critical inhibitor of calcium oxalate crystal formation and retention in renal tubules. *Journal of the American Society of Nephrology,* 14, 139-147.

WIECZOREK, H., BEYENBACH, K. W., HUSS, M. & VITAVSKA, O. 2009. Vacuolar-type proton pumps in insect epithelia. *Journal of Experimental Biology,* 212, 1611-1619.

WIECZOREK, H., BROWN, D., GRINSTEIN, S., EHRENFELD, J. & HARVEY, W. R. 1999. Animal plasma membrane energization by proton-motive V-ATPases. *BioEssays,* 21, 637-648.

WIECZOREK, H., PUTZENLECHNER, M., ZEISKE, W. & KLEIN, U. 1991. A vacuolar-type proton pump energizes K+/H+ antiport in an animal plasma membrane. *Journal of Biological Chemistry,* 266, 15340-15347.

WIESSNER, J. H., GARRETT, M. R., HUNG, L. Y., WILLE, D. F. & MANDEL, N. S. 2011. Improved methodology to induce hyperoxaluria without treatment using hydroxyproline. *Urological research,* 39**,** 373-377.

WILSON, J. M., YOUNG, A. B. & KELLEY, W. N. 1983. Hypoxanthine-guanine phosphoribosyltransferase deficiency: the molecular basis of the clinical syndromes. *New England Journal of Medicine,* 309**,** 900-910.

WITTLE, A., KAMDAR, K. & FINNERTY, V. 1999. The Drosophila cinnamon gene is functionally homologous to Arabidopsis cnx1 and has a similar expression pattern to the mammalian gephyrin gene. *Molecular and General Genetics MGG,* 261**,** 672-680.

WORCESTER, E. M. & COE, F. L. 2010. Calcium kidney stones. *New England Journal of Medicine,* 363**,** 954-963.

XIE, B., HALTER, T. J., BORAH, B. M. & NANCOLLAS, G. H. 2015. Aggregation of Calcium Phosphate and Oxalate Phases in the Formation of Renal Stones. *Crystal growth & design,* 15**,** 204-211.

YANG, J., MCCART, C., WOODS, D. J., TERHZAZ, S., GREENWOOD, K. G., FFRENCH-CONSTANT, R. H. & DOW, J. A. 2007. A Drosophila systems approach to xenobiotic metabolism. *Physiological genomics,* 30**,** 223-231.

YAO, J., KATHPALIA, P., BUSHINSKY, D. A. & FAVUS, M. J. 1998. Hyperresponsiveness of vitamin D receptor gene expression to 1, 25-dihydroxyvitamin D3. A new characteristic of genetic hypercalciuric stone-forming rats. *The Journal of clinical investigation,* 101**,** 2223-2232.

YEPISKOPOSYAN, H., EGLI, D., FERGESTAD, T., SELVARAJ, A., TREIBER, C., MULTHAUP, G., GEORGIEV, O. & SCHAFFNER, W. 2006. Transcriptome response to heavy metal stress in Drosophila reveals a new zinc transporter that confers resistance to zinc. *Nucleic acids research,* 34**,** 4866-4877.

YIN, S., QIN, Q. & ZHOU, B. 2017. Functional studies of Drosophila zinc transporters reveal the mechanism for zinc excretion in Malpighian tubules. *BMC biology,* 15**,** 12-24.

YOO, M.-H., WOO, C.-H., YOU, H.-J., CHO, S.-H., KIM, B.-C., CHOI, J.-E., CHUN, J.-S., JHUN, B. H., KIM, T.-S. & KIM, J.-H. 2001. Role of the cytosolic phospholipase A2-linked cascade in signaling by an oncogenic, constitutively active Ha-Ras isoform. *Journal of Biological Chemistry,* 276**,** 24645-24653.

YOSHIDA, M., ZHAO, L., GRIGORYAN, G., SHIM, H., HE, P. & YUN, C. C. 2016. Deletion of Na+/H+ exchanger regulatory factor 2 represses colon cancer progress by suppression of Stat3 and CD24. *American Journal of Physiology-Gastrointestinal and Liver Physiology,* 310**,** G586-G598.

YU, J., DENG, Y., TAO, Z., LIANG, W., GUAN, X., WU, J., NING, X., LIU, Y., LIU, Q. & HE, Z. 2018. The effects of HAP and macrophage cells to the expression of inflammatory factors and apoptosis in HK-2 cells of vitro co-cultured system. *Urolithiasis,* 46**,** 429-443.

YUEN, J. W., GOHEL, M.-D. I., POON, N.-W., SHUM, D. K., TAM, P.-C. & AU, D. W. 2010. The initial and subsequent inflammatory events during calcium oxalate lithiasis. *Clinica Chimica Acta,* 411**,** 1018-1026.

ZHOU, X. & RIDDIFORD, L. M. 2008. rosy function is required for juvenile hormone effects in Drosophila melanogaster. *Genetics,* 178**,** 273-281.